



PHD

**The use of porcine carotid arteries as a matrix material for tissue engineered small diameter vascular grafts**

McFetridge, Peter Stuart

*Award date:*  
2002

*Awarding institution:*  
University of Bath

[Link to publication](#)

**Alternative formats**

If you require this document in an alternative format, please contact:  
[openaccess@bath.ac.uk](mailto:openaccess@bath.ac.uk)

Copyright of this thesis rests with the author. Access is subject to the above licence, if given. If no licence is specified above, original content in this thesis is licensed under the terms of the Creative Commons Attribution-NonCommercial 4.0 International (CC BY-NC-ND 4.0) Licence (<https://creativecommons.org/licenses/by-nc-nd/4.0/>). Any third-party copyright material present remains the property of its respective owner(s) and is licensed under its existing terms.

**Take down policy**

If you consider content within Bath's Research Portal to be in breach of UK law, please contact: [openaccess@bath.ac.uk](mailto:openaccess@bath.ac.uk) with the details. Your claim will be investigated and, where appropriate, the item will be removed from public view as soon as possible.

# **THE USE OF PORCINE CAROTID ARTERIES AS A MATRIX MATERIAL FOR TISSUE ENGINEERED SMALL DIAMETER VASCULAR GRAFTS**

Submitted by Peter Stuart McFetridge

For the degree of PhD

University of Bath

2002

## **Copyright**

Attention is drawn to the fact that copyright of this thesis rests with its author. This copy of the thesis has been supplied on condition that anyone who consults it is understood to recognise that its copyright rests with its author and that no quotation from this thesis and no information derived from it may be published without the prior written consent of the author.

This thesis may be made available for consultation within the University Library and may be photocopied or lent to other libraries for the purposes of consultation



UMI Number: U601903

All rights reserved

INFORMATION TO ALL USERS

The quality of this reproduction is dependent upon the quality of the copy submitted.

In the unlikely event that the author did not send a complete manuscript and there are missing pages, these will be noted. Also, if material had to be removed, a note will indicate the deletion.



UMI U601903

Published by ProQuest LLC 2013. Copyright in the Dissertation held by the Author.  
Microform Edition © ProQuest LLC.

All rights reserved. This work is protected against  
unauthorized copying under Title 17, United States Code.



ProQuest LLC  
789 East Eisenhower Parkway  
P.O. Box 1346  
Ann Arbor, MI 48106-1346

UNIVERSITY OF BATH  
LIBRARY

75 - 8 MAY 2002

Ph.D.



## ABSTRACT

The failure of the vasculature to deliver blood to the body as a result of vascular disease, accounts for the highest rates of morbidity in western societies. Small diameter (<6 mm) vascular reconstructions have proven to be considerably more problematic than large diameter vessel reconstruction, where reduced diameter and low flow rates compounded by high resistance result in poor performance. In terms of small diameter replacement vessels, autologous arteries are considered the "gold standard" for graft success with patency rates of ~90% at five years. By comparison patency rates as low as 30% over 5 years are obtained when synthetic alternatives. In approximately 30% of all small diameter vascular reconstructions, autologous vessels are unavailable for bypass grafting necessitating the use of synthetic grafting materials. Due to the limited supply of autologous vessels a number of alternative approaches have been developed. The approach favoured in this thesis is a relatively new methodology termed 'tissue engineering'. The essential elements using the principles of tissue engineering are, specific human cell lineages, a scaffolding that supports 3-dimensional cell growth and a bioreactor/perfusion system to apply stresses that mimic *in vivo* haemodynamics. This project has focused on the development of a novel biomaterial with arterial-like mechanical characteristics and the design and implementation of a novel bioreactor that emulates the *in vivo* arterial environment *in vitro*, replicating arterial conditions, which are critical in maintaining correct cellular phenotype.

Porcine carotid arteries, harvested from 6-8 month old Great White pigs, were processed to generate a matrix consisting of mostly collagen and elastin, whilst retaining components of the internal elastic lamina and basement membrane. Matrix processing was aimed at removing the nonstructural components of the native vessel to reduce the potentially immunogenic bioburden, without compromising structural stability. Processing entailed solvent extraction of lipids by multiple washes in ethanol over a 24 hour period, followed by proteolytic digestion with trypsin over 24 hours and washing to remove cellular and nonstructural extracellular matrix debris from the matrix. The matrix was then stabilized against enzymatic degradation (which further reduces the potential for immune rejection) by cross-linking matrix proteins using a photo-oxidative reaction with methylene green as the photoactive agent. The reaction ran for 24 hours at 0°C in a 4M NaCl solution with 0.1% (w/v) methylene green at pH 7.4, using approximately 30000 Lux of visible light as the energy source. Results using reverse phase high pressure liquid chromatography (RP-HPLC) have shown the matrix to be approximately 3 times more resistant to enzymatic digestion than unprocessed tissue. Cell culture under static conditions has shown the matrix to be biocompatible when human umbilical endothelial cells (HUVEC) and human vascular smooth muscle cells (hVSMC) were seeded at 90 cells/mm<sup>2</sup> onto the luminal surface and 333 cell/mm<sup>2</sup> on the abluminal surface respectively. After preconditioning the matrix, HUVEC displayed as high as 1082% seeding and proliferative efficiency after 9 days culture. hVSMC displayed a degree of migration into the matrix (~150-200 µm), but this was speculated to be from the cut edge of the matrix, not by transmural ingrowth.

The development of a novel bioreactor and process flow system allowed analysis of seeding and culture of HUVEC and hVSMC monocultures under pulsed perfusion conditions peaking at 80 beats per minute (bpm) (165.5 ml/min). Luminal HUVEC densities of 632 cells/mm<sup>2</sup> were achieved with hVSMC producing a layer of cells surrounding the abluminal surface. Perfusion cultures of hVSMC of ~ 600 cell/mm<sup>2</sup> were shown to maintain the phenotypic marker,  $\alpha$ -actin, after 5 weeks culture. Confirmation of matrix remodelling and hVSMC migration was assessed by immunohistochemical localisation of MMP-2 and 9 and Cathepsin-L and histological staining.

## ACKNOWLEDGEMENTS

Firstly I would like to thank my wife, Ruth, who has helped and supported me through the challenges of the last few years; with the arrival of new family members to coping with being a student again, it has indeed been an interesting time in our lives.

My thanks go to my supervisors, Dr J.B. Chaudhuri, Professor J.A. Howell, from the Department of Chemical Engineering and Dr Tulin Bodamyali, Dr C.R. Stevens and Professor M. Horrocks from the Department of Medical Sciences, whose encouragement and valuable advice have fashioned the research objectives into a project with positive implications in vascular biology and health.

Thank you to Tissue Science Laboratories (TSL) and the Engineering and Physical Sciences Research Council (EPSRC) who have generously funded this work.

Thank you to all those at the Royal United Hospital, the Bath Clinic and Bath abattoir for providing tissue samples which have been vital throughout this work. Many thanks must also go to all the technicians in Chemical Engineering and the Department of Medical Sciences, who have helped on a day-to-day basis with all that is involved in the training of a PhD student and getting them through their project. I would also like to thank Ursula Potter in the Electron Optics Dept. for her help in producing many of the fine SEM images shown throughout this thesis. A special thanks to all my colleagues both in the UK and abroad who have helped in too many ways to list, including much needed moral support.

My sincere thanks

# TABLE OF CONTENTS

ABSTRACT .....	1
ACKNOWLEDGEMENTS .....	2
TABLE OF CONTENTS .....	3
LIST OF TABLES .....	9
LIST OF FIGURES .....	10
ABBREVIATIONS .....	13
CHAPTER ONE: BACKGROUND TO ARTIFICIAL BLOOD VESSELS .....	14
1.1 INTRODUCTION .....	14
Thesis overview .....	16
1.2 DEVELOPMENT OF THE CURRENT CLINICAL TECHNOLOGY .....	19
1.3 AN OVERVIEW OF THE VASCULATURE .....	21
1.3.1 Blood vessel classification and structure .....	21
Structure of 'normal' arteries .....	22
1.3.2 The extracellular matrix .....	23
Collagen .....	23
Elastin .....	24
Proteoglycans .....	25
Structural glycoproteins .....	26
1.4 DEVELOPMENT OF SMALL DIAMETER VASCULAR GRAFTS .....	27
1.4.1 Strategy 1: Development of biocompatible synthetic materials .....	28
1.4.2 Strategy 2: Acellular biomaterials .....	33
1.4.3 Strategy 3: Tissue Engineering 'living grafts' .....	34
Strategy 3a. Endothelial cell seeding of vascular prostheses .....	36
Strategy 3b. Biopolymer-based biomaterials .....	38
Strategy 3c. Self-assembly model .....	41
Strategy 3d. Polymer-based synthetic materials .....	42
Strategy 3e. Decellularised biological tissues .....	44
Conclusions .....	48
CHAPTER TWO: MATERIALS AND METHODS .....	50
2.1 MATERIALS .....	50
2.1.1 Primary cells .....	50
2.1.2 Collagen matrices .....	51
2.1.3 Cell culture media .....	51
2.1.3.1 Growth media for human vascular smooth muscle cells .....	52
2.1.3.2 Growth medium for human umbilical vein endothelial cells .....	52
2.1.4 Chemicals .....	53
2.2 EXPERIMENTAL METHODS .....	55
2.2.1 Cell isolation protocols .....	55
2.2.1.1 Isolation of Human Umbilical Vein Endothelial Cells .....	55

2.2.1.2	<i>Isolation of adult Human vascular smooth muscle cells: explant method</i>	56
2.2.1.3	<i>Isolation of neonatal vascular smooth muscle cells: enzyme dispersion</i>	56
2.2.2	<i>Cell culture</i>	57
2.2.2.1	<i>Endothelial cell culture</i>	58
2.2.2.2	<i>Human vascular smooth muscle cell culture</i>	58
<b>2.3</b>	<b>ANALYTICAL METHODS</b>	<b>59</b>
2.3.1	<i>Cell counting</i>	59
2.3.1.1	<i>Cell counting on porcine derived dermal collagen</i>	59
2.3.1.2	<i>Cell counting on arterial based matrix after static cell culture</i>	60
2.3.1.3	<i>Cell counting on arterial based matrix after perfusion cell culture</i>	60
2.3.1.4	<i>Cell viability</i>	61
2.3.2	<i>Lipid analysis</i>	61
2.3.3	<i>Protein analysis</i>	62
2.3.3.1	<i>Trypsin stability assay 'whole tissue'</i>	62
2.3.3.2	<i>Trypsin digestion-SDS PAGE</i>	64
2.3.4	<i>Media analysis</i>	65
2.3.5	<i>Cross-linking analysis: reverse phase-high performance liquid chromatography</i>	66
2.3.5.1	<i>Solution Preparation</i>	66
2.3.5.2	<i>Tissue Digests</i>	67
2.3.5.3	<i>Derivatisation</i>	67
2.3.5.4	<i>Chromatography</i>	68
2.3.5.5	<i>Hydroxyproline calibration</i>	69
2.3.6	<i>Matrix mechanical properties</i>	70
2.3.6.1	<i>Pressure testing</i>	70
2.3.6.2	<i>Load-extension tests</i>	71
2.3.7	<i>Histology</i>	72
2.3.7.1	<i>Tissue sectioning, paraffin embedding tissue and dewaxing</i>	72
2.3.7.2	<i>Haematoxylin and eosin staining tissue sections</i>	72
2.3.7.3	<i>Van Gieson stain for elastin fibres</i>	72
2.3.7.4	<i>Mounting sections in DPX</i>	73
2.3.7.5	<i>Cell phenotyping</i>	73
2.3.7.6	<i>Immunofluorescent Staining antibodies</i>	74
2.3.7.7	<i>Immunofluorescent Staining Protocol</i>	74
2.3.7.8	<i>Bromodeoxyuridine incorporation as proliferation marker</i>	75
2.3.7.9	<i>Labelling fixed cells using DAPI</i>	75
2.3.8	<i>Microscopy</i>	76
2.3.8.1	<i>Low-temperature scanning electron microscopy</i>	76
2.3.8.2	<i>Standard scanning electron microscopy</i>	77
2.3.8.3	<i>Phase-contrast light microscopy</i>	77
2.3.8.4	<i>fluorescent microscopy</i>	78

<b>CHAPTER THREE: STATIC CELL CULTURE ON PORCINE TYPE I COLLAGEN .....</b>	<b>79</b>
<b>3.1 INTRODUCTION .....</b>	<b>79</b>
<b>3.2 MATERIALS AND METHODS .....</b>	<b>80</b>
3.2.1 Materials .....	80
3.2.2 Experimental methods .....	80
3.2.2.1 <i>Type I dermal collagen preparation</i> .....	80
3.2.2.2 <i>adhesion and proliferation on standard and modified dermal collagen matrix..</i>	81
3.2.2.3 <i>Investigation of pre-seeding conditions to enhance cell adhesion and proliferation</i> .....	82
3.2.3 Analytical methods.....	83
<b>3.3 RESULTS .....</b>	<b>84</b>
3.3.1 Morphology of the dermal collagen matrix.....	84
3.3.2 Assessment of cell adhesion and proliferation on the dermal collagen matrix.....	87
<i>hVSMC growth analysis</i> .....	87
<i>HUVEC and hVSMC adhesion on Permacol</i> .....	88
3.3.3 Enhancement of cell adhesion and proliferation on the dermal collagen matrix.....	95
<i>Cell proliferation</i> .....	96
<b>3.4 DISCUSSION .....</b>	<b>101</b>
3.4.1 Morphology of the dermal collagen matrix.....	102
3.4.2 Assessment of cell adhesion and proliferation on the dermal collagen matrix.....	102
3.4.3 Enhancement of cell adhesion and proliferation on the dermal collagen matrix ....	106
<b>CHAPTER FOUR: DEVELOPMENT OF A SCAFFOLD FOR TISSUE ENGINEERING BLOOD VESSELS USING PORCINE CAROTID ARTERY .....</b>	<b>112</b>
<b>4.1 INTRODUCTION .....</b>	<b>112</b>
4.1.1 Biologically derived ECM for vascular grafting .....	113
4.1.2 Preparation of biological tissue .....	116
<i>Osmotic shock</i> .....	117
<i>Acid and Alkaline</i> .....	118
<i>Detergents</i> .....	119
<i>Enzyme treatments</i> .....	120
<i>Solvents</i> .....	121
4.1.3 Cross-linking biological tissues.....	123
4.1.4 Process overview.....	126
<b>4.2 MATERIALS AND METHODS .....</b>	<b>127</b>
4.2.1 Materials .....	127
4.2.2 Experimental methods .....	127
4.2.2.1 <i>Mechanical processing</i> .....	127
4.2.2.2 <i>Preliminary decellularisation</i> .....	128
4.2.2.3 <i>Lipid extraction</i> .....	128
4.2.2.4 <i>Cross-linking arterial derived matrix</i> .....	129

4.2.2.5 Post process washing .....	131
4.2.3 Analytical Methods.....	131
<b>4.3 RESULTS .....</b>	<b>132</b>
4.3.1 Mechanical processing and storage .....	133
4.3.2 Removal of cell and cell components .....	133
<i>Initial extraction trials</i> .....	133
<i>Solvent based lipid extraction</i> .....	135
<i>Protein digestion</i> .....	139
4.3.3 Cross-linking .....	143
<i>Enzyme degradation results</i> .....	143
4.3.4 Post process washing to remove disrupted cellular and noncellular components of the ECM .....	145
<i>DNA extraction</i> .....	146
4.3.5 LT-SEM analysis of fully processed matrix/vessel surfaces.....	147
4.3.6 Comparative process analysis.....	149
4.3.7 Mechanical properties.....	151
<i>Pressure test analysis</i> .....	152
<i>Load-extension data - Stress-strain curve</i> .....	152
<i>Mean failure: stress and strain</i> .....	154
<b>4.4 DISCUSSION.....</b>	<b>155</b>
<i>Overview of matrix preparation</i> .....	155
4.4.1 Mechanical processing and storage .....	156
4.4.2 Removal of cells and cell components .....	157
<i>Lipid extraction</i> .....	158
<i>Proteolytic degradation ECM proteins</i> .....	162
4.4.3 Cross-linking .....	165
4.4.4 Washing .....	167
4.4.5 Comparative methodology analysis.....	168
4.4.6 Mechanical properties.....	170
<i>Pressure testing</i> .....	171
<i>Load-extension tests</i> .....	172
<i>mean failure: stress and strain</i> .....	173
<i>Elasticity</i> .....	174
<b>CHAPTER FIVE: STATIC CELL CULTURE ON A PORCINE DERIVED ARTERIAL MATRIX .....</b>	<b>176</b>
<b>5.1 INTRODUCTION .....</b>	<b>176</b>
5.1.1 Matrix remodelling .....	176
<i>Serine Proteases</i> .....	178
<i>Matrix metalloproteinases</i> .....	179
<i>Cysteine Proteases</i> .....	180
<b>5.2 MATERIAL AND METHODS .....</b>	<b>182</b>

5.2.1	Materials .....	182
5.2.2	Experimental methods .....	182
	<i>Matrix sterilisation procedure .....</i>	<i>182</i>
	<i>Preconditioning treatments and HUVEC seeding to the luminal surface of the arterial derived matrix.....</i>	<i>183</i>
	<i>hVSMC seeding to the abluminal surface of the arterial derived matrix.....</i>	<i>183</i>
5.2.3	Analytical methods.....	183
<b>5.3</b>	<b>RESULTS .....</b>	<b>184</b>
5.3.1	Luminal seeding and static culture of HUVEC on porcine derived arterial matrix. 184	
	<i>Treatments to enhance HUVEC adhesion on luminal surface of the porcine derived arterial matrix.....</i>	<i>185</i>
5.3.2	Abluminal seeding and static culture of hVSMC on porcine derived matrix.....	186
5.3.3	Assessment of matrix penetration and remodelling by hVSMC .....	190
	<i>MMP-2 expression by hVSMC on arterial derived matrix .....</i>	<i>191</i>
	<i>MMP-9 expression by hVSMC on arterial derived matrix .....</i>	<i>193</i>
	<i>Cathepsin L expression by hVSMC on arterial derived matrix.....</i>	<i>195</i>
<b>5.4</b>	<b>DISCUSSION .....</b>	<b>197</b>
<b>CHAPTER SIX:</b>	<b>DEVELOPMENT OF A VASCULAR PERFUSION CULTURE SYSTEM ....</b>	<b>205</b>
<b>6.1</b>	<b>INTRODUCTION .....</b>	<b>205</b>
6.1.1	The effect of mechanical forces.....	207
	<i>Responses Endothelial Cells to Mechanical stresses.....</i>	<i>208</i>
	<i>Responses of Vascular Smooth Muscle Cells to Mechanical stresses.....</i>	<i>210</i>
6.1.2	Bioreactors.....	212
	<i>Design Objectives:.....</i>	<i>213</i>
<b>6.2</b>	<b>MATERIALS AND METHODS .....</b>	<b>215</b>
6.2.1	Materials .....	215
6.2.2	Methods .....	215
<b>6.3</b>	<b>RESULTS .....</b>	<b>217</b>
6.3.1	Reactor development.....	217
6.3.2	Process flow development.....	225
	<i>Pulse Pressure Wave Assessment, Development.....</i>	<i>227</i>
	<i>Final process flow with integrated reactor/s .....</i>	<i>229</i>
6.3.3	Media analysis and stabilisation .....	231
<b>6.4</b>	<b>DISCUSSION.....</b>	<b>237</b>
	<i>Reactor Development.....</i>	<i>237</i>
<b>CHAPTER SEVEN:</b>	<b>PERFUSION BIOREACTOR STUDIES OF HUMAN VASCULAR CELLS CULTURED ON PORCINE DERIVED VASCULAR MATRICES.....</b>	<b>243</b>
<b>7.1</b>	<b>INTRODUCTION .....</b>	<b>243</b>
<b>7.2</b>	<b>MATERIALS AND METHODS .....</b>	<b>245</b>
7.2.1	Materials .....	245

7.2.2 Experimental methods .....	245
7.2.2.1 Reactor setup .....	245
7.2.2.2 Reactor and Matrix Assembly .....	245
7.2.2.3 Matrix preparation .....	246
7.2.2.4 Seeding cell suspensions onto the luminal surface of the matrix .....	247
7.2.2.5 Seeding HUVEC.....	247
7.2.2.6 Seeding hVSMC.....	248
7.2.2.7 HUVEC and hVSMC culture within the bioreactor .....	249
7.2.3 Analytical methods.....	249
<b>7.3 RESULTS .....</b>	<b>250</b>
7.3.1 Lumen cultures of HUVEC on the arterial derived matrix.....	250
7.3.2 Abluminal hVSMC cultures on the arterial derived matrix.....	254
<i>Phenotypic expression of <math>\alpha</math>-actin by hVSMC seeded onto the arterial derived matrix .</i>	<i>256</i>
7.3.3. Assessment of matrix penetration by hVSMC .....	257
<i>MMP-2 expression by hVSMC cultured under perfusion conditions on the porcine</i>	
<i>derived arterial matrix.....</i>	<i>258</i>
<i>MMP-9 expression by hVSMC cultured under perfusion conditions on the porcine</i>	
<i>derived arterial matrix.....</i>	<i>260</i>
<i>Assessment of Cathepsin L expression by hVSMC cultured under perfusion conditions</i>	
<i>on the porcine derived arterial matrix.....</i>	<i>261</i>
<b>7.4 DISCUSSION.....</b>	<b>263</b>
7.4.1 Lumen Cultures .....	265
7.4.2 Abluminal Cultures .....	267
<b>CHAPTER EIGHT: CONCLUSIONS AND FUTURE WORK .....</b>	<b>272</b>
<b>8.1 CONCLUSIONS.....</b>	<b>272</b>
<b>8.2 FUTURE WORK .....</b>	<b>276</b>
8.2.1 Biomatrix uniformity .....	276
8.2.2 Development of a variable pulse flow model.....	277
8.2.3 Development of a second generation matrix.....	279
<b>REFERENCES .....</b>	<b>281</b>
<b>APPENDIX .....</b>	<b>290</b>
<b>A1: DETERMINATION OF ENDOTHELIAL CELL PHENOTYPE .....</b>	<b>290</b>
<b>A2: DETERMINATION OF SMOOTH MUSCLE CELL PHENOTYPES .....</b>	<b>292</b>
<b>A3: SDS-PAGE METHOD.....</b>	<b>295</b>
<b>A4: ANALYTICAL TECHNIQUES .....</b>	<b>297</b>
<i>Mechanical testing calculation.....</i>	<i>297</i>
<i>Initial length calculation .....</i>	<i>298</i>
<i>Extension calculation.....</i>	<i>299</i>
<i>Strain calculation .....</i>	<i>300</i>
<i>Stress calculation .....</i>	<i>300</i>



# LIST OF TABLES

Table	Contents
1.01	Genetically distinct collagen types
1.02	Selected proteoglycan families of the ECM
1.03	Selected structural glycoproteins of the ECM
1.04	Strategies for small diameter vascular graft development
1.05	Modification to the materials gross physical structure
1.06	Introduction of functional groups
1.07	Incorporation of biologically active substances
1.08	Acellular biomaterials
1.09	Endothelial cell seeding of vascular grafts
1.10	Gross assessments of approaches to produce viable small diameter grafts
2.01	Materials and suppliers
2.02	Gradient conditions for HPLC analysis of Fmoc derivatized amino acids
4.01	Preparation of biological tissue: a methodology overview
4.02	Solvents used for lipid extraction and their properties
4.03	Qualitative observations of native artery after treatments with 1 x trypsin
4.04	Comparison of unprocessed and cross-linked tissue stability
5.01	An overview of selected MMP and their substrates
6.01	Arterial pressure wave velocities
6.02	Materials for Chapter 6
6.03	Overview of main bioreactor design and modifications
6.04	Component media volumes for perfusion system
A.01	SDS PAGE Resolving gel
A.02	SDS PAGE Stacking gel
A.03	SDS PAGE Running buffer
A.04	SDS PAGE Loading buffer

# LIST OF FIGURES

Figure	Figure title
1.01	Gross structural components of blood vessels
1.02	Elastin content of small diameter arteries
2.01	Counting pattern on dermal collagen disks
2.02	Counting pattern used for assessing cell density on/in matrix samples cultured in the perfusion bioreactor
2.03	Chromatogram of hydroxyproline standards
2.04	Calibration plot to determine experimental hydroxyproline concentration
2.05	Diagrammatic representation of the apparatus used for the pressure testing tests
2.06	Diagrammatic representation of the Instron 1122 test rig
3.01	A transverse section of the porcine derived type I dermal collagen matrix
3.02	Low magnification SEM displaying the variable surface morphology of the type I dermal collagen matrix
3.03	Higher magnification LT-SEM detailing the fibrous structure of the collagen matrix
3.04	High magnification LT-SEM of the flattened or compressed surface fibres of the type I dermal collagen matrix
3.05	Standard growth curve of primary hVSMC on tissue culture plastic.
3.06	HUVEC cultured for 1 day on the dermal collagen matrix
3.07	HUVEC with pseudopodia-like protrusion extending into the matrix
3.08	Cell-cell and cell-matrix interactions of HUVEC after 20 hours static culture
3.09	20 hour static cultures of hVSMC seeded on the dermal collagen matrix
3.10	20 hour static cultures of hVSMC (A) seeded on the dermal collagen matrix
3.11	LT-SEM of HUVEC after 4 days static culture on the dermal collagen matrix
3.12	hVSMC cultured for 96 hours under static conditions on the dermal collagen matrix
3.13	HUVEC reduction in cell density after 7 days static culture on the dermal collagen matrix
3.14	Loss of viability and cell adhesion of hVSMC after 7 days static culture
3.15	Cell viability on type I collagen – assessed by trypan blue
3.16	Conformation of HUVEC proliferation by positive staining by BrdUrd
3.17	HUVEC and VSMC proliferation on washed and non-washed collagen
3.18	SMC on non-washed type I collagen at day 30 (100x).
3.19	hVSMC on washed type I collagen at day 30 (63x)
3.20	Comparative SMC Growth (Heparin vs. NaOH pre-treated Permacol)
3.21	VSMC cultured on heparin treated collagen
3.22	VSMC cultured on NaOH treated collagen
4.01	Main processing steps of the decellularisation process
4.02	Calibration graph: comparison of light intensity
4.03	Cross-linking assembly
4.04	Untreated porcine carotid artery
4.05	NH <sub>4</sub> OH treatments of arterial tissue fragmented ECM framework and failed to remove cell nuclei
4.06	Arterial sections post exposure to ultrasound (directly in ultrasonic bath) for 10 minutes
4.07	TLC plate displaying detected lipids after tissue treatment with butanol
4.08	TLC plate displaying detected lipids after tissue treatment with ethanol and butanol
4.09	TLC plate displaying detected lipids after tissue treatment with 75% ethanol
4.10	A transverse section of the arterial wall post ethanol lipid extraction
4.11	Trypsin activity with and without substrate present
4.12	SDS PAGE analysis of tissue digestion post ethanol treatment
4.13	Identification of matrix elastin content
4.14	Matrix post trypsin digestion (48 hours)
4.15	Presence of crystals within the matrix wall post processing

---

4.16	Luminal surface pre and post cross-linking
4.17	Abluminal surface pre and post cross-linking
4.18	LT-SEM image of fully processed matrix, luminal surface showing hills and valley morphology
4.19	LT-SEM Higher magnification of the processed grafts luminal surface
4.20	Low magnification LT-SEM image of the processed grafts abluminal surface
4.21	High magnification LT-SEM image of the processed grafts abluminal surface
4.22	Comparative analysis of lipid and protein content
4.23	Comparative analysis-Tissue weight loss
4.24	Variation in burst pressure testing between untreated and cross-linked tissue
4.25	Stress-strain curve of uniaxially extended tissue
4.26	Mean failure stress and mean failure strain
4.27	A diagrammatic representation of the complete processing methodology used in this thesis
5.01	HUVEC seeded onto control samples (non-treated) show a lower retention than on pretreated matrix
5.02	Effect of matrix pre-treatment on HUVEC adhesion to fully processed, cross-linked porcine carotid arteries
5.03	Removed
5.04	hVSMC seeded onto the matrix abluminal surface from day 3-7 quantitative results
5.05	hVSMC cultures showing cells have encased the matrix and migrated into the arterial wall via the cut section of the matrix
5.06	$\alpha$ -actin expression by hVSMC on arterial derived matrix
5.07	Random dispersion of hVSMC within the loose adventitial layer
5.08	Control section of hVSMC seeded for 3 weeks on processed matrix and stained for MMP-2
5.09	Matrix staining positive for MMP-2 after 3 weeks culture
5.10	Positive staining for MMP-2 after 5 weeks culture
5.11	Control section of hVSMC seeded for 3 weeks on processed matrix and stained for MMP-9
5.12	Positive staining for MMP-9 after 3 weeks culture
5.13	Positive staining for MMP-9 after 5 weeks in culture
5.14	Control section of hVSMC seeded for 3 weeks on processed matrix and stained for Cathepsin L
5.15	No definite positive staining for Cathepsin L after 3 weeks in culture
5.16	Unlike SMC cultured for 3 weeks and stained for Cathepsin L, 5 week cultures
6.01	An illustration of perfusion conditions and construction theory
6.02	Watson Marlow pump calibration
6.03	Technical specification of Mark 1A reactor
6.04	Mark 1A reactors of differing lengths
6.05	Mark 1 reactor PTFE end caps showing the two different sealing methods
6.06	Reactor showing the tapered male ground glass
6.07	Mark 3 reactor showing the central glass body
6.08	An illustration of the Mark 4 bioreactor displaying inlet and outlet ports of the reactors main body
6.09	Schematic of the final process flow circuit
6.10	Arterial pressure curves
6.11	Pulsatile pressure wave characteristics of the Watson-Marlow 503U peristaltic pump
6.12	Representation of the systems final operating design
6.13	DMEM oxidation under pulsed flow
6.14	Comparative change in pH between static and perfusion systems over time
6.15	Comparative change in glucose concentration between static and perfusion systems
6.16	Comparative change in $\text{PCO}_2$ between static and perfusion systems
6.17	Comparative change in $\text{PO}_2$ between static and perfusion systems
6.18	Comparative change in $\text{HCO}_3^-$ between static and perfusion systems

---

---

7.01	HUVEC adhered to the luminal surface of matrix after trial flow conditions
7.02	Improved HUVEC adhesion after modifying seeding conditions
7.03	Improved HUVEC adhesion after modifying seeding conditions, surface analysis with LT-SEM showing matrix and HUVEC morphology
7.04	Increased cell densities using different seeding methodologies and reactor/system design
7.05	LT-SEM showing matrix and HUVEC morphology (a)
7.06	LT-SEM showing matrix and HUVEC morphology (b)
7.07	LT-SEM showing matrix and HUVEC morphology (c)
7.08	LT-SEM of the abluminal surface displaying loose ECM fibres
7.09	LT-SEM image of hVSMC upon the abluminal surface
7.10	$\alpha$ -actin expression by hVSMC
7.11	hVSMC cultured on the matrix over 5 weeks in the bioreactor
7.12	Control section of hVSMC seeded and cultured for 5 weeks on processed matrix
7.13	Matrix and cell populations staining negative for MMP-2 after 5 weeks culture
7.14	Control, no background or non-specific staining of MMP-9 in the SMC layer
7.15	Positive immunolocalisation for MMP-9 after 5 weeks in perfusion culture
7.16	Control section of hVSMC on processed matrix and stained for Cathepsin L.
7.17	Sections stained for Cathepsin L after 5 weeks perfusion culture
A.01	HUVEC displaying characteristic cobblestone morphology
A.02	HUVEC stained positive for vWF (Factor VIII)
A.03	HUVEC stained positive for CD31 cell surface antigen.
A.04	hVSMC displaying characteristic 'hill and valley' formations
A.05	Neonatal umbilical cord arterial derived and adult saphenous vein hVSMC stained positive for $\alpha$ -actin.
A.06	A stylised stress-strain curve produced by the chart recorder in the load-extension tests.
A.07	Pictorial representation of a tissue ringlet in the form of a strip after bisection
A.08	Side-on view of the ringlet during extension by two hooks on the Instron™ 1122 rig

---

## ABBREVIATIONS

Abbreviation	Full name/title
Ab	Antibody
BAEE	N $\alpha$ -Benzyol-L-Arginine
BrdUrd	Bromodeoxyuridine
DAB	3,3'-diaminobenzidine
DMEM	Dulbecco's Modified Eagle Medium
ECM	Extra Cellular Matrix
EC	Endothelial cell
EDTA	Ethylenediamine tetra-acetic acid
bpm	Beats per minute
ePTFE	expanded Polytetrafluoroethylene (Teflon)
Fb	Fibroblasts
FCS	Foetal calf serum
FITC	Fluorescein isothiocyanate
FMOC-CL	9-fluorenylmethyl chloroformate
GAG	Glycosaminoglycan
GAGS	Glycosaminoglycan side chains
HBSS	Hanks balanced salt solution
HCl	Hydrochloric Acid
HMDI	Hexamethylene diisocyanate
HRP	Horse radish Peroxidase
HSV	Human saphenous vein
HUVEC	Human Umbilical Vein Endothelial Cells
hVSMC	Human Vascular Smooth Muscle Cell
Hyp	Hydroxyproline
ID	Inside diameter
IM	Inner membrane
IMS	Industrial Methylated spirits
ITA	Internal Thoracic artery
LT-SEM	Low Temperature Scanning Electron Microscope
MMP	Matrix metalloproteinase
OD	Outside diameter
P (I,II,III,IV,V,VI,VII,VIII)	Cell passage (number)
PBS	Phosphate buffered saline
PET	Polyethylene Terephthalate (Dacron)
PG	Proteoglycans
PGA	Polyglycolic acid
PTFE	Polytetrafluoroethylene
PU	Polyurethane
PVC	Polyvinylchloride
rpm	Revolutions per minute
r.t.	Room Temperature
SEM	Scanning Electron Microscopy
SIS	Small Intestine Submucosa
SMC	Smooth Muscle Cells
TE	Tissue engineered
TLC	Thin Layer Chromatography
Tween 80	Polyoxyethylenesorbitsan monolaurate
UC	Umbilical cords
VSMC	Vascular Smooth Muscle Cells

# CHAPTER ONE: BACKGROUND TO ARTIFICIAL BLOOD VESSELS

## 1.1 INTRODUCTION

Vascular disease is a major health concern in western society, where the progressive occlusion of blood vessels results initially in symptoms of hypoxia leading to gross organ damage and death. Considerable success has been attained with large diameter synthetic conduits, where higher flow rates compared to peripheral vessels contribute to acceptable patency rates. Bypass surgery of blood vessels less than ~ 6 mm in diameter using traditional prosthetics such as Dacron or ePTFE results in rapid occlusion of the graft yielding unacceptable low patency rates (Ratcliffe, 2000). The grafting material of choice is autologous artery e.g. the mammary artery with patency rates approaching 90% at 5 years, however these vessels are often reserved for heart bypass. It is generally accepted that autologous vein is the next best replacement vessel, unfortunately, for ~30% of patients requiring bypass surgery, autologous vessels (arterial or vein) are either unavailable or inappropriate for use due to prior extraction or inherent vascular disease. In these cases synthetic replacement vessels are used with patency rates as low as 30% over 5 years. It must be noted however that the position and physical dimensions of the replacement vessel have a profound effect on graft patency. With larger diameter vessels exposed to higher flow rates achieving improved patency rates.

The failure of small diameter arteries due to atherosclerotic disease is the leading cause of mortality in the United States, with other western cultures facing similar statistics (Niklason et al., 1999). Mean costs per patient for primary revascularisation operations with autologous vein are approximately £7 512. Limb amputations cost approximately £10 863 with recurring annual costs up to £21 000 per patient per annum for long-term institutional care. With higher reintervention rates for synthetic grafts (PTFE) compared to autologous grafts, the cost is only marginally (6%) cheaper than amputation, though without the additional long-term care (Cheshire et al., 1992). From both a patient care and economic standpoint there is, without doubt, an urgent need for viable small diameter grafts. The ultimate goal of reconstructive vascular research is a procedure that artificially induces a patient's own body to regenerate/grow replacement

vessels *in situ*, as required. This may well be possible in the future; however the current status of vascular reconstruction is limited to by-passing or excision of the diseased tissue, and replacement with one of several options e.g. internal mammary artery, saphenous vein, or a synthetic substitute.

The primary aim of this project is to develop a functional small diameter artery (< 6 mm) for use as a prosthetic graft. An essential requirement is the establishment of a microenvironment that mimics *in vivo* conditions. A key step in this project is the development of a bioreactor that is designed to apply physiological conditions and allow delivery and removal of gases, nutrients, waste etc. Identification of the physical conditions required is based on the premise that the pressure wave, pulse and flow rates have generic properties that can be modelled or replicated over a variety of internal diameters. The importance of local environmental conditions on cell behaviour has been well documented; for example, changes between endothelial cell/substrate contacts (Olivier et al., 1999) and the transition from random to aligned cell focal contacts when exposed to laminar flow (Nerem and Seliktar, 2001).

### Essential requirements for functional arterial grafts:

Immunological acceptance by patient

Availability i.e. time to produce

Durability i.e. ability to withstand haemodynamic stresses

Positive handling characteristics i.e. suturability and simplicity of handling

Resistance to thrombosis and graft infection

Post implantation healing c.f. scar tissue formation

## THESIS OVERVIEW

In this thesis the progress made towards solving the problem of poor vascular graft patency has been described. As discussed previously, this thesis is directly applicable to small diameter (<6 mm) vascular reconstructions as larger vessel replacements such as the abdominal aorta, achieve acceptable patency rates using current technology. This is not to preclude the technology discussed in this thesis for use in larger grafts, particularly in growing children, where a graft must be able to 'grow and remodel' as the child develops. Only the said technology is directed at an area where demand far exceeds supply.

An important issue in vascular reconstructive surgery is the time required to produce a viable graft due to patient morbidity; for this reason emphasis has been placed on increasing the efficiency of process and design. Each of the results chapters begins with a brief introduction to that specific aspect of the thesis, followed by a literature review, unless the topic has been previously covered, that aims to summarize the current state of the art in direct relation to that specific chapter. Here, comprehensive reviews obtained from the literature may be summarised in order to complement literature and experimental procedures described in later chapters. After detailing results, the discussion with conclusions follows in each chapter.

Chapter 1 has begun with a general introduction and brief historical overview of the current technology to introduce the reader to the extent of the clinical problem. This is followed by a gross description of the human vascular system, which later details components of the arterial wall such as collagen, elastin, glycoproteins, proteoglycans etc. As the research to develop successful small diameter vascular grafts is a field where the problem is engaged from several angles, the various strategies to accomplish this are discussed. The chapter finishes by reviewing the current state-of-the-art with direct relation to tissue engineering of small diameter vascular grafts. The remainder of this introduction gives a brief overview of the content and aims of this thesis on a chapter-by-chapter basis.

Chapter 2: Materials and Methods, contains general materials and experimental



methods. Primary adult human vascular smooth muscle cells (hVSMC) and human umbilical vein endothelial cells (HUVEC) have been used throughout this thesis. Adult human cell growth is considerably slower and more problematic than either neonatal or non-human cells, it would have been preferable to use all adult human cells due to the works clinical relevance, unfortunately only adult hVSMC were available, requiring the use of neonatal EC.

The chapter concludes with all analytical methods used throughout this thesis. Each of the results chapters contains a materials and methods section describing only materials and experimental methods specific or discrete to that chapter.

Chapter 3: Static cell culture on porcine type I collagen, describes the analysis of a porcine derived dermal type I collagen matrix. The primary aim was to assess the matrix for its potential as a scaffold for applications in tissue engineering of small diameter vascular grafts. Primary human vascular smooth muscle cells (hVSMC) and human umbilical vein endothelial cells (HUVEC) were seeded and cultured on the matrix to assess cell adhesion, proliferation and maintenance over time. This was followed by exploring various methodologies to enhance cell compatibility and growth dynamics by modifying the material to improve its potential as a matrix for vascular tissue engineering.

Chapter 4: Development of a scaffold for tissue engineering blood vessels using porcine carotid arteries, was based on knowledge and experience gained in Chapter 3 to develop a specific, tailor-made material, for vascular tissue engineering. To this extent the progressive development of a unique porcine derived arterial matrix is described. The chapter is introduced with a literature review of methodologies currently used to generate acellular biomaterials. Methodologies are examined to efficiently strip porcine cells and non-structural components of the artery and stabilise against enzymatic degradation to yield a theoretically immunologically inert, or near inert acellular biomaterial that maintains an acceptable degree of native biomechanical characteristics.

Chapter 5: Static cell cultures on a porcine derived arterial matrix, has focused on assessing the developed biomaterial in terms of cell biocompatibility. Specifically, adhesion and maintenance of HUVEC on the luminal surface and hVSMC on the

abluminal surface of the matrix. These analyses were conducted under static culturing conditions to reduce variables. Methods have been explored to improve cell adhesion and proliferation as a prelude to culturing specific human cells under pulsed flow conditions. Cell migration into and remodelling of the matrix by seeded cells, specifically hVSMC, is of critical importance to graft development. A variety of enzymes have been assessed immunohistochemically with antibody probes for MMP-2 and 9 and cathepsin L.

Chapter 6: Development of a vascular perfusion culture system, is introduced with an overview of the effects mechanical forces have on the two main cell types of the vasculature, endothelial cells (EC) and VSMC. The chapter then details the progressive development of a novel bioreactor and process flow support system. The bioreactor development has aimed to focus attention on the matrix supported between the luminal inlet and outlet of the reactor, where conditions such as pressure, pulsed wave form, flow, gas content, glucose and pH have been assessed to emulate physiological arterial conditions. It is believed that an accurate representation of *in vivo* conditions is the key to cell phenotype stability and thus graft success.

Chapter 7: Perfusion bioreactor studies of human vascular cells on porcine derived vascular matrix, describe the natural progression from Chapter 5 and 6 to deliver chemical, gas and mechanical forces to both hVSMC and HUVEC seeded and cultured on the matrix that is representative of the *in vivo* conditions described in Chapter 6. Similarly to Chapter 5, the ability of the matrix to support cell adhesion and proliferation are key to the success of this project. Given the perfusion conditions under which cells are cultivated, particularly the high shear in the lumen (compared to static culture) a number of seeding methodologies have been explored to increase the efficiency of both HUVEC and hVSMC adhesion on their appropriate surfaces. In line with the data gathered in Chapter 5, static cultures on the arterial derived biomaterial, hVSMC have been immunohistochemically assessed under defined flow conditions for expression of MMP-2 and 9 and cathepsin L, and their ability to migrate within the matrix as a comparative analysis to static cultures.

Chapter 8, the final chapter, gives final conclusions to each of the experimental chapters and a description of future work. Appendices brings the thesis to a close.

## 1.2 DEVELOPMENT OF THE CURRENT CLINICAL TECHNOLOGY

Vascular diseases such as arteriosclerosis (e.g. atherosclerosis, arteriolosclerosis and Monckebergs's calcific medial sclerosis) are major health concerns within western society. The natural development of these diseases is the progressive occlusion of blood vessels where the initial symptoms are manifested as hypoxia, ultimately leading to gross organ damage and death unless treated. Methodologies to halt or repair diseased blood vessels include: diet modifications, stent installation, angioplasty and complete vessel replacement. Although autogenous artery is considered to be the best vessel replacement, such as the internal-thoracic-artery (ITA) or internal mammary artery, they are seldom used due to limited availability. Previous studies (Loop et al., 1986), (Zeff et al., 1988) have shown the ITA graft to be a superior conduit and (Cameron et al., 1996) evaluated ITA versus saphenous vein when used as coronary-artery bypass. Due to the higher performance of the ITA graft, it is usually reserved for heart bypass operations. The American Registry of the Coronary Artery Surgery Study (24958 patients) over a 15-year period, found that the ITA graft conferred a distinct survival advantage, regardless of age, sex or disease state over other procedures.

The saphenous vein is understood to be the next best option (site specific) and considered superior to current synthetic replacements. The saphenous vein, like other veins including; cephalic or basilic vein, cryopreserved saphenous vein allografts, umbilical vein grafts and the superficial femoral vein, is susceptible to late complications. These include aneurysmal degeneration, intimal fibrosis, intimal hyperplasia and accelerated atherosclerosis. By comparison autogeneous arteries, specifically the ITA grafts have been shown, in post-mortem examinations, to have little if any evidence of atherosclerosis (Cameron et al., 1996). Unfortunately, 30-40% of femoropopliteal reconstructions (Charlesworth et al., 1985) or in general, 15-30% of cases the veins, like arteries, are found to be unsuitable for use due to "gross abnormalities" or their prior use has precluded them (Esquivel and Blaisdell, 1986).

These findings are significant in the choice of matrix material used to develop a tissue engineered graft, where the preferred option for vessel replacement is autogeneous biological artery, displaying fewer disease symptoms long-term, compared with vein grafts. Importantly the most successful graft materials are firstly biological and

secondly those which are structurally and mechanically similar to the original vessel being replaced. As an alternative to autogenous material, synthetic conduits are used in vascular reconstructive surgery. Voorhees et al (1952) pioneered this work by proposing the use of Vinyon 'N' cloth to bridge arterial defects (Voorhees et al., 1952). Later Blakemore and Voorhees, (1954) continued this work with limited success in clinical trials (Blakemore and Voorhees, 1954).

Since these early trials, research has concentrated on improving graft biocompatibility. This has led to the widespread use of synthetic materials such as Dacron (polyethylene terephthalate or PET), polyurethane and Teflon (expanded polytetrafluoroethylene or ePTFE) as graft material. Vascular reconstructive surgery has had considerable success with the use of large diameter synthetic conduits (> 6 mm) as replacement vessels. By contrast, small diameter synthetic conduits occlude rapidly resulting in very low patency rates. This is particularly so in the peripheral vasculature where high resistance is compounded by low flow rates cumulating in graft thrombosis (Callow, 1982). Prosthetic materials are typically found to be inferior to autologous saphenous vein as replacement vessels, where thrombosis and graft infection reduce patency rates of synthetic materials (Thomas et al., 1999). Larger diameter synthetic replacements have proved more reliable than small diameter grafts and with long term use of anticoagulants and platelet inhibitors, grafts attain patency rates in excess of 10 years (Antiplatelet Trialists' Collaboration, 1994). Principally the development of neointimal hyperplasia and the absence of a fully biocompatible luminal surface, compounded by low flow rates and high resistance are the main causes of graft occlusion and failure. This is particularly so in smaller diameter vessels of the peripheral vasculature. One of the synthetic materials available for use in reconstructive surgery, ePTFE is commonly used for femoropopliteal bypasses (Bos et al., 1998). Surgical assessments of ePTFE have found cumulative patency rates at 6-years to be 20-30% in comparison to autologous vein with cumulative patency rates at 5-years of 70% and 60% at 10-years, when used in femoropopliteal bypasses. Charlesworth et al (1985) proposed that when autologous material was unavailable for use it "may be wiser to elect non-operative management than perform reconstructions of limited durability" (Charlesworth et al., 1985). These results have been further iterated in later studies reviewed by Jeschke et al (1999) where "long-term" (in this case 2-years) patency rates of ~30% for ePTFE grafts were achieved (Jeschke et al., 1999). Thus, an alternative replacement prostheses to

native vessels in which patency rates are deemed acceptable is of the highest priority and is a task that tissue engineers and others have set to solve.

### **1.3 AN OVERVIEW OF THE VASCULATURE**

To recognize the prerequisites for development of a successful conduit, an overview of basic structure and function of the vasculature is provided.

#### **1.3.1 BLOOD VESSEL CLASSIFICATION AND STRUCTURE**

Within the circulatory system, blood vessel function has been classified into four groups based on their role within the vasculature. Firstly, the *conductance* vessels, with internal diameters ranging from 4-25mm and wall thicknesses of 2mm, these have a low resistance to fluid flow and are designed for rapid fluid transport. Vessels in this category are the elastic and muscular arteries, which deliver blood to distal vessels. Secondly, *resistance* vessels, with internal diameters ranging from 30 $\mu$ m – 4mm and wall thicknesses from 30 $\mu$ m – 1mm, which are the terminal arteries and arterioles, these act to control local blood flow. Through contraction or dilation of the smooth muscle fibres of the vessel wall, (controlled predominantly through the sympathetic nervous system and the adrenal medullary hormones) blood flow to downstream capillary beds is controlled (Wheater et al., 1979). Thirdly, *exchange* vessels, with internal diameters approximately 8 $\mu$ m and wall thicknesses of 1 $\mu$ m, which are the capillaries themselves. These characteristically have a single layer of flattened endothelial cells that form a continuous epithelium that optimises mass transfer between blood and tissues. Finally *capacitance* vessels, the veins and venules of the vasculature. These vessels are thin-walled and offer low resistance to blood flow. With the exception of venous components of the microcirculation, capacitance vessels function as a low-pressure collection system and a variable capacity blood reservoir (containing approximately 65% of the bodies blood volume), which ultimately returns blood to the heart.

## STRUCTURE OF 'NORMAL' ARTERIES

Blood vessel structure, whether arterial or venous, basically consist of three main layers or tunicae. Tunica intima, the innermost layer, comprises an inner layer of flattened epithelial cells, termed the endothelium, which lines the lumen. Outside the endothelium is a zone of connective tissue, a basement membrane of type IV collagen. This supports the endothelium that is encased by the internal elastic lamina, a 'sleeve' of elastic tissue that limits the distension of the blood vessel (Hampton, 1983). The tunica media, an intermediate muscular layer, forms a tube around the internal elastic lamina. In the larger arteries, elastin is entwined within the collagen fibres whereas in the aorta, elastin is the dominant structural protein. At the boundary between the tunica media and adventitia lies the external elastic lamina, less defined than the internal lamina and absent from some arteries e.g. the cerebral arteries. The tunica adventitia is an outer layer of loose connective tissue that merges with adjacent structures, containing lymphatic vessels, autonomic nerves and vasa vasorum. The increased wall thickness of the larger vessels and diffusion implications of wastes, nutrients and gases within the vessels predicts the requirement for a network of small arteries, vasa vasorum, within the vessels themselves to supply nutrients and gases. Vasa vasorum are predominantly within the tunica adventitia though some capillary beds are found to extend into the tunica media (Sunthareswaran, 1998), see Figure 1.01. Although the basic structure of the vasculature remains constant throughout the circulatory system, there is considerable variation between tunica from one type of vessel to another. The major histological difference is the density of smooth muscle cells and the structural protein elastin. The function of the arterial system is to deliver blood from the heart to capillary beds throughout the body, thus supplying the necessary gasses and nutrients for tissue maintenance. Delivery is via the cyclic pumping of the heart, forcing blood into the arterial network in a pulsatile flow. The effect of this flow regime cumulates in distension of the arterial wall and its subsequent recoil as the pressure wave passes. Vessel structure (e.g. muscular arteries, veins) display physical characteristics pertinent to their function. Arteries for example have increased demands from a pressure standpoint, therefore have an increased wall thickness to accommodate increased mechanical stresses.

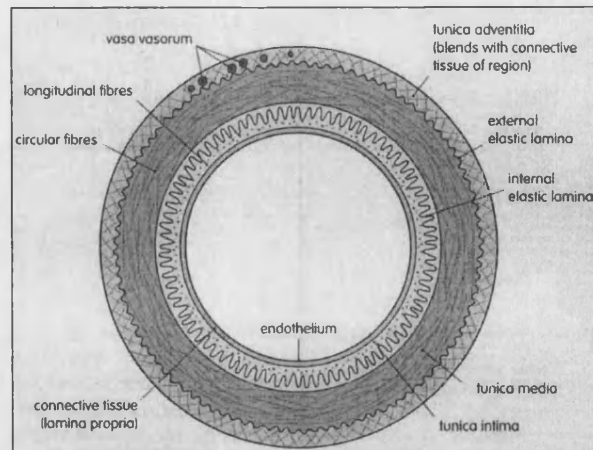


**Figure 1.01:** Gross structural components of blood vessels, Sunthareswaran, (1998).

### 1.3.2 THE EXTRACELLULAR MATRIX

ECM components are of fundamental importance to the efficient functioning of the vasculature and are therefore a significant aspect of vascular research. In this section, an overview of the structure and function of these vascular components is presented. The ECM consists of four major classes of macromolecules: collagen, proteoglycans, structural glycoproteins and elastin, each of which are discussed in the following sections.

#### COLLAGEN

Collagen can be described as a multifunctional family of structural proteins where one or more domains have the conformation of a triple helix (Van der Rest and Garrone, 1991). It is the most abundant protein in the animal kingdom, accounting for 30 - 40% of the protein in the human body and is found in all multicellular organisms. Table 1.01 shows the diversity of the collagen molecule, with 18 genetically distinct collagen types. The predominant collagen types within the vasculature are types I and III in the arterial wall and type IV as the major constituents of the basement membrane. By providing a scaffold with inherent mechanical properties, collagen allows for cell attachment and motility thus empowering specific tissues to perform their function. From ligaments to blood vessels, collagen is the main structural component within connective tissue which

holds, binds and strengthens individual tissues. In most living systems structure and function have a close relationship that results in efficient design; collagen is no exception. The importance of the extra-cellular matrix in tissue engineering cannot be understated. The matrix composition provides various cell types with ‘local’ information, from topological arrangement to dynamic interactions with its surroundings or environment. For example, the pulsatile nature of blood flow on the blood vessel wall, as a mechanical effect, is one of the determinants in maintaining vascular smooth muscle cell (VSMC) phenotype. VSMC in traditional culture will ultimately revert to a non-specialised fibroblast-like state and subsequent loss of function, for example, it has been shown that vascular smooth cells not only increase expression of h-caldesmon, a marker for the differentiated SMC state when exposed to cyclic strain but are also induced to proliferate (Birukov et al., 1995).

**Table 1.01:** Genetically distinct collagen types (Ramshaw et al., 1995). The predominant collagen types in blood vessels have been highlighted.

Group	Structure	Type/s
1	Collagen forming long fibrils	I, II, III, V, XI
2	Fibril-associated collagen with interrupted triple helices	IX, XII, XIV
3	Fibril-associated collagen forming beaded filaments	VI
4	Collagen that form sheets	IV, VIII, X
5	Collagen that form anchoring fibrils	VII
6	Others	XVII
7	Unknown functions	XIII, XV, XVI, XVIII

## ELASTIN

The second most abundant structural protein in blood vessels is elastin, the main component of elastic fibres. Where collagen confers strength to tissues, elastin gives tissues resilience in order to recoil after each stretching action. Collagen fibres are interwoven with the elastic fibres in order to delimit extension and prevent tearing of the tissue. Elastin is of particular importance in blood vessels as it confers elasticity thus allowing the blood vessels to recoil as the pressure pulse wave propagates through the arterial vasculature, Figure 1.02 (Alberts et al., 1994).



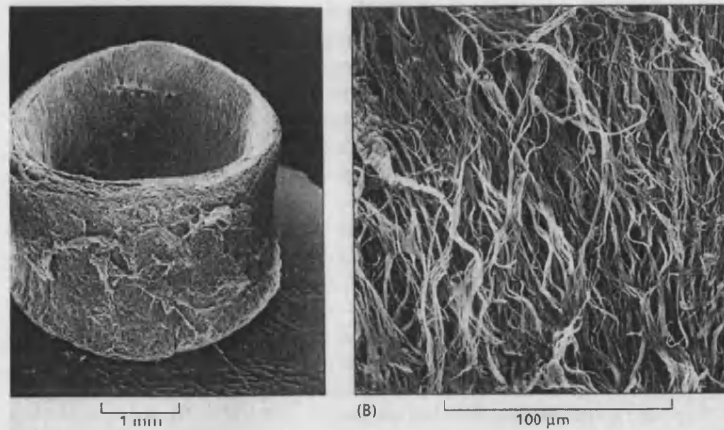


**Figure 1.02:** Elastin content of small diameter arteries. This LT-SEM micrograph shows the network of elastic fibres as dense and longitudinal aligned, all other components have been digested away with enzymes and formic acid (Alberts et al., 1994).

Like collagen, elastin is rich in proline and glycine but differs dramatically in that it is not glycosylated, contains few hydroxylated proline residues, no hydroxylysine and is encoded by a single gene product, tropoelastin (Haralson and Hassell, 1995). Once secreted by the cell, elastin becomes highly cross-linked, in a manner similar to collagen covalent cross-linking, between lysine residues forming substantial lattice of fibres and sheets. Alanine and lysine rich,  $\alpha$ -helical, hydrophobic segments alternating along the polypeptide chain of elastin form cross-links between adjacent molecules, each of these  $\alpha$ -helical segments is coded by separate DNA exons. Although the molecular structure and the action of elastin is well documented, the exact mechanism by which its elastic properties are conferred is still debated. Theoretically elastin molecules form a 'random coil' when relaxed. When stretched, fibres extend until straightened while adjacent cross-links hold the fibre intact, until the strain is released and the fibre can recoil, much like a rubber band (Alberts et al., 1994).

## PROTEOGLYCANS

The basic structure of proteoglycans (PG) consists of a protein core to which one or more carbohydrate components, glycosaminoglycan side chains (GAGs) are covalently bound via a serine residue. Potentially 18 genetically different core proteins have been elucidated, which have 1 or more domains that can interact with other ECM components

and cell surface proteoglycans. Proteoglycan gene families associated with cells and the ECM are shown in Table 1.02. An important member of the orphans, is perlecan, located in basement membranes and associated with cell attachment (Haralson and Hassell, 1995). The basic structural feature of GAG chains is the alteration of two monosaccharide units. GAGs can be subdivided into three major groups: chondroitin/dermatan sulphate, heparin and heparan sulphate and keratan sulphate (Haralson and Hassell, 1995). The biological properties and functions of proteoglycans are diverse. These functions range from stabilising the ECM mechanically to effects on cell adhesion and migration to influences on cell differentiation and morphogenesis. The functionality of PG is not limited to the core protein but its activity is often related to the GAG side chain component or the two components working in concert.

**Table 1.02:** Selected proteoglycan families, modified from (Haralson and Hassell, 1995)

Family	Source	Examples	Proposed Function (examples)
Syndecan	Cell surface	Syndecan I-IV	Binds matrix constituents and growth factors via GAG side chains
Orphans (a)	Cell surface	CD44	Binds collagen IV
Leucine-rich	ECM	Fibromodulin	Associates with fibrillar collagens
Hyaluronate binding	ECM	Aggrecan	Cartilage, resists compression
Collagenous	ECM	Collagens IX and XII	Cartilage, resists compression
Orphans (b)	ECM	Perlecan	Basement membrane, filtration and cell attachment

## STRUCTURAL GLYCOPROTEINS

Structural glycoproteins of the ECM exhibit several common features in that their primary structure is both structural and functional, have independent binding sites for matrix and cell ligands and commonly have multiple protein subunits. Examples of these ECM components in terms of location and function are outlined in Table 1.03.

**Table 1.03:** Selected structural glycoproteins of the ECM, modified from (Haralson and Hassell, 1995).

Glycoprotein	Location (examples)	Function (examples)
Fibronectin	Cellular fibronectin (produced by fibroblasts, epithelial, EC and chondrocytes)	Cell adhesion; Thrombosis and wound repair Binds heparin collagens I and III, and fibrin
Laminin	Basement membranes	Interaction with collagen IV, entactin and heparin sulphate; cell binding to ECM; cell differentiation; wound healing and angiogenises
Entactin	Basement membranes	Binds laminin, type IV collagen and fibronectin; RGD sequence and EGF-like domains
Thrombospondin	Produced by EC SMC bone cells and fibroblasts	Cell attachment; platelet adhesion, proliferation and migration of SMC; binding sites for fibrinogen, fibronectin, laminin and plasminogen
SPARC/ Osteonectin	Basement membranes; tissue undergoing remodelling	Binds collagen I, II and IV, calcium and cells; influences cell migration
Vitronectin	Liver, platelets, plasma and macrophages	RGD mediated attachment of fibroblasts and EC; associated with elastin; binds heparin
Fibrillin	Aorta, skin, lung, muscle	Constituent of elastic fibres

## 1.4 DEVELOPMENT OF SMALL DIAMETER VASCULAR GRAFTS

Techniques to create/generate small diameter replacement vessels with acceptable patency rates vary greatly. Generally these methodologies can be grouped into three distinct strategies which have been previously reviewed (Bos et al., 1998). The differences within each strategy group represent the choice of matrix or support structure used to support cell growth; these generally fall into three categories: synthetic (e.g. ePTFE), biologically derived (e.g. collagen), or a combination of both (see Table 1.04).

**Table 1.04:** Alternative strategies to develop vascular prostheses, (Bos et al., 1998) including additions and omissions.

Strategies for small diameter vascular graft development	
1	Development of biocompatible synthetic materials <ul style="list-style-type: none"> <li>1a. Modification to the materials gross physical structure</li> <li>1b. Introduction of functional groups</li> <li>1c. Incorporation of biologically active substances</li> </ul>
2	Development of biopolymer biomaterials
3	Tissue engineering: 'living grafts' <ul style="list-style-type: none"> <li>3a. Endothelial cell seeding onto vascular prostheses</li> <li>3b. Biopolymer-based materials</li> <li>3c. Self-assembly model</li> <li>3d. Polymer-based synthetic materials</li> <li>3e. Decellularised tissues</li> </ul>

The first strategy is often the reapplication of an existing material from either non-medical applications or a material that has proven biocompatibility characteristics and modified to suit a specific need. Advantages of the reapplication of a material previously accepted for human implantation is that most of the regulatory steps have already been approved, and materials with previous surgical success are more likely to be accepted by the procuring surgeon.

#### **1.4.1 STRATEGY 1: DEVELOPMENT OF BIOCOMPATIBLE SYNTHETIC MATERIALS**

Gore-Tex (PTFE), like other synthetic materials has been modified to offer a variety of characteristics such as internal diameter variation, wall thickness variation, ringed, ringed thin walled, tapered, bifurcated and patches. Thus, Gore-Tex is not one product that fits all, but one that has been modified over time to improve characteristics and offer a larger, more diverse product range. Table 1.05 illustrates some of the many methodologies that have been used to alter the physical or chemical structure of existing synthetics.

**Table 1.05:** Techniques used to modify the gross physical structure and surface morphology of existing synthetic vascular grafts, (Bos et al., 1998) including additions and omissions.

Strategy 1a. Modification to the materials gross physical structure			
Modification	Method	Effect	Reference/s
Gross structure	Alternative knitting procedures e.g. woven	Increases in structural stability	(Mary et al., 1997)
Denucleation	Removal of gas nuclei	Decreases thrombogenic effects	(Vann et al., 1993)]
Surface chemical groups	Mild hydrolisation	Allows attachment of biomolecules	(Phaneuf et al., 1995)
	Gamma-radiation	Improved cell growth on modified matrix	(Kirkpatrick et al., 1991)
	Radio frequency glow discharge e.g. conversion of PET to PTFE	Resistance to thrombosis and embolism deposition	(Kiaei et al., 1992)

Polyurethane (PU), was initially used in the form of intravenous catheters where it displayed excellent blood compatibility and cellular adhesion properties. In the mid-eighties PU became a popular ‘potential’ material for vascular conduits due to its durability, elasticity and compliance. However, some of the past successes have not been reproducible, with continued structural failures (Jeschke et al., 1999), thrombosis and embolism (Bos et al., 1998a) resulting in PU being perceived as a less promising option. PU has recently seen a revival of interest. As with other synthetic materials, modification of either the chemical structure, addition of other polymers, or variations in manufacturing processes aim to enhance the material characteristics. Recently a modified PU has been produced with ‘improved’ hydrolytic and oxidative stability. Assessment of the material in terms of biocompatibility compared to ePTFE was carried out in a small animal study (Jeschke et al., 1999). Of the parameters studied, PU displayed faster luminal endothelialisation, less chronic neointimal proliferation and a thinner neointima compared to ePTFE grafts. These advantages in biocompatibility were not realised in terms of patency rates, as no significant differences between PU (82% at 6-months) and ePTFE (81% at 6-months) were observed. Like previous work comparing patency rates between ePTFE and autologous vein, initial patency of ePTFE grafts is comparable, though lower, to autologous vein patency, where as long-term implantation (2-years and over) saphenous vein patency is considerably better (Charlesworth et al., 1985; Jeschke et al., 1999). The authors also acknowledged

limitations of the study in that although the study is comparative between ePTFE and PU in a rat model, no conclusions can be drawn relating to the effectiveness of PU as a prosthetic graft in humans. Both of these factors are important to the long-term patency of any prosthetic vascular material. They conclude with a positive outlook on PU as a grafting material due to increased biocompatibility compared with ePTFE. Importantly, the choice of animal model and the site of graft implantation are critical in determining graft outcome. For example, grafts placed in the rat abdominal aorta, a small diameter vessel with *high blood flow* and *low resistance*, are quite unlike diseased tissues of the peripheral human vasculature which show *low blood flow* and *high resistance* may lead to false positives. In many animal models spontaneous endothelialisation occurs, whereas in humans only small regions of the prosthetic graft may gain endothelial cell coverage immediately adjacent to the anastomosis, termed transanastomotic endothelialisation (Davids et al., 1999).

The development of synthetic materials is an important area of research for vascular replacement technology. Particularly when a surgical procedure is urgent, the material maybe taken directly from bulk storage, without requiring cell culture such as tissue engineering methodologies. In addition synthetic materials have a significant advantage over competing technologies in that they are likely to be less expensive, considerably less complicated and less problematic than methodologies requiring a cell culture phase prior to implantation. For these reasons a synthetic material displaying extended patency may ultimately be the prosthetic of choice; this is however not in the foreseeable future.

Reapplication of an existing material facilitates the process of regulatory acceptance, while the use of a previously accepted graft further simplifies this process. Within this overall strategy, a huge variety of research has been conducted that encompasses direct surface modification of the graft material, application of biologically inert and biologically active substances. Each of these ‘general’ methodologies is to a large extent interrelated and boundaries between groups are often not clear. Strategies are discussed in the three groups mentioned above. Table 1.06 summarises the methods that introduce functional groups to enhance performance of vascular grafts *in vivo*. Based on Bos et al (1998a), with omissions and additions (Bos et al., 1998)

**Table 1.06:** Introduction of functional groups and/or the incorporation of biologically active substances to existing synthetic vascular grafts (Bos et al., 1998) including additions and omissions.

Strategy 1b. Introduction of functional groups			
Modification	Method	Effect	Reference/s
Chemical treatment	Treatment with ammonia or alkylamine plasma to covalently biomolecules	Improved cell adhesion to matrix	(Sipehia et al., 1993) (Tran and Walt, 1989)
Binding specific biomolecules	Chemical modification and addition of e.g. collagen, gelatin	Seals graft pores negating the requirement for pre-clotting	(Guidoin et al., 1989) (Guidoin et al., 1987) (Weadock and Goggins, 1993) (Marois et al., 1995)
	e.g. albumin	Biocompatibility Healing	(Kottke-Marchant et al., 1989) (Marois et al., 1996)
Cross-linking	Glutaraldehyde etc to bind biomolecules	Reduces risk of, Aneurysm Thrombosis Hyperplasia	(Schmidt et al., 1998) (Werkmeister et al., 1995)
Variation of cross-linking agents	glutaraldehyde vs. carbodiimide	Differential effects on cell cytotoxicity Calcification of matrix	(Slimane et al., 1988)

The aim of modifying existing vascular prostheses is to enhance *in vivo* characteristics whereby cell adhesion, reduced thrombogenicity and post-implantation healing processes maybe optimised. Surface or structural modifications vary from relatively simple changes in the method of production, where fibres of the material maybe woven, knitted, of variable thickness, tapered etc. to chemical modification. A further study has reported on four different types of tubing used in bypass surgery and evaluated under static *in vitro* conditions. Silicon elastomer tube with a platinum cured catalyst, silicon elastomer tube cured with a peroxide initiator, Polyvinylchloride (PVC) and PVC coated with heparin using ionic bonding. Each of the four materials where monitored for biomarkers of the complement system, coagulation, and fibrinolytic cascades using both direct contact (cells seeded directly on the material) and extracts of the materials (conditioned media) to Balb/3T3/A31 cells. Variations in pH of liquid extracts of each material range from 7.82 to 8.50, extracts of liquid heparin-coated-PVC resulted in a decrease in cell densities of 24% ( $P < 0.01$ ), whereas other materials showed no statistical difference in cell densities. Both PVCs displayed no significant cytotoxic effects when in direct cell contact, whereas the heparin-bonded material displayed a

38% reduction in cell density (Harmand and Briquet, 1999). The authors suggest that this is likely to be due a component of the heparin binding process as heparin itself is well characterised and considered to have no cytotoxic potential. None of the materials exhibited any significant haemolytic effects or platelet activation. Where the heparin-bonded material displayed negative results in some of the cytotoxic evaluations, it contrasted the other materials with a lower thrombogenicity. Although this paper has only characterised a few of the important cell/material interactions, it highlights the subtleties of graft/cell behaviour. Table 1.07 summarises the methods that modify or add compounds/molecules to enhance performance of vascular grafts *in vivo*. Based on (Bos et al., 1998), with omissions and additions.

**Table 1.07:** The incorporation of biologically active substances to existing synthetic vascular grafts, (Bos et al., 1998) including additions and omissions.

Strategy 1c. Incorporation of biologically active substances			
Modification	Method	Effect	Reference/s
Anticoagulants	Immobilising heparin, to collagen-coated and gelatine-coated grafts	Anticoagulation Influence cell function	(Gemmell et al., 1998) (Kodama, 1990) (Laemmel et al., 1998) (Wilson et al., 1993)
	Immobilising hirudin to collagen-coated and gelatine-coated grafts	Inhibits thrombin Minimise platelet formation (or not)	(Ito and Lo Gerfo, 1990) (Phaneuf et al., 1997)
	Immobilising, benzamine, pentamine, pyridoxal-5-phosphate, cysteine, N-acetyl-aspartyl glutamic acid	Prevention of platelet adhesion by inhibition of complement cascade	(Gemmell et al., 1998)
Growth factors	aFGF/bFGF	Promote cell growth proliferation Differentiation of specific cells (EC)	(DeBlois et al., 1994) (Gray et al., 1994) (Doi and Matsuda, 1997)
Antibiotics	e.g. rifampin	Prevention of graft infection (Dacron, PU)	(Gahtan et al., 1995) (Galdbart et al., 1996)



### 1.4.2 STRATEGY 2: ACELLULAR BIOMATERIALS

Similar to the development of synthetic materials, acellular ‘biomaterials’ aim to develop a successful material that is immunologically inert and structurally sound that can be supplied immediately to patients in critical care in sufficient quantities, and implanted into the patient without the requirement of a pre-implantation culture phase. The development of acellular biological prosthetic substitutes stemmed from the positive aspects of synthetic grafts when biological molecules were bonded or cross-linked to the synthetic matrix. Table 1.08 displays a selection of biologically derived matrix materials used as acellular implants. Similar to many synthetic grafts, these materials are designed to be implanted directly into the patient.

**Table 1.08:** Selected biological materials used as direct implants.

Strategy 2. Acellular biomaterials			
Matrix Type	Research	Cells seeded	Reference/s
Small Intestine Submucosa	Matrix characterisation	3T3, 3T3/J2 fibroblasts human fibroblasts, keratinocytes and microvascular EC	(Badylak et al., 1998)
	Mechanical properties	-	(Hiles et al., 1995)
	SIS <i>in situ</i> development	-	(Robotin-Johnson et al., 1998)
Umbilical vein	Vessel replacement	-	(Dardik et al., 1988)
Bovine carotid artery	Vessel replacement	-	(Rosenburg et al., 1976)
Porcine carotid artery	Vessel replacement	-	(Tamura et al., 1999)

A biological material receiving considerable attention in recent years is the porcine derived small-intestine submucosa (SIS). The initial material is harvested by removing the superficial layers of the mucosa and the external muscle layers from the porcine small intestine. The 80 µm thick sheet is then disinfected, sterilised and all cellular components removed with the final structure retaining its native 3-D structure and composition (Badylak et al., 1998). Hiles et al (1995), have shown after 1 month of implantation that the SIS (when used as an arterial graft) induces a post implantation healing response, whereby the graft is remodelled to form an artery-like vessel that is both structurally and functionally similar to natural vessels (Hiles et al., 1995). Further

studies were carried out by Robotin-Johnson et al (1998), where autologous SIS was implanted into 11 piglets (superior vena cava) and assessed by the grafts ability to develop or remodel as the piglets matured. Of the nine surviving piglets (2 died of non-related causes) the mean weight gain from  $10.3 \pm 2.0$  kg before the operation to  $59.2 \pm 16.7$  kg, compared favourably with controls at  $58.5 \pm 6.6$  kg (Robotin-Johnson et al., 1998). This study illustrates the potential of SIS as a grafting material; nevertheless long-term implantation studies must be carried out to determine ultimate patency rates. An issue with all biological material used with the intention of applying for certification for human implantation is that of consistency or uniformity of the final product. Our own experience has shown the extensive variation in porcine carotid arteries, within animals of the same breed, age and sex. It is this variation that may undermine the feasibility of scaling-up these processes.

#### **1.4.3 STRATEGY 3: TISSUE ENGINEERING 'LIVING GRAFTS'**

As the search for replacement blood vessels with prolonged patency rates continues, a new strategy 'Tissue Engineering', has become an important player in the field of vascular research. Tissue engineering aims to circumvent the dire shortage of donor organs by 'growing' *de novo* replacement organs, neo-organs. From skin to livers, tissue engineers aim to replicate the body's natural processes of development to create "off-the-shelf" whole organs thereby alleviating this shortage. Although the creation of a complete biological neo-liver is unlikely to occur in the near future, due to the organ's sheer complexity, major inroads to neo-liver (as well as other organs) development are underway. Notably, the first tissue engineered product to achieve American FDA approval was "Transcyte", produced by Advanced Tissue Sciences in 1997, as a non-living wound covering. This construct was developed by culturing human foreskin fibroblasts on a synthetic polymer, which could then be frozen for later use (Naughton, 1999). Since then, other living tissues have been developed for skin replacements and being marketed internationally. Complex organs such as blood vessels (L'Heureux et al., 1998; Weinberg and Bell, 1986); (Niklason et al., 1999) and heart valves (Shinoka et al., 1997) are being intensively studied with the same eventual aim of developing efficient grafts.

The question, “what does tissue engineering offer, or potentially offer, that traditional synthetic substitutes do not”, is important as it lays down the foundation for this research. The fundamental difference between a discrete synthetic substitute and a tissue engineered vessel is that the tissue engineered replacement tissue is 'grown' using either the patients own cells or another cell source that maybe recognised as 'self', in the laboratory or a clinical environment prior to surgical implantation. Once implanted the organ remains a fully functional and an interactive 'device' (Bos et al., 1998). In addition the graft maybe exposed to mechanical forces that mimic the *in vivo* environment, providing the necessary cues for correct development. All cells within any individual, with the exception of *n* germ cells and non-specific mutations, have exactly the same genetic content or genotype. In order for a cell to perform a specific function it must first differentiate e.g. a neurone, osteoblast or muscle cell. *In vivo* cells are maintained within a dynamic perfusion system, where cells interact with chemical signals, such as growth factors, signals associated with the ECM, such as adhesion molecules and mechanical stimuli, e.g. shear stress and cyclic strain. It is this dynamic physical environment that allows cells to firstly differentiate and secondly maintain their specific function or phenotype. Without external queues a cell is likely to dedifferentiate back to a non-specialised state, for example vascular smooth muscles cells revert to a non-specialised fibroblast state, with resulting loss of function. Mechanical influences on cellular growth, proliferation and differentiation have become an increasingly important factor in the biocompatibility and healing processes involved in graft acceptance. The incorporation of fundamental engineering principles into experimental design has become a major factor in mimicking the *in vivo* environment within an *in vitro* experimental setting of tissue engineering applications. Effects on cell phenotype resulting from the application of mechanical forces is further discussed in Chapters 6 and 7, where the development of a perfusion bioreactor has enabled the application of mechanical forces on the construct developed in this thesis.

Current research relating to tissue engineering vascular grafts can be broadly categorised into five generic approaches utilising different matrix types or methodologies: 1. EC seeded synthetic graphs, 2. reconstituted biological macromolecules e.g. reconstituted collagens, 3. self-assembled vessels 4. polymer based synthetics e.g. ePTFE, and 5. decellularised tissue, see Table 1.04. The primary constituents of a tissue engineered vascular graft are vascular cells, which may include:

EC, SMC and fibroblasts in concert with an extracellular matrix (ECM) to provide the framework by which the development of the 3D organ is guided. The following section highlights the critical observations reported previously and the current knowledge that relates to this project. To introduce the reader to the developmental process preceding this project, selected articles have been reviewed that represent landmarks or critical observations that have been made in tissue engineering of small diameter vascular grafts.

### STRATEGY 3A. ENDOTHELIAL CELL SEEDING OF VASCULAR PROSTHESES

A replacement prosthesis that could be removed from sterile packaging in the operating theatre ready for immediate use, with high patency rates would be the simplest and most cost effective option for reconstructive surgery. While manufactures of synthetic replacements work towards this goal, methodologies to enhance both existing and prototype graft patencies are actively researched. The first application of surgically implanting 'living-grafts' was the concept of seeding endothelial cell lined synthetic matrices (Schmidt and Bowlin, 1999). This process aims to enhance graft patency by providing optimal biocompatibility at the blood/matrix interface. Unlike the first two strategies (1 and 2), endothelial cell seeding adds a new level of complexity and cost to production. Firstly, cells must be isolated from patient tissue (until immunologically inert cells such as stem cells or genetically modified cells are available for use, (Nerem and Seliktar, 2001) and seeded onto the graft material prior to graft implantation.

Much of the current tissue engineering research utilised either HUVEC or other animal EC, which are relatively simple to isolate, however the relevance of these investigations has been questioned because of the origin and nature of these terminally differentiated cells. Isolation of autologous vascular EC in adequate quantities is a more difficult and expensive task. Not only is the isolation method more technically challenging but also cells isolated from adult tissue behave very differently from HUVEC used for preliminary research. Zilla et al (1994) and others have shown the human EC isolated from the jugular vein were unlikely to proliferate if autologous serum with elevated levels of lipoprotein A was used in cultures (Zilla et al., 1994). An important issue with the use of 'living' grafts is the increased costs associated with graft production and maintenance prior to clinical use. A promising method to obtain vascular endothelial

cells is to isolate them from adipose tissue associated with the omentum, containing adipocytes and microvascular EC (Williams et al., 1989). Williams et al (1994) confirmed that EC derived from adipose tissue are indeed EC and not mesothelial in origin (Williams et al., 1994). Purification of EC from contaminating fibroblasts (and others) had been a problem associated with this procedure, however by repetitive positive selection with *Ulex Europaeus Agglutinin I*-coated paramagnetic beads to EC, contaminating cells maybe removed from culture (Jackson et al., 1990).

Early studies concluded no significant advantage in graft patency with the use of EC seeded grafts (Fasol et al., 1987; Herring et al., 1987; Walker et al., 1987), and also reported an increase in platelet activation, of both seeded and unseeded grafts compared to saphenous vein grafts (Fasol et al., 1989). Variation in clinical procedure including, graft placement, diameter, material, EC type, cell seeding method and use of anticoagulants, has made interpretation of results difficult (Bos et al., 1998). The adhesion of endothelial cells is an important issue in tissue engineering blood vessels. To reduce the thrombogenicity of the graft surface, the stage or state of endothelisation prior to the grafts clinical use is critical to the success of the graft. Meinhart et al (1997) reported low patency rates when the growth and proliferation of EC had not reached confluence prior to implantation. Allowing the EC layer to reach confluence and mature for a period ( $12 \pm 3$  days) of incubation prior to implantation, has proven a significant advantage in graft patency compared to unseeded grafts at three-years (Meinhart et al., 1997). Zilla et al (1994) with a patient group of 49 with a mean age of  $65.2 \pm 9.8$  years, reported on combined above and below knee reconstructive surgery. Autologous EC were harvested from a section of the right external jugular vein, cultured to a final density of  $16 \times 10^6$  cells and seeded onto 6 mm ePTFE grafts 'preclotted' with a fibrinolytically inhibited fibrin glue. Prior to implantation EC confluence was shown to be 88.9%, with 77.8% grafts confluent and 14.8% grafts subconfluent. The clinical follow-up after 32 months implantation showed patency rates for controls at 55.4% and EC seeded grafts at 84.71% (Zilla et al., 1994). Although these studies have shown an improvement in graft patency, the added complication of a two stage process has proven a significant hurdle to the wide spread uptake of this technology.

Further techniques and studies in endothelial cell seeding and growth are tabulated below, Table 1.09. Methodologies to enhance cell seeding onto bioprotheses are

discussed in context with the cell seeding studies carried out in this thesis Chapter 7.4.

**Table 1.09:** Endothelial cell seeding of vascular grafts from (Bos et al., 1998) including additions and omissions.

Endothelial cell seeding	Study	Effect	Reference/s
	Preclinical studies	Increased biocompatibility reduction in platelet adhesion	(Herring et al., 1979) (Schmidt et al., 1991) (Belden et al., 1982) (Stanley et al., 1982)
	Models/problems	Spontaneous endothelialisation EC loss	(Szilagyi et al., 1991) (Graham et al., 1980) (Schmidt et al., 1991)
	Improvements	Culturing and seeding techniques	(Schmidt et al., 1991) (Watkins et al., 1984) (Meinhart et al (1997)
	EC seeding in humans	Isolation of human EC Adhesion studies, RGD, other binding sequences Graft porosity	(Jackson et al., 1990) (Hubble et al., 1991) (Hynes, 1992)
		Shear-stress preconditioning	(Boyd et al., 1988) (Bull et al., 1995)
		Genetically modified EC	(Ott and Ballermann, 1995) (Shayani et al., 1994)

### STRATEGY 3B. BIOPOLYMER-BASED BIOMATERIALS

The concept of allowing an entire graft to develop *in vitro* using tissue engineering principles was first conducted by Weinberg and Bell (1986), where an entirely biological, multi-layered structure with the gross physical appearance of an artery was developed. Earlier trials using this methodology failed under physiological pressures, later constructs supported by a Dacron mesh were able to withstand higher pressures. The development of the tissue engineered construct was modelled around a three-layered tissue using bovine derived EC, SMC and fibroblasts and animal collagen. The intima had an endothelial cell lining; the media had SMC and *de novo* matrix materials. The vascular media was made by casting a gel forming collagen with SMC within an annular mould and left to gel (37°C), for a period of several days to allow the gel to contracted to form a tubular lattice around a central mandrel. The Dacron mesh was then slipped over the lattice. The adventitial layer was constructed with fibroblasts and matrix materials that was supported by a Dacron mesh to provide structural integrity

and was cast around the first layer. When the outer layer (adventitia) was fully contracted the mandrel was removed and an EC suspension was seeded into the lumen. The matrix was rotated at 1 Hz for 1 week to allow cells to adhere evenly on the matrices luminal surface. Histological analysis showed SMC displayed bipolar differentiation with bundles of filaments, dense bodies and secreted collagen. EC formed a near complete monolayer (92.1%) with intercellular junctions acting as a permeability barrier to large molecules such as albumin. The EC also released prostacyclin, a potent inhibitor of platelet aggregation and produced von Willebrand factor an established marker for the EC phenotype. The authors attributed the vessel's structural integrity to: the Dacron mesh, collagen contraction, initial seeding density and time lapsed for casting. Unfortunately this model did not display the required mechanical strength, even when reinforced with Dacron. Burst pressures without Dacron mesh were < 10 mmHg, and with one mesh layer 40-70 mmHg and two mesh supports 120 –180 mmHg. Although 180 mmHg is at the top end of normal blood pressure, there is zero tolerance. Maximal burst strength was attained between 3-6 weeks post casting with the structural integrity declining after 6 weeks. This was attributed to collagenase activity. This model displays important features of a natural graft but was limited by reduced mechanical strength, lack of elastin, SMC orientation and the longitudinal alignment of collagen fibres unlike that *in vivo* with LH and RH alternating spirals. Finally SMC density was 1/8 to a 1/4 of *in vivo* densities (Weinberg and Bell, 1986). An important point with this earlier work was that once the graft had been developed it was not exposed, or cultivated under pulsed pressure conditions. Had it been so, the ability of the graft to withstand higher pressures may have improved significantly.

Further to this work L'Heureux et al (1993) using a similar methodology to Weinberg et al, (1986) and human vascular cells, developed a Tissue Engineered blood vessel. Again problems with low burst pressures have shown this technique in its current form to be limited (L'Heureux et al., 1993). Hirai and Matsuda (1996), again with a similar methodology using canine jugular cells, poured a cold mix of VSMC ( $5 \times 10^5$  cell/ml) and type I collagen (1.5 mg/ml) into a glass mould and incubated with the inner mandrel at 37°C for 10 d. The inner 8 mm mandrel was then removed and a smaller support consisting of 6 stainless steels wires was inserted, a 2 ml solution of EC ( $1 \times 10^6$  cell/ml) was then inoculated into the lumen. After incubation at 37°C for 20 minutes

the vessel was rotated 90° and a further 2 ml solution of EC ( $1 \times 10^6$  cell/ml) was inoculated to improved EC density. This process was repeated four times. The 3 cm long grafts were implanted into the posterior vena cava position of 14 dogs. All grafts utilised autologous canine tissue. A Dacron mesh was used to support the graft and the two anastomoses as cases of severe bleeding were noted due to the graft tearing. Importantly, neither anti-platelet nor anti-coagulant treatment was used throughout the implantation period (up to 24 weeks) other than intraoperative heparin. Results showed an overall patency of 64% (9 out of 14), with confluent EC (from 1 week), circumferential orientation of VSMC, fibroblast in growth, vessel wall contraction and the appearance of fibrous collagen, giving the appearance of near complete remodelling over the 24 week implantation period (Hirai and Matsuda, 1996). From the same group, Kobashi and Matsuda (1999) using a similar process have uniquely developed a branched prosthesis reinforced with a Dacron sleeve. In an attempt to improve the graft's structural integrity, twice the concentration of type I collagen (3mg/ml) and six fold increase in VSMC density (to  $3 \times 10^6$  cell/ml) was employed. After a total of three weeks in culture EC were seeded (several times) at  $3 \times 10^6$  cell/ml until confluence was reached. After EC seeding the graft was exposed to pulsatile pressure of 1 Hz, between 30 and 60 mmHg for 24 h. Without the Dacron mesh support the graft ruptured at 40 mmHg. With Dacron the graft remained viable at 250 mmHg (Kobashi and Matsuda, 1999). Advantages with this technique are clear, high densities of VSMC can be directly incorporated into the developing medial layer of the vessel, subsequent seeding of EC immediately positions cells in their native 'setting' within effective communication distances (Francis and Palsson, 1997). Although the orientation of the VSMC is not circumferential and EC do not align with the direction of flow, the applied haemodynamic stresses will encourage cell alignment, and subsequent improvements in phenotypic expression of cellular constituents over time. While the 24 h period in this article is likely to be too short for full development of cellular orientation and density, an extended culture period under progressive pulsed flow will improve strength through increased collagen deposition and VSMC density. Like all current methods using cells seeded within a collagen gel, the inherent floor is the weakness of the initial gel. The very fact that a permanent synthetic sleeve is used to reinforce the matrix limits the ultimate remodelling potential of the graft by preventing the potential vasotone, which may eventually result in intimal hyperplasia (Nerem and Seliktar, 2001).



### STRATEGY 3C. SELF-ASSEMBLY MODEL

Described as the self-assembly model this technique was pioneered by L'Heureux et al (1998) who created a tissue engineered blood vessel based exclusively on cultured human cells without exogenous biological materials. This is the first model to show sufficient structural integrity to withstand physiological conditions. Key to this result was culturing cell types in ascorbic acid to induce increased production of ECM, resulting in cohesive cellular sheets. Graft development was a four-step process: 1. Production of an acellular inner membrane (IM) using a dehydrated fibroblast sheet formed into a tube, 2. The IM is slipped around a tubular, perforated PTFE mandrel (OD 3.0 mm) and a sheet of SMC is rolled around the IM, creating the vascular media. This was placed in a bioreactor, providing luminal flow and support for one week, 3. A sheet of fibroblasts was rolled around the smooth muscle cell layer, creating the adventitial layer; this was incubated in a bioreactor for a further 8 weeks when the PTFE mandrel was removed. Finally, step 4, the inner PTFE mandrel was removed and either used for EC seeding or mechanical testing (L'Heureux et al., 1998). The total culture time necessary for the graft developed by L'Heureux et al (1998) was 12 weeks, excluding cell expansion and IM production. The final structure was 'artery-like' in appearance; displayed differentiated tissues, intima, media and adventitia; SMC did not penetrate the inner membrane (8 weeks) and the EC layer reached 99.2% confluence. SMC density was lower than *in vivo* tissue, but was considered high by the authors for an *in vitro* model. Collagens type I, III and IV were present, and burst pressures up to 2594 mmHg were achieved at 8 weeks. Animal studies carried out in a canine model implanted with the graft, less the human endothelial cell lining to prevent chronic rejection, results show the graft to be thrombogenic. The authors suggest this is due to the lack of an EC cell layer. They conclude that the graft is "clearly" more compliant than ePTFE grafts, but less than human saphenous vein (HSV) grafts. Any foreign material implanted into either an animal model or human is subjected to the host immune system, clearly some materials are potentially more thrombogenic or immune-reactive than others. With the exception of grafts grown within the recipients own body (Campbell et al., 1999) all other tissue engineering applications employ a foreign matrix and are thus subjected to the host immune system. Therein lies the major advantage with this particular method, minimal, if any immune response. Although the results presented by the authors show a poor performance of the graft, the use of autologous

cells (both EC and VSMC) would without a doubt show a vast improvement (L'Heureux et al., 1998). Present applications for this type of graft are limited by the time scales required to generate the complete graft. This obstacle may become less of an issue as improved methods are explored to speed up initial cell densities, such as application of growth factors, larger biopsy material or the use of stem cells.

### STRATEGY 3D. POLYMER-BASED SYNTHETIC MATERIALS

Early designers of synthetic grafts concentrated on developing immunologically inert materials. In recent years there has been a drive to develop materials that interact with the biological environment in which they are implanted. Examples of the introduction of functional groups and/or incorporation of biologically active substances to synthetic materials are shown in Table 1.07. Variation of cellular response to different synthetic materials is not only dependent on the material but also the manner in which it is presented, for example the weave pattern and porosity of the same synthetic material (Greisler et al., 1996).

Shinoka et al (1998), used a synthetic biodegradable matrix (polyglactin woven mesh, sealed with a polyglycolic acid nonwoven mesh) 20 mm x 15 mm (L x W), designed to degrade over a 6-8 week time course. Mixed autologous ovine vascular cell populations (2-3% EC, with the remaining being VSMC and Fb) were seeded at  $1 \times 10^7$  cells onto the matrix and cultured for 6-9 weeks prior to surgical implantation of a 2 cm section into the pulmonary artery (PA). The aim of this work was to develop a living graft that would 'grow' with the animal, as a preliminary study for pediatric vascular reconstruction. Results showed all grafts remained patent after 12 weeks (n=7) with no evidence of thrombus formation or calcium deposition. By two weeks the graft material had almost entirely disappeared, with a reduction in wall thickness compared to native PA. Immunohistochemical staining showed EC presence on the graft lumen, with the hydroxyproline analysis of the graft material displaying about 70% natural collagen (Shinoka et al., 1998). This model has shown it has potential to remodel and grow over the 12-week implantation period, with the graft remaining viable after the degradation of the synthetic matrix.

The use of a complete or near complete matrix prior to cell seeding is a method to reduce development times. To achieve this Niklason et al (1999) have used a synthetic polymer, a non-cross-linked PGA scaffold sewn into a tubular form. Bovine aortic SMC were seeded onto the PGA vessel and cultured for 8 weeks under pulsatile conditions using a bioreactor in a parallel flow system. A compliance chamber was used to reduce high frequency vibrations (300ml) and the pulsatile radial stress set at 165 beats/min (Niklason et al., 1999). SMC migrated into matrix creating a smooth luminal surface onto which the EC were seeded followed by 3 days of continuous perfusion culture. The resulting vessel displayed burst pressures well in excess of physiological conditions (8 weeks  $2150 \pm 709$  mm Hg), compared to native saphenous vein  $1680 \pm 307$  mm Hg. Advantages with the use of pulsatile pressure were an increase in collagen deposition, though SMC density was unaffected by pulsatile pressure conditions. SMC densities were higher than systems using collagen gels. The authors speculated that this is due to space being occupied by matrix (15% of total after 5 weeks). Vessel contraction in response to various hormones was considered to be evidence of retained phenotype; often lost in standard culture. The EC lining the luminal surface inhibited SMC proliferation. Implantation studies conducted with 6-month old pigs, grafts were implanted into the right saphenous artery and monitored up to 4 weeks before explantation. Results from these studies are promising with all grafts remaining patent for 2 weeks postoperatively. The pulsed (prior to implantation) xenograft remained patent for 24 days with no evidence of stenosis or dilation. The pulsed autologous vessel was patent at 4 weeks with a reduced flow rate, non-pulsed autologous vessel occluded at 3 weeks. Histological analysis of the explanted vessels displayed a highly organised structure with minimal inflammation. Importantly the effects of pulsatile culturing conditions have produced positive effects on the viability of engineered vessels. Long-term implantation studies are required to fully test the effectiveness of this methodology. Again, the choice of model is critical. Kim et al (1999) have shown the addition of 10% serum increases VSMC proliferation of rat aortic cells grown on both PGA and collagen type I scaffolds. The application of pulsatile pressure on seeded grafts prior to implantation and the resulting benefits seen through the maintenance of cell phenotype and the up regulation of both elastin and collagen genes has lead to a significant increase in tensile strength of the engineered tissues (Kim and Mooney, 1998). These distinct effects will bring the graft closer to its *in vivo* phenotype and potentially improve graft success through the first three critical

months after vascular reconstruction.

In a more recent publication Niklason et al (2001), have expanded on their earlier studies, where neovessels are created *in vitro* (Niklason et al., 2001). Again using bovine cells seeded onto a biodegradable PGA scaffold, the group has focused on a variety of culture parameters to understand the mechanisms affecting graft development. The effects of the degradation or presence of PGA scaffold residues on SMC phenotype has been previously noted (Greisler et al., 1993), where SMC dedifferentiated to a fibroblast-like state resulting in a hyperplastic response. In this model, cultures at 5-8 weeks showed similar histology and burst strength, however the lack of elastin expression prevented native mechanical behaviour and the contractility of the graft was a fraction of native vessels. The group is currently exploring ways to induce elastin expression in order to extend mechanical compatibility (Niklason et al., 2001). Interestingly the model Kim et al (1999) used, confirmed elastin expression with murine cells. This effect can be attributed either to the increased mechanical stresses used or different cells types and their differential reactions to the *in vitro* environment. Both groups used PGA scaffolds, which weakens the argument that PGA residues dedifferentiate SMC under these conditions. These positive results will need to be introduced into a more stringent model where graft diameters are reduced, implanted in lower flow rate systems and adult primary human cells used to determine the effectiveness of this method. As discussed in Chapter 4, a fine balance must be acquired with the use of biodegradable matrices, reduced growth rates and culture times associated with primary humans.

### STRATEGY 3E. DECELLULARISED BIOLOGICAL TISSUES

To reiterate several of the prescription details for a matrix for use in vascular tissue engineering it is clear that the matrix must have sufficient porosity to allow rapid cell invasion to populate all aspects of the graft, maintain haemostasis, be immunologically inert to reduce thrombotic effects at the blood interface and tolerance at the abluminal surface, non-cytotoxic, must degrade progressively to allow complete remodelling, have matched compliance to the replaced vessel, mechanical strength to cope with haemodynamic stresses and have adequate handling characteristics for surgical implantation. As described in Table 1.01 graft designers have taken several

approaches to encompass as many of the listed items as possible, including full synthetic matrices, biological polymers and combinations of each. Most of these materials do not provide biomechanical properties that mimic the natural artery, such that the compliance mismatch between grafted matrix and patient artery is excessive, which may lead to early graft failure by intimal hyperplasia (Schmidt and Baier, 2000; Seifalian et al., 1999). No other replacement material has the same biomechanical properties as the body's own arteries due to the complex relationship between collagen, elastin and associated ECM molecules. A method employed to provide improved mechanical properties and cell adhesion properties more akin to a natural artery is the use of decellularised xeno or allograft tissue. Much of the earlier work has focused on bioprosthetic devices such as heart valves that have preferential properties, e.g. reduced noise, improved haemodynamics and immunological tolerance by the patient immune system over mechanical valves. Unfortunately biologically derived valves tend to have a shorter lifespan (7-10 years) compared to mechanical man-made valves (>25 years) in which the patient is required to maintain lifelong immune suppression. In order to minimise host immune response and prevent rapid degradation once implanted, biomaterials are cross-linked to stabilise the material ensuring the maintenance of structural integrity. The failure of biological materials, in particular glutaraldehyde fixed prostheses has been associated with cytotoxicity, mechanical failure and calcification (Schmidt and Baier, 2000). Alternatives to glutaraldehyde have been pursued that minimise these negative responses and are further discussed in Chapters 3 and 4.

The extraction of cellular components aims primarily to reduce the immunological response to the implanted tissue and thus improve graft patency by removing as many of the foreign epitopes from the tissue as possible. Chapter 4 reviews the main methodologies used and their effects on the tissue. Most tissue decellularised for arterial replacement has been used as a direct grafting material, (Badyalak et al., 1998; Dardik et al., 1988; Rosenberg et al., 1976; Tamura et al., 1999). Karim et al (1999) used enzyme treatments to extract porcine cells from aortic specimens. The treatment was shown to remove cytoskeleton components, integrins, collagen IV and fibronectin leaving fibrillar collagen and elastin of the aortic wall. After seeding and culture with human myofibroblasts production of ECM components such as human pro-collagen I, fibronectin and laminin was shown as an evidence of matrix remodelling *in vitro* (Karim et al., 1999). Teebken et al (2000) applied a decellularisation process on

thoracic aortas of adult large German pigs using enzymatic extraction of protein, DNA and RNA, no cross-linking step was reported as described in Section 4.1.2. After the extraction process, human saphenous vein myofibroblasts and EC were seeded onto the luminal surface of the matrix and assessed under both static and pulsed conditions. After 4 days in perfusion culture, (flow rates 120-190 ml/min. pressure 70-140 mmHg) EC density increased from initial numbers to produce a near confluent endothelial cell layer. Myofibroblasts generally formed monolayers on the grafts luminal surface, though one sample displayed cells in multiple layers (Teebken et al., 2000). Like synthetic polymers used in tissue engineering, biological matrices are designed to either remain intact, i.e. be stable against host degradation, or to remodel over time. Teebken et al (2000) have chosen not to cross-link the prepared matrix. Advantages of this method are seen as enhanced tissue remodelling processes by seeded cells, which would otherwise be prevented by cross-linking. Cross-linking procedures certainly reduce, the ability of seeded cells to remodel the tissue by proteolytic means such as MMP. Further, by not introducing toxic chemicals and the negative effects cross-linking often has on the mechanical properties of biological tissues (Schoen and Levy, 1999), seeded cells are likely to have improved performance over treated tissues in the remodelling process. Importantly with this method, like bioresorbable synthetics is the relationship between host remodelling and graft structural integrity. Excessive host degradation of the matrix prior to autologous cells laying down newly synthesised structural proteins may result in graft dilatation and failure.

Another approach has seen the use of only the elastin component of the arterial wall as a matrix for tissue engineering purposes. Gregory et al., (2000) have prepared an elastin matrix from processed porcine carotid arteries and have seeded porcine aortic endothelial cells. Using a bioreactor (not described) endothelial cells (EC) were exposed to a progressive flow regime up to 90 ml/min. SEM and histological analysis have shown EC to form a confluent endothelium serving as a barrier between the internal elastic membrane and the lumen of the vessel. Similarly Berglund et al., (2002), have produced an elastin matrix by exposing porcine carotid arteries to treatments to remove all other extracellular matrix (ECM) components to leave only the elastin component of the artery. Cells (either human dermal fibroblasts or rat aortic SMC) were seeded to the abluminal surface suspended within a collagen gel. After 8 and 23 days of culture, construct had shown improved mechanical properties over the

initial elastin matrix which approach those of native arteries. It is important to note that in both these cases the cell types used limit the applicability to aged patients where autologous cells must be used.

The use of natural ECM components in the native structure is seen as positive step forward in attaining mechanical properties similar to native arteries, critical to the success of a small diameter vascular graft. An issue surrounding the use of grafts without polymeric reinforcement, may face problems with regulatory acceptance and the surgeons approval, which may delay the wide spread use of this type of replacement vessel (Bos et al., 1998).

Sceptics of the tissue engineering approach have foreseen cell availability, graft length, development time and difficulties transferring laboratory base technology into a clinical situation as areas that will prevent this technology being successful in the clinical arena. A clinical application of tissue engineering principles has recently been described by Shin'oka et al., (2002), where a 4 year old girl with a total occlusion of the right intermediate pulmonary artery was treated by inserting a tissue engineered 'living' graft. Using a copolymer of PCL-PLA (50:50) reinforced with PGA (10 mm diameter, 20 mm long by 1 mm thick) designed to degrade by 8 weeks, autologous venous cells were taken by biopsy and bulked up to approximately  $1.2 \times 10^7$  cells at 8 weeks. These cells were seeded onto the matrix, which was cultured for 10 days before surgical implantation. At 7 months post implantation the graft remains patent with no signs of occlusion or aneurysm. Although this graft is not placed in a more stringent 'model', such as an aged person in an area of restricted blood flow an of a smaller diameter, it give a glimpse of the potential this field has to offer. New developments discussed above using the methodology of tissue engineering will ensure a promising outlook for improved grafts with extended patency rates.

## CONCLUSIONS

The problems that require solving in order to provide for the continued health and longevity of persons with progressive vascular disease are numerous. In short the current technology provides a poor substitute for the bodies natural vasculature. The first choice the vascular surgeon has, given the current technology, is to excise and relocate arteries or veins to repair diseased sections of the vasculature. As these vessels may be diseased or previously used, options are limited to synthetic replacement vessels. Current prosthetic grafts are manufactured from synthetic polymers, which are maintained as permanent structures within the body. By their very nature they lack the ability to remodel, preventing integration into the patient as 'self tissue' and as such elicit varying degrees of immune rejection. Critical to graft success is the initial period of implantation where graft thrombosis or neointimal hyperplasia restricts and eventually blocks blood flow in a majority of synthetic grafts. Table 1.10 summarises various important aspects of different approaches to small diameter graft development.

**Table 1.10:** Advantages and disadvantages of graft developmental approaches, where increased (+) indicates positive aspects and increasing (–) indicates negative aspects.

Grafting Strategy	Lead time	Uniform	Potential to remodel	Cell-cell communication		Potential for vascular tone	Immune response
				Initial	Secondary		
Permanent synthetics	+++	+++	---	---	---	---	+
Modified synthetics	+++	++	---	---	---	---	+
Biological biomaterials	+	--	+++	---	+++	++	+
E C seeding	-	++	---	+	+	---	+
T.E. degradable synthetics	---	---	+++	++	+++	+++	++
T.E. biological biomaterials	---	---	+++	++	+++	+++	++

Of the essential requirements necessary for a replacement vessel, listed in Section 1.1, areas that synthetic grafts excel in are availability, durability, handling characteristics



and acceptable costs. Where they fail is in immunological tolerance, resistance to thrombosis and infection; these are the primary reasons for early graft failure, coupled to the production of a neointima at the graft-native vessel anastomosis, which may block the graft. Two primary reasons (theorised) for early failure of traditional synthetic grafts is the lack of compliance matching, or matched mechanical properties, and the fact the graft is inert. Early biomaterials focused on achieving the highest degree of 'inertness' so that the body essentially ignores the materials presence. In recent years the complex communication between cell types associated within the arterial wall have been shown to modulate cell behaviour, in particular the hyperplastic response of VSMC at the graft anastomoses. Of the options available to generate a neoartery only the tissue engineering approach has the potential to deliver into the patient a developed artery that has a reduced lag time to fully integrate once implanted, it is this time that most other grafts fail as the body attempts to heal the 'damaged' area.

***Given the current literature, novel aspects of this thesis are:***

- Characterisation, modification and utilisation of a porcine dermal biomaterial to guide cell growth and proliferation to develop a small diameter vascular graft.
- Development of a novel processing methodology that strips cellular and non-structural components from porcine carotid arteries, whilst maintaining the matrices native mechanical properties in addition to the potential reduction in calcification and host immune response with the novel use of multiple treatment regimes.

Assessed by: TLC, RP-HPLC, burst pressure and stress strain analysis

- Design and application of a novel bioreactor and process flow system that allow has allowed long term culture of the 'living' tissue engineered graft, under conditions that mimics human peripheral arterial conditions. Where human primary cells (HUVEC and hVSMC) and culture under defined haemodynamic-like conditions, followed by assessment of expressed hVSMC matrix remodelling enzymes.

In this thesis the principles of tissue engineering have been applied to produce a 'living' graft that has aimed to fore fill all the essential requirements of the ideal vascular graft. By culturing a biomaterial that contains many of the native arteries extracellular matrix (ECM) cell signalling systems, with the patients own cells in a bioreactor that mimics the gas, chemical and physical environment of a native artery, a 'living' graft may be generated in which cell phenotype has been retained. With an intact endothelium and VSMC within communicative distance of the endothelium 'growing' within the graft, it is hoped that early graft failure be minimised due to functional neovessel and long-term implantation may equal if not exceed the patency rates of autologous arteries.

## **CHAPTER TWO: MATERIALS AND METHODS**

This chapter details the general materials and methods used in this thesis. Any further specific experimental methods are described in the appropriate chapters.

### **2.1 MATERIALS**

#### **2.1.1 PRIMARY CELLS**

During the course of this work a variety of different human cell lineages were isolated and grown in culture. Human vascular smooth muscle cells (hVSMC) and endothelial cells (EC) have been used for experimental purposes in this thesis. All human tissue was obtained and used with appropriate ethical consent.

The hVSMC were sourced from either adult human saphenous vein or human umbilical cord veins, described as human vascular smooth muscle cells (hVSMC) for the adult cells and neonatal hVSMC from umbilical cords. Saphenous vein segments were refrigerated at +5°C until processing (<12 hours post operatively) for cell isolation. Umbilical cords were stored at +5°C until processing for isolation of neonatal hVSMC (between 2 hours and 3 days of child delivery). Refer section 2.2.1.2/3 for isolation protocols

EC were sourced from human umbilical cord veins (sourced and processed as above). Refer section 2.2.1.1 for isolation protocols.

### **2.1.2 COLLAGEN MATRICES**

The acellular matrix utilised in Chapter 3 was derived from porcine dermal tissue processed to generate a matrix material substantially free of cellular components (Permacol, Tissue Science Laboratories, Aldershot, UK). The matrix was received in a sterile condition as flat sheets measuring 50 x 50mm (L x W) in two thicknesses, 0.75 or 1.5mm (see Section 3.1).

Porcine vascular tissue was also used to develop a tubular scaffold. Porcine carotid arteries were extracted from 6-8 month old Great White pigs at the Bath Abattoir (Cheltenham Street, Bath). Briefly, the porcine carotid arteries were removed from the heart, liver, lung and throat section that had been removed (1-3 minutes previously) from the animal's carcass during the slaughtering process. Extraction required washing excess blood from the organs and isolating any intact arteries, (as the slaughtering process aims to cut one or both of the animals carotids, to 'bleed' the animal) running from the heart up and along the remnants of the animals' oesophagus. Once isolated a butchers knife was used to gently remove connective tissue around artery and the ends were severed to free the artery. The arteries were then placed in a sterile container (for not more than 2 hours prior to storage at 5°C). All tissue processing was complete within 48 hours of extraction.

Initial tissue processing involved removal of loose connective tissue surrounding the vessel with forceps and scalpel, (Chapter 4.2.1). The overall process described in Chapter 4, utilises several steps to extract arterial lipid, remove non-structural proteins and stabilise the vessel by cross-linking proteins within the ECM.

### **2.1.3 CELL CULTURE MEDIA**

Two fundamentally different cell culture medias were used for HUVEC and hVSMC culture, firstly the DMEM and M199 based medias with 10-20% foetal calf serum. For two reasons the media was changed to a lower serum containing media. Firstly due to lower serums ability to maintain physiological pH in the bioreactor and secondly the

lower pH media is preferential from an FDA approval perspective, where defined medias are required for all human implantation studies. The reduced serum medias will allow the use of minimal quantities of autologous serum for patient trials.

#### 2.1.3.1 GROWTH MEDIA FOR HUMAN VASCULAR SMOOTH MUSCLE CELLS

Two growth media were used for the culture of human vascular smooth muscle cells (hVSMC), DMEM and low serum media, as follows.

**DMEM based VSMC media:** Experiments using the porcine dermal collagen matrix utilised Dulbecco's Modified Eagle Medium (DMEM) with Na, Pyruvate, L-glutamine (Cat. No 31885-023, Gibco Life technologies, Paisley, Scotland). 500 ml aliquots were supplemented with 75 ml (100%) Foetal calf serum (heat inactivated), (Cat. 10108-165, Gibco Life technologies, Paisley, Scotland), 86 U/ml penicillin and 86 µg/ml streptomycin, (Cat. No 15149-114, Gibco Life Technologies, Paisley, Scotland). Media were stored at 4°C.

**Low serum VSMC media:** Later work (Chapters 5 and 8) used a low serum media, Human vascular smooth muscle cell Growth Media (C-22062 PromoCell, Heidelberg, Germany) with SupplementMix (C-39267, PromoCell, Heidelberg, Germany). The SupplementMix once mixed with the base media resulted in final ingredient concentrations within the media of: 5% (v/v) Foetal Calf Serum, 0.5 ng/ml Epidermal Growth Factor, 2 ng/ml basic Fibroblast Factor, Insulin 5 µg/ml, 50 ng/ml Amphotericin B, 50 µg/ml Gentamicin. Media was stored at 4°C.

#### 2.1.3.2 GROWTH MEDIUM FOR HUMAN UMBILICAL VEIN ENDOTHELIAL CELLS

Two growth media were used for the culture of human endothelial cells (EC), M199 and a low serum media, as follows.

**M199 based EC media:** Experiments in Chapter 3, utilised the M199 based media (500 ml) with Modified Earls Salts (Cat. 31153-026, Gibco Life technologies, Paisley, Scotland). Media was supplemented with 100 ml (100%) Foetal calf serum (heat inactivated), (Cat. 10108-165, Gibco Life Technologies, Paisley, Scotland), 83 U/ml

penicillin and 83 µg/ml streptomycin, (Cat. No 15149-114, Gibco Life Technologies, Paisley, Scotland). 15 mg Endothelial cell growth supplement (from bovine neural tissue) (Cat. No E-2759, Sigma, Poole, Dorset), Heparin 5000 IU (monoparin, CP Pharmaceuticals, UK). All quantities are final concentrations. Media was stored at 4°C.

**Low serum EC media:** Experiments in Chapters (5 and 7) utilised Endothelial Cell Growth Media (C-22010) with the SupplementMix (C-39215), (PromoCell, Heidelberg, Germany). Final media (media mixed with SupplementMix pack) contained 0.4% Heparin, 2% Foetal Calf Serum, 0.1 ng/ml Epidermal Growth Factor, 1 µg/ml Hydrocortison, 1 ng/ml basic Fibroblast Factor, 50 ng/ml Amphotericin B, 50 µg/ml Gentamicin. All quantities are final concentrations 500ml.

## 2.1.4 CHEMICALS

**Table 2.01:** Materials and suppliers

Material	Cat. No.	Supplier	Address
Accutase	AT104	TCS CellWorks	Bucks, UK
Acetone	10386 6 x	BDH, UK Ltd.	Poole, UK.
Acetonitrile	10477 4P	BDH, UK Ltd.	Poole, UK.
Acrylamide (40%)	20-2400-05	Anachem	Luton, UK
Alpha-Actin	M 0851	DAKO	Ely, UK
Amino acid standards (HPLC)	A-9531	Sigma Chemical Co.	Gillingham, UK
Ammonium hydroxide	A-6899	Sigma Chemical Co.	Gillingham, UK
Ammonium Bicarbonate	A-6141	Sigma Chemical Co.	Gillingham, UK
Ammonium persulphate (AMPS)	A-9164	Sigma Chemical Co.	Gillingham, UK
Anti freeze (universal)	T-216-6652	Silkolene Lubricants	Henley, UK
Aquamount slide adhesive (aqueuous)	36226 2H	BDH, UK Ltd.	Poole, UK.
Arginine	A-4881	Sigma Chemical Co.	Gillingham, UK
Boric acid	B-0252	Sigma Chemical Co.	Gillingham, UK
Bovine albumin serum	A-8667	Sigma Chemical Co.	Gillingham, UK
Bromophenol blue	H5011	Promega	Southampton, UK
1-Butanol	34867	Riedel-de Haen	Gillingham, UK
Calcium Chloride	C-3881	Sigma Chemical Co.	Gillingham, UK
CD 31 EC antibody	M0823	DAKO	Ely, UK
Chloroform	277105X	BDH, UK Ltd.	Poole, UK.
Citric acid	C-0759	Sigma Chemical Co.	Gillingham, UK
Collagenase (bovine)	C-9891	Sigma Chemical Co.	Gillingham, UK
DAPI	D-9542	Molecular Probes	London, UK
Sigma-Fast DAB	D-4293	Sigma Chemical Co.	Gillingham, UK
di-Sodium hydrogen orthophosphate	102494C	BDH, UK Ltd.	Poole, UK.
DL-Dithiothreitol (DTT)	V3151	Promega	Southampton, UK
DNase 1 (Deoxyribonuclease 1)	DN-25	Sigma Chemical Co.	Gillingham, UK
Dodeca-Molybdophosphoric acid	101613k	BDH, UK Ltd.	Poole, UK.
DPX slide adhesive (non-aqueous)	36029 2F	BDH, UK Ltd.	Poole, UK.

Eosin	35084 41K	BDH, UK Ltd.	Poole, UK.
Ethanol	10107EP	BDH, UK Ltd.	Poole, UK.
9-fluorenylmethyl chloroformate	F-0378	Sigma Chemical Co.	Gillingham, UK
9 fluoroenylmethyl	F-0378	Sigma Chemical Co.	Gillingham, UK.
Formaldehyde (37%)	20910-328	BDH, UK Ltd.	Poole, UK.
Formal saline	36136 7L	BDH, UK Ltd.	Poole, UK.
Fungizone – Squibb	16-723-46	Flow Lab	UK
Glutaraldehyde	R1312	TAAB	UK
Glycerol	G-7893	Sigma Chemical Co.	Gillingham, UK
Harris Haematoxylin	35194 5S	BDH, UK Ltd.	Poole, UK.
Hanks Balanced Salt Solution (HBSS)	TH2513	Sigma Chemical Co.	Gillingham, UK
Horse Radish Peroxidase	P 6782	Sigma Chemical Co.	Gillingham, UK
Hydrochloric acid (concentrated)	28507BF	BDH, UK Ltd.	Poole, UK.
Hydroxyproline (standards)	H-7279	Sigma Chemical Co.	Gillingham, UK
Industrial methylated spirits (IMS)	35194 4R	BDH, UK Ltd.	Poole, UK
Methanol	15250 6X	BDH, UK Ltd.	Poole, UK.
Methylene Green	M-7766	Sigma Chemical Co.	Gillingham, UK
Molecular weight marker (rainbow)		Amersham	Bucks, UK
TEMED	V3161	Promega	Southampton, UK
N-A-Benzoyl-L-Arginine Ethyl Ester	B-4500	Sigma Chemical Co.	Gillingham, UK
Osmium tetroxide EM (2% w/v)	15	TAAB	UK
Nunc chamber slides	154461	GibcoBRL Lifetech	Paisley, Scotland
nystatin	15340-045	GibcoBRL Lifetech	Paisley, Scotland
Oxalic acid	O-0376	Sigma Chemical Co.	Gillingham, UK
Penicillin-Streptomycin	30339316	GibcoBRL Lifetech	Paisley, Scotland
Pentane	15334 6U	BDH, UK Ltd.	Poole, UK.
Pepsin	P-6887	Sigma Chemical Co.	Gillingham, UK
Peracetic acid Solution	77240	Fluka	Gillingham, UK
Poly (2-hydroxyethyl methacrylate)	P-3932	Sigma Chemical Co.	Gillingham, UK
potassium permanganate	29644	BDH, UK Ltd.	Poole, UK.
RNase 11-A (ribonuclease A)	R-50000	Sigma Chemical Co.	Gillingham, UK
Silica gel 60 TLC plates (20 x 20 cm)	155552J	MERCK UK Ltd.	Poole, UK.
Slide cover slips	406/0188/34	BDH, UK Ltd.	Poole, UK.
Slides (histology)	406/0179/00	BDH, UK Ltd.	Poole, UK.
Smooth muscle growth medium 2	C-22062	PromoCell	Heidelberg Germany
SMC growth medium supplement mix	C-39267	PromoCell	Heidelberg Germany
Sodium acetate	S-7670	Sigma Chemical Co.	Gillingham, UK
Sodium azide	S-8032	Sigma Chemical Co.	Gillingham, UK
Sodium chloride	102415	BDH, UK Ltd.	Poole, UK.
Sodium dihydrogen orthophosphate	102454R	BDH	Poole, UK.
Sodium dodecyl sulphate (SDS)	L-4509	Sigma Chemical Co.	Gillingham, UK
Sodium Hydroxide	S-5881	Sigma Chemical Co.	Gillingham, UK
Sucrose	S-7903	Sigma Chemical Co.	Gillingham, UK
Tetramethylammonium chloride	15309 2R	BDH, UK Ltd.	Poole, UK.
Tris/base	H5131	Promega	Southampton, UK
Trizma Hydrochloride	T-3253	Sigma Chemical Co.	Gillingham, UK
Trypan Blue	T-8154	Sigma Chemical Co.	Gillingham, UK
Trypsin-EDTA solution (1X)	25300-054	Life Technologies,	Paisley, Scotland
Trypsin-EDTA solution (10X)	35400-027	Life Technologies,	Paisley, Scotland
Triton-X100	T9284	Sigma Chemical Co.	Gillingham, UK
Tween 80	560234H	BDH, UK Ltd.	Poole, UK.
van Gieson (elastin stain)	351154S	BDH, UK Ltd.	Poole, UK.
von Willebrand factor antibody	M 0616	DAKO	Ely, UK
Weigerts Resorcin Fuchsin	AS021	R.A. Lamb	Eastbourn, UK
Xylene	305756G	BDH, UK Ltd.	Poole, UK.

## **2.2 EXPERIMENTAL METHODS**

Experimental methodologies used throughout this thesis, have been divided into two groups, firstly, those methods having been used in more than one section of work, such as cell culture protocols, are described in this chapter, Chapter 2. Secondly, methods specific or unique to any one of the experimental chapters (Chapters 3-7) are described separately in the appropriate chapter.

### **2.2.1 CELL ISOLATION PROTOCOLS**

#### **2.2.1.1 ISOLATION OF HUMAN UMBILICAL VEIN ENDOTHELIAL CELLS**

The method of HUVEC isolation was a modification of the method first described by Jaffe et al (1973). Sheets of gauze were laid out on a suitable sterile plate, measuring at least 250 x 250mm (to prevent spillage of blood) and soaked with IMS to collect excess blood and minimise the possibility of infection. Umbilical cords (UC) were then laid onto the plate and wiped clean using additional gauze soaked in IMS. UC were then checked for perforations resulting from injection or clamping. A suitable cord was selected and a plastic luer adapter was inserted into one end of the vein. Plastic zip ties (Cat. No 221/0371/01, BDH, Poole, UK) were then used to secure the UC to the luer adapters. Using a new 40ml syringe, sufficient sterile PBS was run through the cord to remove all traces of visible blood. The open end was then tied off with another zip tie, thus forming a chamber. Bovine collagenase (1 mg/ml) was made in sufficient volumes for the number of cords to be processed, approximately 20 ml per cord, in PBS, mixed, filter sterilised and preheated to 37°C prior injecting into the UC via a syringe and attachment. The collagenase was repeatedly injected into and drawn out of the UC to displaced air within the vein. The collagenase solution was then fully injected into the vein and incubated at 37°C for 35 minutes. After incubation the adapter furthest from syringe was cut off and the collagenase was drained into a sterile 50 ml Falcon tube. The cord was then flushed with a further 20 ml of sterile PBS into the same Falcon tube to remove any remaining cells. 10 ml of DMEM-based HUVEC media was then pipetted into the Falcon tube to inactivate the collagenase. The solution was then

centrifuged (ACL PK130, Jencons, London, UK) for 5 minutes at 1100 rpm (164 mm rotor radius) to pellet cells. The resulting supernatant was discarded. The cell pellet was then resuspended in 5 ml of HUVEC media and transferred into a T25 flask for culture (Jaffe et al., 1973).

#### 2.2.1.2 ISOLATION OF ADULT HUMAN VASCULAR SMOOTH MUSCLE CELLS: EXPLANT METHOD

Diseased saphenous veins were collected and stored overnight in HBSS at 5°C, as described in section 2.1.1. The protocol used to isolate hVSMC from explanted tissue is a modification of the method described by (Kirschenlohr, et al. 1996). The samples were then placed in a sterile Petri dish containing 10 ml of sterile HBSS. Sections of vein that were devoid of, (or had reduced diseased) symptoms were isolated and the remaining tissue discarded. The selected tissue was then sliced/cut longitudinally and laid luminal surface uppermost in a Petri dish. The luminal surface was then scraped with a sterile scalpel to remove the endothelial cell lining and rinsed with HBSS to remove free endothelial cells. A pair of forceps was used to 'pinch' the medial layer and pull away from the adventitial layer in strips. The strips of medial tissue (essentially the basement membrane of the internal elastic lamina and surrounding cells) containing hVSMC were then placed individually into the well of a 24 well culture plate and covered with 0.5 ml of either low or high serum SMC media, as described in materials Section 2.1.3. and incubated at 37°C in a 5% CO<sub>2</sub>/air atmosphere. Tissue was left for 3 days to allow adhesion to the plastic, after which normal feeding protocols were followed, see Section 2.2.2. After approximately 10-14 days hVSMC began to migrate from the tissue explant. Media was replenished three times a week until the cells reached sufficient density for either passaging or experimental use. (Kirschenlohr, et al. 1996).

#### 2.2.1.3 ISOLATION OF NEONATAL VASCULAR SMOOTH MUSCLE CELLS: ENZYME DISPERSION

The isolation of venous derived hVSMC was carried out as part of the isolation of HUVEC process (Section 2.2.1.1) and was a modification of the method described by



(Kirschenlohr, et al. 1996). Once the EC had been extracted, a fresh solution (approximately 25 ml for a 300 mm long cord) of filter sterilised collagenase (1 mg/ml) in PBS was prepared and preheated to 37°C. The distal end of the cord was tied closed and the collagenase solution injected into the vein using the same methodology as described in Section 2.2.1.1 and incubated for a further 30 minutes at 37°C. After incubation the adapter furthestmost from the syringe was cut off and the collagenase/cell suspension was drained into a sterile 50 ml Falcon tube. The UC was then flushed with 20 ml of sterile PBS to flush out any remaining cells into the tube. 10 ml of medium was then pipetted into the solution to inactivate the collagenase. The solution was then centrifuged for 5 minutes at 1100 rpm, (conditions as in Section 2.2.1.1) to pellet cells with the resulting supernatant being discarded. The cell pellet was then resuspended in 5 ml of SMC media and transferred into a T25 flask for cell culture, (Kirschenlohr, et al. 1996).

## **2.2.2 CELL CULTURE**

All cell populations were maintained in a routine manner, incubated at 37°C in an atmosphere of air supplemented with 5% CO<sub>2</sub>. Cell cultures requiring passaging were dissociated from the plastic culture dish by exposure to a solution of sterile 1 x trypsin-EDTA (trypsin 2.5 mg/ml and 1 mg/ml EDTA in PBS) for 5-10 minutes (used in Chapter 3) or a 100% solution of Accutase (used in Chapters 5 and 6) within the 37°C incubator. Once cells had dissociated from the plastic culture plate and were free in solution an equal volume of the appropriate media was added to inactivate the enzyme solution. The cell suspension was then centrifuged for 5 minutes at 1100 rpm as before. The resulting supernatant was then removed leaving a pellet of cells which were resuspended in 5 ml of the appropriate media. Initial density determination was carried out visually by standard low power light microscopy. Cell counts were routinely carried out to determine appropriate seeding densities for replating cells into fresh culture flasks. Cell cultures were then incubated at 37°C with 5% CO<sub>2</sub> as described above (Kirschenlohr, et al. 1996; Morgan 1996).

### 2.2.2.1 ENDOTHELIAL CELL CULTURE

Media replacement for all 'static' HUVEC cultures was three times a week, in accordance with guidelines from (Morgan 1996) for M199-based media. Protocols for the use of media supplied by PromoCell for endothelial cell cultivation (PromoCell, Heidelberg, Germany) were carried out as per the manufactured instructions where the media was changed three times a week. After initial cell isolation cultures were allowed to reach near confluence (2-4 days) then passaged, as described above. All further passages were carried out at ~80-90% confluence to maintain cell proliferation (Morgan 1996).

### 2.2.2.2 HUMAN VASCULAR SMOOTH MUSCLE CELL CULTURE

Media replacement for DMEM based media in 'static' hVSMC cultures was twice a week, in accordance with guidelines from (Kirschenlohr, Metcalfe et al. 1996). Cell cultured with the PromoCell media, (PromoCell, Heidelberg, Germany) had the media changed three times a week in accordance with the manufacturers protocols for human vascular smooth muscle cell growth media. hVSMC were allowed to reach full confluence before passaging, as before.

## **2.3 ANALYTICAL METHODS**

Unless specified otherwise all images throughout this thesis are representative of the sections (either cut sections or surface microscopy) viewed.

### **2.3.1 CELL COUNTING**

Cells were removed from the plastic culture flasks using the standard protocol with trypsin EDTA or Accutase, as described previously in Section 2.2.2. The cell suspension was spun down (1000rpm for 5 minutes, as before) and resuspended in the cell specific media to an appropriate volume for counting purposes (i.e. if cells from T25 flasks are being harvested, 5 ml media is used to resuspended cells, if cultured on T75 flasks, 20 ml of media is added). Samples were then loaded into an improved Neubauer haemocytometer (Cat. No. 403/0024/00, BDH, Poole, UK) and counted as per manufactures instructions giving a total of ten individual counts per sample lot.

#### **2.3.1.1 CELL COUNTING ON PORCINE DERIVED DERMAL COLLAGEN**

This method was used exclusively in Chapter 3. In this chapter collagen was cut into 16 mm diameter discs, with a surface area of 201 mm<sup>2</sup>. The microscope, (Mod. 68040 phase contrast microscope, Carl Zeiss, UK), was calibrated using a stage micrometer (Cat. No. 316/1212/26, BDH, Poole, UK), and an eyepiece graticule, (Cat. No. 316/1212/20, BDH, Poole, UK) with a grid formation 10 x 10 squares, such that the total grad area was calculated to be 750 x 750 µm, resulting in a surface area of 0.56 mm<sup>2</sup>. Semi-random counting areas were assigned by moving the microscope stage to a new area (according to a prescribed plan, see Figure 3.01), without looking through the eyepiece. In this way it was possible to objectively select the area (random) without the subjectivity of actually viewing cell density until the area had been preselected. A total of 12 counts were taken on each disk (see Figure 3.01) with a total of 36 counts over the triplicate data set. Representing approximately 10% of one disks surface area (20.16 mm<sup>2</sup>) which was deemed an adequate representation of the entire disc. Counts were taken using a prescribed pattern as far as possible to ensure each of the 12 counts per disc were representative of the entire disc area.

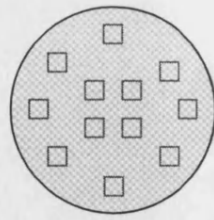


**Figure 3.01:** Counting pattern on dermal collagen discs: semi-random

#### 2.3.1.2 CELL COUNTING ON ARTERIAL BASED MATRIX AFTER STATIC CELL CULTURE

This method was used exclusively in Chapter 5, with a Carl Zeiss Axioskop2 fluorescent microscope described in Section 2.3.7. Primary human cells were cultured on sections of the arterial based matrix under static conditions. On completion of the culture duration, tissue sections (approximately 5 x 5 mm) with cells seeded onto either the luminal or abluminal surface were removed from culture, fixed, then stained with DAPI as described in Section 2.3.5.10. Image analysis equipment was set up with an image size of 762 x 480 pixels, which when calibrated equalled approximately 625 x 400  $\mu\text{m}$  (250000  $\mu\text{m}^2$  or 0.25  $\text{mm}^2$ ) using the 10 x objective. Five semi-random sites were selected (total of 1.25  $\text{mm}^2$ ) per tissue section (duplicate) and cells counted resulting in the number of cells per  $\text{mm}^2$ .

#### 2.3.1.3 CELL COUNTING ON ARTERIAL BASED MATRIX AFTER PERFUSION CELL CULTURE

This method was used exclusively in Chapter 7, perfusion cultures. Counting HUVEC on the luminal surface of the matrix was conducted in a similar fashion to static cultures (Section 2.3.1.2). After each experiment, where two reactors were run in series, matrix sections were removed from the reactor and fixed in the normal manner for DAPI staining (see Section 2.4.2.3). Each matrix had a total length of 100 mm, of which 30 mm from the proximal and 20 mm from the distal ends were discarded to reduce error from end effects. The remaining 50 mm sample was sectioned in half (2 x 25 mm) and then cut longitudinally to produce a total of 4 x 25 mm sections with the lumen exposed. These sections were stained with DAPI in the normal manner. Five counts were taken

from each section, (total of 20 per vessel) evenly spaced along the entire length in a zigzag fashion, see Figure 2.02. In the same manner as Section 2.3.1.2 the image analysis equipment was calibrated to view matrix sections  $625 \times 400 \mu\text{m}$  ( $250000 \mu\text{m}^2$  or  $0.25 \text{ mm}^2$ ) and results expressed as cells/ $\text{mm}^2$ . Cells were counted in each semi-random section from the two matrices (run in series) and pooled to yield the final data set for each run.

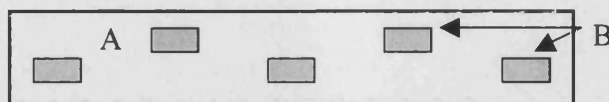


**Figure 2.02:** A diagrammatic representation of the cell counting pattern used for assessing cell density on/in matrix samples cultured in the perfusion bioreactor. **A**, the matrix and **B** counting zones.

#### 2.3.1.4 CELL VIABILITY

Determination of cell viability with Trypan Blue (0.4%). Trypan Blue is used as a dye exclusion assay for cell viability procedures. This method is based on the principle that live (viable) cells will not take up the dye, whereas dead cells (non-viable) will. Total solution volumes equal 1.0 ml, comprising 0.5 ml of 0.4% Trypan Blue, 0.3 ml HBSS and 0.2 ml of cell suspension (dilution factor = 5). The suspension is mixed thoroughly and allowed to stand for 5-15 minutes. Cells that stained dark blue after the incubation period are deemed non-viable.

#### 2.3.2 LIPID ANALYSIS

Ascending one-dimensional thin layer chromatography (TLC) was used to evaluate, qualitatively, the extent of lipid extraction using dodeca-molybdophosphoric acid as the detection reagent. The protocol used was a modification of methods described by (Sherma 1986; Stevens, et al. 1988).

The experimental methodology followed prior to lipid analysis is described in Chapter 4.2.2.3. At each prescribed time point samples were collected, cut and weighed to

approximately  $0.4 \pm 0.03$  g, 5 mm sections were removed and discarded from the exposed end to reduce end effects on total lipid extraction. Samples were then diced using a sterile scalpel and liquidized in a glass homogeniser with 1 ml of butanol. Prior to spotting the sample onto the TLC plate, plates were 'activated' by immersion in the mobile phase, consisting of 100% solutions of chloroform, methanol and distilled water in ratio 30:10:1.2, for 2-3 minutes. The plates were then air dried and activated by heating at 120°C for 15 minutes. The homogenate was then spun down with one pulse for 5 s (Techne Genofuge Cat. 193-980, Jencons PLS, London, UK) to remove suspended particulates remaining the supernatant. The supernatant was collected in a 500  $\mu$ l Epindorf tube and subsequently spotted in aliquots of 1  $\mu$ l onto the silica gel 60 TLC plates. Once the spots had air dried the plates were run in the mobile phase (enough volume to immerse the bottom 5 mm of the TLC plate) for 15 –18 minutes, resulting in a migration distance of approximately 85 mm. The chromatogram was then air dried and washed in a suitably sized glass container with the detection reagent, (250 mg dodeca-molybdophosphoric acid, dissolved in 50 ml ethanol with 4 ml of concentrated HCl per 100 ml of reagent solution) for a further 2 minutes. The TLC plates were air dried then heated to 150°C in a vented lab oven for 15 minutes. Lipid appeared as dark blue zones on a yellow background. Exposure of the TLC to the gaseous vapour from a 25% ammonia solution (gas) for 3-5 minutes bleached the yellow background white.

The delipidised tissue was tested for stability by immersion in a 1 x solution of trypsin at 20°C. Tissue degradation was observed qualitatively over time.

### **2.3.3 PROTEIN ANALYSIS**

#### **2.3.3.1 TRYPSIN STABILITY ASSAY 'WHOLE TISSUE'**

This analytical technique was a modification of Sigma quality control test procedure ('Enzymatic Assay of Trypsin' Sigma, Dorset, UK). Continuous spectrophotometric rate determination was attained using a Hitachi U-2010 spectrophotometer, Jencons-PLS, London, with UV-Solutions software at A253 nm. The substrate, N $\alpha$ -Benzyol-L-Arginine Ethyl Ester (BAEE), is hydrolysed to form N $\alpha$ -Benzyol-L-Arginine and

ethanol. The result was a linear relationship between absorbance (Abs) and time. The gradient was calculated, yielding the enzyme's activity in absorbance units/min.

Four analyses were completed which included two controls. Arterial sections digested in trypsin, trypsin alone, and controls 1. enzyme solution heated to 75°C for 30 minutes and 2. buffer less BAEE substrate. For tissue digestion analysis, porcine carotid artery sections weighing 0.5 g, post lipid extraction, were aseptically transferred to 15 ml Falcon tubes and trypsin solution (filter sterilized) was added in a ratio of 1 g tissue to 15 ml trypsin solution (1 x). Samples were placed on a rock/roll table at room temperature  $19 \pm 2^\circ\text{C}$  for the duration of the experiment. At prescribed time intervals samples were collected for analysis as shown in results, Section 4.3.2, protein digestion. A 67 mM di-sodium hydrogen orthophosphate (anhydrous), (BDH, Dorset, UK) buffer was prepared, adjusted to pH 7.6 with 1 M NaOH to a total volume of 50 ml. BAEE was made up to a final concentration of 0.25 mM in the buffer solution. All Trypsin-EDTA solutions were diluted from 10 times concentration to 1 times concentration in PBS (10 x trypsin concentration: 5.0 g/L porcine trypsin and 2.0 g/L EDTA in 0.9% sodium chloride). 67  $\mu\text{l}$  of sample solution was added to the buffer/BAEE solution and the reaction recorded as an absorbance change over time (as above) at 25°C.

### 2.3.3.2 TRYPSIN DIGESTION-SDS PAGE

#### ***Preparation of sample protein***

Tissue samples with a mean weight of  $0.3 \pm 0.02$  g were immersed in a 1 x trypsin solution (15:1 as described previously). Samples were placed on a rock/roll table at room temperature  $19 \pm 2^{\circ}\text{C}$  for the duration of the experiment. Due to the insolubility of the ECM proteins a more comprehensive method to solubilise whole tissue was followed. Tissue was firstly weighed and dried with blotting paper then diced as small as possible with a scalpel. Tissue samples were then placed in a ceramic mortar and pestle and approximately 50 ml of liquid nitrogen was added. Liquid nitrogen was applied until tissue had frozen. When the liquid nitrogen had evaporated the sample was ground until a fine powder was produced. Finally the sample was homogenising in the glass mortar and pestle in 1 ml  $\text{H}_2\text{O}$  with 20% w/v SDS. The homogenate was then spun down with one pulse for 5 s (Techne Genofuge Cat. 193-980, Jencons PLS, London, UK) to remove particulates remaining the supernatant.

#### ***Bradford's Assay: protein concentration***

Samples were prepared as above for SDS PAGE protocol above. Calibrations of bovine serum albumen (BSA) standards were prepared by serial half dilution. 35  $\mu\text{l}$  of BSA (20 mg/ml) was made up to 160  $\mu\text{l}$  in distilled  $\text{H}_2\text{O}$ , 80  $\mu\text{l}$  of which was pipetted into the first well of a 96 well microplate (NUNC, UK). A further 80  $\mu\text{l}$  of distilled water was added and mixed thoroughly to the same well bring the total volume to 160  $\mu\text{l}$ . Into each of the remaining 6 wells adjacent to the first well 80 $\mu\text{l}$  of distilled water was added. Then 80  $\mu\text{l}$  from the 160  $\mu\text{l}$  in the first well was removed and added to the second well, this was mixed thoroughly. The process was repeated to each of the remaining wells, removing 80  $\mu\text{l}$  from the previous well and adding to the next, so that each well was left with a final volume of 80  $\mu\text{l}$ . Well number 6 was the last well that had the protein standard, well 7 was distilled water only. Into a separate well 80  $\mu\text{l}$  of neat protein sample was added. 20  $\mu\text{l}$  Coomassie Brilliant Blue was added to each well bring the total volume to 100 $\mu\text{l}$  and mixed thoroughly. After 5 minutes the optical densities of the samples is read at 595 nm using a microplate reader (Mod. 448-127 MRX microplate reader, Jencons PLS, London UK). A calibration was completed with each protein analysis, where BSA standards were read against wave length, from which the total protein content was read.



#### ***Preparation of the loading buffer***

10 µl of sample protein was added to 10 µl of sample buffer, although this was not an absolute ratio due to variation in the samples total protein content (determined by the Bradfords assay, (above), up to 16 µl of sample and 4ml buffer was deemed to be acceptable. The sample/buffer was mixed and denatured by heating at 100°C for 1 hour. This solution was then spun down. 10 µl of sample buffer was added to 6 µl of Rainbow Marker as an indicator of sample molecular weights on the gels. The samples were then loaded, lid fitted, power reconnected and the power pack set to run for 2 hours at 100V. Once finished the power supply was disconnected and the gels removed from the tank. Gels were removed from the glass plates and placed in the staining solution for two hours. Gels were then washed and destained until a majority of the background staining was removed. Gels were then scanned for reference.

SDS PAGE gels utilized an 8 % acrylamide resolving gel and 4% stacking gel (Laemmli 1970), loaded with 5-10 µl of sample in 10 µl loading buffer (as above) which had been mixed and denatured by heating at 99°C for 5-10 minutes. Gels were run at 80 volts until migration was complete, stained using Coomassie blue for 4 hours and destained in 5% methanol, 7.5% acetic acid. Further details of the SDS-PAGE methodology are provided in Appendix A3

#### **2.3.4 MEDIA ANALYSIS**

Analysis of media parameters: pH, PCO<sub>2</sub>, PO<sub>2</sub> and HCO<sub>3</sub> was conducted with the use of an integrated AVL blood gas analyser, model OMNI, Stone, UK. Glucose testing utilized a hand held glucose monitor 'Accu-Chek, Advantage, Boots, pharmacy, UK, used for diabetic analysis of blood glucose concentration. At prescribed time intervals the sample (5 µl) from the media solution was removed under sterile conditions and stored on ice for periods not more than 15 minutes before analysis with either the AVL blood gas analyser or the Accu-Chek glucose monitor mentioned above.

### **2.3.5 CROSS-LINKING ANALYSIS USING REVERSE PHASE-HIGH PERFORMANCE LIQUID CHROMATOGRAPHY**

The procedure for the assaying for hydroxyproline (Hyp) was derived from a method described by (Bank, et al. 1996). The procedure uses RP-HPLC to separate the amino acids. In order to detect the separated amino acids, they are derivatized using 9-fluorenylmethyl chloroformate (FMOC-Cl), a fluorescing agent, before the separation step. Due to the sample volume required by the auto-sampler, the sample volume for the derivatisation step was increased, the volumes of all other reagents used were increased proportionately to maintain the ratios used in the original method. After early runs the number of extraction steps used to remove excess FMOC-Cl and its hydrolysis product FMOC-OH was increased to improve background 'noise' in the chromatogram. The method described below is the result of the refinements made to the Bank et al (1996) protocol to suit the C18 RP-HPLC column used.

A Gilson 715 HPLC system (Gilson, UK) was used, consisting of Gilson model 305 and 306 pumps, 811C mixer and a 231 auto-sampler. A Perkin Elmer LC240 fluorescence detector was used to detect derivatized amino acids. The C18 reverse phase HPLC column (4.6 x 250 mm; Kromasil KR100-5C18-4498, BDH, UK) was maintained at 40°C in a water bath with a Grant temperature controller.

#### **2.3.5.1 SOLUTION PREPARATION**

Borate buffer was prepared from boric acid (0.1M) adjusted to pH 8.0 with 5N sodium hydroxide. Amino acid standards were prepared by adding 120µl of the stock solution to 100ml 0.1M borate buffer. Hydroxyproline standards were prepared by adding 120µl of the concentrated Hyp stock (20mg Hyp/10ml water) to 100ml 0.1M borate buffer resulting in a Hyp concentration of 15.25 µmol/ml. To achieve lower concentrations for generating calibration plots, this stock solution was mixed in the appropriate ratios with 0.1M borate buffer to produce the desired Hyp concentrations. For the enzyme digested tissue samples, the remaining intact tissue was removed, and the solution was filtered with a 0.2 µm filter to remove solid particles.

### 2.3.5.2 TISSUE DIGESTS

Both control and cross-linked matrix materials were exposed to increasing concentrations of pepsin (results from 1000 and 5000 activity units/ml shown) to yield quantitative data of the Hyp and total free amino acids in solution. Unless otherwise stated the following procedure was used. Enzyme solutions were made up in ultra pure water and adjusted to pH 4.2 with HCl. All sample weights were recorded,  $0.102 \pm 0.01$ g. To each tissue sample a 3ml aliquot of enzyme solution was added and placed in a water bath maintained at  $37^{\circ}\text{C}$  for the appropriate time.

Repeatability and accuracy of the assay was tested, running  $15.25 \mu\text{mol/ml}$  of Hyp standard, recording the retention time and Hyp peak area. Figure 2.03 shows a chromatogram of the Hyp standard for initial repeatability tests. A mean retention time of  $13.479 \pm 0.19$  minutes was determined with a mean peak area of  $47300 \pm 2580$  units.

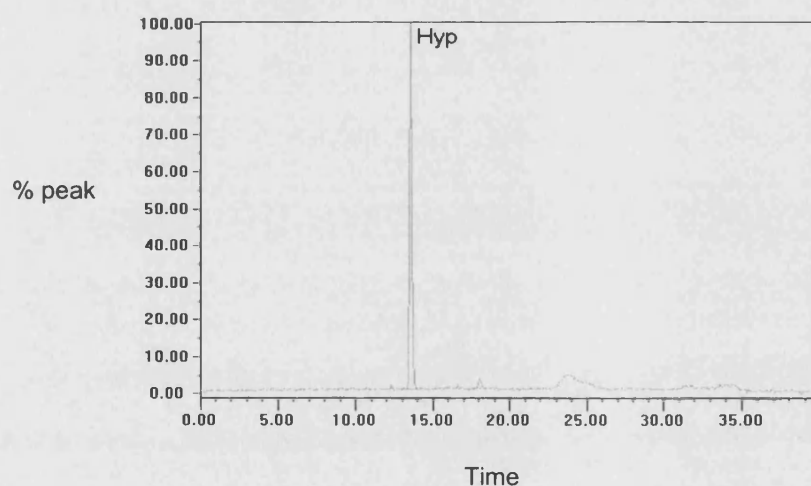


**Figure 2.03:** Chromatogram of hydroxyproline standards

### 2.3.5.3 DERIVATISATION

The reactant solution consisted of FMOC-Cl dissolved in acetone ( $1.5 \text{ mg/ml}$ ,  $6 \text{ mM}$ ).  $2 \text{ ml}$  of FMOC-Cl solution was added to  $2 \text{ ml}$  of sample solution mixed immediately and allowed to stand at room temperature for 10 minutes. Termination of the reaction and removal of excess reagent (FMOC-Cl), and its hydrolysis product FMOC-OH, and acetone were performed by extraction with  $6 \text{ ml}$  of pentane. After mixing and a short

period (~1 minute) to allow phase separation, the upper layer was discarded. After 4 additional extractions, 4 ml of 25% (v/v) acetonitrile in 0.1 M borate buffer was added. 20 µl aliquots of this diluted sample were injected into the HPLC.

#### 2.3.5.4 CHROMATOGRAPHY

Derivatized amino acids were separated using the ternary gradient system described below, see Table 2.02 for a summary of gradient conditions (Bank, et al. 1996). All solvents were filtered through a 0.2 micron filter and degassed with helium for a minimum of 30 minutes

**Eluent A:** was 20 mM citric acid containing 5 mM tetramethylammonium chloride and 0.015 (w/v) sodium azide, adjusted to pH 2.85 with 20 mM sodium acetate containing 5 mM tetramethylammonium chloride and 0.01% (w/v) sodium azide.

**Eluent B:** 80% (v/v) of 20 mM sodium acetate solution containing 5 mM tetramethylammonium chloride and 0.01% (w/v) sodium azide (adjusted to pH 4.5 with concentrated phosphoric acid) plus 20% (v/v) methanol.

**Eluent C:** Acetonitrile.

For elution the gradient was as given in the table below. The flow rate was maintained at 1.4 ml/min throughout the analysis. The separation was performed at a column temperature of 40°C and fluorescence was monitored at 254 and 630 nm (excitation and emission wavelengths respectively).

**Table 2.02:** Gradient conditions for the elution of derivatized amino acids (Bank, et al. 1996)

Time (min)	Eluent A (%)	Eluent B (%)	Eluent C (%)
0	75	-	25
11.5	60	-	40
13	60	-	40
13.1	-	64	36
18	-	62	38
25	-	30	70
30	-	25	75
32	-	25	75
32.1	75	-	25
40	75	-	25

### 2.3.5.5 HYDROXYPROLINE CALIBRATION

Calibration of Hyp to chart peak area was carried out to determine the concentration of Hyp in free solution, see Figure 2.04. Hyp standard solutions were made up to the following concentrations 1.53, 3.05, 3.81, 6.10, 7.63, 9.15, 12.20 and 15.25  $\mu\text{mol/ml}$ .

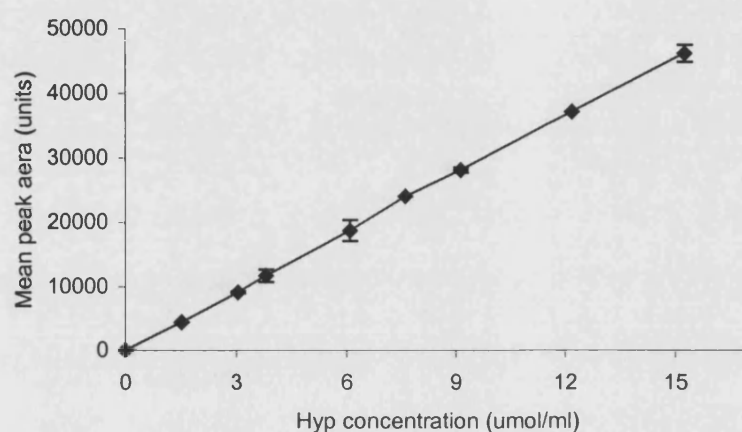


**Figure 2.04:** Calibration plot to determine experimental Hyp concentration,  $n = 3, \pm 1 \text{ sd}$ .

## 2.3.6 MATRIX MECHANICAL PROPERTIES

### 2.3.6.1 PRESSURE TESTING

A stainless steel reservoir was filled with distilled H<sub>2</sub>O and air pressurized to deliver a regulated pressure increase to the arterial section (pressure control valve, Swagelok, UK). Pressure increments were monitored with a 7 bar pressure transducer connected to a data acquisition system (Model PCL 818L Bede Technology Ltd, Tyne and Wear, UK). Genie Builder Version 3.0, Advantech™ (Bede Technology Ltd, Tyne and Wear, UK), running Windows 3.1, was used to record the data at a sample rate of 5 per second into the computer-based format, Figure 2.05.

Tissue samples were attached to tapered glass adapters directly into the 3.2 mm ID PVC tubing (275/0100/06, BDH, Poole, UK) circuit and tensioned to remove slack. Wall thickness and internal diameter were measured at each end of the arterial section to obtain an average dimension. The control valve was progressively opened, pressurising the arterial section until vessel failure. From the computerised data, the observed maximum pressure (mmHg), at which bursting occurred, was collected.

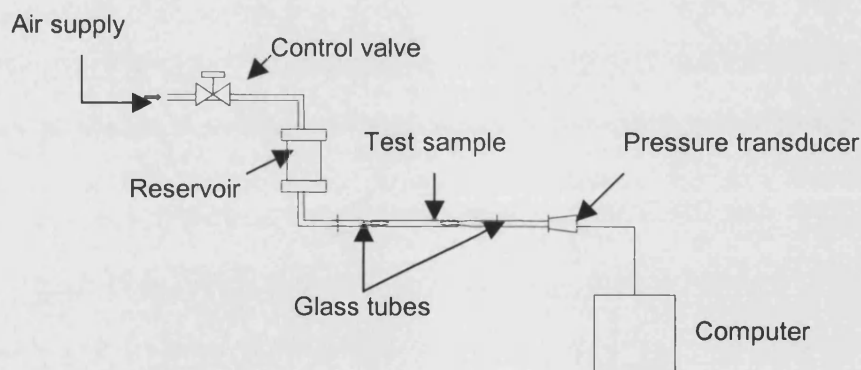


**Figure 2.05:** Diagrammatic representation of the apparatus used for the pressure testing tests.

### 2.3.6.2 LOAD-EXTENSION TESTS

Arterial sections greater than 2 mm in length were cut off each end to eliminate end effects caused by damage during explantation (Courtman, et al. 1994). The artery was then cut into 5 mm long circular ringlets. Hiles et al (1995) used 3-5 mm length sections, and Courtman et al (1995) used 4 mm sections in similar procedures (Courtman, et al. 1994; Hiles, et al. 1995). 5 mm sections were chosen, as these were similar in size and using a larger size would reduce the effect of error for stress calculations, where the cross-sectional area is required. The average wall thickness and internal diameter were measured for each ringlet. The wall was considered to be the bulk tissue of the medial layer, which was distinguishable from the loose, adventitial tissue. A stress/strain analysis rig (Instron 1122 test rig, Instron, UK) was used to obtain load-extension data, where individual ringlets were attached to stainless steel hooks and extension data was acquired until matrix/ringlet rupture, see Figure 2.06. The equipment was calibrated and zeroed; chart drive speed was set to 50 mm/min. The maximum deflection on the chart was set to 5000 g. The cross-head control was set to 5 mm/min. Similar tests by Courtman et al (1995) and Hiles et al (1995) worked with strain rates from 10 to 25 mm/min. A lower value of 5 mm/min was used to decrease the strain rate to improve graphical results. Results were expressed as a stress strain trace on a chart recorder, as illustrated in Appendix A4.

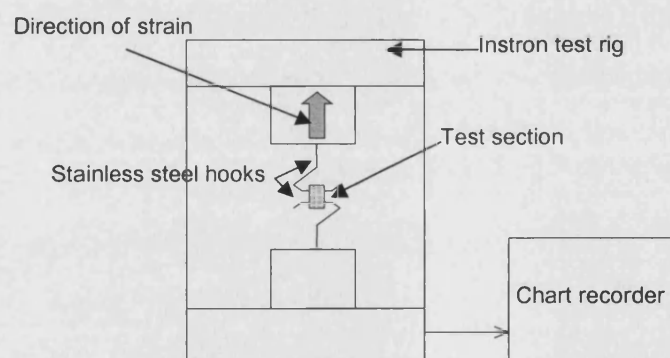


**Figure 2.06:** A representation of the Instron 1122 test rig, used for obtaining load-extension data. Arterial ringlets were attached to the stainless steel hooks and pulled apart till rupture. A chart recorder records the increase in load required for the constant increase in extension.

## **2.3.7 HISTOLOGY**

### **2.3.7.1 TISSUE SECTIONING, PARAFFIN EMBEDDING TISSUE AND DEWAXING**

Tissue used in histological analysis was first processed in an automated system (HistoCentre1, Shandon Inc., Pittsburgh, USA) to fix and prepare the tissue for paraffin embedding. After processing the tissue was paraffin embedded (HistoCentre2, Shandon Inc., Pittsburgh, USA) into an appropriately sized carrier block. After the wax blocks had cooled the metal blocks were removed and excess wax was trimmed, sections of 5  $\mu\text{m}$  thickness were cut on a standard sledge microtome (Wetzler sledge microtome, Leitz, UK). Sectioned tissue was floated in  $\text{H}_2\text{O}$  (45°C) to flatten, then mounted on glass slides. Slides were then heated at 65°C overnight and then stored for later use. When required, slides were dewaxed in xylene for 2 x 2 minutes followed by 2 x 1 minutes in IMS then rehydrated in slow running tap water for 5 minutes.

### **2.3.7.2 HAEMATOXYLIN AND EOSIN STAINING TISSUE SECTIONS**

Following dewaxing (xylene for 2x 2 minutes followed by IMS for 2x 1 minutes) sections were immersed in Harris's haematoxylin for 5 minutes followed by washing in tap water for 5 minutes. Samples were then differentiated acid alcohol (1% (v/v) HCl [conc.] / IMS) for 30 seconds with gentle shaking followed by washing in tap water for 5 minutes. If staining of the cells cytoplasm was required an additional step of Eosin for 30 seconds followed by a further 5 minutes wash in tap water was required. Finally slides were dehydrated by immersion in IMS for 2x 1 minute followed by xylene for 2x 2 minutes. Slides were mounted with DPX, see Section 2.3.3.4.

### **2.3.7.3 VAN GIESON STAIN FOR ELASTIN FIBRES**

Following dewaxing, sections were immersed in acidified potassium permanganate for 2 minutes then rinsed in tap water for 5 minutes. This was followed by immersion in 1% Oxalic acid 30 seconds and again rinsing in tap water for 5 minutes. Samples were then washed in 70% alcohol for 1 minute then stained in Weigerts Resorcin Fuchsin, at



room temperature for 20 minutes followed by washing for 10 minutes. Samples were then differentiated in acid alcohol for 30 seconds, see Section 2.3.3.2, washed in tap water for a further 5 minutes then stained in van Gieson for 5 minutes. Finally samples were washed in tap water for 5 minutes prior to clearing and mounted in DPX.

#### 2.3.7.4 MOUNTING SECTIONS IN DPX

After dehydrating the sections through graded alcohols and xylene an appropriately sized coverslip was selected and placed on a sheet of fibre-free paper. A drop of DPX was applied to the coverslip and using forceps slides were removed from the holding rack, excess xylene was drained away and the cover slips were then gently lowered onto the slides containing the section, such that the section is sandwiched between its slide and the coverslip. The slides were then turned over allowing the DPX to spread between the slide and coverslip. Excess DPX was removed with the fibre free tissue and the slides were left to dry overnight.

#### 2.3.7.5 CELL PHENOTYPING

All phenotypic characterisation (including cells on tissue culture plastic as well as those seeded onto the biomatrix) was carried out using the R.T.U. VectorStain (code PK-7800, Vector Labs, UK), universal quick kits containing reagents in ready-to-use form, including: prediluted normal horse serum, prediluted biotinylated secondary antibody and a preformed streptavidin/peroxidase complex solution. Two primary antibodies were used for the immunocytochemical phenotype characterisation of HUVEC, both of which were monoclonal mouse antibodies, Monoclonal Mouse–Anti-human Von Willebrand Factor (vWF), Clone F8/86 (500:1 dilution) (code No. M0616 Lot 039 DAKO Ltd. Ely, UK) and Monoclonal Mouse – Anti-human endothelial cell, CD31: clone JC/70A (50:1 dilution) (code No. M0823, Lot 028 DAKO, Ely, UK). The antibody used for hVSMC identification was Monoclonal Mouse – Anti-human smooth muscle actin: clone 1A4 (40:1 dilution) (code No. M0851 lot 028 DAKO Ltd. Ely, UK). See Appendix A1-2 for results of cell phenotyping.

Following dewaxing (above) sections were rinsed in tap water for 5 minutes. Slides were incubated with prediluted blocking serum for 10 minutes, followed by incubation with the primary antibody for 1 hour at room temperature. Slides were then washed in PBS for 5 minutes (x3), followed by incubation with the prediluted biotinylated secondary antibody then washed in PBS for 5 minutes (x3). Slides were then incubated in the preformed streptavidin/peroxidase complex reagent for 5 minutes, followed by washing in PBS for 5 minutes (x3). Slides were then incubated in the peroxidase substrate solution (VectorLabs, No. SK-4600) until the desired staining intensity was achieved. Finally slides were rinsed in tap water for 5 minutes and counterstained (if required) before clearing in graded alcohols and mounting with DPX.

#### 2.3.7.6 IMMUNOFLOUORESCENT STAINING ANTIBODIES

**Primary Antibodies:** Goat anti-cathepsin L (S-20) polyclonal antibody (Santa Cruz Biotechnology Inc. Cat No. SC-6500) used at 1:100 dilution, MMP-2 mouse anti-human-MMP-2 monoclonal antibody (Cat. MAB3308 Chemicon, UK) and MMP-9 mouse anti-human-MMP-9 monoclonal antibody (Cat. MAB3309 Chemicon, UK).

**Secondary Antibodies:** Mouse anti-goat rhodamine conjugated secondary antibody (100:1 dilution) (Cat, AP300R Chemicon UK) MMP-2 and MMP-9 used a horse-anti-mouse-FITC conjugate in a 1:100 dilution (Cat, 5024 Chemicon UK).

#### 2.3.7.7 IMMUNOFLOUORESCENT STAINING PROTOCOL

Slides were dewaxed in xylene 2 x 2mins followed by IMS 2 x 1min then washed in PBS 2 x 5mins. Slides were then incubated in blocking solution (0.5 mg bovine serum albumin, 333 µl FCS, 10 ml PBS) for 20 minutes at room temperature. The blocking solution was removed and the primary antibody (made up in blocking solution) applied, then incubated at 4°C overnight. Slides were washed in PBS (2 x 5 minutes), followed by incubation in the appropriate fluorescently tagged secondary antibody made up in blocking solution for 30 minutes at room temperature; slides were protected from light. Finally the slides were washed 2 x 5 minutes in PBS and mounted using DAKO fluorescent mounting medium (DAKO, Cat No. S3023 Ely, UK).

#### 2.3.7.8 BROMODEOXYURIDINE INCORPORATION AS PROLIFERATION MARKER

Assessment of cell proliferation used the incorporation of pyrimidine bromodeoxyuridine (BrdUrd), an analogue of the nucleotide uracil during DNA replication. Mitotic cells are identified by immunocytochemistry as those with nuclear DNA stained dark brown. BrdUrd is prepared to a final concentration of 10  $\mu$ M in the growth media, which is added to the cell culture. This is then incubated for 24 hours in standard cell culture conditions. After 24 hours the growth media was aspirated off leaving the cell/matrix, which was then fixed with 70% ethanol in PBS/0.5% Tween 80 for 30 minutes at room temperature. The fixative was then diluted in equal volumes 4M HCl for a further 30 minutes. After washing twice (2 x 10 minutes) with PBS/0.5% Tween 80, mouse anti-BrdUrd (DAKO, Ely, UK) in PBS/1% Bovine Serum Albumin (BSA) added at a dilution of 1:50, and incubated over night at 4°C. After a further two washes (2 x 10 minutes) with PBS/0.5% (v/v) Tween 80, the secondary antibody, Horse radish Peroxidase (HRP) conjugated rabbit anti-mouse IgG (DAKO, Ely, UK) in PBS, 1% (v/v) BSA, was added to a dilution of 1:200 and incubated for 30 minutes at room temperature. After further washings (2 x 10 minutes) with PBS/0.5% (v/v) Tween 80, the chromogen DAB was added. Its development was monitored using the light microscope and arrested at completion (approximately 5-10 minutes) by rinsing with tap water thus identifying nonmitotic cells. Cell proliferation was assessed by microscopic visualisation of dark brown stained cells (BrdUrd nuclear stain).

#### 2.3.7.9 LABELLING FIXED CELLS USING DAPI

From a stock solution of DAPI (m.w. 350) at 10 mg/ml made up in distilled H<sub>2</sub>O, a 5000-fold dilution in PBS was prepared for labelling cells. Cell media was aspirated and the samples rinsed in PBS for 5 minutes (x3). Samples were then fixed in a freshly made up 3.7% formaldehyde solution for 10 minutes followed by permeabilization of the cells by immersion in 0.2% Triton X-100 for 5 minutes. This solution was then aspirated and samples rinsed in PBS for 5 minutes (x3). Samples were then incubated in the prepared DAPI labelling solution for 1-5 minutes at room temperature. Samples were then rinsed in PBS for 5 minutes (x3) and mounted. Observation of DAPI labelled DNA was carried out with a Zeiss Florescent microscope and image analysis with

software from Image Associates, UK. The excitation wavelength maximum is near 359 nm and the emission wavelength maximum is approximately 461 nm when bound to DNA. It is believed that DAPI associates with the minor groove of double-stranded DNA with a preference for the-AT clusters. Fluorescence increases approximately 20-fold when DAPI is bound to double-stranded DNA.

## **2.3.8 MICROSCOPY**

### **2.3.8.1 LOW-TEMPERATURE SCANNING ELECTRON MICROSCOPY**

Prior to examination with the low temperature SEM specimens are washed (gently) with PBS (3x) to remove any protein residues left from the media. Then specimens were fixed with 1% (v/v) glutaraldehyde being added per well for two hours prior to viewing. Both low temperature scanning electron microscopy and standard vacuum SEM, used the JEOL JSM-6310 SEM (Jeol Tokyo, Japan).

The cold stage and anticontaminator were cooled with nitrogen gas at a pressure of 0.5 kg/cm<sup>2</sup> (7psi) for 1-2 minutes. The dewar was then filled with liquid nitrogen (the inlet was checked to ensure it was not restricted). The dewar was topped up and gas flow adjusted as was necessary as the temperature on the control monitor dropped to approximately -180°C as the system cooled. Likewise the cryo-preparation chamber dewar was filled with liquid nitrogen, until the temperature fell below -160°C. Both dewar were topped up as necessary throughout the session to maintain temperature. The specimens were fixed to the rod/holder with glue (Tissue tek, OTC compound plus carbon, EM Supplies, UK) and plunged into nitrogen slush for several minutes to allow the specimen plus holder to fully cool. The specimen was then transferred from the nitrogen slush into the vacuum transfer device. The chamber was then flushed with N<sub>2</sub> gas. Once completed the specimen and holder were located onto the cold stage of preparation chamber.

The temperature was set on the controller to -85 to -95°C to allow sublimation at a controllable rate. The heater was then activated whilst observing the specimen at a

low KV monitoring the sublimation. When completed the specimen was transferred back to the cryo-preparation stage. The stage temperature was maintained at -170°C or colder and the vacuum set to 0.1 torr. The splutter was then activated and volts set to maximum (30 seconds). The argon valve was slowly opened until the current rose and stabilised at approximately 1-2 milliamps. The timer was reset to 2-3 minutes and specimen was positioned directly beneath the splutter head. The timer is activated to commence coating. When complete the argon valve was closed and volts set to zero. The specimen holder (plus specimen) was transferred from the cryo-preparation stage to the SEM cold stage and viewed in the normal way at 10-15 KV.

#### 2.3.8.2 STANDARD SCANNING ELECTRON MICROSCOPY

Specimens were fixed in two stages firstly as in section 2.4.2.1. secondly with osmium tetroxide to stabilise cellular lipids. Fixation was carried out by preparing a 25% (v/v) solution of osmium tetroxide in which tissue sections were immersed. Fixation required 1 hour with specimens held in a slow revolving mixer. After fixation specimens were dehydrated in graded acetone treatments (50, 60, 70, 80, 90, 95 and 100% dry acetone). Samples were then critical point dried (Polaron 3000, Agar Scientific, Stanstead, UK), by draining acetone and replacing with liquid CO<sub>2</sub> in the critical point dryer. The temperature was then gradually raised above 31°C at a pressure of 1150 p.s.i. (critical point) to 35°C, at which the liquid CO<sub>2</sub> behaves as a gas and is bled away. Samples were coated in gold in a similar fashion to the LT-SEM method described above. Samples were viewed under vacuum with the JEOL JSM-6310. Both LT-SEM and standard SEM images were saved as TIFF files.

#### 2.3.8.3 PHASE-CONTRAST LIGHT MICROSCOPY

Specimens of both tissue and collagen are fixed in the same manner as for standard histological analysis with formal saline (room temperature) for a minimum of two hours prior to staining. Once fixed, specimens stained as appropriate and visualised electronically. All digital images other than SEM derived images were obtained using a Carl Zeiss Axioskop2 phase-contrast microscope utilising a JVC 3-CCD KY-F55B colour video camera with a KS 300 Imaging System (Imaging Associates Ltd, Thames,

UK). All light microscopy images (including florescent) were saved as JPEG files.

#### 2.3.8.4 FLUORESCENT MICROSCOPY

All florescent image analysis was carried out using a Carl Zeiss Axioskop2 florescent microscope at wave lengths described in section 2.2.5.

## CHAPTER THREE: STATIC CELL CULTURE ON PORCINE TYPE I COLLAGEN

### 3.1 INTRODUCTION

Considerable efforts have been made to produce non-toxic, stable and non-immunogenic biomaterials that retain natural mechanical characteristics. Cross-linking methodologies, which include glutaraldehyde, carbodiimides, hexamethylene diisocyanate (HMDI) and a variety of other fixation methods, often proved problematic due to issues of toxicity. This is of particular significance to this chapter as the process used to stabilize, or cross-link this particular collagen matrix utilises HMDI as the cross-linking agent. HMDI is proposed to degrade to hexamethylene diamine and is cited to be minimally cytotoxic (Chvapil, 1992 and Khor, 1997). Further evidence of its cytotoxic nature has been reported e.g. (van Luyn et al., 1992a), in particular Bellincampi and Dunn, (1997), declared that the compound in their hands was “impractical for use in a tissue engineering device”. Using a methylcellulose cytotoxicity cell culture test (van Luyn et al., (1991) reported that HMDI elicited both primary and secondary cytotoxicity; the primary toxicity being the direct diffusion of the residual compound and the secondary cytotoxicity by enzymatic actions, and aqueous hydrolysis. Although the bulk of the toxic compounds were released by 6 days, glutaraldehyde, by contrast was shown to elicit a secondary response for as long as 42 days (van Luyn et al., 1992b). van Luyn et al (1992b) concluded the residual secondary response would not “seriously influence biocompatibility over time”. Bellincampi et al (1997) compared several methods of cross-linking collagen fibres, including ultraviolet radiation, dehydrothermal treatment and HMDI, and found that fibroblast attachment, proliferation and morphology on HMDI cross-linked collagen was significantly lower than other methods of cross-linking. The primary cytotoxic response to both glutaraldehyde and HMDI is reduced after the application of controlled washing regimes. Repeated exposure of human fibroblasts to HMDI cross-linked materials eliminated all cytotoxic substances by day 18 (Bellincampi and Dunn, 1997). Published methodologies for the preparation of biological tissues for biomaterial development and components of the extracellular matrix (ECM) are further discussed in Chapter 4.11 (ECM components) and 4.1.2 (processing biological tissues).

This chapter describes the gross morphology of the type I dermal collagen matrix used in this thesis, where preliminary growth studies to characterise (qualitatively) the ability of cells (HUVEC and hVSMC) to adhere, grow and proliferate under static conditions followed by modifications to the matrix to improve cellular compatibility have been conducted.

## **3.2 MATERIALS AND METHODS**

### **3.2.1 MATERIALS**

General materials and methods are described in Chapter 2, including protocols for the isolation and culture of primary HUVEC and hVSMC, SEM sample preparation, processing, histology, immunohistochemistry and image analysis. Discrete protocols, unique to this chapter are described within Section 3.2.2.

### **3.2.2 EXPERIMENTAL METHODS**

#### **3.2.2.1 TYPE I DERMAL COLLAGEN PREPARATION**

The initial stages of this project assumed that, since this matrix had been cleared for human implantation there would be negligible, if any, cytotoxic effects. The first step in preparation therefore was to simply cut uniform sections of equal surface area that allows an accurate assessment of cell numbers per unit area. To this extent a simple set of protocols were developed to cut and wash the collagen matrix whilst maintaining sterility. The material were cut manually under sterile conditions with a scalpel into 10 x 10mm (100mm<sup>2</sup>) sections immediately prior to experimental use. Later cutting methods utilized a circular (16 mm diameter, 2 cm<sup>2</sup>) leather punch. The protocol was altered to ensure the collagen surface area remained consistent, as manually cutting squares proved inconsistent. Also circular disks would fit directly into the wells of standard culture plates without any exposed plastic. The benefit of this is that no compensation is required for seeding volume to actual seeded density. An added benefit is that the collagen is handled less thus reducing the risk of contamination.



### ***Washing potentially contaminating toxic compounds from the matrix***

In order to achieve increased cell adhesion, growth and continued proliferation, a protocol of washing the collagen was developed to ensure removal of non-bound cross-linking agent (HMDI) and any other potentially toxic compounds, including acetone. Other than using the matrix material directly from its sterile packaging, two other methods were used to remove potentially contaminating compounds:

**Method one:** A preliminary washing protocol was used to establish the effectiveness of washing the matrix prior to cell seeding. The matrix (no more than 9 disks/50ml) was washed for two weeks in 100 ml HBSS containing Penicillin, Streptomycin (250µl) and Fungizone (50µl) to guard against potential bacterial contamination, with the solution being changed twice over the two week period.

**Method two:** The second method was designed to maximise the washing process, as follows. Square cut sections 10x10x1.5 mm (LxWxD), or disks (1.5x16 mm diameter) were cut to size and placed in 25 ml Sterilin tubes, eight separate washes (no less than 3 hours each) in sterile PBS were applied followed by two washes in the appropriate media for the cell type to be cultured. The final solution (media) included 100 µl Fungizone per 20ml media in addition to the standard 100U/ml penicillin and 100µg/ml streptomycin to guard against potential bacterial and fungal contamination.

### **3.2.2.2 ADHESION AND PROLIFERATION ON STANDARD AND MODIFIED DERMAL COLLAGEN MATRIX**

HUVEC and hVSMC were seeded onto the sterile matrix directly from its packaging, for culture periods of 20, 96 and 168 hours prior to assessment by LT-SEM. Studies of cell growth and cytotoxicity were conducted with VSMC and HUVEC (PII-PV), at densities ranging from  $1.4 \times 10^4$  and  $4.5 \times 10^5$  cells/ml. Removal of cells from plastic and matrix material was achieved with the use of the proteolytic enzyme trypsin to digest adhesion molecules binding the cells to Permacol, thus releasing it into solution, see Section 2.2.2 for details on cell passaging and general culture. Viability as determined with Sigma's standard protocol, see Section 2.3.2.9. Prior to counting sample wells were washed gently with PBS to remove cells in free solution. Standard tissue culture techniques were carried out, where media was changed every three days.

### ***Cell viability***

A quantitative assessment of cell and viability on type I collagen was assessed with (0.4%) Trypan Blue, Sigma 192 protocol. HUVEC (PIII) were seeded at density of  $6.5 \times 10^4$  cell/ml ( $3.25 \times 10^4$  cell/cm<sup>2</sup>) onto 10x10x0.75 mm (LxWxD) type I collagen. The matrix was prepared as per protocol 1, Section 3.2.2. The Matrix was removed directly from the packet i.e. not washed prior to cell seeding. Samples were cultured in 4 well tissue culture plates with a total surface area of 2 cm<sup>2</sup>. Each culture plate (4 wells) contained 2 controls and 2 matrix samples. The cell suspensions were pipetted evenly over the entire surface area of both controls and matrix samples. Removal of cells from both plastic and Permacol was achieved with the use of the proteolytic enzyme trypsin. Prior to counting sample wells were washed gently with PBS to remove cells in free solution. For details on cell passaging and general culture, see Section 2.2.2. Procedure: Total solution volumes equal 1.0 ml, comprising 0.5 ml of 0.4% Trypan Blue, 0.3 ml HBSS and 0.2 ml of cell suspension (dilution factor = 5). The suspension is mixed thoroughly and allowed to stand for 5-15 minutes. Cells that stain dark blue after the incubation period are deemed non-viable.

### **3.2.2.3 INVESTIGATION OF PRE-SEEDING CONDITIONS TO ENHANCE CELL ADHESION AND PROLIFERATION**

#### ***Bromodeoxyuridine Proliferation Assay***

The BrdUrd protocol has been described previously in Section 2.3.3.8. Cell types used: hVSMC and HUVEC. Seeding densities for hVSMC (PIV) and HUVEC (PIV) were  $4 \times 10^4$  and  $9 \times 10^4$  cell/well respectively. A preliminary washing protocol was used to establish the effectiveness of washing the matrix prior to cell seeding. The matrix was washed for two weeks in 100 ml HBSS containing Penicillin, Streptomycin (250µl) and Fungizone (50µl) with the solution being changed twice. Comparisons between washed and non-washed matrix in terms of cell proliferation were conducted with both HUVEC and VSMC. Primary cell cultures were cultured as per standard protocols and seeded onto 16 mm diameter matrix disks (see section 3.2.2.1). Cells were seeded at  $1.08 \times 10^5$  (HUVEC) and  $1.21 \times 10^5$  cell/well (VSMC), [to convert to cell/mm<sup>2</sup> divide total cell number by matrix disk area 201 mm<sup>2</sup>, 537 and 600 cell/mm<sup>2</sup> respectively]. Cells were seeded either directly onto non-washed matrix, straight from packaging, or washed matrix. A standard washing protocol was adopted. A total of nine, 16 mm disked could

be cut from each 5 x 5 matrix sheet. These 9 disks were washed in 50 ml of sterile PBS followed by two washes in the appropriate media for the cell type to be cultured on a standard bottle roller. Washes were no less than 2 hours between each wash. The final solution (media) included 100U/ml penicillin, 100 µg/ml streptomycin with 100 µl/20ml Fungizone (final concentrations) to minimize any potential contamination. Cell counts were conducted as described in Section 2.3.1.1.

#### ***Chemical modification with sodium hydroxide***

Matrix disks were immersed in a 0.2 M solution of NaOH for 4 minutes (matrix begins to turn opaque) at room temperature ( $16 \pm 3^\circ\text{C}$ ). Disks were then washed (2x rapidly) plus 3 further washes with a minimum of 1 hour between each. Disks were stored at 4°C in the final wash (media as above) until required.

#### ***Matrix modification by heparin***

Matrix disks were immersed in 5 ml Heparin (Heparin 5000 U/ml<sup>-1</sup> monoparin, CP Pharmaceuticals, UK) plus 20 ml PBS for 48 hours on the rock/roll table. Solution is then drained and replaced with high serum SMC media containing additional 250 U/ml penicillin and 250 µg/ml streptomycin and 100 U/ml of nystatin (final concentration), stored at 5°C until required. At prescribed days, samples were removed from culture, and fixed for analysis. Controls were seeded onto culture plates, without collagen disks.

### **3.2.3 ANALYTICAL METHODS**

All analytical methods used in this chapter are described in Chapter 2, Material and Methods.

### 3.3 RESULTS

#### 3.3.1 MORPHOLOGY OF THE DERMAL COLLAGEN MATRIX

The aim of this section was to characterise the matrix in terms of its morphological microstructure, whereby transverse sections of matrix samples were cut and prepared for histological analysis as described in Section 2.3.3.1 and viewed by either phase contrast microscopy or LT-SEM. Cross-sections of the dermal collagen display large interwoven collagen fibres characteristic of type I collagen, Figure 3.01. The surface of the matrix exhibited open areas that lead into the matrix, where areas of free space are visible between the large collagen fibrils. Spaces or gaps in the fibrous structure are important for cell migration into the matrix.

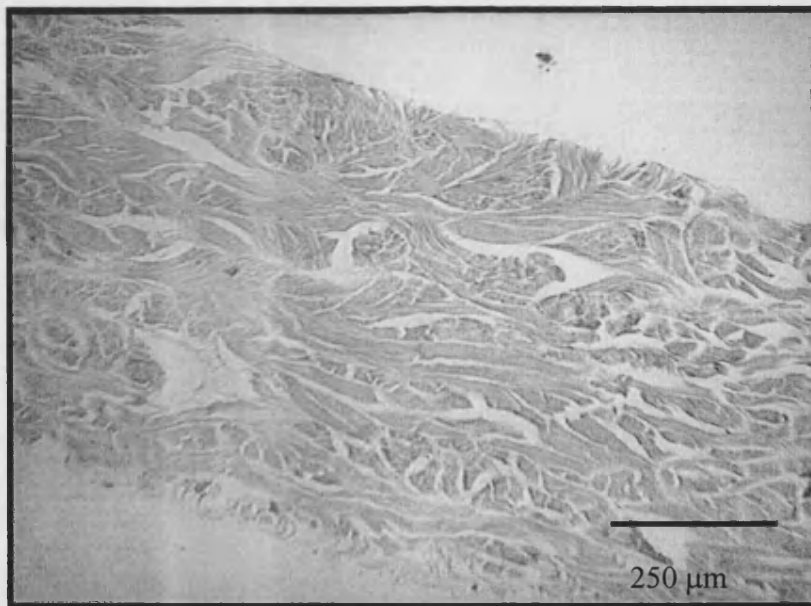


**Figure 3.01:** A transverse section of the porcine derived type I dermal collagen matrix. The matrix (0.75 mm thick) displays the interwoven nature of the predominantly type I collagen, H & E stained.

The surface morphology of the collagen matrix was assessed using low-temperature scanning electron microscopy (LT-SEM). These images detail this matrix surface structure, as predominately flatted or compressed areas confirming the phase contrast microscopy results that show a nonuniform matrix surface see Figures 3.02. Figure 3.03, a higher magnification of the fibrous matrix surface shows pores in the matrix fibres as up to 15  $\mu\text{m}$ . Figure 3.04, like Figure 3.03, shows a higher magnification detailing the flattened or compressed collagen fibres that are unlikely to allow cell migration via passive motility.

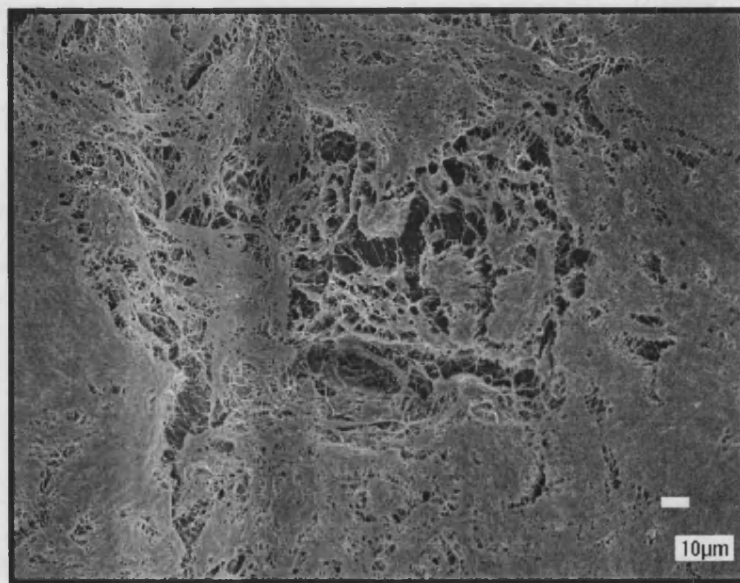


**Figure 3.02:** Low magnification LT-SEM displaying the variable surface morphology of the type I dermal collagen matrix. In addition to the flat or compressed sections a more open porous structure is noted with 'pores' up to 30 x 15  $\mu\text{m}$ .

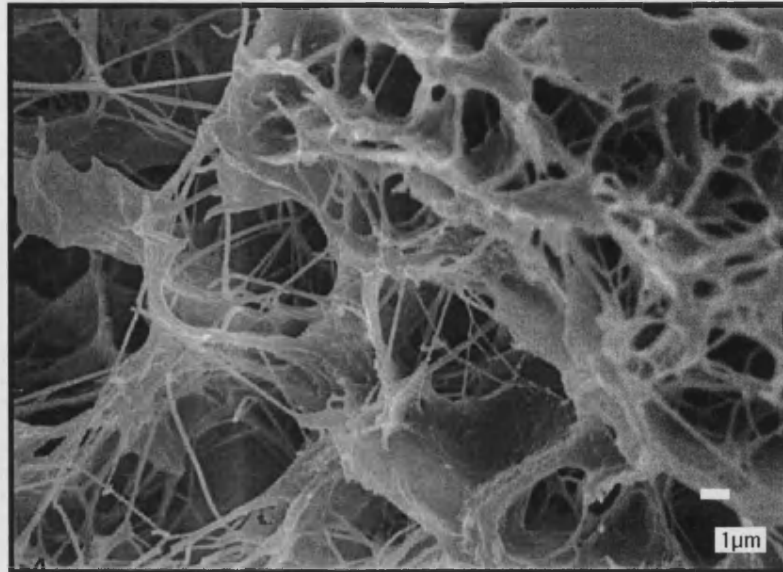


**Figure 3.03:** Higher magnification LT-SEM detailing the fibrous structure of the collagen matrix. Pores ranging from 1-10  $\mu\text{m}$  are evident.

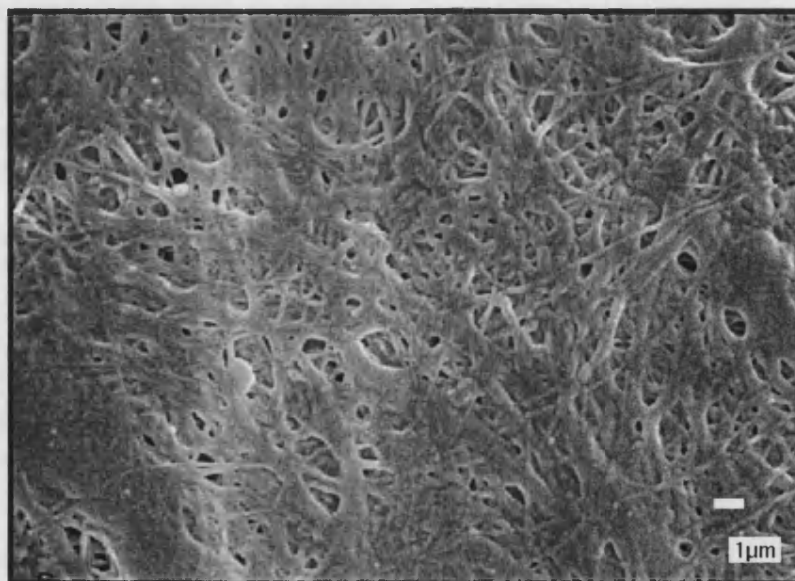


**Figure 3.04:** High magnification LT-SEM of the flattened or compressed surface fibres of the type I dermal collagen matrix. Compared to pores in the fibrous regions this compressed morphology has pores less than 1  $\mu\text{m}$  (qualitative assessment).

### 3.3.2 ASSESSMENT OF CELL ADHESION AND PROLIFERATION ON THE DERMAL COLLAGEN MATRIX

#### hVSMC GROWTH ANALYSIS

A growth analysis was conducted with SMC resulting in a typical growth curve, Figure 3.05. Cells were enzymatically removed from the surface of the plastic culture plate. Results were expressed as the mean number of cells/mm<sup>2</sup>. Although this growth analysis indicates a 'typical' growth curve it was noted that large variations occur in cell doubling times between different individuals (patients) with differing stages of disease. A standard growth analysis of hVSMC was conducted to use as a base or reference point for hVSMC culture directly on the type I dermal collagen matrix. Results show an expected increase in cell density of approximately 114 cells/mm<sup>2</sup> until proliferation plateaus at approximately 1150 cell/mm<sup>2</sup> at 3 weeks after cell seeding.

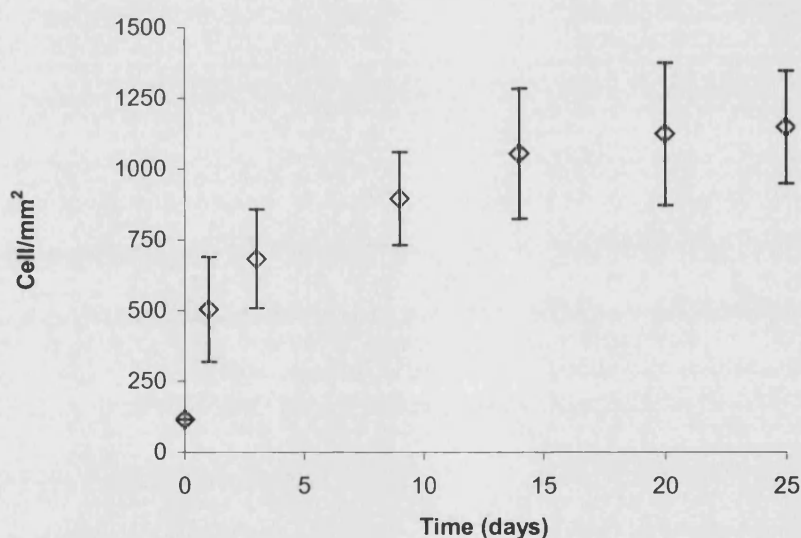


**Figure 3.05:** Standard growth profile of primary hVSMC on tissue culture plastic, error is shown as from triplicate samples from one tissue/cell isolation.

## HUVEC AND hVSMC ADHESION ON PERMACOL

These experiments were designed to assess the ability of human cell lineages (HUVEC and hVSMC) to adhere, maintain adhesion, grow and proliferate in static growth conditions on the type I dermal collagen matrix. Cells were seeded onto the dermal collagen matrix and cultured using techniques described in Section 2.2.2. At prescribed time points (approximately 1, 4 and 7 days) samples were removed from culture rinsed in PBS and fixed in glutaraldehyde in preparation for LT-SEM, as described in Section 2.4.2.1.

HUVEC seeded at  $1 \times 10^5$  and  $2 \times 10^5$  cells/ml and cultured for approximately 1 day have adhered to the matrix with pseudopodia-like structures extending into the matrix, cell-cell contacts have formed indicating a maturation of adhesion post initial contact. Cells appear both singularly (see Figure 3.07) and in clusters (see Figure 3.06) randomly dispersed over the entire matrix surface. As a qualitative assessment, densities are an order of magnitude less than plastic controls. Visual assessment of HUVEC seeded onto the matrix displayed little difference in cell density when seeded at twice the density  $1 \times 10^5$  and  $2 \times 10^5$  cells/ml. Both HUVEC and hVSMC were found in higher concentrations randomly dispersed over the matrix surface, with other areas completely void of all cells. Figure 3.07 a LT-SEM of HUVEC after 1 day static culture showing a single cell with a pseudopodia-like protrusion (A) extending into the matrix pores. Further details of cell-cell contacts are shown in Figure 3.08. Similar results were found with hVSMC, Figure 3.09.



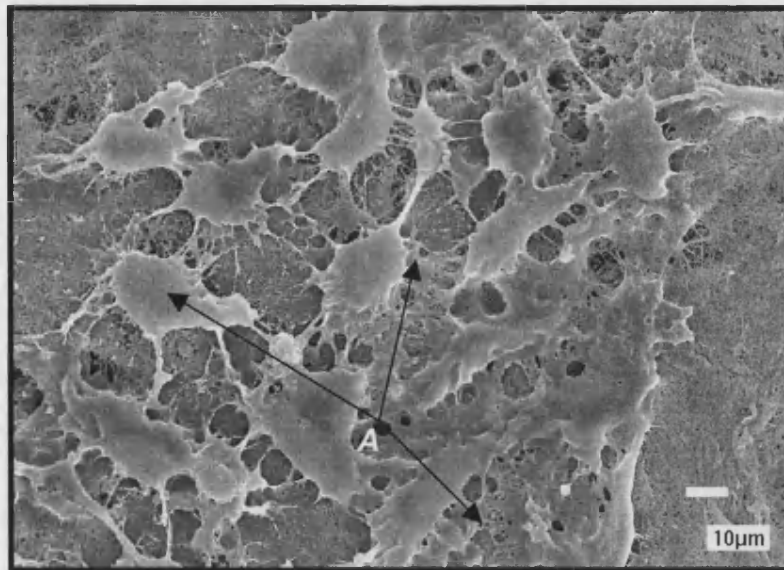


**Figure 3.06:** HUVEC (A) cultured for 1 day on the dermal collagen matrix. Cells were seeded onto the matrix at  $1 \times 10^5$  cell/ml.

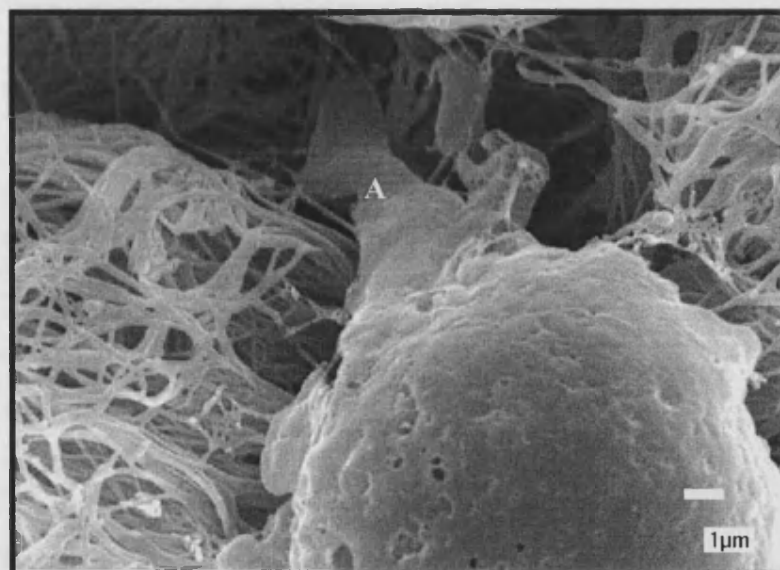


**Figure 3.07:** A HUVEC cell displaying pseudopodia-like structures (A) extending into the matrix

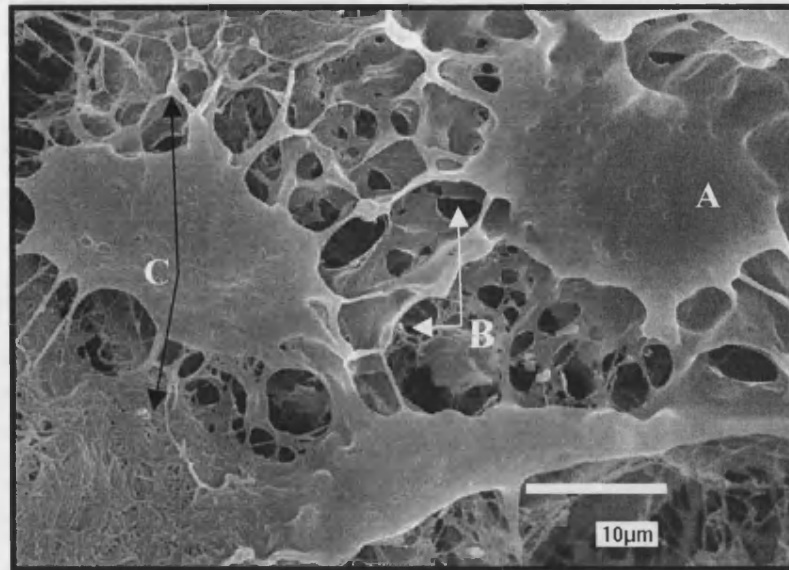


**Figure 3.08:** Cell-cell (B) and cell-matrix (C) interactions of HUVEC (A) after 20 hours static culture. At higher magnifications these interactions are clearly visible; HUVEC were seeded at  $2 \times 10^5$  cells/ml

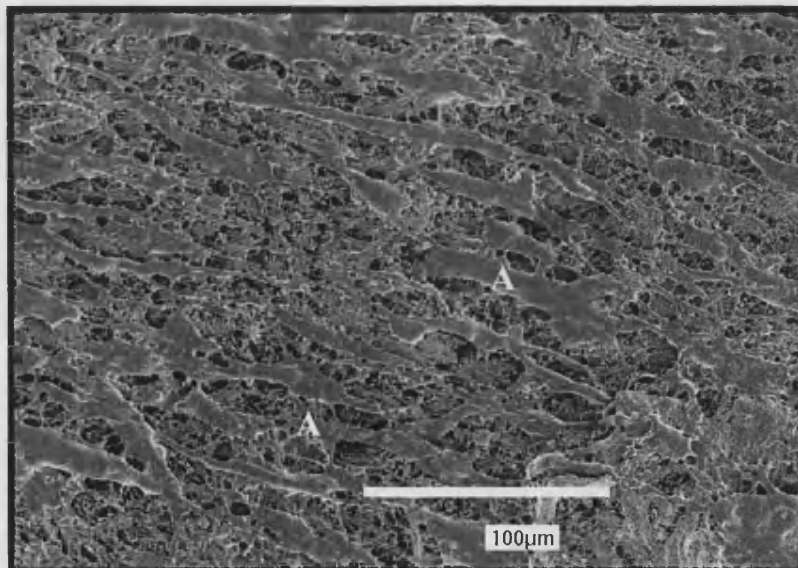


**Figure 3.09:** 20 hour static cultures of hVSMC (A) seeded on the dermal collagen matrix. hVSMC seeded at  $1 \times 10^5$  cell/ml displayed similar densities to HUVEC cultures, where both high and low densities of cells were present. In this image hVSMC appear longitudinally orientated.

After 4 d culture periods, LT-SEM analyses of HUVEC show cells remain adhered to the matrix and display similar morphologies and densities to 20 hour cultures. Figure 3.10 shows HUVEC seeded at  $1 \times 10^5$  cell/ml onto the type I collagen matrix (non-washed), again regions of higher densities were observed randomly over the matrix surface. The only distinct difference noted between the two time points was the appearance of more advanced cell-cell contact, Figure 3.11. Little difference, if any, is noted between seeding densities of  $1 \times 10^5$  cell/ml and  $2 \times 10^5$  cell/ml (qualitative assessment). hVSMC cultured over the 4 d period, like HUVEC, had adhered to the matrix displaying similar densities to HUVEC cultures seeded at the same density. Again cells appear both singularly on the matrix and in clusters, see Figure 3.12 where hVSMC morphology was difficult to interpret in this series of images. Compared to confluent cell layers on flat-bottomed T25 culture flasks (controls) cell densities are considerably lower (qualitatively).

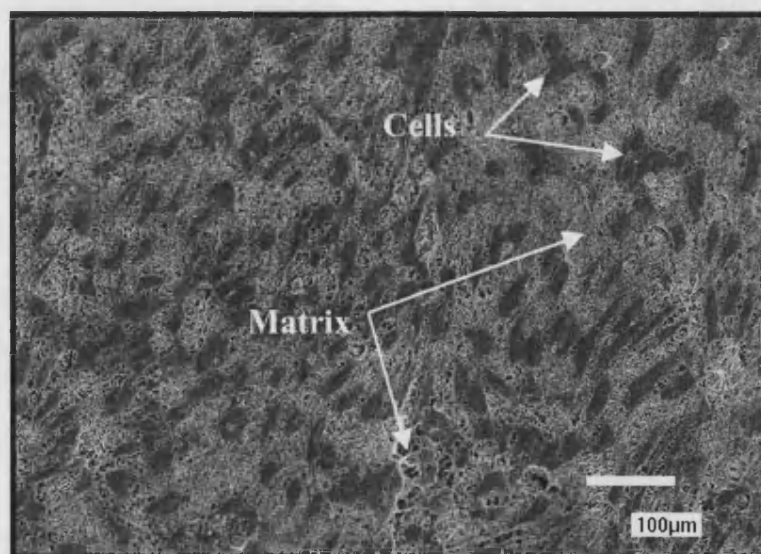


**Figure 3.10:** 96 hour culture of HUVEC on the dermal collagen matrix. HUVEC were seeded at  $1 \times 10^5$  cell/ml onto the type I collagen matrix and cultured under static conditions.

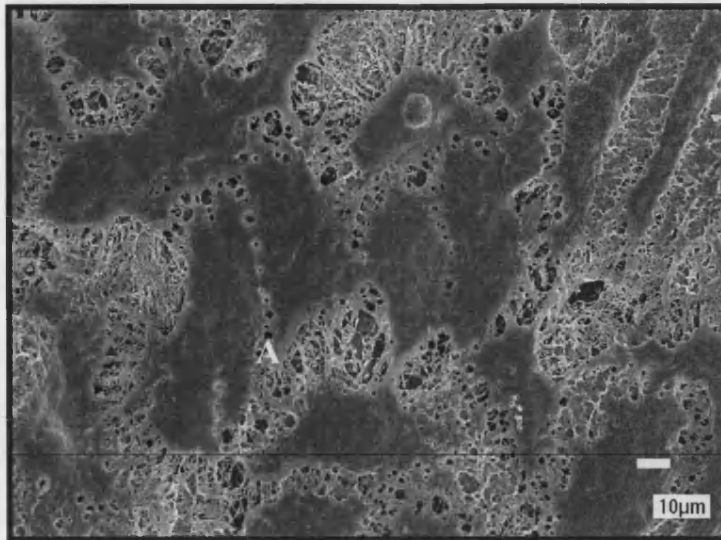


**Figure 3.11:** LT-SEM of HUVEC after 4 days static culture on the dermal collagen matrix. Cells display signs of more established cell-cell contact (A).



**Figure 3.12:** hVSMC cultured for 96 hours ( $1 \times 10^5$  cell/ml) under static conditions on the dermal collagen matrix, cell morphologies were more difficult to interpret.

Few cells remain adhered to the matrix after 7 days culture. Both HUVEC and hVSMC appear stressed (rounded and globular) compared with cells cultured for 1 and 4 days, Figures 3.13 and 3.14. Both cell types are morphologically similar, displaying a contracted globular nature as cells loose adhesion to the surface of the collagen matrix followed by detachment, cumulating at 7 day culture period.

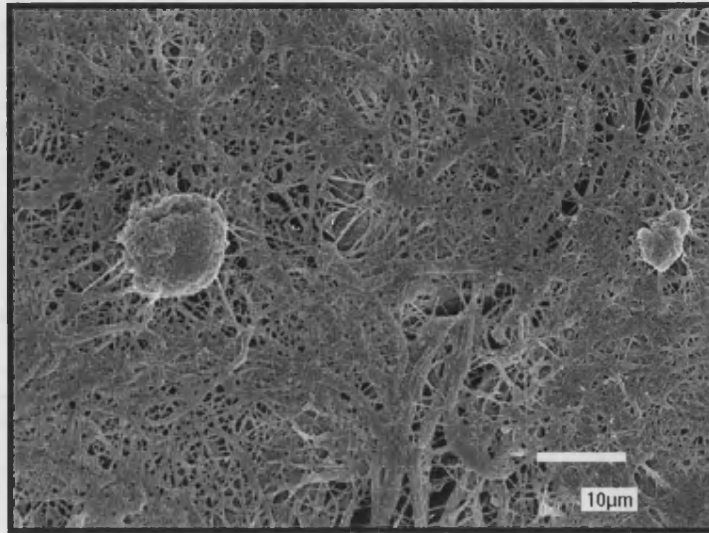


**Figure 3.13:** HUVEC reduction in cell density after 7 days static culture on the dermal collagen matrix. HUVEC seeded at  $2 \times 10^5$  cell/ml, on non-washed dermal collagen

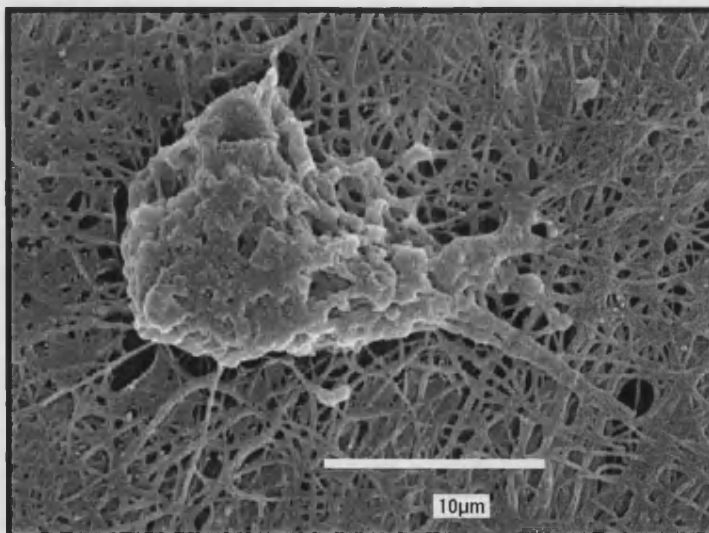


**Figure 3.14:** Loss of viability and cell adhesion of hVSMC after 7 days static culture, as noted by the qualitative reduction in total cell density over the experimental time course.

### ***Expanding zone of cell necrosis***

This experiment was designed to assess (qualitatively) if any cytotoxic compounds were leaching from the matrix resulting in a loss in cell viability. Previous observations noted an expanding zone (over time) of cell exclusion emanating from the collagen matrix, where controls display normal cell growth and morphology. Square sections, 10x10x1.5 mm (LxWxD) of the dermal collagen were placed into larger (35 mm OD), circular culture plates (6-well Nunc. UK), where an area of plastic void of collagen remained for cells to adhere and monitor cell morphology over time. SMC (PIII) and HUVEC (PV) were seeded at a density of  $4.5 \times 10^5$  cell/ml and  $2.5 \times 10^5$  cell/ml respectively onto the matrix and surrounding plastic of the culture well. Cultures were observed with an inverted phase-contrast microscope, observational evidence only.

From the initial seeding through to day-3 cells (both HUVEC and hVSMC) display 'normal' morphology surrounding the matrix. After 5 days cells adhered immediately adjacent to the matrix and were showing gross changes in morphology compared to controls. By day-7 both hVSMC and HUVEC in the zone immediately around the matrix appear to have lysed, with cells of typical morphology present only at the extreme edge of the culture wells, again controls normal. Day-10 results where as day-7. After 10 days an increase in cell density was observed at the periphery of the culture well. Controls displayed normal cell morphologies and typical confluent densities.

### ***Cell viability on Permacol***

Cell viability was assessed with trypan blue, used as a dye exclusion assay for cell viability procedures, see section 2.3.7.9. Post seeding there is an initial decline in cell density, considered normal when seeding primary human cells onto any surface. Control data show a consistently higher cell density compared with cells seeded on Permacol. Cells seeded onto the dermal collagen matrix follow a similar pattern of decline to control samples immediately post seeding, though cell numbers did not recover and remained low compared to controls. Non-viable cell numbers were also lower compared to controls, which indicates a lower total cell number.

The general trend indicates a low percentage cell adhesion and little if any cell growth and/or proliferation. Results displayed in Figure 3.15 show HUVEC adhesion and proliferation as the mean number of cells per  $\text{cm}^2 \pm$  one sd.



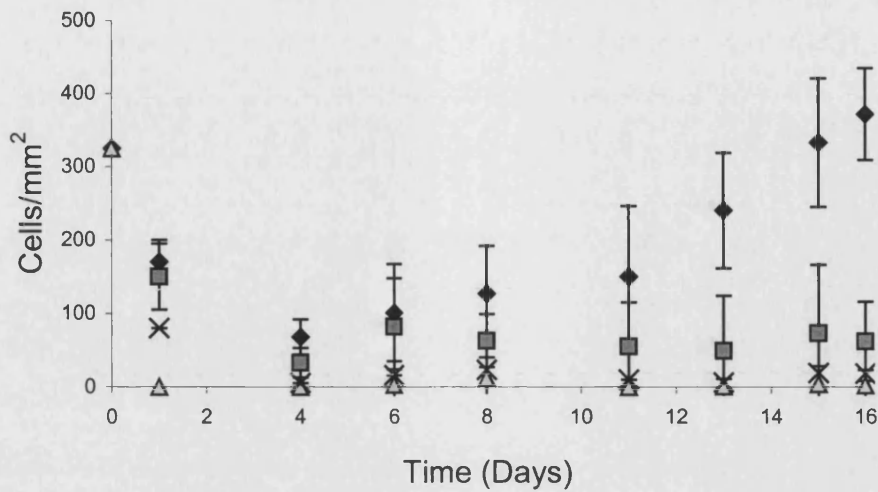


**Figure 3.15:** HUVEC viability on collagen matrix and plastic controls: ♦ control-viable, ■ control-nonviable, x collagen-nonviable, △ collagen viable.

### 3.3.3 ENHANCEMENT OF CELL ADHESION AND PROLIFERATION ON THE DERMAL COLLAGEN MATRIX

A critical issue in tissue engineering is the lead-time from the isolation of (autologous) cells, the bulking-up phase through to the mature Tissue Engineered construct within the bioreactor. Particularly so with replacement organs such as the heart, vascular tissue, liver etc., where extended culture periods may impact directly of patient mortality. The rate at which a population of cells reach an optimal density is critical; an important step to optimise. With the aim to further enhance initial cell adhesion and subsequent proliferation rates, methodologies were assessed to determine if modifying the surface of the dermal collagen matrix would affect cell adhesion/growth. In this series of experiments cell proliferation was assessed after the dermal collagen matrix had been washed. The effect of further washing the matrix was then assessed in terms of cell density over time. In order to further improve adhesion and growth dynamics, the matrix surface was modified by exposure to heparin and NaOH, with comparative analysis. NaOH modifies the surface structure of the collagen matrix by attacking acidic residues, were as heparin has been shown to improve cell adhesion (Bos et al.,

1998), enhance vascularisation (Doi and Matsuda, 1997) and reduce the incidence of intimal hyperplasia (Laemmel et al., 1998).

#### CELL PROLIFERATION

The presence of an unknown cytotoxic compound (possibly residues from the HMDI cross-linking process, known to be cytotoxic) diffusing from the collagen matrix was clearly affecting cell viability. To determine whether or not a simple washing step may reduce or eliminate this compounds effect, HUVEC PIV ( $9 \times 10^4$  cells/well) and hVSMC PIV ( $4 \times 10^4$  cell/well) were seeded onto a pre-washed matrix (matrix preparation see method 1, Section 3.2.2.1) with the aim of confirming cellular proliferation as opposed to adhesion and growth during the early stages of cell culture. Cell proliferation was assessed by assaying for the primidine bromodeoxyuridine (BrdUrd), a nucleotide analogue and its incorporation into DNA during DNA replication. Figure 3.16 displays BrdUrd positive cells with nuclear regions stained brown. The time point of day 5 was chosen being immediately after the last day of confirmed cell adhesion (day 4) and was prior to the loss of cell adhesion by day 7. Clearly cells are proliferating at day 5, indicating the washing step had improved conditions for cell culture compared to non-washed controls.

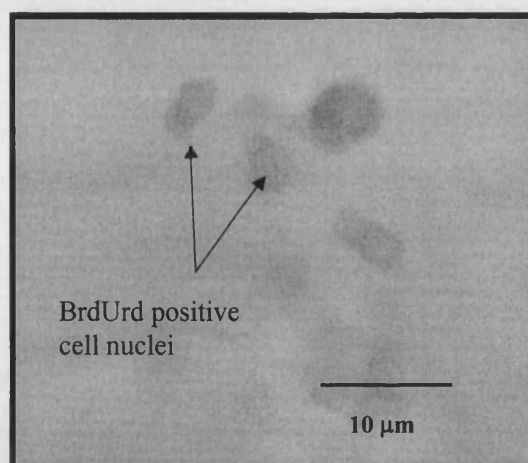


**Figure 3.16:** Conformation of HUVEC proliferation by positive staining by BrdUrd. After a preliminary matrix washing step and 5 days in static culture, mitotic (or post mitotic) cells (proliferating cells) were identified by dark stained nuclear DNA (BrdUrd assay).



### Matrix washing

In order to maximise the washing process collagen sections were cut to size and a more comprehensive washing protocol applied, method 2, as described in Section 3.2.2.1. This experiment emphasised the need to wash thoroughly the collagen matrix, where a near eight-fold increase in cell density of hVSMC and HUVEC over 30 days to non-washed collagen is observed, Figures 3.17-19. At day 16 cells (both hVSMC and HUVEC) on the washed matrix displays a four-fold increase in cell density from day 16 through day 30, Figure 3.17. In contrast densities of cells seeded directly onto matrix (non-washed) continue to decline until day 22 where densities begin to rise from a low of 27 cell/mm<sup>2</sup> back to 65 cell/mm<sup>2</sup> approximately equivalent densities at day 16 (66 cell/mm<sup>2</sup>). See Figures 3.18 and 3.19 for comparative smooth muscle cell growth at 30 days.

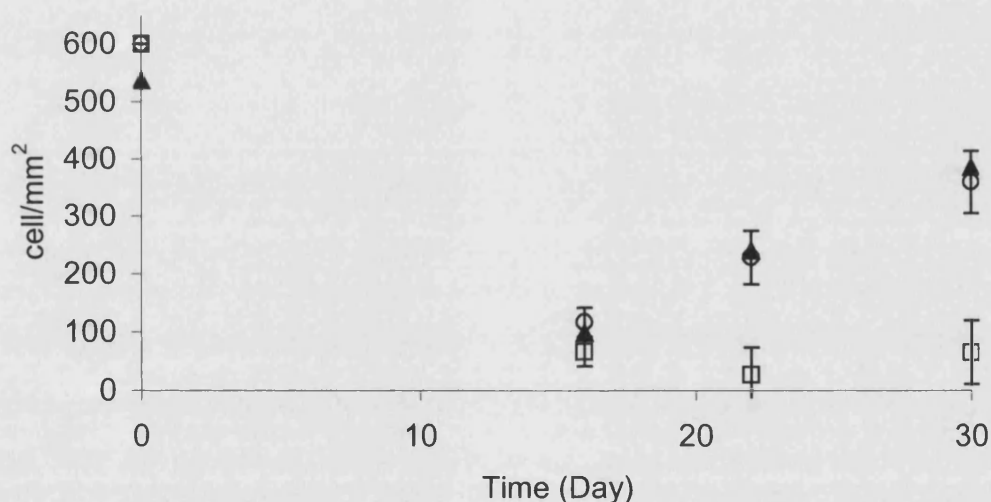


**Figure 3.17:** Comparative analysis of HUVEC and hVSMC cell density on washed and non-washed matrix. (▲) HUVEC and (○) hVSMC on washed matrix, compared to (□) non-washed matrix. Cell density shown as the mean number of cell/mm<sup>2</sup>,  $\pm$  1 standard deviation.

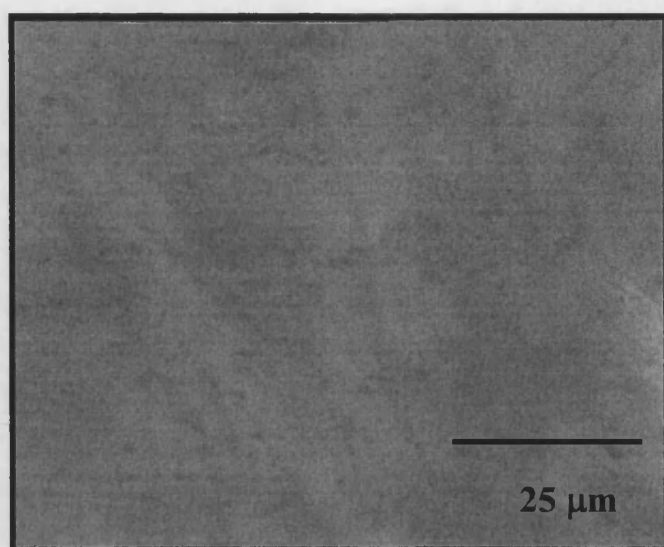


**Figure 3.18:** Cell density of hVSMC cultured on the non-washed type I dermal collagen matrix at day 30.

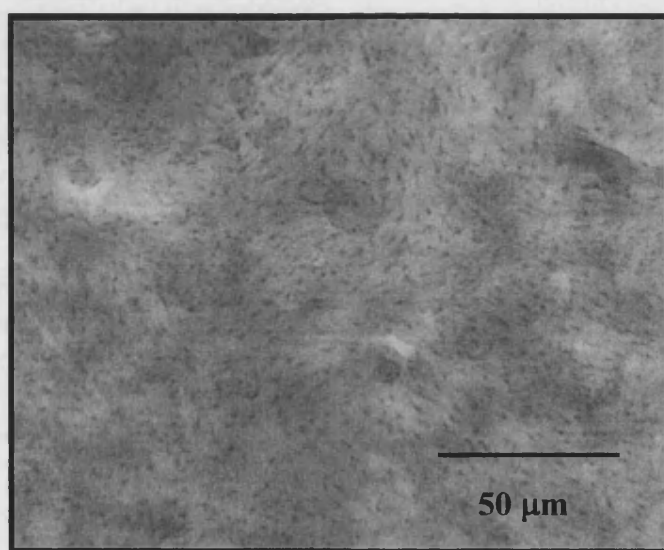


**Figure 3.19:** Cell density of hVSMC cultured on washed type I dermal collagen matrix at day 30.

### Matrix modification

Prior to matrix modification the matrix was washed with the more comprehensive washing protocol, method 2, as described in section 3.2.2.1. Sample pre-treatments are described in section 3.2.2.3. In addition to the washing procedure, NaOH treated disks were washed 2x rapidly plus 3 further washes with a minimum of 1 hour between each in PBS to neutralise the alkaline pH. Results from these data suggest that NaOH treated dermal collagen offers a better environment for cell adhesion and subsequent growth. Results from heparin treated collagen displayed higher densities over days 3 and 7, however between day 7 and 11 cell density declines rapidly, Figure 3.20. hVSMC cultured days 21 on heparin treated collagen, displayed large 'sheets' of what appeared to be the heparin layer losing adhesion from the collagen matrix, Figure 3.21. In contrast hVSMC cultured on NaOH treated collagen at 21 days, remained adhered to the matrix and continued to increase in density through to the termination of the experiment, Figure 3.22.

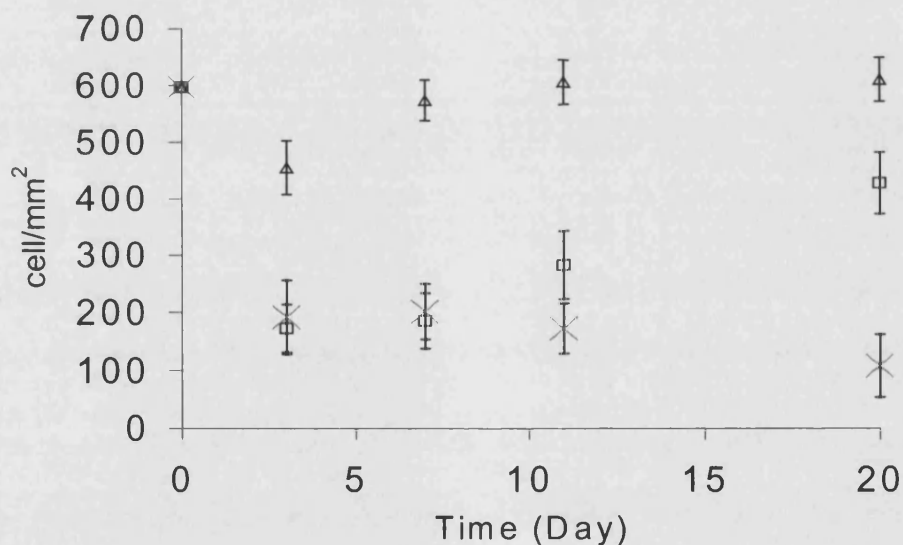


**Figure 3.20:** Comparative matrix treatments of heparin and NaOH in terms of hVSMC density over time. Analysis of hVSMC density over time between heparin (x), NaOH (□) treated matrices and plastic controls tissue culture plates (Δ).

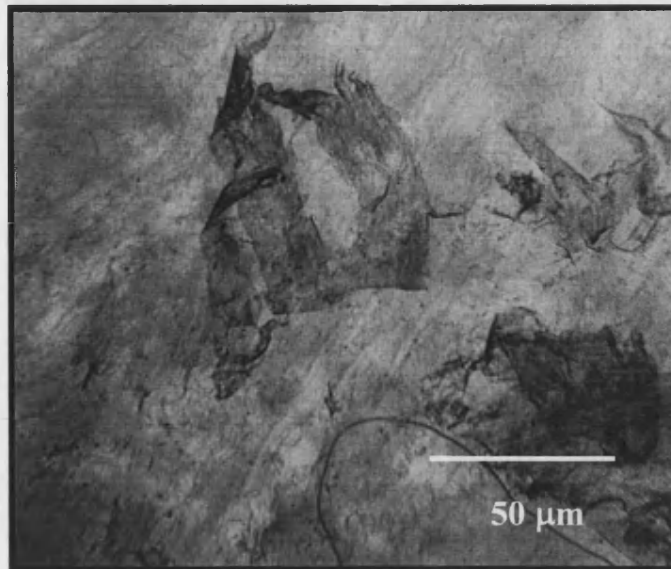


**Figure 3.21:** hVSMC cultures at day 21 on heparin treated collagen, large 'sheets' of what appears to be the heparin layer have detached collagen matrix.

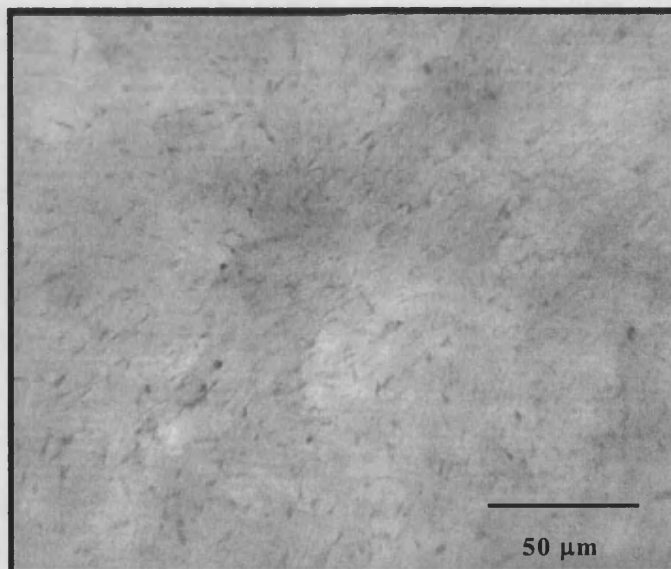


**Figure 3.22:** hVSMC cultured on NaOH treated collagen at 21 days, remained adhered to the matrix.

### 3.4 DISCUSSION

This chapter describes the use of a modified porcine dermal collagen as a scaffold for three-dimensional cell growth and proliferation. The matrix consists primarily of collagen and elastin and has been treated to remove cells, cell debris, cross-linked to increase immune tolerance and stabilise against host degradation. The aim was to determine the suitability of this material for use as a matrix for tissue engineering vascular prostheses. Supplied by Tissue Science Laboratories, London, Permacol has been described in the patent WO 85/05274 invented by Roy Oliver and Roy Grant as; “A collagenous fibrous tissue preparation of human or animal origin which is suitable for homo- or hetero transplantation as a permanent implant. The fibrous tissue preparation is preferably in sheet form and is prepared by a process which results in the tissue being substantially free of non-fibrous tissue proteins, glycoproteins, cellular elements, lipids and lipid residues. This process involves the treatment of the fibrous tissue with a polyisocyanate which unlike earlier processes using, for example, dialdehyde treatment agents, provides a fibrous tissue preparation which is non-cytotoxic and is stable to endogenous proteolytic enzymes” (Oliver and Grant, 1985). Two important aspects of Permacol with regard to its use as a matrix in tissue engineering vascular prostheses are, that Permacol is derived from dermal collagen which is primarily type I collagen with lesser amounts of type III collagen, whereas the predominant collagen type in native blood vessels is type III, with a small amount of type IV collagen associated with the basement membrane. However, the molecular formulas of type I,  $[\alpha 1(I)]_2\alpha 2(I)$  and type III,  $[\alpha 1(III)]_3$ , both contain similar  $\alpha 1$  polypeptides and polymerise to form fibrils. Secondly, the content elastin within Permacol estimated between 2 and 4% by the patent holders, is considerably lower than in native blood vessels (depending on the vessel type and location) (Sunthareswaran, 1998). The impact of these discrepancies is discussed in relation to cell adhesion, growth and proliferation. It has not been the aim of this project to comprehensively characterise the type I dermal collagen matrix (Permacol). Studies have been limited to understanding fundamental aspects describing the matrices gross morphology and ability to confer cell adhesion, growth and proliferation under *in vitro* conditions with the aim to develop a small diameter vascular graft.

### **3.4.1 MORPHOLOGY OF THE DERMAL COLLAGEN MATRIX**

Initial observations of transverse sections of the dermal collagen matrix analysed by phase contrast microscopy show clearly the fibrous nature of the dermal matrix with open spaces of sufficient size that may allow cellular penetration (non-proteolytic migration) into the matrix. Given appropriate stimuli, cells seeded onto the matrix surface will migrate into the matrix ultimately conferring a cell dense biomaterial. LT-SEM characterisation of matrix surface structure iterates the transverse sections, showing both fibrous and compressed areas. The fibrous areas are seen to be critical to allow cell migration into the collagen matrix, particularly so if cellular mechanisms to digest the matrix are unable to digest the collagen fibres due to excessive cross-linking.

A porous structure will improve mass transfer of nutrients/waste products into and out of the matrix essential if high densities of cells are to develop within the matrix wall. Of the samples studied with the LT-SEM a qualitative assessment that approximately 50-65% of the matrix surface is in the form of compressed fibres that are unlikely to allow passive migration of cells into the matrix.

### **3.4.2 ASSESSMENT OF CELL ADHESION AND PROLIFERATION ON THE DERMAL COLLAGEN MATRIX**

Cell proliferation rates will vary dramatically depending on the patients age and the disease state of the tissue from which the cells were originally isolated. This can be explained by the nature and origin of the cell types used, not least variation between species. hVSMC used in this report are primary cell lineages, isolated from diseased venous tissue, having variable growth characteristics from one individual to the next. In addition hVSMC are isolated from tissue in various stages of vascular disease and origin, which again results in variability of growth characteristics. This is in direct contrast to cell lines (e.g. Hela cells), which can potentially maintain consistent growth and proliferation rates, indefinitely. A standard growth analysis was conducted using hVSMC as the 'gold standard' by culturing on tissue culture plastic. hVSMC have the slowest replication rates of the cells cultured in this project and are likely to be the time limiting step in generating the tissue engineered blood vessel. Throughout this

thesis primary human cells, with regard to the hVSMC sourced predominantly from or near diseased tissue (e.g. saphenous veins), the rationale behind this was that any product or protocol generated by this project would use patient cells, as discussed in the literature review. In order to better understand limitations in terms of diseased cell growth and proliferation it was preferential to use the patient group as a source of cells. Results from the growth analysis were therefore limited as each individual cell lineage exhibits differing growth and proliferation properties. Similar growth rates will be achieved from other tissue samples, however there is considerable variation in primary cell growth rates between individuals.

As explained above, the results have provided limited information about hVSMC growth as an independent lineage of cells was used that have been grown *in vitro* on an unnatural substrate. Furthermore this culture is 2-dimensional, where migration into a tissue is not possible with the effects of contact inhibition preventing continued cell proliferation. It is hoped that 3D culture will allow cells to migrate into a matrix to reach densities approaching physiological levels, where EC form an endothelium and hVSMC have a sufficient density to confer vascular tone, whereby VSMC contraction within the matrix wall will confer physiological control over blood flow.

An interesting issue is the phenotypic state of hVSMC in relation to their proliferative activity and the method cells are isolated for *in vitro* cultivation. hVSMC isolated by the 'explant method' (used in this thesis) have a higher proliferation rate and lower expression of  $\alpha$ -actin than cell isolated by the 'enzymatic method' (Kirschenlohr, et al. 1996). It has been postulated that the latter method is less phenotypically damaging to cell populations, hence they are likely to retain the phenotypical gene expression pattern of *in vivo* cells. As cells proliferate increased resources, such as  $\alpha$ -actin expression, are potentially compromised thus the reduced immunocytochemical staining for this protein (Kirschenlohr, et al. 1996). The substrate cells are grown on dramatically influences their phenotype. It is possible that the higher proliferative rate of hVSMC gained from the explant method and grown on tissue culture plastic revert back to a more phenotypically correct state with reduced proliferation, when cultivated on a 3D collagen matrix, more akin to the *in vivo* environment. Experimentation was not conducted to confirm this, however these results are valuable as an indirect comparison for later cell culture on the collagen matrix.

Cell adhesion studies on the type I dermal collagen matrix was confirmed with the LT-SEM, 1 day after cell seeding. HUVEC had adhered to the matrix displaying pseudopodia-like structures extending into the matrix, Figure 3.07. Further evidence of more mature adhesion was the establishment of cell-cell contacts was noted in Figure 3.08. Although this initial study was qualitative, it could be clearly seen that comparative densities to cells cultured on plastic tissue culture flasks, cell densities on the collagen matrix were considerably lower. Cells appeared both singularly and in clusters of higher densities that are randomly dispersed over the entire matrix surface, which did not change after 4 days culture. HUVEC and hVSMC adhered to the matrix and displayed similar morphologies and densities to 1 day cultures, though possibly more advanced, Figure 3.11. These observations appeared consistent across all samples, where seeding density ranged from  $1 \times 10^5$  cell/ml to  $2 \times 10^5$  cell/ml. By 7 days very few cells (hVSMC and HUVEC) are adhered to the matrix. Remaining cells appear stressed (rounded and globular) compared with cells cultured over shorter periods (see Figures 3.13 & 3.14)

As this matrix had been granted a rating for human implantation, it was expected, based on the literature provided by the company that human cells would adhere grow and proliferate on the matrix (Oliver and Grant, 1985). The first set of experiments was designed to characterise (qualitatively) the ability of HUVEC and hVSMC to adhere to the matrix under static growth conditions (1, 4 and 7 day culture periods). No preparation of the matrix was performed prior to cell seeding, the matrix was simply removed from its packaging, cut to size and the cell suspension seeded directly on top. After seeding cells onto the collagen matrix and through the period of culture, cells that were initially confluent around the matrix material (adhered to the plastic culture dish) either lost adhesion or became necrotic. It was observed that over time the zone of cell disruption expanded from the matrix towards the periphery of the culture plate. With evidence from the SEM adhesion studies, where a reduction in cell density was noted and the additional evidence in the literature concerning cytotoxic residues the presence of a cytotoxic compound was speculated e.g. (van Luyn et al., 1992a) and (Bellincampi and Dunn, 1997). To assess (qualitatively) this observation, small sections of Permacol were seeded with cells, such that the surrounding tissue culture plastic was also covered with cells. The samples were monitored over time to indirectly observe if any potentially cytotoxic compound was leaching from the matrix resulting in cell necrosis.



The observed results indicated a toxic compound was leaching from the matrix being diluted over time with normal tissue culture practices. This allowed the remaining cells (that survived the initial toxic shock) to recover and begin proliferating approximately 15 days post seeding. The experimental design did not take into account the possibility that matrix movement (during culture maintenance) could be the cause of the observable effect, however, care was taken to minimise this effect and the expanding zone extended well past any potential area the matrix may have inadvertently moved, i.e. no more than 3-4 mm.

To quantify changes in cell density over time and assess cell viability, an assay using 'Trypan Blue' was utilised. Results have shown an initial decline in cell numbers post seeding, which is consistent with cell adhesion/densities on plastic controls, although the reduction in cell density is much less on plastic controls. This decline in cell density is amplified in the collagen matrix samples to the point where viable cell numbers fall below statistically significant levels. Non-viable cells on the matrix are lower (80 cell/mm<sup>2</sup>) than plastic non-viable cells (150 cell/mm<sup>2</sup>), this is possibly due to the presence of cytotoxic compounds stressing cells on the matrix prior to the development of mature adhesion where the production of secondary matrix proteins aids the binding of cells, thus non-viable cells maybe washed away during standard cultivation. It is also possible that the trypsin treatment did not remove all of the cells from the collagen surface, resulting in lower counts, however this is not consistent with the LT-SEM micrographs.

Previous results had been based on empirical (LT-SEM) or data taken from cell counts, where cells had been removed from the matrix by trypsin digestion. Although the LT-SEM is an effective method to observe cells adhered on the surface of a matrix material, it is neither cost nor time efficient to use on a daily basis. The later method relied on the ability of trypsin to effectively remove all cells from the collagen matrix. Personal communication with Dr. Philip Chan (Sheffield General Hospital, UK.) expressed concern that not all hVSMC would be removed from the collagen substrata by enzymatic digestion, particularly if cells were cultured for extended durations. hVSMC secrete collagen producing a secondary matrix around cells, in addition cells may migrate into the matrix further complicating the removal process. In order to reduce the subjectivity and improve accuracy of data collection and analysis a more cost effective,

quantitative method was required to determine specific cell densities. Standard methodologies, such as H & E, excessively stained the opaque matrix to the point where cells were not discernable from the background collagen. The first stage required the development of a cell staining protocol, where cells adhered to the matrix could be visualized with a phase-contrast microscope. In order to visualise cells on the surface of the collagen matrix a modification of the standard H & E histological technique was developed where only Haematoxylin was used, see Section 2.3.7.2. The combination of maximum illumination and a reduced H & E protocol with no eosin step, resulted in cells being observable on the surface of the collagen matrix with the phase-contrast microscope, from which counts were made. Although cells, particularly hVSMC, may migrate into the matrix and distort results, the protocol was reliable when the principal question was whether or not the material was capable of supporting cell adhesion, growth and proliferation.

### **3.4.3 ENHANCEMENT OF CELL ADHESION AND PROLIFERATION ON THE DERMAL COLLAGEN MATRIX**

The application of a preliminary washing protocol was used to establish the effectiveness of washing the matrix prior to cell seeding as a method to reduce or eliminate the toxicity effect. Previous studies had shown that by day 5 virtually all cells had detached from the matrix. The aim of this experiment was to firstly confirm the presence of cells and a brief analysis of the proliferative state using the BrdUrd assay. Results from this experiment confirmed cells (at 5 days) have both adhered and proliferated on the matrix. Although a qualitative assessment, these results are encouraging in that previous experiments with non-washed collagen have shown a near complete loss in cell numbers/density over the same time period. Here, where the matrix has been through a rudimentary washing protocol cells have adhered and more importantly, are proliferating Figure 3.16. Control samples (collagen matrix without cells) displayed minimal non-specific antibody binding. The experiment was not repeated to give a more quantitative result, as the aim was to determine cell proliferation, to this extent the results were positive. Washing the matrix in terms of cell proliferation was evaluated further in the next section.

A specific requirement in tissue engineering to obtain tissue that approximates the native organ is to firstly attain an appropriate cell density within the matrix material and secondly to do so as rapidly as possible. With particular reference to a vascular prosthesis, the ability of cells to adhere, grow and proliferate is vital, particularly so if the patient's condition is life threatening, where the delay whilst waiting for the graft to 'grow' *in vitro* may decrease patient mortality, and secondly to provide a sound economic basis for graft production. Initial experiments with the LT-SEM (visual conformation) and enzymatic removal of hVSMC off collagen (actual counts) indicate percentage cell adhesion is very low. To further reduce the cytotoxic potential of the unwashed matrix and hence improve biocompatibility, a more comprehensive washing protocol was applied followed by two washes in the appropriate media for the cell type. This experiment was conducted to determine the effect of washing and pre-soaking in media prior to cell seeding comparative to non-washed collagen (controls) determining the effects on cell adhesion, growth and proliferation on this type I collagen matrix.

Heparin sulphate and NaOH have been used to potentially increase the performance (both in terms of cell adhesion and *in vivo* biocompatibility), where hVSMC growth was compared on heparin and NaOH pre-treated matrix, Figure 3.20. These data suggest that the NaOH treated matrix offers a better environment for cell adhesion and growth, however, cells adhered heparin treated Permacol at higher densities over days 3 and 7. Between day 7 and 11 heparin cell density declines rapidly as a result of the heparin 'layer' formed upon the matrix surface disengaging from the matrix resulting in loss of the cell layer, see Figure 3.21. NaOH treated samples continue to increase in density through day 21. This experiment used plastic culture plates as a control matrix material, which, since having determined the effectiveness of washing the collagen matrix and soaking it in media prior to its use should ideally have been used in conjunction with the plastic culture plates.

Previous use of heparin (Gemmell et al., 1998), (Laemmel et al., 1998) and (Bos et al., 1999) has successfully been used to increase the grafts performance, in terms of cell adhesion and *in vivo* biocompatibility. The basic structure of the heparin and heparan sulphate GAG chains, which are covalently bound to a protein core, is the alteration of two monosaccharide units, polymers of alternating glucosamine and glucuronic/iduronic acid units (Haralson and Hassell, 1995). Although not a native product of the arterial

wall the main advantage seen with heparin, which in vivo is stored in mast cells found in connective tissues, as an anticoagulant that blocks the conversion of prothrombin to thrombin (enzymes in the blood clotting cascade that converts fibrinogen to fibrin).

The loss of heparin/cell adhesion between day 7 and 11 is almost certainly due to the inability of heparin to bind the collagen matrix securely. Although there is no direct evidence that the heparin substrate attached to the matrix in the first place, the formation and subsequent loss of an entire cell layer would indicate this possibility. Secondly heparin is known in some cases to be a direct inhibitor of hVSMC proliferation (Laemmel et al., 1998), methods to improve heparin binding are cited in the literature (Chanda et al., 1999) and (Laemmel et al., 1998). A previous study by Greisler et al (1996) had shown that lower concentrations of heparin (5 and 50 U/ml<sup>-1</sup>) significantly increased SMC proliferation, whereas concentrations as high as 500 U/ml<sup>-1</sup> significantly decreased proliferation (Greisler et al., 1996). Soaking the dermal collagen matrix in 25000 U<sup>-1</sup> heparin does not provide the necessary information as to the final concentration of the heparin additive once the matrix was rinsed in media and cells seeded. It does appear that hVSMC recovered in a similar fashion to NaOH treated samples up to day 7 prior to declining in cell density.

NaOH was used to modify the surface of the collagen matrix by attacking the acidic residues of the collagen molecule, resulting in a semi controlled degradation of the material. The explanation for improved cell adhesion and subsequent growth is not fully understood. Speculatively, as the matrix degrades with the NaOH treatment, noted by the material turning opaque, the ability of cells to enter and populate deeper into the matrix increases.

The effective distance with which communication is possible has been theoretically estimated at approximately 250 µm, (Francis and Palsson, 1997). For this to occur between SMC seeded onto the grafts abluminal surface and EC seeded to the luminal surface, cells will need to migrate up to 500 µm on material 0.75 mm thick to be within this theoretical distance. If the initial adhered population is higher than control tissues, even if in mono-culture, proliferation rates are likely to be higher due to the proximity of neighbouring cells, where proliferation is density dependent.

This type I collagen matrix 'Permacol', as described previously, is delivered as flat sheets of porcine derived collagen (initially with thickness of either 0.75 and 1.5 mm in a variety of pre-cut lengths and widths). Several advantages are noted for its use as tissue engineering matrix for a vascular graft. A proven durability (Oliver and Grant, 1985) that is 'likely' to be more than capable of withstanding local haemodynamic stresses. Previous surgical experiences have shown the material to have positive handling characteristics i.e. suturability and simplicity of handling, is relatively immunologically inert (as an implanted dermal graft), and is available at a relatively low cost.

Based on these positive attributes the question must therefore be asked "Is this collagen matrix suitable as a biomaterial for small diameter vascular grafts?" For this reason, the less attractive aspects of Permacol for use as a potential vascular biomaterial for tissue engineering purposes have been evaluated. As such, the experimental design has focused on compatibility issues of this matrix to culture *in vitro* of human primary cells. It is a specific requirement that primary cells can adhere, grow and proliferate to attain significant densities and secondly to do so as rapidly as possible. With particular reference to a vascular prosthesis, the ability of cells to adhere with high efficiency then proliferate to the required density *in vitro* is critical. The patient may well be in a life threatening condition throughout the graft preparation time, thus any reduction in terms of the grafts 'lead time' is advantageous. In addition extended *in vitro* culture periods would lead to potentially unfeasible economics of graft production. Although product optimisation is a critical step, it is a secondary issue in this project.

Flat sheets of dermal collagen are in principle relatively simple to process into tubular form, it is however considered second rate to a pre-formed tube specifically designed (artificially or naturally) elastic material that may be adaptable as a vascular prosthesis. Several considerations were taken into account when deciding to develop a specific or novel matrix rather than modify the existing dermal collagen matrix (Permacol). 1. Initial experimental studies with washed matrix have displayed time lags in excess of 30 days before cell densities begin to approach initial seeding densities, see Figure 3.17. In order to create a 'tube' from Permacol it is necessary to roll the material, resulting in a large luminal ridge (when wetted approximately 1 mm) running longitudinally along the matrix. Although this effect has not been quantified, it is considered an inferior

attribute compared to existing or alternative materials. 3. Although this material has a proven durability when implanted subcutaneously, no data is available with regard to haemodynamic stresses, only assessments based on the materials mechanical properties. 4. The matrix has been shown to elicit a “mild immune response” (Oliver and Grant, 1985) which maybe acceptable when used as a subcutaneous graft, however the increased sensitivity of small diameter grafts to thrombosis from even “mild” reactions is likely to render the prosthesis invalid. 5. In respect to an active or functional arterial graft, EC must form an endothelium and hVSMC, ideally, need to approach *in vivo* densities to confer vascular tone. The heavily cross-linked nature of this material appears to inhibit or indeed prevent cellular migration into the matrix by one of the primary methods of cell migration, proteolytic digestion, for example matrix metalloproteinase, matrix remodelling enzymes. The dermal collagen matrix, as stated previously, is specifically cross-linked with HMDI, a strong mechanism to stabilise collagen molecules. In addition to this specific cross-linking step the material is exposed to both acetone (lipid extraction) and gamma radiation (matrix sterilisation) both of which add to the materials ability to withstand *in vitro* and *in vivo* degradation. Although the porous structure characteristic of type I collagen has been essentially maintained, it is evident from the low temperature scanning electron micrographs that sections of the matrix surface are as compressed collagen fibres which form a non-porous structure, approximately 50-65% Section, 3.3.1. The two distinct surface morphologies of this dermal collagen are likely to be an artefact, resulting from the processing methods used during manufacture. The open, more fibrous, areas of the collagen matrix are closer in nature to the unprocessed fibrous networks of type I collagen. From the Figure 3.03, it is possible to hypothesise that the compressed sections are areas that have contracted either during the HMDI or  $\sigma$ -radiation processes resulting in the exposure of the underlying fibrous collagen and compression or compaction of the surface collagen. It is however speculation and beyond the remit of this project to determine structural changes that occur from native to fully process collagen. If indeed the compressed sections have a higher ratio of cross-links compared to the underlying tissue, cellular penetration by proteolytic activity will indeed be impaired in these regions. Cellular migration into the matrix is an important factor in communication within and between multiple cell populations (SMC and EC) (Ziegler and Nerem, 1994).

The effect of these structural deviations with respect to graft performance has not been fully evaluated, other than a qualitative visual analysis that had shown that cells, particularly HUVEC, appear to have a propensity for the compressed or non-fibrous regions. Importantly with regard to cell adhesion, the luminal surface of blood vessels is lined by type IV collagen, a non-fibril forming two-dimensional basement membrane. Implications of attempting to seed EC onto type I collagen (fibrous), in contrast to native type IV basement membrane may account for (in concert with cytotoxic compounds) some of the difficulties observed in cell adhesion and proliferation with this cell type. The significance of the basement membrane and internal elastic lamina with reference to cell adhesion is discussed further in Chapter 5.

In this chapter a porcine derived dermal collagen has been assessed to determine its potential use as a small diameter graft. Conclusions drawn from this chapter show that this biomaterial is not a suitable biomaterial for applications in vascular tissue engineering where cellular ingrowth is a fundamental requirement. However after extensive washing and possible modification to the matrix structure (such as NaOH treatments) the material may prove adequate. This section of work has shown that although this material maybe used to generate a tissue engineered artery it is not ideal. In seeking an alternative matrix material for small diameter vascular graft several options were considered, including the alternative of full synthetic materials. Based on the current literature supporting natural materials for their mechanical characteristics (Schmidt and Baier, 2000) and our background in biological materials, a native muscular artery was chosen, specifically, the porcine carotid artery. This particular artery was chosen to serve as a model, representing approximate dimensions for arterial replacement, although it is envisaged that other arteries (possibly veins) would serve equally as well, in addition availability and ease of extraction promoted this choice.

The next chapter in this thesis describes the development an acellular matrix utilizing porcine carotid arteries as a starting material and the progressive removal of non-structural components of the ECM. The matrix is stabilised to host degradation by a non-cytotoxic cross-linking step which also known to reduce immunological response to implanted foreign materials.

# CHAPTER FOUR: DEVELOPMENT OF A SCAFFOLD FOR TISSUE ENGINEERING BLOOD VESSELS USING PORCINE CAROTID ARTERY

## 4.1 INTRODUCTION

The objective of the tissue engineering approach is to utilise a prosthetic material/matrix onto which the patients own cells are seeded or when technology allows, immunologically inert cells such as stem or genetically modified cells. Once seeded the combination of matrix and cells are cultured in a purpose built bioreactor that emulates physiological conditions, both mechanically and chemically, to produce an immunologically inert bioprosthetic graft with patency rates equal to or better than current autologous arterial transplantation methodologies.

In addition to the general characteristics detailed in Chapter 1.1, the ideal vascular prosthesis requires further properties that may give a tissue engineered graft increased patency over traditional synthetic materials.

Immunologically inert

Chemically inert (non-toxic)

Resistance to infection and calcification

Durability i.e. ability to withstand haemodynamic stresses

Mechanical characteristics emulating native arteries

Able to be remodelled by the patient

ECM components that regulate cell phenotype, growth and proliferation

High efficiency of cell seeding

Positive handling characteristics i.e. suturability and simplicity of handling

Post implantation healing as self tissue

Patency rates equal to or better than autologous artery (>90% at 5 years)



There are currently no (bio) prostheses that encompass this ‘ideal’ list of graft characteristics. The choice of primary material in the development of a prosthesis is of particular importance. The matrix material must provide structural, mechanical and appropriate chemical stimuli that may ultimately produce a compliant prosthetic graft. Blood vessels of the vascular system, like other organs of the body have evolved to provide the body with a specific service/function, where, amongst other things, blood is transported efficiently to all cells of the body. The efficiency of natural vessels function is due in large to the physical characteristics of the extracellular matrix (ECM) where not only chemical stimuli is received by cells but by the manifestation of the physical characteristics when haemodynamic stresses are applied. Synthetic, biosynthetic or biological prosthetic graft research has aimed to replicate the natural vessel.

This section of work aimed to develop a material that can be shown to embody the requirements (above) by modifying, for generic use, the material whose biomechanics are second to none - biological vessels.

#### **4.1.1 BIOLOGICALLY DERIVED ECM FOR VASCULAR GRAFTING**

Clinical usage of non-living grafts has predominantly used either human umbilical vein or cryo-preserved vessels such as the saphenous vein. A variety of pre-treatments (such as fixation with glutaraldehyde), have been applied to these vessels to improve both their biocompatibility and mechanical strength under arterial pressures.

Results from prepared biological tissue, in particular human umbilical vein (HUV) stabilised with glutaraldehyde cross-linking for arterial (or venous) grafting have had mixed results, in some cases a lack of stability has shown the graft to be aneurysmal, with an incidence of 33% beginning at three years and increasing with time (Karkow et al., 1986). Early graft degeneration and aneurysm formation have also been reported, (Hasson et al., 1986; Nevelsteen et al., 1988). Other data suggests this particular graft does in fact out perform polytetrafluoroethylene (PTFE), with patency rates 2.1 times higher (Eickhoff et al., 1987). Dardik et al (1982), who first described the formation of aneurysms in HUV grafts has since remarked that due to the poor rates of PTFE patency the HUV is an “acceptable alternative to the absent or deficient autologous vein”.

Further describing the half-life patency of the HUV graft (popliteal, tibial and peroneal bypass) being 6.5, 2.3 and 1.7 years respectively, with overall infection rates of 4.3% (Dardik et al., 1988). In addition reduced infection rates have been shown by Koskas *et al* (1996), where human cadaver arteries (n=6), stored for >1 month in a preservation media at 4°C prior to implantation in a dog model were not infected after a *Staphylococcus aureus* challenge, whereas 4 out of the 6 ePTFE grafts were infected (Koskas et al., 1996). Although the mechanism for reduced infection is unclear, the biological model has, in this example, is clearly superior to the synthetic model. Further evidence by Johnson et al (2000) has again shown the potential suitability of biological grafts over synthetic alternatives, particularly PTFE, where five year cumulative assisted primary patency rates of 80% for saphenous vein (SV), 56% HUV, 33% PTFE and in cases of critical ischemia 68% SV, 52% HUV, 37% PTFE (Johnson and Lee, 2000). It must be noted the site of graft placement, in terms of flow and vessel diameter largely determines the grafts 'expected' patency irrespective of the grafting material. Larger diameter grafts (e.g. femoral artery) generally achieve higher rates of patency compared to smaller diameter vessels (e.g. popliteal artery), although this is also dependent on the stage of vascular disease, age and sex of the patient.

The general mechanism through which prosthetic grafts fail at any point can be summed up as initial thrombosis, progressive intimal hyperplasia and degradation leading to graft dilation and aneurysm. Bioprosthetics achieve high initial patency but tend to fail due to progressive graft dilation (Courtman et al., 2000). Traditionally the basis for treating biological tissues has been to reduce or prevent chronic immune rejection by the patient and to stabilise the tissue to host proteolytic degradation. Cross-linking or tanning of prostheses, particularly prosthetic heart valves with the use of glutaraldehyde has concentrated on prevention of chronic immune rejection, mechanical stability and infection resistance. Other agents such as formaldehyde or low concentrations of glutaraldehyde have resulted in either mechanical graft failure or bacterial/fungal contamination (Schoen and Levy, 1999). Host cells are prevented from migrating into the matrix, by secretion of proteolytic remodelling enzymes by the barrier of 'stabilised' ECM proteins. Previous attempts to prepare biological tissue for arterial (or venous) grafting proved aneurysmal due to lack of stability, or being thrombogenic as a result of a 'naked' basement membrane (inherently thrombogenic) being exposed to host blood and its constituents (Hasson et al., 1986; Karkow et al., 1986; Nevelsteen et al., 1988;

Niklason et al., 1999). Recently the role of cross-linking tissue has been questioned, Courtman et al (2000), using a unique acellular matrix glutaraldehyde, polyglycidyl-ether and carbodiimide where used to cross-link the matrix material. It was found that although the matrix was stabilised to cellular infiltration, by either an exclusion barrier or cytotoxic residues in the tissue; compared to the untreated acellular matrix there was an increase in humoral immune response. The importance of extracting cells, cell debris and other non-structural proteins from the starting material may indeed play a more important role in an immune response than tissue stabilisation through cross-linking. Where immunological and structural resistance, provided by cross-linking, is in fact the inhibition of immune cell penetration into the matrix and prevention of matrix degradation (Courtman et al., 2000).

The importance of local environmental conditions on cell growth, proliferation and phenotypic expression have been well documented, for example, (Birukov et al., 1995; Kim et al., 1999; Nerem et al., 1993; Olivier et al., 1999; Osol, 1995; Zilla et al., 1994). Mechanical properties are widely acknowledged as crucial to graft performance, allowing replication of natural arterial elasticity and compliance. Without doubt a natural biological blood vessel with matched compliance, offers the closest mechanical characteristics to an autologous vessel. Using experiences gathered with biological materials for tissue engineering purposes in Chapter 3 and published data in (Smith et al., 2000), an acellular porcine tubular matrix has been developed for use as small diameter vascular prostheses. Arterial tissue was chosen, over venous tissue due to the mechanical properties inherent with the artery, where the artery has a considerably strengthened medial layer (compared to veins), to accommodate arterial pressures. In addition it has been speculated that the mechanical properties associated with the artery wall to give explanation to improved patency associated with autologous arterial revascularisation compared to venous tissue.

The prosthesis is expected to have reduced immunogenicity and resistance to calcium deposition which, following implantation is aimed to extend the current rates of patency of biosynthetic grafts. Our investigations have focused on the development of this acellular tubular matrix derived from carotid arteries extracted from 6-8 month old Great White pigs. The matrix is initially stabilised through a solvent lipid extraction process, followed by an enzymatic digestion to reduce any potential immunogenic

epitopes. Finally the matrix is preconditioned and cross-linked with the non-toxic photo-active dye, methylene green (Mechanic, 1994), further stabilising the tissue and minimising host rejection by concealing immunogenic epitopes (Moore et al., 1994).

#### **4.1.2 PREPARATION OF BIOLOGICAL TISSUE**

As discussed above, processing native tissue to remove cells, cell debris in concert with crosslinking the tissue; aims to reduce the implants immune reactivity and stabilise the tissue to rapid host degradation. Methods including: chemical, enzymatic and mechanical treatments have been explored by others with the aim to produce an acellular matrix. Unlike a majority of other methods that rely exclusively on, for example SDS treatments to remove the matrix lipid content, the process developed in this thesis uses a combination of methods to remove both cellular materials and non-matrix proteins/carbohydrates.

The literature describes a variety of methodologies used to intentionally remove lipids and host cells/cell components from tissue, either singularly or in concert with other treatments. These include: osmotic shock, solvent extraction, ionic and non-ionic detergents, acid treatments and enzymatic digestion with DNase, RNase, lipase and proteases, see Table 4.01.

These methodologies were assessed based on effectiveness of component removal, structural change of the matrix pre- and post-extraction and the retention of the vessel's mechanical attributes, then used as a guide for the development of the biomaterial outlined in this chapter. The methods described in table 4.01 are a representative selection of treatments including: enzyme, ionic and non-ionic detergents, acids, alkaline and solvent-based systems. Although they have been segregated into these categories many are a combination of more than one type of treatment.

**Table 4.01:** Preparation of biological tissue: a methodology overview

METHOD	PROCEDURE	EXAMPLES
Osmotic shock	0.5 M sucrose (step1), 4M NaCl (step 2)	(Mechanic, 1994)
	1 M NaCl	(Probst et al., 1997)
Acid	0.1% peracetic acid. Complete cell removal, no data given on matrix structure, though both dehydrated and hydrated forms support HMEC adhesion	(Badylak et al., 1999)
	4% desoxycholate (bile acid)	(Probst et al., 1997)
Alkaline	DMSO (6%) plus Na <sup>+</sup> , K <sup>+</sup> and Ca <sup>++</sup> solutions at pH > 13	(Goissis et al., 2000)
Detergents	1% Triton X-100	(Courtman, et al 1994) (Tamura et al., 1999)
	1% SDS plus 0.2% Glutaraldehyde	(Bodnar et al., 1986)
Enzymes	Acetone (multiple washes) followed by trypsin (multiple exposures)	(Oliver and Grant, 1985)
	0.1% trypsin with 0.02% EDTA in PBS	(Teebken et al., 2000)
	1% Triton X100 + 0.02% EDTA. RNase + DNase	(Bader et al., 1998)
Solvents	Ethanol	(Goissis et al., 2000) (Malone et al., 1984) (Vyavahare et al., 1997)
	Butanol	(Reid and Rojkind, 1987)
		See Section 4.3.2
	Acetone	(Oliver and Grant, 1985)
	Xylene	See Section 4.3.2

## OSMOTIC SHOCK

Several authors have reported the use of osmotic shock, with either hypo or hypertonic solutions to rupture cells thus releasing cellular material into free solution for removal. The method described by Mechanic (1994) has made no direct attempt to remove cells prior to dye mediated photo-oxidation other than the use of high osmolarity solutions (0.5M C<sub>12</sub>H<sub>22</sub>O<sub>11</sub> and 4M NaCl) as part of the preconditioning and cross-linking steps. The effectiveness of this method to completely remove cell lipid is perhaps limited, though there is no evidence of DNA at the end of the treatment, see Section 4.3.6 (Mechanic, 1994).

## ACID AND ALKALINE

Badylak et al (1999) have published extensively on a matrix material derived from the porcine jejunum or the small intestinal submucosa (SIS) as it is commonly referred to. In this method the superficial layers of the tunica mucosa are removed leaving a material approximately 80-100  $\mu\text{m}$  thick. The SIS is said to be essentially cell prior to any treatments to remove cells/cell debris. A treatment of 0.1% peracetic acid followed by rinsing in PBS removes residual cells and cell components. The study showed that cells (human dermal microvascular endothelial cells) adhered to the hydrated matrix over a twenty-minute incubation period in greater densities than the dehydrated form, tissue culture plastic, collagen types I and IV, fibronectin and laminin (Badylak et al., 1999). As our previous studies have shown, initial adhesion is a very different issue than long-term growth and proliferation where residual cytotoxic compounds may leach from the matrix material (Smith et al., 2000). However the treatment described by Badylak et al (1998), in a comparatively thin material is unlikely to retain processing compounds if washed appropriately and has been shown to provide a suitable support for extended cell culture (Badylak et al., 1998). This methodology to remove cells and cell debris, although suitable for thin near acellular materials, was deemed inappropriate due to differences in the thickness of the two tissue types. Peracetic acid (0.1% (v/v)) has not only been shown as an effective method to disrupt cellular material but an effective treatment to sterilise matrix materials prior to use, Badylak, S. (1999) Department of Biomedical Engineering, Purdue University, personal communication.

Probst et al (1997), developed a matrix material derived from a heterograft rat bladder, the 'bladder acellular matrix graft' (BAMG). The treatment or preparation protocol combines osmotic shock with enzyme and acid process steps. The matrix is washed repeatedly with 0.1%  $\text{NaN}_3$  (sodium azide), followed by a 1M solution of  $\text{NaCl}$ , presumably to disrupt any remaining whole cells by osmotic shock and precipitate DNA. The final treatment was with a solution of 4% desoxycholate, a bile acid, plus 0.1%  $\text{NaN}_3$ . The results from an implantation study of 34 rats (a mortality of >32%), the matrix by 10 days had developed a new mucosal lining and by 4 weeks all components of the bladder wall were complete. By 12 weeks the BAMG was histologically similar to the host bladder tissue (Probst et al., 1997). More recent studies with the BAMG as an acellular matrix in a dog model have also shown

promising results with the implanted BAMG at 7 months showing near complete regeneration, the group is currently applying for approval for a human study (Probst et al., 2000).

Goissis et al (2000), employed a method with strong alkalines, where tissue is firstly 'preserved' in a 70% EtOH solution, not part of the said 'devitalisation process' as a step prior to 'cell removal'. Tissue preservation in a 70% ethanol solution will, in addition to preserving the tissue, solubilise a high percentage of lipids. The 'devitalisation process' consists of a 6% DMSO solution containing alkaline salts  $\text{Na}^+$ ,  $\text{K}^+$  and the alkaline earth metal  $\text{Ca}^{++}$  in the form of chlorides or sulphates, at a pH greater than 13. This was followed by a neutralisation step of 3% boric acid and pH correction in PBS. Concluding that both collagen and elastin fibres were 'highly preserved' although the removal of cells and cell debris is dependent on tissue type and diameter (Goissis et al., 2000).

## DETERGENTS

The predominant method, or treatment regime described in the literature to decellularise tissue has been incubation with detergents such as *t*-octyl-phenoxypolyethoxyethanol (Triton-X100) or sodium dodecyl sulphate (SDS) to solubilise lipids. Cell components such as DNA, RNA, non-structural protein and carbohydrates are released into the extracellular matrix to be subsequently digested enzymatically or removed by a series of washes. For example, Bader et al (1998), used a combination of Triton X-100 with DNase and RNase in PBS to decellularise porcine aortic valves, reporting that the structure was 'largely' cell free across the valve leaflet, with a general loosening or widening of the interfibrillar spaces within the collagen and elastic fibres. The matrix was washed several times in PBS prior to seeding EC onto the surface of the acellular structure. EC were found to form a monolayer over the surface of the construct, which were maintained for a three-day culture period. The process described, although not removing all cell remnants appears largely successful in as much as confirming the viability of seeded EC and maintaining the gross structure of the matrix (Bader et al., 1998). Also reporting success, Tamura et al (1999), have shown that a 48 hour treatment of porcine carotid arteries with 1% Triton X-100 had completely removed cell

nuclei. By 18 weeks confluent EC were evident in a dog model (Tamura et al., 1999). Courtman et al (2000), have developed a four-step process that utilizes both ionic and non-ionic detergents to decellularise canine arteries. First step is with protease inhibitors to prevent matrix degradation, followed by a 1% Triton X-100 solution tris buffer to pH 8 (including protease inhibitors), followed by DNase and RNase treatments. A fourth step is incorporated with 1% SDS tris buffered at pH 9 (Courtman et al., 2000). Interestingly work by Wilson and Courtman et al (1994), had previously concluded that the final treatment with SDS had proved detrimental porcine aortic leaflets (Courtman et al., 1994), citing Bodnar et al (1986), where 1% SDS treatments resulted in “profound degenerative changes” (Bodnar et al., 1986).

Cartmell and Dunn (2000) compared the efficiency of three chemical treatments: A non-ionic detergent Triton X-100, an organic solvent tri (*n*-butyl)phosphate (TnBP) and a ionic detergent SDS on rat tail tendon cellularity, structure, nativity and the subsequent alterations to the tissues mechanical properties. Results from the Triton X-100 displayed a disrupted tendon structure with the treatment failing to remove cells at lower concentrations (Cartmell and Dunn, 2000). This again contrasts Courtman et al (1994) who found the bovine pericardium maintained its mechanical properties after a 1% Triton X-100 treatment (Courtman et al., 1994). Treatments with 1% SDS for 24 hours did not cause significant denaturation of the rat tail collagen and found of the three treatments (SDS, Triton X-100 and TnBP) to have better retention of the tissues mechanical and structural properties. Finally tissue exposure to TnBP over any period of time (independent of concentration) resulted in a significant reduction in cell density. 1% TnBP for 48 hours removed cells with the least damage to the matrix (structurally or its mechanical properties).

## ENZYME TREATMENTS

In most cases enzymes have been used to degrade DNA and RNA with DNase and RNase with the intention of reducing the risk that these macromolecules maybe recognised as foreign. Teebken et al (2000), aimed to generate a biocompatible and mechanically stable porcine aortic (thoracic) graft with exclusive use of enzymes. Their method involved a trypsin digest (0.1% with 0.02% EDTA) for 24 hours, followed by incubation with DNase (0.2mg/ml), RNase (20 µg/ml) all at 37°C 5%



CO<sub>2</sub> (Teebken et al., 2000). These results displayed positive removal of DNA, examined by H & E and immunohistochemically with CD 31, and  $\alpha$ -actin for cellular debris. The use trypsin, a serine protease, is directed to the proteolysis of non-matrix proteins in particular cell remnants after a lipid extraction with multiple washes in acetone. The matrix described in Chapter 3 of this thesis has been exposed to a multi-step process, where porcine dermal collagen is firstly exposed to multiple acetone washes followed by an extensive enzymatic digestion of non-matrix proteins with trypsin. The remaining matrix is said to retain less than 5% of the tissues original non-fibrous tissue proteins, glycoproteins and lipid. The material is then cross-linked with HMDI (Oliver and Grant, 1985). The result of acetone treatments, specific cross-linking with hexamethylene diisocyanate and its subsequent sterilisation with gamma radiation renders a material that becomes a permanent implant. The matrix becomes impenetrable to cells, other than physical migration into fibrous pores, as cells are unable to digest heavily cross-linked matrix proteins. The choice of enzyme in this application is important to selectively reduce structural protein degradation. Trypsin is only active against the peptide bonds in protein molecules that have carboxyl groups donated by arginine and lysine, therefore collagen whose structure maintains the basic formula (Glycine-X-Y)<sub>n</sub> where X maybe any residue other than glycine and Y is typically hydroxyproline (Williams, 1998), is particularly resistant to trypsin digestion (Friess, 1998).

## SOLVENTS

Industrial processes have extensively used solvents to extract lipids from tissue, for example the separation of lipid from fish tissue. Many of these processes are concerned with the complete extraction of a variety of lipids not the resulting properties of the tissue itself. Solvents used in these processes have traditionally been methanol and chloroform, which are both considered toxic (Undeland et al., 1998). Similarly, Reid and Rojkind (1987) patented a method describing the isolation of a connective tissue biomatrix. The patent describes a methodology to isolate connective tissue fibres, including basement membrane components and components of the “ground substance”, providing improved adhesion and growth properties compared with the then current culture substrates. The two steps in this process relevant to this project are the DNase, RNase digestion and lipid extraction. The solvents used for lipid extraction is 100

ml of distilled H<sub>2</sub>O and an equal volume of butanol/ether (40:60) is added and stirred approximately every 5 minutes for 0.5-1 hour at room temperature (Reid and Rojkind, 1987). The process aims to remove lipid from dissolved collagen solutions (retained lipids and nucleic acids are not quantified) with no interest in the mechanical properties of the original tissue.

As discussed above in the *detergents* subsection, EtOH has been used during decellularisation procedures as a wash to remove remnants of detergents (Malone et al., 1984) or preserve tissue (Malone et al., 1984) and (Goissis et al., 2000). Several researchers have investigated EtOH as an integral part of tissue processing as a method to reduce calcification of bioprosthetic heart valves. The hypothesis is that EtOH pre-treatment, results in structural changes of tissue proteins and extraction of lipids that inhibits the deposition of calcium (Vyavahare et al., 1997). Reduced calcification as a consequence of ethanol treatment cannot be solely put down as the removal of lipid, where more extensive lipid extraction methods such as chloroform and methanol do not offer the same protection against calcification (Demer, 1997). Vyavahare et al (1997) have shown that a concentration of 40% EtOH did not remove cholesterol and phospholipids, whereas treatments 60% and greater were very effective. Treatments of 60% EtOH extracted up to 98% cholesterol and 71% phospholipid whereas 80% EtOH extracted 99% cholesterol and 94% phospholipid. Using a sheep mitral valve replacement model with treated (EtOH concentrations 60 – 80%) porcine bioprosthetic heart valves calcification was almost completely inhibited (Vyavahare et al., 1997). Vyavahare et al (1998), have also shown that ethanol pre-treatment stabilise the material to collagenase digestion and reduces the total water content within the tissue, assessed with NMR (Vyavahare et al., 1998).

In a later study from the same group, Lee et al (1998) have used an 80% treatment of EtOH with aortic wall implants in rat subdermal implants and porcine valves implanted into the mitral position of a sheep model. Results with this treatment were less conclusive than previous studies, where calcification of the bioprostheses was reduced from  $129.90 \pm 7.24$   $\mu\text{g}/\text{mg}$  to  $71.80 \pm 8.45$   $\mu\text{g}/\text{mg}$  in the rat model. In the sheep model the reduction in calcification was less significant falling from  $56.35 \pm 6.14$   $\mu\text{g}/\text{mg}$  in control tissue to  $28.02 \pm 4.42$   $\mu\text{g}/\text{mg}$  in the treatment sample. In contrast to Vyavahare et al (1998) the water content was not found to differ significantly as a result of the

ethanol treatments. The conclusion of this work stated that ethanol treatment of bioprosthetic heart valves had significantly reduced calcification from control samples but would require the addition of a further agent to completely inhibit tissue calcification (Lee et al., 1998). Shen et al (2001), studied pretreatments of bovine pericardium with combinations ethanol, ether and Tween 80, their results found the combination with ethanol and surfactant or ethanol, ether and surfactant were more effective at preventing calcification than treatments of surfactant alone (Shen et al., 2001).

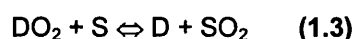
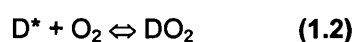
#### **4.1.3 CROSS-LINKING BIOLOGICAL TISSUES**

The use of collagen based biomaterials for tissue regeneration necessitates a degree of tissue processing to stabilise the tissue (against both pre- and post-implantation degradation) and prevent a chronic immune reaction against matrix epitopes (in this case porcine) associated with the biomaterial, Schmidt and Baier (2000). Cross-linking biological tissues has been shown to prolong the materials structure and mechanical characteristics *in vivo* while reducing the potential immune load on the graft recipient, Khor (1997). Chapter 3 has introduced the topic of cross-linking where the porcine derived dermal collagen matrix which had been previously been cross-linked with hexamethylene diisocyanate (HMDI) was used as a potential biomaterial for this project, as discussed in Chapter 3, Sections 3.1 and 3.4.

Cross-linking methodologies can be grouped into two major sections, chemical and physical methods. Of the chemical methods, glutaraldehyde has been the most frequently used preservative in bioprosthetic tissue. The stabilising effect is said to be a complex, degradation-resistant, Schiff base and pyridinium salt-derived cross-links between collagen molecules. Compared to formaldehyde, which forms less stable methylene-based protein cross-links, Schoen and Levy (1999). Issues concerning these and other chemical methods to cross-link tissue have been with cytotoxic residues remaining within the matrix material post processing, Khor (1997). Bioprosthetic implanted as heart valves for example are continually perfused in the recipient's body. Whereby potential cytotoxic compounds are continually removed from the implant giving the impression of 'minimal' toxicity. This was clearly noted with the HMDI

cross-linked dermal collagen matrix used in Chapter 3. *In vivo* analysis had shown the matrix to elicit a minimal immune response, Oliver and Grant, (1985), where the more sensitive *in vitro* analysis had shown seeded HUVEC and hVSMC to loose adhesion between 4 and 7 days of static culture, see Figures 3.11-14. Extensive washing of the matrix was shown to improve this situation see Chapter 3.4.3. A number of other chemical treatments have been analysed, that have aimed to reduce toxicity, improve retention of the tissues mechanical characteristics, with better stability and reduced calcification; including carbodiimides, azide and polyether oxide, (Khor 1997).

The primary benefit of physical methods, such as heating, freeze drying and irradiating is that no potentially cytotoxic compounds are introduced into the tissue. The method favoured in this thesis is that of dye-mediated photo-oxidation, where the tissue is incubated in a photoactive dye and irradiated to introduce intermolecular cross-links that stabilised the tissue against degradation. Modification of amino acid residues histidine, tryptophan, methionine and tyrosine can be oxidised in the presence of visible light and a photosensitiser such as methylene blue or green; and that the reaction does not cause the cleavage of the peptide bond, (Tomita et al., 1969). Weil et al (1965) had shown a reduced yield of histidine after 24 hours hydrolysis of insulin after irradiation in the presence of methylene blue. The mechanism of action is said to be complex and may vary from system to system, Oster et al (1959) proposed that the dye (D) is raised to a higher energy level by exposure to visible light where it forms a  $DO_2$  complex that can then react with the substrate,  $\rho$ -toluenediamine (in this case). Equations 1.1-3 have been abbreviated, where  $D$  represents the dye,  $D^*$  the dye in an excited electronic state (after visible light activation) and  $S$  the substrate.



Gerdes et al., (1997) state that the dominant initial step is the formation of singlet oxygen, followed by oxidation of the substrate. In another model *N*-benzoyl-L-histidine has been used as a model system to analyse the chemical nature of the His-His cross-link(s) that form during photo cross-linking of proteins. His-His covalent cross-link(s)

were formed when samples were incubated in singlet oxygen producing photosensitiser and illuminated with visible light. The His-His cross-links form between the  $\delta^2$ -carbon of one residue and the  $\epsilon^2$ -nitrogen of the other residue mediated by the singlet oxygen pathway, Shen et al., (2000).

In terms of the photo oxidation of collagen fibrils, Ramshaw et al (1994) have shown that exposure of rat-tail collagen fibrils to methylene blue and visible light (or UV light) resulted in reduced yields of amino acids, particularly histidine after irradiation. Concluding that the reduced yields were the result of introduced intermolecular cross-links in the tendon collagen. Further discussion of cross-linking by means of this method, applied to whole tissue is discussed in Section 4.3.3.

Although much of the later work has been conducted with methylene blue, methylene green has a similar mode of action, the difference being the addition of a  $\text{NO}_2$  group on methylene green which very slightly affects the wave length at which light is absorbed, the mechanism is energy transfer will however be the same, Price (2001), Department of Chemistry, University of Bath, UK, personal communication.

It is generally accepted that the more exogenous bonds introduced to the tissue the increased durability and resistance to host degradative mechanisms such as matrix remodelling enzymes. Iterated throughout this thesis is the importance of the extent of cross-linking within the tissue. If a biomaterial is designed to behave similar to a permanent implant a high degree of cross-linking is required. However if desired, the tissue has the ability to remodel then exposure to the chemical or physical methods are reduced. The concept of tissue engineering is to seed cells onto the matrix to guide cell growth and proliferation to generate a neo-organ; if the matrix is excessively cross-linked cell ingrowth is likely to be inhibited. A balance is therefore required between stability, whereby the matrix remains stable long enough for the patient's cells to infiltrate and remodel the matrix before matrix degradation and failure under arterial pressure conditions.

In this thesis a general methodology modified from Mechanic (1994) using methylene green as a photoactive dye to cross-link processed porcine arterial tissue has been described.

#### 4.1.4 PROCESS OVERVIEW

Clearly a multitude of different paths available to remove cells and cellular debris from tissue, the aim of this chapter is to describe a methodology that removes cells and their components, fatty tissue and physically removes connective tissue, and many non-structural proteins within the ECM without destroying the gross structural integrity of the native vessel. Due to reported problems associated with SDS and Triton X-100 detergent on destabilising the matrix and benefits foreseeable with a solvent extraction process, organic solvents was the method of choice to extract tissue lipid. With the goal to reduce, ideally eliminate the potential for *in vivo* calcium deposition and immunogenic components with solvent extraction, non-structural protein digestion and cross-linking will ideally produce a 'clean', immunologically inert biomaterial, with a structurally intact matrix, as tested: histologically, pressure testing and load extension analysis, in a condition ready to seed the desired cell type/s for tissue engineering applications. Briefly, the process developed in this thesis is a stepwise procedure that incorporates a variety of mechanisms to extract cellular and non-cellular components from the matrix material, Figure 4.01.

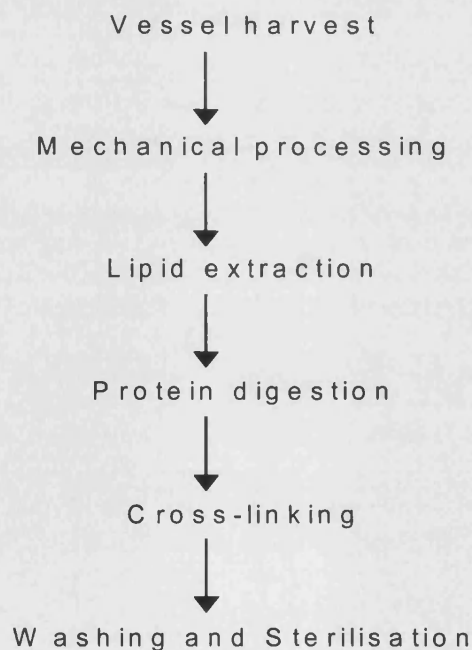


**Figure 4.01:** Main processing steps of the decellularisation process.

## **4.2 MATERIALS AND METHODS**

### **4.2.1 MATERIALS**

Unless stated otherwise all reagents and material details including vendor and are shown in Chapter 2.

### **4.2.2 EXPERIMENTAL METHODS**

All solution volumes to tissue weights are in a ratio of 15 ml solution to 1g tissue unless stated otherwise. This ratio was established due to the size and form of the arterial sections. It was found that this ratio of solution to tissue weight 'arbitrarily' covered or immersed the tissue section/s being treated within 15 or 50 Falcon tubes.

#### **4.2.2.1 MECHANICAL PROCESSING**

Carotid arteries were harvested from 6-8 month old Great White pigs slaughtered at a local abattoir. Warm ischemic time was no more than two hours from the time of tissue extraction to storage at 5°C and subsequent processing; see Section 2.1.2 for harvest details. Initial tissue processing tissue involved removal of loose connective tissue surrounding the vessel with forceps and scalpel. Arteries selected for experimental use measured 80-110 mm in length with lumen diameters from 2.5-6.5 mm. Vessels were then stored at -20°C until required.

#### 4.2.2.2 PRELIMINARY DECELLULARISATION

##### ***Ammonium hydroxide***

Porcine carotid artery sections ( $0.5 \pm 0.1\text{g}$ ) were exposed a 10% solution of ammonium hydroxide (v/v) in 15 ml Falcon tubes for 12 hours in a temperature controlled water bath at 20°C. Samples where removed from the  $\text{NH}_4\text{OH}$  solution, rinsed twice (10 minutes each) in  $\text{dH}_2\text{O}$  (same volumes). Following wax imbedding, sections were cut to 5  $\mu\text{m}$ , then dewaxed and stained with haematoxylin, refer Chapter 2.3.7 for protocols.

##### ***Ultrasound treatments***

Porcine carotid artery sections ( $0.5 \pm 0.1\text{g}$ ) were exposed to high frequency sound waves with a Grant ultrasonic water bath (Model XB5, BDH, Poole, UK). Samples were either placed directly in the water bath or within a 15 ml Falcon tube for 12 hours in a temperature controlled water bath at 20 °C. Samples where removed from the water bath, rinsed twice (10 minutes each) in distilled  $\text{H}_2\text{O}$  (same volumes). Following wax imbedding, sections were cut to 5  $\mu\text{m}$ , dewaxed and stained with haematoxylin, refer Chapter 2.3.7 for histology protocols.

#### 4.2.2.3 LIPID EXTRACTION

Tissue sections were incubated in 2 x 75% ethanol treatments for 10 minutes followed by 1 x 24 hr treatment. Unless stated otherwise samples where then incubated in the described solvent for 1, 2, 3, 6 and 24 hours on a rocking/rolling plate at room temperature (13-15°C.). Glass capillary tubes (1.5 x 125 mm) were inserted into each vessel to prevent kinking, which may have reduced tissue exposure to the solvent. In all cases tissue sections were cut, weighed and incubated in solvent (xylene, n-butanol or ethanol), see Table 4.02 for solvent properties, with a 1:15 ratio tissue weight (g) to solvent volume (ml) at room temperature and placed in a Duran bottle on a rolling/rocking table for the experimental duration. Sections were removed at prescribed time points and prepared for TLC as described in Section 2.3.2.



**Table 4.02:** Solvents used for lipid extraction and their properties, (Tennant, 2000).

	Xylene	n-Butanol	Ethanol
Molecular formula	$C_6H_4(CH_3)_2$	$CH_3(CH_2)_3OH$	$C_2H_5OH$
Molecular mass	106	74.12	46.07
Solubility in $H_2O$ (%)	-	7.8	100

#### 4.2.2.4 CROSS-LINKING ARTERIAL DERIVED MATRIX

The method used to cross-link the processed porcine carotid arteries was a modification of a method described by (Mechanic, 1994). The cross-linking process consisted of four main steps: 1. preconditioning tissue in 100mM  $NaPO_4$  with 0.5 M sucrose (682 mOsm) pH 7.6, for 24 hr. 2. A second preconditioning step where the tissue was again soaked for a 24 hour period in the cross-linking solution (100mM  $NaPO_4$  with 4M NaCl plus 0.1% w/v methylene green, pH 7.4). 3. Cross-linking the tissue in a modified 2.5 L stainless steel tank with the same solution as step 2 for a period of 22 hours (see below). 4. Rinsing to remove remnants of the processing steps entailed washing the tissue sections in sodium phosphate buffer (pH 7.4) on a rolling/rocking table until the samples were substantially free of the dye catalyst. This required a minimum of 10 washes, no less than 2 hours each, over a 2 week period.

The cross-linking step required the design and manufacture of a reaction chamber that enabled multiple arteries to be processed simultaneously, supplying an even exposure of light from the 300 watt halogen bulb and maintained at  $0 \pm 1^\circ C$ . The published method neither describes the type of bulbs used nor the energy output in terms of Lux, heat of spectrum, only that visible light provide the reaction energy. The method was described using 2 x 150 watt flood light bulbs 7-15 cm from the sample tissue. Due to the variation in tissue dimension from the pericardium (used in the Mechanic et al (1994) protocol) to blood vessels (this thesis) the light source was changed to a more appropriate designed halogen bulb that better suited the physical characteristics of the cross-linking equipment. A calibration was performed using a Gossen Luna III light meter (Hedges and Wright, Swindon, UK) to ensure a similar light intensity was used between the floodlights (2 x 150 watt) and the 300 watt halogen.

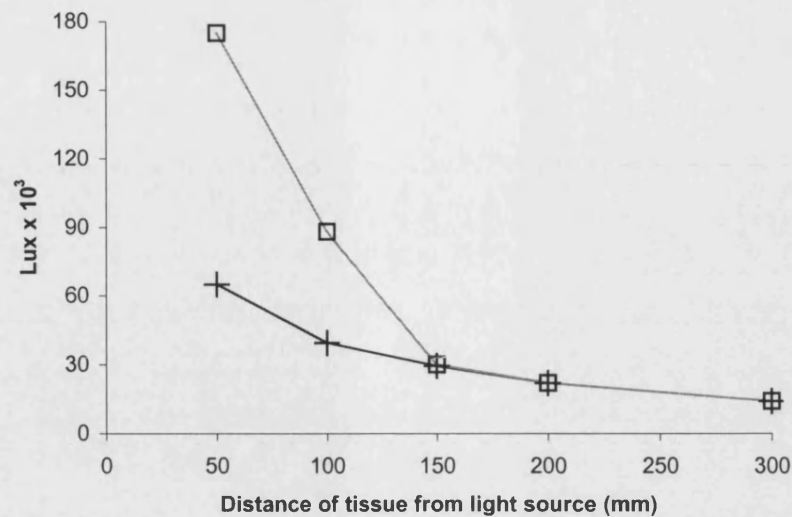


**Figure 4.02:** A calibration graph comparing two 150 watt flood lights (+) to one 300 watt halogen lamp (□). Illustrating a comparable light intensity at approximately 150 mm from the tissue surface.

Figure 4.03 displays the apparatus used for the cross-linking procedure, utilizing using a high-energy light source and methylene green as the photo-catalyst. Each artery had a 1 mm stainless steel rod inserted through its lumen and placed in a purpose built perspex holder that held up to 10 arteries in a parallel formation 8 mm apart. The pre-cooled (5°C) cross-linking solution was poured into the reaction vessel, covering the arteries by not more than 2.5 mm. The reaction chamber was placed in the cooling unit, maintained at  $-4^{\circ}\text{C}$  and vigorously stirred throughout the process. When the cross-linking solution fell to  $0^{\circ}\text{C}$ , the 300 watt halogen light source, suspended 150 mm above the surface of the solution, was turned on to irradiate the methylene green solution. During the cross-linking step 10 ml/min of air was sparged through the reaction chamber. The reaction chamber equilibrated at  $0^{\circ}\text{C} \pm 0.5^{\circ}\text{C}$  as a result of the heat generated by the light source (a requirement of Mechanic et al 1994 protocol).

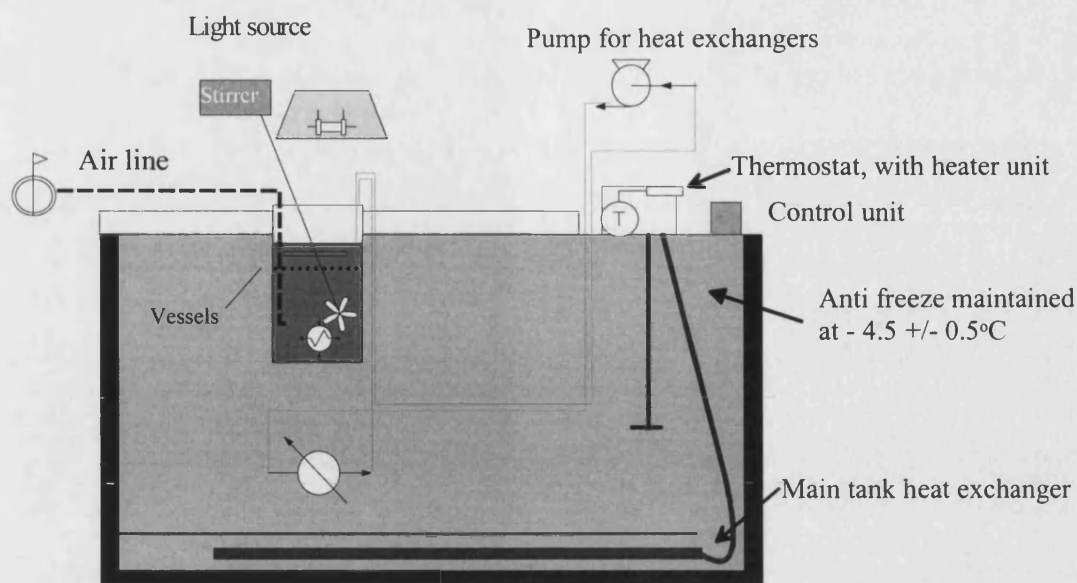


**Figure 4.03:** Cross-linking assembly

#### 4.2.2.5 POST PROCESS WASHING

Post cross-linking; the matrix was washed to remove components of the cross-linking reaction (methylene green, sucrose, NaCl) and to further aid the extraction of remaining cell debris. Processed arteries were washed in batches of 10, with a combined weight approximately 14-18g, in 2L of distilled H<sub>2</sub>O on a rocking rolling plate. A minimum of 7 complete changes over a 7 day period were carried out or until the bulk methylene green had been removed from the tissue. Extended washes to remove crystal substances exposed by LT-SEM, see Figure 4.15 required a further 7 days (7 further equidistant changes of H<sub>2</sub>O) eliminated these crystals from the matrix/arterial wall. Cross-linked matrix was cut in transverse section for LT-SEM analysis and prepared as in Section 2.3.8.1.

#### 4.2.3 ANALYTICAL METHODS

All analytical methods used in this chapter are described in chapter 2, Material and Methods, analytical methods Section 2.3.

### 4.3 RESULTS

Results from experiments to modify the native porcine carotid artery to give a functional matrix for tissue engineering purposes are described in this section. Figure 4.01 displays an overview of the theme followed to generate a stable acellular tissue, whereas this section details the incremental steps within each of the main headings. In addition, a comparative analysis was conducted between the acellular matrix produced by the method described by Mechanic et al (1994), and the methodology employed in this study. Finally mechanical properties, such as burst pressure and stress-strain relationships were measured and compared to the native porcine artery.

Unless stated otherwise all images and observations taken of the tissue or processing methods are representative of the sections or samples studied. Figure 4.04, illustrates a transverse section of unprocessed porcine carotid artery, displaying the major functional and histological components of the arterial wall. Note the high density of VSMC throughout the media and EC lining the vessels basement membrane. This representative image is referred throughout this chapter as the native or unprocessed tissue to distinguished changes induced by vessel processing described in this chapter.

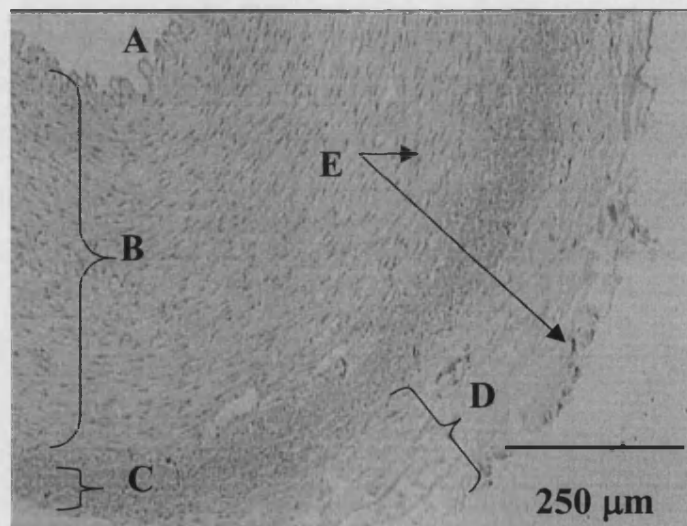


**Figure 4.04:** An H & E stained transverse section of control (untreated) arterial wall. Showing the lumen and convoluted intimal lining (A), medial layer (B), adventitial layer (C) and connective tissue joining the artery to other tissues (D). Cell nuclei are stained purple (E).

#### **4.3.1 MECHANICAL PROCESSING AND STORAGE**

In order to minimize the immunological load on the patient (once tissue engineered product is implanted) as much nonessential porcine arterial component was removed as possible. As the connective tissue provides little or no strength to the artery, in terms of resistance to mechanical failure imposed by haemodynamic stresses, it was removed, leaving as few 'foreign' immunological components as possible.

Observations of the mechanically processed arteries abluminal surface display the adventitial layer largely intact around the medial layer of the vessel wall, with the bulk of the connective collagen removed. In some instance the adventitial layer had been partially removed, this was due to difficulty discerning between the said layer and the surrounding loose connective tissue. Storage of the vessels prior to processing at -20°C to rupture cells was not tested independently as a specific step.

#### **4.3.2 REMOVAL OF CELL AND CELL COMPONENTS**

##### **INITIAL EXTRACTION TRIALS**

Early investigations focused on methodologies to extract nonstructural components of the arterial wall, including cells and their components, in a 'one-step' process. Two different treatment methodologies utilising  $\text{NH}_4\text{OH}$  and ultrasonic radiation were assessed. Figure 4.05 shows an H & E stained section of porcine carotid artery exposed to 10% solution of  $\text{NH}_4\text{OH}$  at 20°C as described in 4.2.2.2. Collagen fibres are severely fragmented with large spaces appearing between the elastin and collagen ECM. Cell nuclei are observed throughout the tissue section. Porcine carotid arterial sections immersed in  $\text{H}_2\text{O}$  within separate tubes and exposed to ultrasound displayed no histological change in structure from control tissue over the experimental duration. Arterial sections immersed directly in the ultrasound water bath and exposed to ultrasonic sound waves displayed similar histology to  $\text{NH}_4\text{OH}$  treated samples. Fragmentation of the ECM was evident within the ECM (A) while cell nuclei remain in the tissue (B) see Figure 4.06.

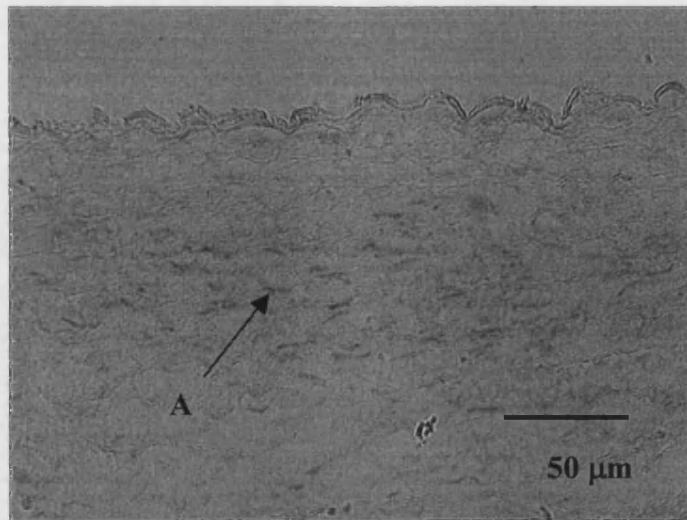


**Figure 4.05:**  $\text{NH}_4\text{OH}$  treatments of arterial tissue fragmented the ECM framework and failed to remove cell nuclei (A).

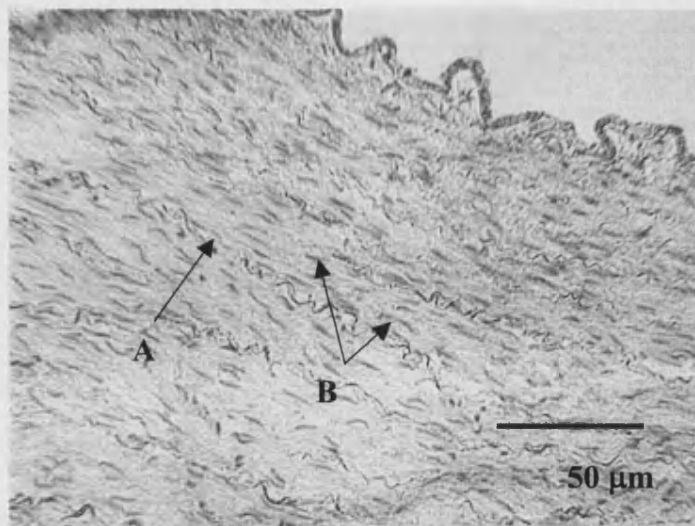


**Figure 4.06:** Arterial sections post exposure to ultrasound (directly in ultrasonic bath) for 10 minutes. Note ECM fragmentation (A) and retention of cell nuclei (B).

## SOLVENT BASED LIPID EXTRACTION

Due to the negative outcome of both  $\text{NH}_4\text{OH}$  and ultrasound treatments, a two step process was designed that used a lipid extraction step followed by proteolytic digestion to allow non-structural components to be removed. A variety of solvents were tested and evaluated in terms of lipid extraction and effect on the structure of the arterial ECM.

### ***Xylene***

Sections of artery ( $0.5 \pm 0.1\text{g}$ ) washed in xylene on a rocking rolling table at room temperature ( $14\text{-}17^\circ\text{C}$ ) for 24 hours. A barrier of  $\text{H}_2\text{O}$  formed around the tissue as a result of xylene hydrophobicity, see Table 4.02. This layer diminished by approximately 75% (qualitative reduction from  $\sim 0.5$  to  $< 0.1$  mm) by 6 hours but remained present ( $\sim 10\%$  of original size) after 24 hours. The treatment was altered to include 25% and 75% EtOH dehydration steps prior to, and 75% and 25% EtOH rehydration steps after exposure to xylene, for 2 hours. The tissue dehydrated severely when exposed to xylene after the 75% EtOH dehydration step, forming a rigid structure that did not rehydrate, irrespective of the duration (up to 72 hours) of washing in  $\text{H}_2\text{O}$ . The vessel did not regain any of its previous mechanical characteristics due to its compacted (dehydrated) state. The vessels (after EtOH-xylene-EtOH treatment) were exposed to trypsin (1 x) at room temperature ( $14\text{-}17^\circ\text{C}$ ) for 24 hours and maintained its bulk structure with the vessels lumen remaining open.

### ***Butanol***

Tissue sections with a mean weight of  $0.314 \pm 0.03$  g were incubated in 100% butanol solution on a rocking/rolling plate at room temperature (15-18°C) as described in Section 4.2.3. Tissue was prepared for TLC as described in Section 2.3.2 and 4 $\mu$ l aliquots were run for each sample on silica gel 60 TLC plates as described in Section 4.2.3. Detectable lipids display a banding pattern of 5 spots on control samples. Over the experimental time course these bands faded as more lipid was extracted from the tissue. By the end of the third wash (3 hours) a significant reduction in banding intensity is noted. By 6 hours only small molecular weight lipid is noted at the top of the chromatography plate, which was further reduced by 24 hours see Figure 4.07. After 24 hour rehydration, samples were rigid with the bulk mechanical severely compromised, typical of tissue in a dehydrated state. Unlike EtOH-xylene-EtOH treatments, trypsin digestion of the butanol treated samples resulted in complete tissue collapse after 3 hours in a 1x solution at  $16 \pm 1.5^\circ\text{C}$ .

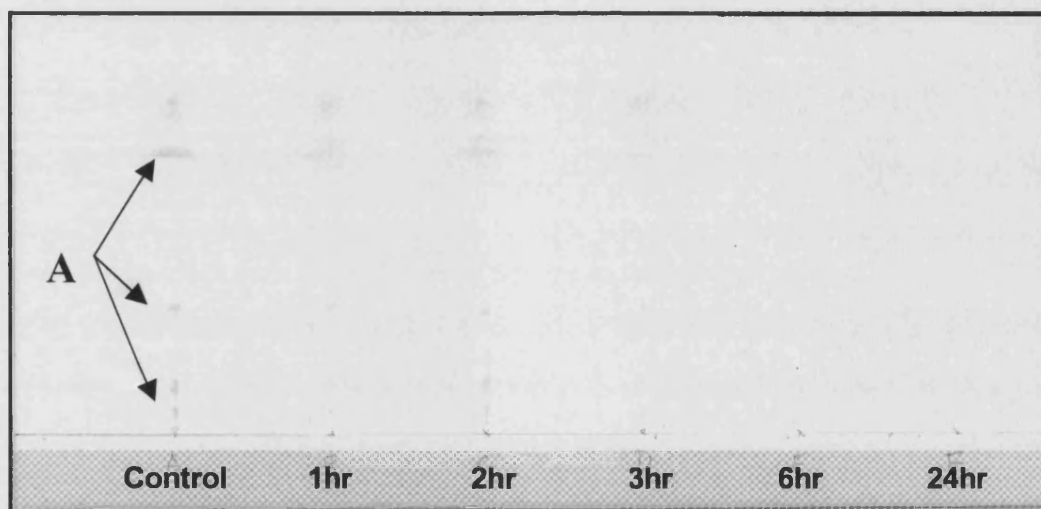


**Figure 4.07:** TLC plate displaying detected lipids (A) as vertical marks on the chromatogram. The butanol treatment has removed all detectable lipids by the 5<sup>th</sup> wash at 24 hours.



### ***Ethanol-Butanol-Ethanol***

Tissue with mean weights of  $0.20 \pm 0.03$  g was prepared and run on silica gel 60 TLC plates as described in Section 4.2.3. Detectable lipids display a banding pattern of 5 spots on control samples. Results show that ethanol dehydration treatments, prior to butanol, have removed the bulk of the detectable lipid. Samples remained pliable after the ethanol dehydration step, only after exposure to butanol did the tissue become rigid and lose beneficial mechanical properties, see Figure 4.08. Digestion of the treated tissue with trypsin showed, like the EtOH-xylene-EtOH treatments, samples had retained their structural integrity though the 24-hour digestion period.

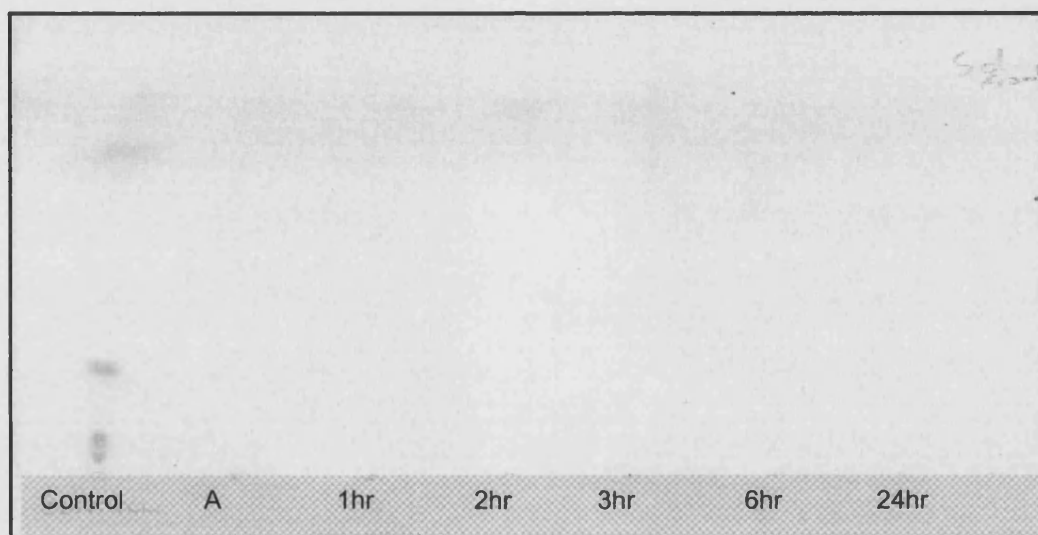


**Figure 4.08:** EtOH-butanol extraction of tissue lipids. TLC plate showing an almost complete extraction of lipid by the end of step A (2 x 10 minute washes EtOH (25%), 1 wash overnight EtOH (75%)). The extent of any further lipid extraction by the butanol treatments (1, 2, 3, 6 and 24 hours) past the initial dehydration steps is subjective with this methodology.

### Ethanol

Tissue sections with a mean weight of  $0.31 \pm 0.012$  g were incubated with 75% ethanol as described in Section 4.2.3. By 3 hours the ethanol treatments had removed the bulk of the detectable lipid, with no further lipid being extracted by 48 hours see Figure 4.09. On rehydration the tissue had returned (qualitatively) to a near 'native' state. Trypsin digestion post ethanol treatment showed, like the EtOH-xylene-EtOH treatments, the tissue had retained its bulk mechanical properties after the 24 hour digestion period. Two controls were tested 1. non-washed unprocessed tissue and 2. tissue washed in the same manner as experimental samples except in H<sub>2</sub>O for the full duration of the experiment, neither of which showed a loss of lipid content.

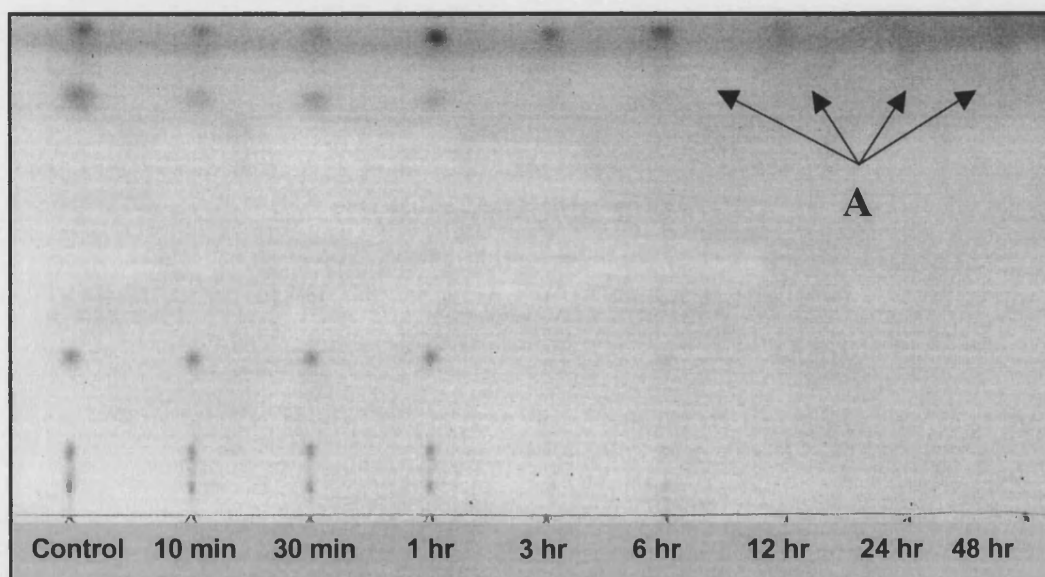


**Figure 4.09:** TLC plate displaying detected lipids after tissue treatment with 75% ethanol. A chromatogram showing the progressive reduction in lipid content over a 48 hour period. At the 3<sup>rd</sup> wash after 1 hour, the 75% ethanol treatment was unable to extract further detected lipid (A) at the top of the chromatogram remaining throughout the 48 hour treatment.

Treatment with EtOH resulted in a matrix material with reduced lipid content and retention of its bulk mechanical properties, unlike previous treatments that had detrimental effects on tissue mechanical properties, see Figure 4.10. EtOH treatment (progressive washes for 24 h) was therefore used as the lipid extraction protocol.

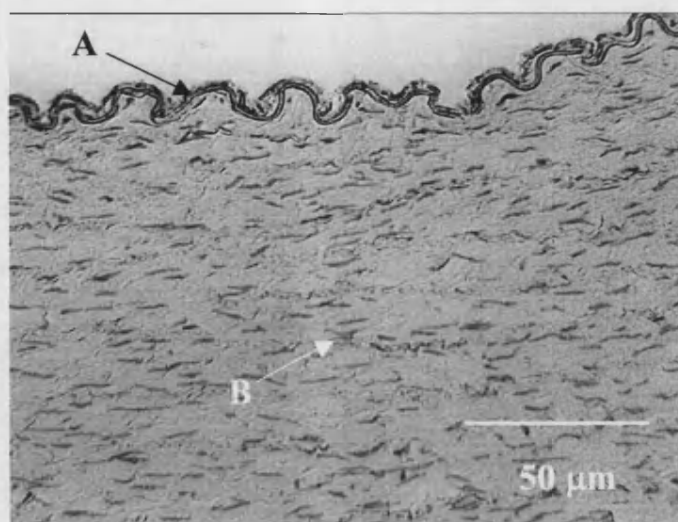


**Figure 4.10:** An H & E transverse section of the arterial wall post ethanol lipid extraction. The internal elastic lamina remains intact (A) along with cell nuclei (B).

#### PROTEIN DIGESTION

Following treatment in EtOH for 24 h with washes in new solutions of EtOH at the prescribed time points, as illustrated in Figure 4.09, the tissue incubated in a trypsin solution, see Section 2.3.3. Structural change in the tissue was qualitatively monitored (tissue elasticity and collagen/elastin histology) and for the presence of cell nuclear material (histological analysis) over time, see table 4.03. These results were used to determine an optimal digestion period (48 hours) where a compromise was required that retained the tissues elastic nature whilst removing cell nuclear debris.

**Table 4.03:** Qualitative observations of native artery after treatments with 1 x trypsin

Time	Elasticity	Cell nuclei	Collagen / elastin
Unprocessed	control	Present & intact	Normal & intact
Post EtOH treatment	small reduction	Present & intact	slightly compressed
24 hr trypsin	reduced from t=0h	partial disruption	"
48 hr trypsin	reduced from t=24h	complete disruption	"
72 hr trypsin	reduced from t=48h	none present	partial fragmentation
96 hr trypsin	tissue collapsed	"	↓
120 hr trypsin	"	"	extensive fragmentation

Trypsin activity over time showed the enzyme's activity was stabilized when arterial sections were present comparative to trypsin alone. This is likely to result from a reduction in autolysis as the enzyme competes with an increasing quantity of partially digested protein hydrolysed from the arterial section. Although trypsin activity declines over 120 h, the reduction in catalytic activity over the 48-hour incubation period is not significant to require changing the trypsin solution, see Figure 4.11. Controls were 1. enzyme solution heated to 75°C for 30 minutes to inactivate the enzyme and 2. buffer less BAEE substrate. Both displayed no change in absorbance over time.

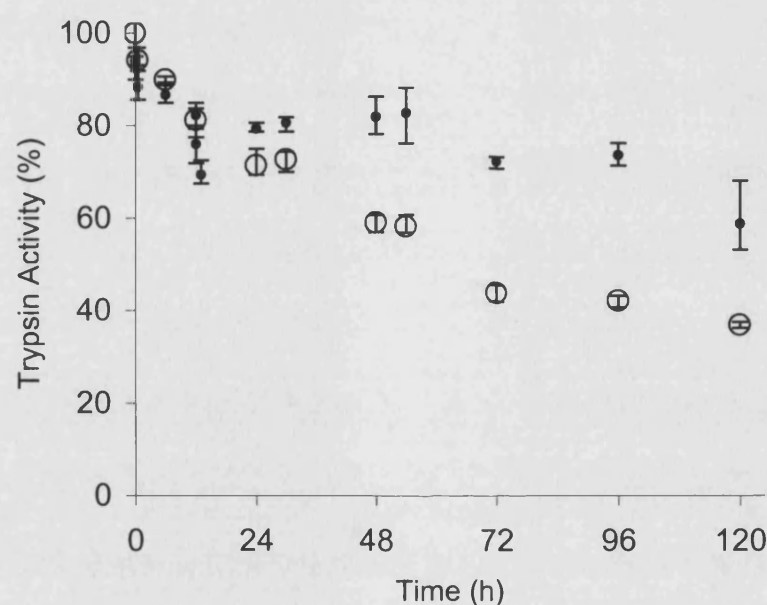


**Figure 4.11:** Trypsin activity without arterial sections present (□) reduced 63% (120 hours) and 38% (48 hours) from initial activity  $n = 3 \pm 1$  sd. Trypsin activity when the arterial substrate is present (○) reduced 41% (120 hours) and 10% (48 hours) respectively.

SDS PAGE analysis of tissue digestion (post ethanol treatments) shows the progressive extraction of matrix proteins, particularly small molecular weight proteins. By 24 hr the bulk of proteins less than ~75 kD have been removed, Figure 4.12. Staining the arterial derived matrix with van Gieson (specific for elastin) displayed retention of the internal elastic lamina and components of the basement membrane, see Figure 4.13.

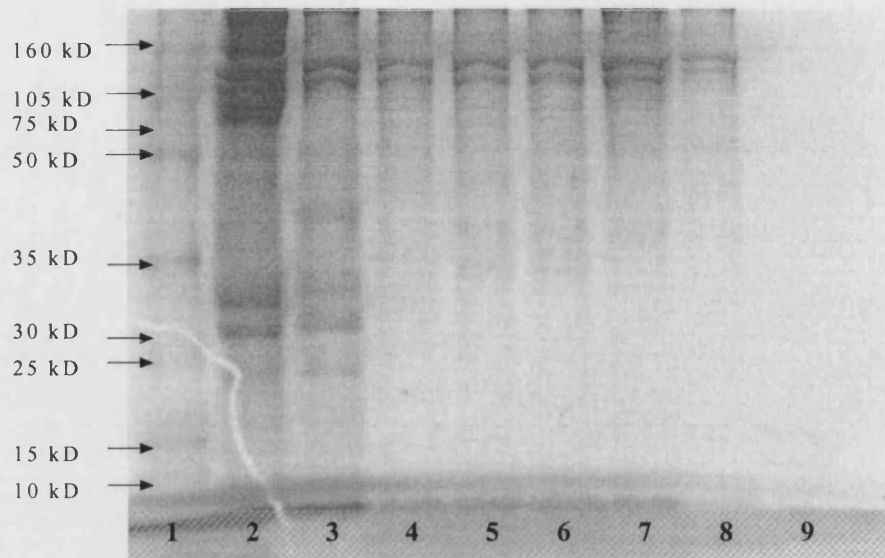


**Figure 4.12:** SDS-PAGE analysis of arterial protein after incubation to trypsin. Lanes: **1** molecular weight marker, **2**. untreated raw tissue, **3**. tissue post EtOH lipid extraction, **4**. trypsin digestion 24 hr, **5**. 48hr, **6**. 72hr, **7**. 96hr, **8**. 120 hr, **9**. Trypsin (10x).

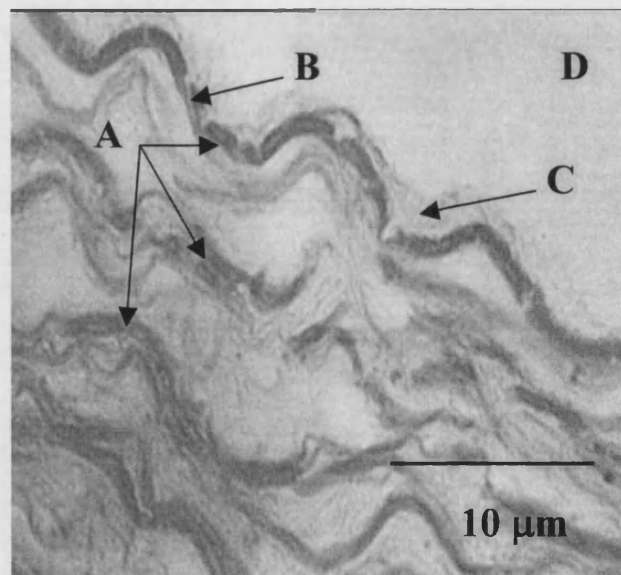


**Figure 4.13:** Identification of matrix elastin content. Matrix post trypsin digestion (48 hours) with elastin stained dark purple (A). Note retention of the internal elastic lamella (B) and basement membrane (C). Vessel lumen (D). van Gieson (Specific elastin stain).

Similarly, Figure 4.14, an H&E stained section of processed tissue shows the presence of the internal elastic lamina stained as a dark band beneath the translucent basement membrane on the luminal surface of the section. Importantly, cell nuclear material have been disrupted and is no longer visible by staining with H&E compared to control unprocessed tissue, see Figure 4.04.

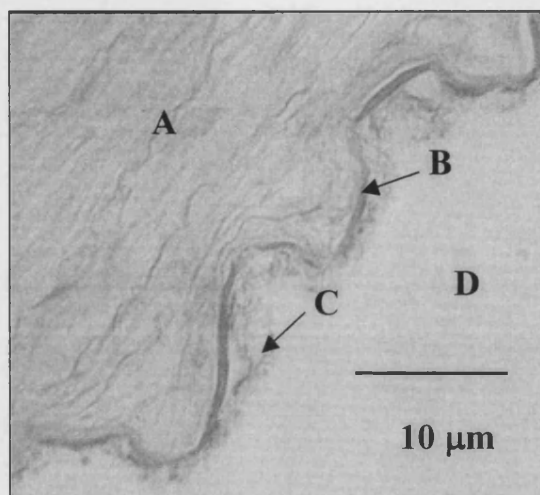


**Figure 4.14:** H & E stained matrix post trypsin digestion (48 hours), no nuclei are present within the arterial wall (A). The internal elastic membrane (B), basement membrane (C) have been retained. Vessel lumen (D).

Based on the results from the observable changes in matrix structure, cell nuclei disruption and SDS-PAGE analysis of protein extraction, a 48 h digest was chosen as the preferred method to disrupt residual cell components (after solvent treatment) for clearing from the tissue.

### 4.3.3 CROSS-LINKING

As discussed in Section 4.1.3 the distinctive amino acid composition of collagen is used as a diagnostic tool to determine Hyp (hydroxyproline) content (Vincent, 1982). By assaying the proteolytic degradation products (particularly Hyp) with RP-HPLC a comparison was made between untreated (less resistant to degradation) to cross-linked tissue (more resistant to degradation).

#### ENZYME DEGRADATION RESULTS

The results in table 4.04 show tissue samples from the cross-linked arteries were resistant to degradation in the 1000 activity unit/ml pepsin solution for the duration of the enzyme treatment. The Hyp samples from the untreated (raw) arteries displayed moderate levels of degradation indicated by the free Hyp concentration and total peak area. Comparative to cross-linked samples (total peak area only) the control group displayed consistent concentrations/total peak areas. Cross-linked samples were not degraded sufficiently to yield a discrete Hyp peak with this concentration of enzyme. Evaluation of the total peak area indicates that the extent of tissue degradation is almost 6 times (5.73) less than that of the cross-linked samples, although this is not representative of specific collagen (Hyp) degradation, rather the total amino acids in solution post-pepsin treatment.

Standard cross-linked samples were compared to untreated tissue post digestion with 5000 activity unit/ml pepsin at 37.5°C for 16.5 hours. At this higher enzyme activity, the extent of the tissue degradation of the cross-linked tissue was sufficient to result in a measurable level of free hydroxyproline in solution. Free hydroxyproline per gram from the cross-linked tissue is less than a quarter (21.4%) of raw tissue samples. The total peak area per gram of tissue in the cross-linked samples was approximately a third (32.5%) of the value for the uncross-linked tissue; see Table 4.04.

**Table 4.04:** Comparison of unprocessed and cross-linked tissue digested with 1000 and 5000 activity units/ml pepsin for 20 hours at 37.5°C. Mean peak areas and total free Hyp in solution digested (n=6).

	Free hydroxyproline $\mu\text{mol/g}$		Total Peak Area (units)	
	Mean	S.D.	Mean	S.D.
1000 activity units/ml pepsin				
Unprocessed artery	16.54	2.08	1055000	6961
Cross-linked	0	0	184100	17990
5000 activity unit/ml pepsin				
Unprocessed artery	31.51	1.19	2200000	21320
Cross-linked	6.74	1.01	714600	11430



#### 4.3.4 POST PROCESS WASHING TO REMOVE DISRUPTED CELLULAR AND NONCELLULAR COMPONENTS OF THE ECM

As described in Section 4.2.2.5, the processed porcine arteries were washed in H<sub>2</sub>O to remove vessel components that had been disrupted through the processing steps. Over the 7 day duration of vessel washing it was observed that the dye was progressively removed, until day four when no further dye was removed, the final 3 days having no effect on dye removal, with the vessel remained light blue in colour. Transverse sections of the vessel wall with LT-SEM showed the presence of crystalline substance/s imbedded throughout the vessels medial layer. No direct analysis was conducted to determine the nature of the substance, however it was believed to be residual salt from the cross-linking step where vessels were incubated in 4M NaCl, see Figure 4.15, where crystals are clearly visible. Extending the washing process a further 7 days eliminated these crystals from the matrix/arterial wall.

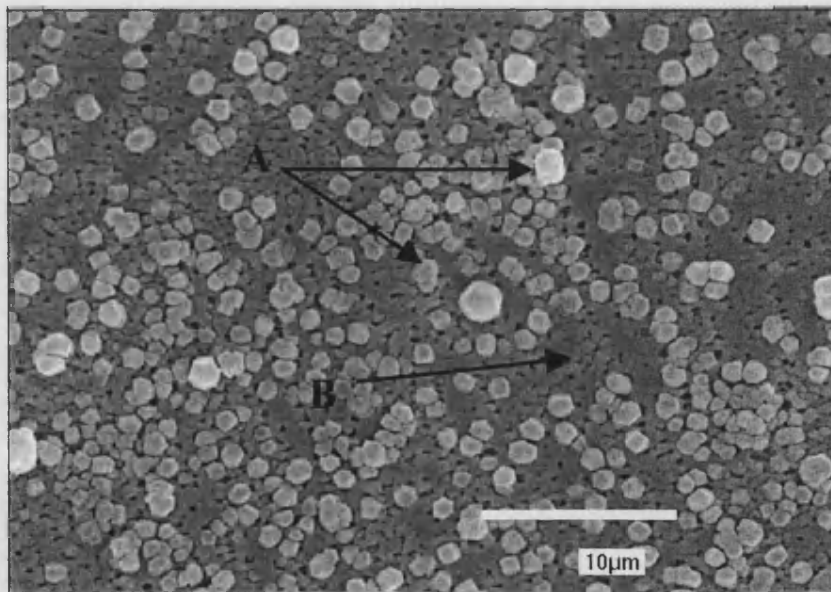


**Figure 4.15:** Presence of crystals within the matrix wall post processing. LT-SEM, vessel wall in transverse section (cut immediately prior to viewing) of a fully processed and 'washed' matrix wall. Note the abundance of crystals (A) exposed at the cut edge of the collagen/elastin matrix (B), approximately 2-4µm in diameter.

## DNA EXTRACTION

In order to determine the effectiveness of the washing steps at removing residual cell components, sections of matrix (post trypsin treatment, pre-cross-linked and not washed) were compared to sections of matrix that had been washed for two weeks, as described in Section 4.2.2.5. These Figures (4.16a/b and 4.17a/b) show DNA as bright 'light-blue' strands (A) against a darker blue background. Figures 4.16a and b shows the vessels luminal surface, with Figures 4.17a and b the vessels abluminal surface. Figures 4.16a and 4.17a represent the matrix pre-cross-linking with Figures 4.16b and 4.17b displaying DNA remaining post cross-linking and washing steps. These images show the near complete removal of DNA from both the luminal and abluminal surfaces.

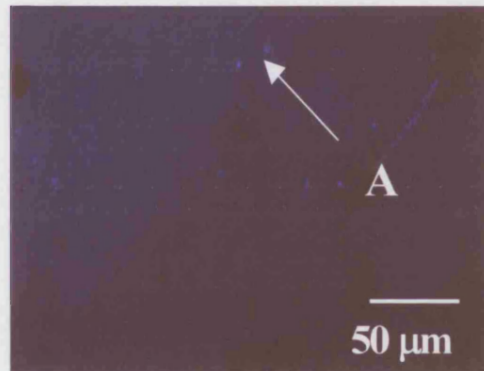
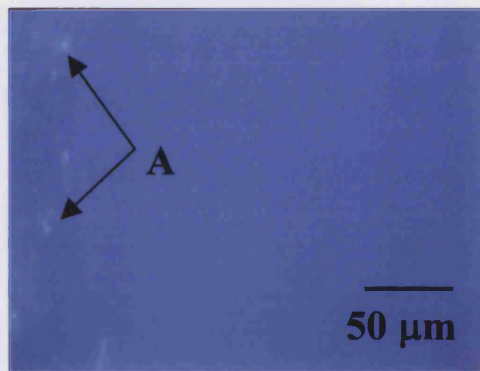


**Figure 4.16a:** Luminal surface pre cross-linking and **Figure 4.16b:** post cross-linking and washing, DNA is stained by DAPI (A).

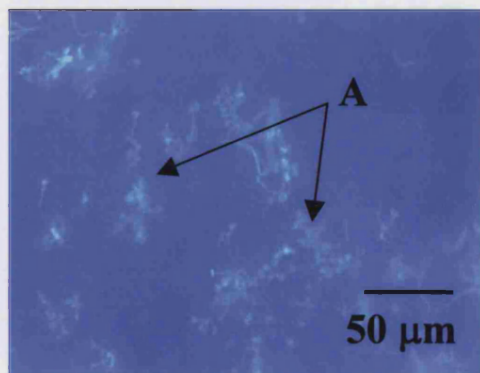


**Figure 4.17a:** Abluminal surface pre cross-linking and **Figure 4.17b:** post cross-linking and washing, DNA is stained by DAPI (A).

#### 4.3.5 LT-SEM ANALYSIS OF FULLY PROCESSED MATRIX/VESSEL SURFACES

To assess the presence of other non-specific cell debris retained on the surfaces of the matrix LT-SEM image was conducted. Fully processed and washed matrix displays a luminal surface void of EC or large cellular debris with the undulating basement membrane retained (luminal surface), see Figure 4.18. Although the basement membrane remains largely intact, gaps or holes were noted in some areas. Figure 4.19 shows a higher magnification of the luminal surface, clearly showing gaps in the basement membrane. Like the luminal surface there was no evidence of intact porcine cells on the abluminal surface, Figure 4.20. Figure 4.21, a higher magnification of the matrices abluminal surface shows the presence of particulate matter bound to the surface fibres. The compressed or matted appearance of the ECM was believed to be an artefact of LT-SEM sample preparation where surface H<sub>2</sub>O is blotted which compacts the free surface fibres, standard SEM (not low temperature) has been used in Figure 7.08 to display of the outer fibrous nature of the matrix surface of the matrix.

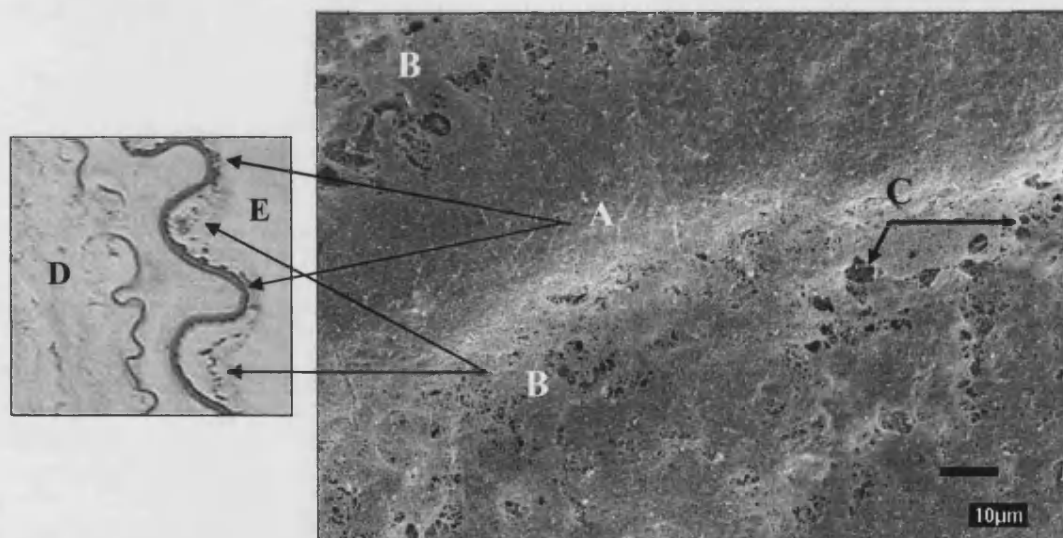


**Figure 4.18:** LT-SEM image of fully processed matrix displaying the luminal surface morphology. Showing the hills (A) and valleys (B) associated with undulating luminal surface. Breaks in the basement membrane can be seen (C). **Inset:** van Gieson stained arterial transverse section showing the equivalent surface structures (A and B) with the matrix wall (D) and vessel lumen (E).

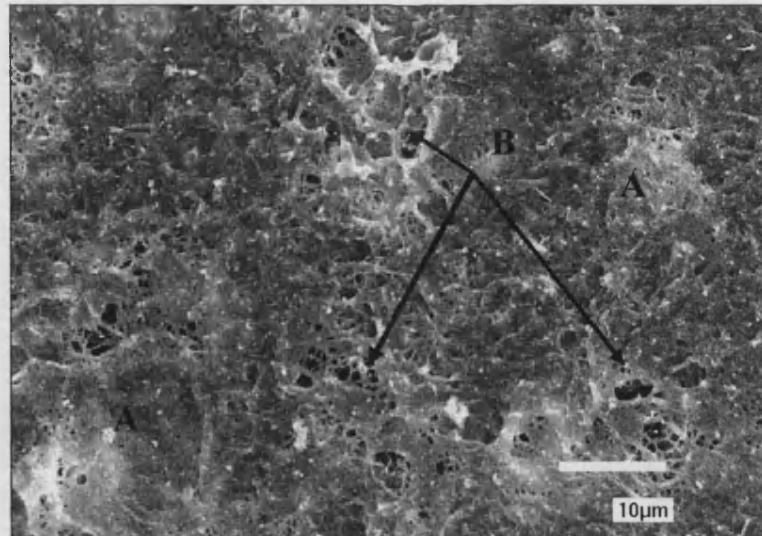


**Figure 4.19:** Higher magnification of the processed grafts luminal surface. Holes in the basement membrane can be clearly seen (B) compared to continuous areas (A).

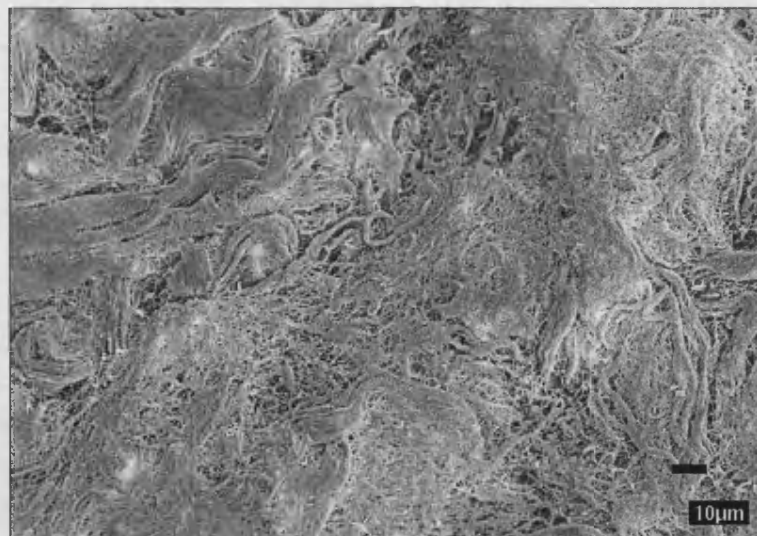


**Figure 4.20:** Low magnification LT-SEM image of the processed grafts abluminal surface. Like Figure 4.27, the bulk of the matrix appears free of particulate matter. Note the compressed or matted appearance of the ECM fibres lying flat on the surface of the matrix.

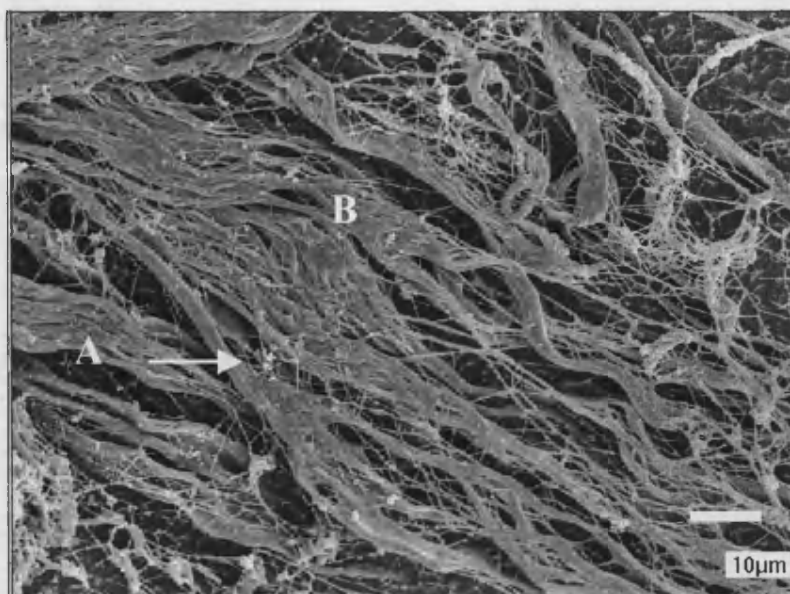


**Figure 4.21:** A higher magnification LT-SEM image of the processed grafts abluminal surface. Particulate matter (A) remains amongst the matrix fibres (B). No intact or partially lysed cells are noted on the matrix surface.

#### 4.3.6 COMPARATIVE PROCESS ANALYSIS

In order to determine the process described in this thesis was an improvement over the processes published by Mechanic (1994) a comparative analysis between the final processed matrix described in this thesis and that published by (Mechanic, 1994) was conducted. The two key steps in this process were the lipid extraction using the EtOH washing protocol and digesting the vessel in trypsin to remove non-structural proteins. Results from TLC chromatograms have shown additional lipid has been extracted by the process described in this thesis compared to the method described by Mechanic (1994) protocol, see Figure 4.22a. SDS-PAGE analysis of ECM protein content is similar to the lipid analysis, where the total protein content is considerably reduced from both control (A) and Mechanic (1994) process (B) to the method in this thesis (C), see Figure 4.22b.



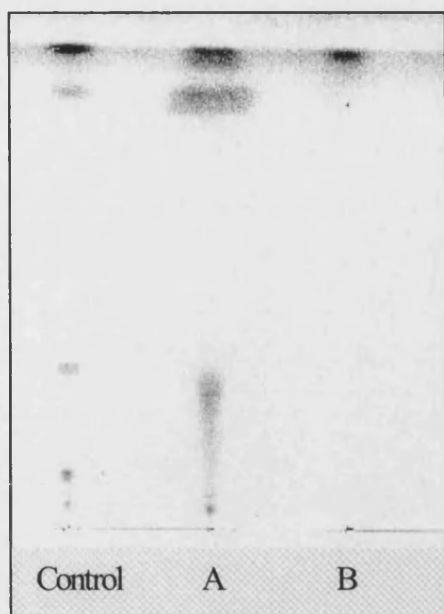


Figure 4.22a

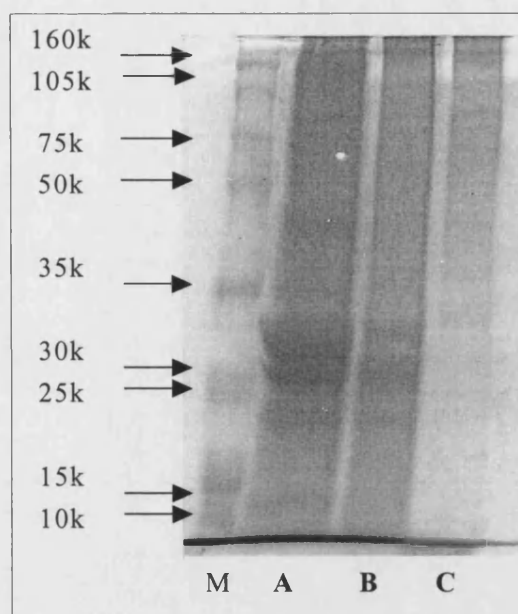
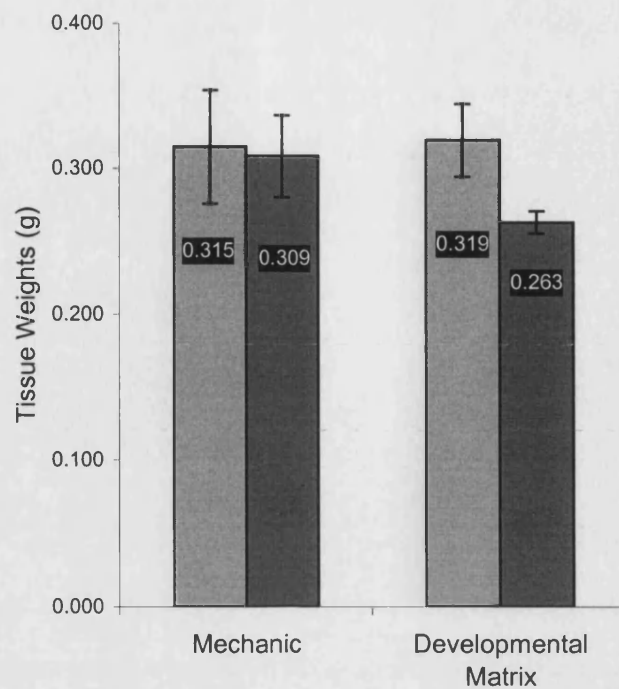


Figure 4.22b

**Figure 4.22a:** Sample A, using 0.5 M sucrose followed by 4 M NaCl and cross-linked as described in Section 4.2.3.1/2. Sample B, lipids remaining in the tissue after the completed treatment developed and described in this thesis. **4.22b:** Total protein content in (C), the method in this thesis, is considerably reduced from both, controls (A) and Mechanic's process (B). Gel loading 10 $\mu$ l/well.

SDS-PAGE had shown a visual loss of protein, Figure 4.22b. To determine if the reduction in protein content was detectable in gram quantities, initial weights were recorded and compared to post processing tissue weights. Tissue sections ( $n = 12$ ) with mean weights pre-treatment of (Mechanic  $3.15 \pm 0.39$  g and the matrix developed in this thesis  $3.19 \pm 0.03$  g) were treated in accordance with each method. Figure 4.23 illustrates the physical loss in tissue weight between the two processing methods expressed as a percentage weight loss, with mean values  $\pm 1$  sd, Mechanic 2.01% and the matrix developed in this thesis 17.92%. The student's t-test was used to determine significance between pre and post-treatments. No significant difference was found with the Mechanic process from start to finish weight, with a t-test value of 0.327 resulting in a  $p > 0.05$ . Conversely the matrix developed in this thesis showed a significant loss in weight  $p < 0.01$  with a t-test result of 9.449. Critical values for  $p=0.05$  (2.07) and  $p=0.01$  (2.82), see Figure 4.23.



**Figure 4.23:** Tissue weight loss: ■ pre-treatment and ■ post-treatment. Error bars indicate  $\pm$  one standard deviation.

#### 4.3.7 MECHANICAL PROPERTIES

Critical to the success of this matrix is the ability to withstand applied haemodynamic stresses imposed by the human arterial system. Arterial pressure rarely exceeds 200 mmHg, it was therefore important that the described material maintains integrity to a level exceeding this working load. A pressure test was conducted to determine the mean rupture point of the fully processed matrix comparative to unprocessed tissue. In addition the mechanical strength, a stress strain analysis was conducted to compare the elastic properties between untreated and fully processed tissue.

## PRESSURE TEST ANALYSIS

The t-test was used to determine any significance between untreated porcine carotid sections and cross-linked samples. No significant difference was found between the two sample sets with a t-test value of 0.111 with 8 degrees of freedom ( $n=10$ ) and a critical value of 2.306 results in a  $p > 0.05$ , (n.s.), see Figure 4.24.

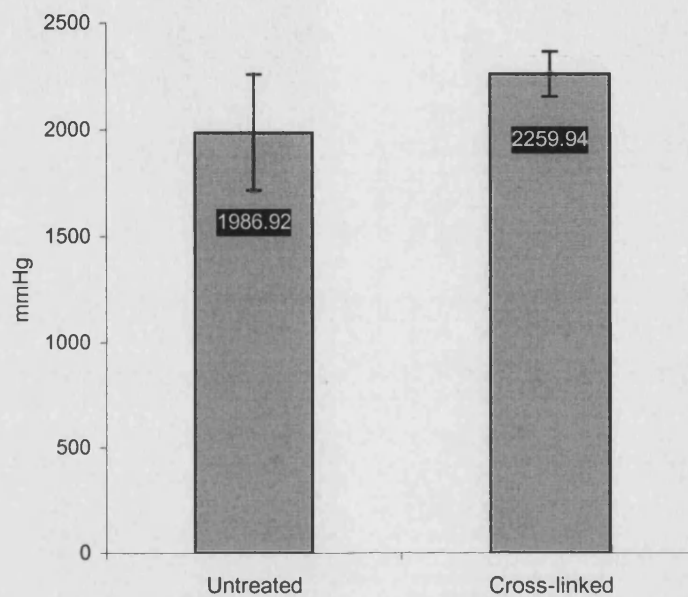


**Figure 4.24:** Variation in burst pressure between untreated and cross-linked tissue. No significant difference was found  $p > 0.05$ . Error bars indicate  $\pm$  one standard deviation.

## LOAD-EXTENSION DATA - STRESS-STRAIN CURVE

Stress strain analysis has shown a significant difference between untreated and cross-linked arterial segments. Untreated tissue segments display the characteristic biphasic relationship between matrix proteins, elastin and collagen. This is shown at the point where the graph becomes non-linear at approximately 90% strain from which the trend line curves upwards. Cross-linked tissue did not display the same biphasic relationship between the two main matrix proteins. Cross-linked tissue displayed increased variation around mean values, compared to untreated tissue, see Figure 4.25. The termination of each trend line represents the mean failure stress and strain  $602 \text{ g/mm}^2$  (untreated) and  $830 \text{ g/mm}^2$  (cross-linked).



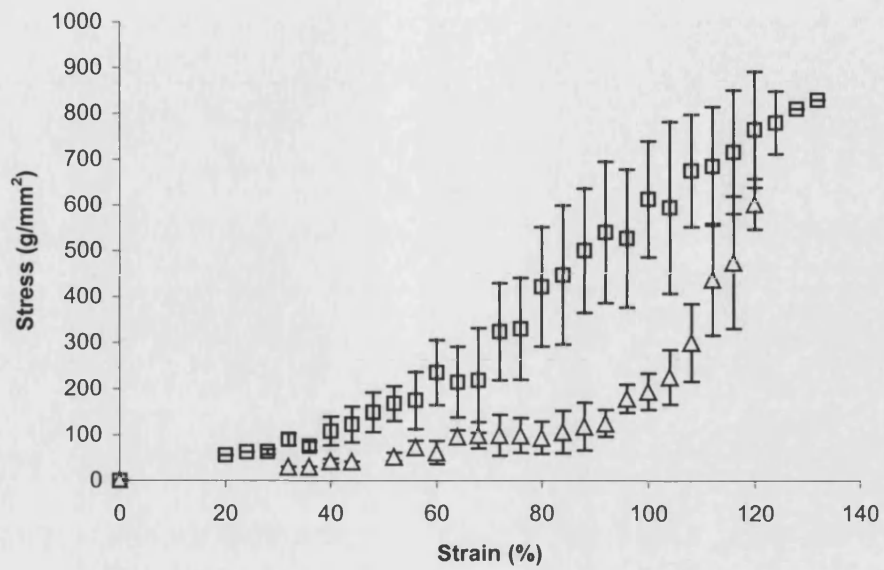


**Figure 4.25:** Stress-strain curve: Untreated tissue  $\Delta$  ( $n = 18$ ) and cross-linked  $\square$  ( $n = 38$ ). Error bars indicate  $\pm$  one standard deviation.

## MEAN FAILURE: STRESS AND STRAIN

The ultimate tensile strength of cross-linked tissue was higher than untreated tissue with results for the mean failure stress  $631.89 \pm 192.92$  and  $188.17 \pm 86.21$  ( $\text{g/mm}^2$ ) respectively. To determine any significance differences between untreated and cross-linked tissue the student T-test was used. Between the two data sets, *failure stress* ( $\text{g/mm}^2$ ), a T-test value of 3.87 was calculated, with a critical value of 2.66 ( $p = 0.01$ ) and 53 degrees of freedom. This confirms a significant increase in the failure stress point of the cross-linked tissue over the untreated tissue at the 1% level. Conversely the *percentage failure strain* no significant difference was found, with a t-test value of 0.001, where the mean failure strain (%) for untreated tissue was  $85.06 \pm 18.97\%$  and  $103.5 \pm 14.37\%$ , Figure 4.26.

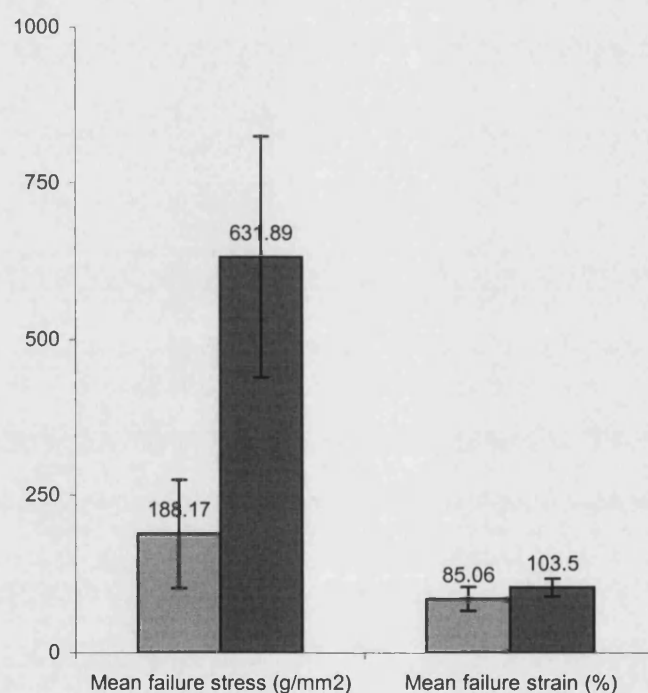


**Figure 4.26:** A graph to show the variation mean failure stress ( $\text{g/mm}^2$ ) and the mean failure strain (%) between untreated tissue and processed tissue. Error bars indicate  $\pm$  one standard deviation.

## 4.4 DISCUSSION

### OVERVIEW OF MATRIX PREPARATION

This section of work has focused on the generation of a matrix for vascular tissue engineering purposes, derived from porcine carotid arteries. In this section the discussion has been divided up into topic headings, in the order the work was carried out. Figure 4.27 details the stepwise process leading from collection of the carotid artery from the abattoir through to the fully processed matrix.

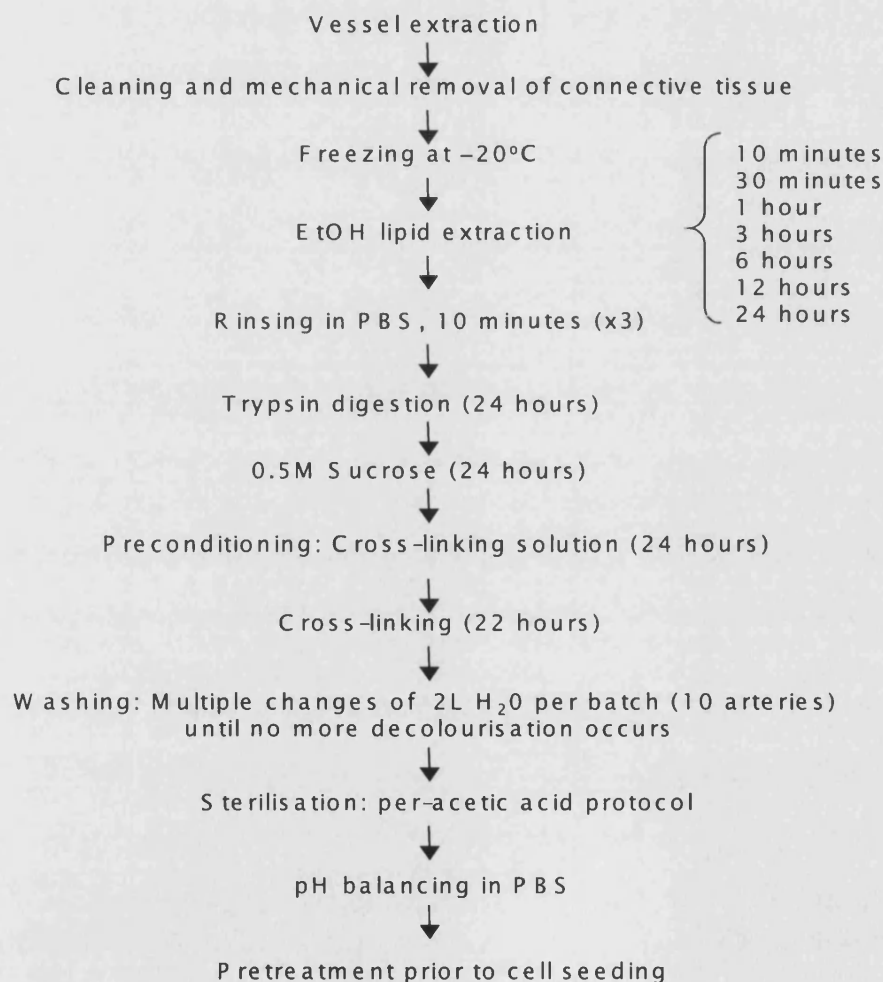


**Figure 4.27:** A diagrammatic representation of the complete processing methodology used in this thesis.

#### 4.4.1 MECHANICAL PROCESSING AND STORAGE

The first step in the process was the actual harvesting of the arteries whereby arteries of an appropriate size and undamaged during the extraction process were selected. The selection criterion encompassed intact arteries measuring between 80-110 mm in length with lumen diameters from 3.5 - 6.5 mm (proximal) tapering to 2 - 3 mm (distal). Observable variation in the physical parameters of the porcine carotid between individual animals was marked, with many intact arteries falling outside the selection criteria. The selected arteries were then washed and trimmed to reduce the artery to its minimum effective components that will allow it to withstand applied haemodynamics stresses, whilst retaining its mechanical properties. As such the final implant will present to the recipient as few as possible 'foreign' immunological components. For this reason the loose connective tissue surrounding the exterior of the vessel was removed.

The stability in terms of haemodynamic tolerance that the adventitial layer provides to a muscular artery is minimal compared to the considerably larger (and retained in this process) medial layer (Nerem and Seliktar, 2001). A qualitative decision was made to retain this layer in order to preserve the tissues mechanical properties as much as possible throughout the processing steps. The extent of this 'retention of mechanical properties' by retaining (or not) the adventitial layer was speculative and specific tests to prove or disprove this were not carried out. It was assumed that retention of the adventitial layer would not be detrimental from a mechanical perspective as it was an integral part of the natural artery; it was therefore retained in the processing. The mechanical removal of loose connective tissue surrounding the unprocessed arteries proved to be a delicate and lengthy operation. Results have shown the adventitial layer to be largely intact around the medial layer of the vessel wall with the bulk of the connective tissue removed. Considerable care was required to excise the surrounding connective tissue, as there was no clear boundary between the arteries outer adventitial layer and the adjoining connective tissue. In some instances the adventitial layer had been completely removed with the medial layer exposed.

An issue favouring the removal of this outer layer would be a decrease in the distance between EC seeded on the luminal surface and SMC seeded onto the outer or

abluminal surface. Effective communication at both the cellular and molecular level plays an important role in retention of the endothelium as a whole and the maintenance of cell phenotype (Nackman et al., 2000). The domain around which a single cell can effectively communicate with surrounding cells has been estimated to be ~250  $\mu\text{m}$  (Francis and Palsson, 1997). The thickness of the porcine carotid arterial wall ranges between ~500-2000  $\mu\text{m}$ , including the adventitial layer, (~ 50- 500  $\mu\text{m}$ ), see Figure 4.04, by reducing this distance it is speculated that the culture time required to generate a biofunctional artery with cell populations within communicative distances, maybe decreased. Additionally the removal of the adventitial and associated connective tissue layers (retaining only the intimal and medial layers), would increase the efficiency of later processing steps by decreasing the thickness of the wall. These initial decisions were made without the benefit of hindsight, where the final experimentation conducted in this thesis has proven the matrix to be over cross-linked preventing cellular migration into the matrix. Based on these results it would be beneficial to completely remove the adventitial layer prior to lipid extraction.

Storage of the vessels at -20°C after the mechanical removal of connective tissue was chosen not only to preserve the vessels prior to completing the processing steps, but to rupture porcine cells by formation of ice crystals, releasing cellular components into the ECM aiding the later, more specific decellularisation processes. Damage to the ECM as a result of the freezing process, for example fractures within the collagen matrix were not observed. In support, (Hunt et al., 1994) have shown that collagen fibres are resistant to fracturing at these temperatures. Vessels were maintained in storage no more than 4 weeks prior to processing to reduce the potential of damage by freeze-drying.

#### **4.4.2 REMOVAL OF CELLS AND CELL COMPONENTS**

Initially procedures were investigated that could employ a one-step process to extract as much non-structural protein, lipid, including cellular components as possible without affecting the mechanical properties of the ECM. Advantages of a one-step process, if successful, would be favourable from both manufacturing and ultimately cost perspectives. Several methodologies were employed to extract these components, including; ammonium hydroxide and ultrasound followed by multiple H<sub>2</sub>O washes to

remove both residual chemical and disrupted components within the ECM. Preliminary tests, see Figure 4.05 (NH<sub>4</sub>OH) and Figure 4.06 (ultrasonic irradiation) show despite severe fragmentation within the collagen/elastin matrix and the appearance of large spaces between the elastin and collagen frameworks, cell nuclei remain visible in histological sections. After these initial experiments a more rational approach was taken where two major components of whole tissue were specifically targeted for extraction, lipid and non-structural matrix protein.

The order in which treatments were carried out was based on improving the accessibility of the tissue to the following treatment, refer to Figure 4.27. In addition to a potential reduction in immunogenicity by component removal, connective tissue would inhibit diffusion of all treatments into the arterial wall. By firstly removing this outer layer of connective tissue all following treatments will have improved access to the inner medial layer and thus increase the effectiveness of each treatment. The lipid extraction step was aimed to remove cellular and tissue lipids, by dissolving the cell lipid membrane many cell proteins will be washed from the tissue and the following proteolytic treatment will be more effective, through better access to cellular proteins.

#### LIPID EXTRACTION

The second step of the process was extraction of the vessels lipid content a number of different solvents or combinations of solvents were initially tested to evaluate both lipid extraction and alterations to the vessels gross mechanical characteristics, these included xylene, butanol and ethanol. Progress towards extraction of the lipid content within the arterial vessel began with xylene, an extremely hydrophobic solvent requiring excessive agitation before the (observable) H<sub>2</sub>O boundary layer was reduced, not removed, see Table 4.02 for solvent properties. The treatment was modified to include ethanol dehydration and post treatment rehydration steps (25-75%). Tissue rehydration post xylene treatment failed to return the tissue to its former elastic state resulting in a rigid structure irrespective of the duration (up to 72 hours) of washing in H<sub>2</sub>O.

As part of the processing methodology for the type I dermal collagen matrix used in chapter 3, trypsin is used after the acetone treatments to digest non-matrix protein (Oliver and Grant, 1985). This published treatment utilizes a 2-6 week digest in

trypsin, clearly either the matrix material is strongly resistant to degradation by the neutral protease trypsin, as discussed by (Friess, 1998) or acetone pretreatment has a stabilizing effect, either through modification of the structure of the collagen/elastin molecule or mass transfer of the enzyme is limited due to compaction of the matrix after dehydration. Oliver and Grant (1985) state that less than 5% of the original non-matrix protein and cell debris remains after processing. A reduction in matrix water content may act as a barrier to the enzyme entering the matrix thus preventing excessive matrix degradation.

LT-SEM images of this biomaterial Chapter 3.3.1 show a matrix void of all visible cell debris supporting the findings of Oliver et al (1985). In order to determine the effect, if any, the solvent extraction process was having on the matrix sections, treated tissue was immersed in a 1x trypsin solution for 24 hours and assessed in terms of gross visual and structural properties. Tissue sections exposed to xylene and EtOH-xylene-EtOH remained viable with each vessel lumen remaining open and appearing structurally sound. The only noticeable effect of the trypsin digestion was the outer extremities of the arterial wall began to loosen with strands of attached ECM floating freely. This result is likely to be due to excessive dehydration of the matrix preventing the enzyme entering the arterial wall with only the exterior of the matrix rehydrating. The resulting loss of mechanical properties was so severe that regardless of the efficacy of lipid extraction the process was not deemed favourable. In addition xylene is rated as a Class II toxic solvent by the American Food and Drug Agency, where extensive extraction procedures are required post treatment, which may become problematic for human implantation studies.

Assessment of butanol as a solvent extraction mechanism was based on improved solubility in H<sub>2</sub>O, see Table 4.02 for solvent properties. Increased solubility would negate the requirement for EtOH dehydration/rehydration steps, reducing processing steps and additional handling. Results from TLC trials display a near complete removal of detectable lipid by 24 hours, Figure 4.07. However the tissue, like xylene without the EtOH treatments, failed after 24 hours washing in H<sub>2</sub>O to rehydrate, remaining rigid with the bulk mechanical severely compromised. Unlike xylene or EtOH-xylene-EtOH treated tissue, the butanol treatment failed to provide any stability to the matrix, which was severely compromised by 24 hours exposure to trypsin. The vessel wall had

collapsed with the lumen folding in on itself after 3 hours despite being excessively dehydrated. This result suggests another mechanism for matrix stability other than sole protection from reduced water content. Vyavahare *et al* (1998) have also shown that ethanol pretreatments stabilise biomaterial to enzymatic digestion. In this example the enzyme treatment was with collagenase, an enzyme that (unlike trypsin) specifically targets collagen. EtOH alone was shown by NMR studies to have reduced the total tissue water content (Vyavahare *et al.*, 1998). It is hypothesised to be minimal by comparison to the more hydrophobic butanol treatments, thus unlikely to be the sole reason for tissue stability. It was concluded that excessive dehydration and the tissues subsequent failure to rehydrate, in concert with reduced stability to trypsin, necessitated further modification to the process.

To assess the effect on EtOH on tissue stability and rehydration in concert with butanol treatments, samples were dehydrated with EtOH treatments (25 and 75%), exposed to butanol and once again rehydrated in graded EtOH treatments. The chromatogram of this treatment regime, Figure 4.12, shows that by the end of the initial EtOH dehydration step the bulk of the detectable lipid has been extracted. It was also observed that the tissue remained (qualitatively) pliable up to the point of butanol treatments. After 24 hours exposure to trypsin the vessels, like the xylene treatments, had retained their bulk mechanical properties. Like xylene, exposure of the matrix to butanol compromised the mechanical properties of the tissue due to the inability of the matrix to rehydrate post treatment. Under these conditions butanol was rejected as a solvent for lipid extraction. A reduction of butanol concentration in concert with EtOH may have produced the desired results, however from a simplicity point, trials progressed with EtOH alone as a sole mechanism to extract lipid and stabilise tissue. As discussed in the introduction to this chapter EtOH also reduces tissue calcification which has been a major issue in replacement collagen heart valves, for example (Vyavahare *et al.*, 1997) and (Lee *et al.*, 1998). Demer *et al* (1997) with the use of more volatile extraction solvents (chloroform and methanol) have shown a minimal reduction in calcification compared to EtOH treatments (Demer, 1997). Thus lipid extraction alone is not the sole factor in the prevention of tissue calcification. The hypothesis put forward by Vyavahare *et al* (1997) is that EtOH pre-treatment, in addition to extraction of lipid, results in structural changes of tissue proteins that inhibits the deposition of calcium (Vyavahare *et al.*, 1997). Further evidence that EtOH



stabilises the ECM framework is shown by Pieper et al (1999) where 1-ethyl-3-(3-dimethyl aminopropyl) carbodiimide (EDC) was used as a cross-linking agent. When the cross-linking reaction was conducted in the presence of ethanol matrix porosity was preserved. The reduction in structural change by comparison to controls was clearly demonstrated when EtOH was used as a pretreatment (Pieper et al., 1999). Figure 4.13, illustrates the progressive extraction of lipid from the tissue using EtOH washes (at each time point the EtOH solution is replaced). By 3 hours no further lipid is extracted (A) with a total tissue exposure of 48 hours in the treatment solution. Unlike any of the previous treatments the EtOH treated tissue rehydrates to its near native state, though a slight increase in rigidity was noted. As expected, exposure to trypsin over a 48 hour time course showed no obvious signs of degradation, at the macroscopic level.

Analysis of the solvents tested with the porcine vascular tissue has made it clear that a degree of compromise is required between the complete removal of tissue lipid and retention of the tissues mechanical properties. Aggressive solvents such as xylene and butanol extract more lipid than the EtOH treatments but their use results in a matrix with severely compromised mechanical properties through dehydration. As discussed the presence alone of lipid is not the sole cause of calcification, but the extraction solvent and its secondary effects on the matrix conformation play an important role, which is not fully understood. Butanol offers no protection or stabilising effect to matrix structural proteins to the trypsin digestion, used to extract non-structural proteins of the ECM. This again supports the premise that protection against ECM calcification is a multi-variable process that involves aspects of lipid content and the lipid extraction process, which further affects ECM stability against enzymatic degradation and structural change in denaturing conditions.

In this section of work the lipid content has been specifically targeted for removal by the application of a variety of solvents. Proteins associated with lipids, such as lipoproteins of the cell membrane removed in the washing, is secondary, though beneficial, to the aim of this step, which has been lipid extraction and retention of the vessels bulk physical/mechanical characteristics. Figure 4.10 a micrograph of the arterial wall post EtOH treatment, shows that cell nuclei have not been disrupted and are clearly present in the tissue, though slightly elongated, possible due to tissue dehydration.

## PROTEOLYTIC DEGRADATION ECM PROTEINS

After the removal of tissue lipids the process aimed to remove as much of the non-structural ECM (including cellular) proteins. Tissues were exposed to a proteolytic (trypsin) digestion. The aim of this step was to remove, in the same fashion as lipid extraction process, potential immunogenic porcine epitopes that may elicit an immune response to the engineered graft on implantation. Reduction in 'non-self' recognition of an implanted device/prosthetic by an individual's immune system is a positive step towards biocompatibility.

This section of work aimed to determine several factors: an effective enzyme digestion period to disrupt cell nuclei and remove non-matrix proteins; to assay the activity of trypsin over time determining its effective life-span in relation to the optimal tissue digestion period and to assess macro and microscopic changes in the arterial wall through the digestion period. In order to optimise this process it was necessary to determine parameters of the enzymes activity. Firstly, trypsin activity was monitored over time to establish the enzymes operational stability. Arterial specimens were exposed to proteolytic digestion and studied both histologically and for gross protein reduction. Collagen is inherently resistant to neutral proteases (Friess, 1998), none-the-less it was critical to establish an optimal digestion period. Excessive proteolysis will render the matrix susceptible to failure under haemodynamics stresses, whereas a reduced digestion period may not remove residual cell components and other non-matrix materials. Analysis of trypsin activity over the experimental time course and temperature range had shown 10.6% reduction in activity over 48 hours, a reduction not seen as significant to warrant changing the enzyme solution over the digestion period.

Similar to the lipid extraction process, a compromise was necessary, in this case between a digestion period that removes significant amounts of ECM protein and a digestion period, if too long, that damages the structure of the collagen/elastin fibres. Table 4.03 summarizes qualitative data that assessed effects of extended trypsin digestion on the ECM in terms of its elasticity, fibre morphology and the presence, or not, of porcine cell nuclei. Based on these results a 48 hour digestion period was selected. At this time point porcine cell nuclei had been completely disrupted and were no longer visible as independent structures, see Figure 4.14. Morphologically the

ECM fibres appear slightly compressed or flattened at 48 hours with a marginal reduction in tissue elasticity. Digestion past 48 hours resulted in a more noticeable reduction in elasticity with partial fragmentation of collagen/elastin fibres, however no cell nuclei were present nor any nuclear material assessed by haematoxylin staining. The mechanism for nuclear disruption is speculated to be the proteolytic digestion of the molecules e.g. histones, which maintain the coiled nature of non-proliferating DNA within cell nuclei. As cell membranes have been disrupted by the solvent treatment the uncoiled DNA molecules are dispersed through the ECM.

In terms of protein extraction, SDS-PAGE analysis of processed arterial sections after ethanol treatments, taken at 24 hour intervals during trypsin digestion showed a progressive extraction of tissue proteins, particularly small molecular weight proteins. All samples displayed a reduction in the smaller molecular weight protein ( $< \sim 75$  kD). The end of the first 24 hour digestion SDS PAGE gels showed a loss of protein bands between  $\sim 25$ -40 kD, from all tissue up to the point of the trypsin treatment. From 48 hours and on to 120 hours further loss in protein is qualitatively noted. The aim of this experiment was to observe the gross loss of protein not identify individual proteins. Further analysis of loss in tissue weight is discussed in Section 4.4.5.

Images such as Figure 4.04 display variation of the 'preliminary' material developed in Chapter 4. Showing sections of the adventitial layer remain attached to the abluminal surface of the matrix, further and more importantly from an EC adhesion perspective the basement membrane has in some places been digested away altogether and in other areas (the majority) the basement membrane appears intact. Figures 4.18, show the basement membrane attached to the internal elastic lamina whereas Figure 4.19 shows regions where the underlying collagen of the medial layer is clearly evident. Although the importance of this layer is debatable as a tissue engineering product, it is undoubtedly critical within living systems where it provides cellular cues, aids EC adhesion, acts as a filtration barrier and as a barrier to VSMC migration into the vessel lumen which may result in neointimal hyperplasia. The argument for its complete removal, along with all other non-structural proteins and carbohydrates is that as the product must be considered a foreign body, irrespective of attempts to reduce its immunoreactivity through extraction processes and cross-linking, an immune response to the material is to be expected. Even if this response is considered 'minor' blood

vessels, particularly small diameter vessels are extremely sensitive to thrombosis, due largely to their immediate proximity to blood and cells of the thrombolytic cascade. The argument to retain this membrane and other adhesive components of the ECM became clearer as the project matured. Again this is a qualitative assessment, but it appeared that EC have a propensity to adhere to regions of the matrix where the basement membrane has been retained. Although under static conditions (the bulk of the work) this was less obvious; when flow conditions were applied EC appear to have a higher retention in regions that the membrane has been retained. Apart from the adhesive components the membrane offers a relatively smooth surface for EC to adhere. The more fibrous sections, where the membrane has been removed, do not offer EC a uniform support surface that allows the EC to resist shearing off under flow conditions. Although the concept of a tissue engineered graft is that the graft is 'grown' *in vitro* prior to implantation the time required for EC to lay down a new and complete membrane may prove too long as time is a critical factor in production criteria. In my view, the maintenance of the membrane is advantageous to the final product, providing a confluent endothelium can be produced prior to implantation thus allowing some time for remodelling and the patient autologous cells to mask foreign epitopes remaining within the porcine tissue.

Processing steps involve chemical, physical (or other) agents to alter/modify a material will be subjected to variation associated with mass transfer within biological tissue. In particular a prolonged enzymatic digestion, a degenerative process, results in damage to the vessel wall, whereas a reduced digestion period fails to remove all the desired cellular and non-structural components. With uniform materials an acceptable balance can be found, by contrast observations of porcine carotid arteries have shown that the vessels taper and can have in excess of 50% variation in wall thickness from one end to the other. This variation results in thinner tissue being excessively digested in order for the cell nuclei etc. to be visually removed from thicker regions of the arterial wall.

#### 4.4.3 CROSS-LINKING

The final step, whereby the matrix material was physically altered was matrix cross-linking or stabilising the matrix, whereby potentially immunogenic epitopes are masked and the tissue modified in such a manner that it is resistant to host proteolysis. The process used to cross-link the matrix in this thesis was a modification of the method published by (Mechanic, 1994). The process utilizes methylene green as a photo-catalyst to cross-link amino acids forming covalent bonds between adjacent chains of the collagen macromolecule (Kuntz, 1964). This was followed by an extensive washing step to aid removal of ECM components, including cellular and noncellular components that had been disrupted in previous steps such that washing would remove them from the tissue. In addition, mechanical characteristics: pressure test, stress-strain analysis and tensile strength were compared to non-processed material to ensure the matrix would remain viable if exposed to arterial haemodynamics, see Section 4.3.6.

As a methodology to cross-link collagen, the approach used in this thesis with methylene green as a photo-catalyst has been very successful. Firstly the method is simple and once set-up is relatively inexpensive to treat large quantities of tissue, secondly, the design and system application effectively cross-links the arterial tissue. This directly supports others e.g. (Mechanic, 1994) demonstrating the resistance of treated materials to both pepsin and collagenase digestion and (Moore et al., 1994) using xenogenic pericardial tissue, demonstrate the retention of physical and biochemical durability of the tissue implant, an essential quality for heart valve replacement. Photo-oxidation is an alternative method to what could be called 'traditional' methodologies, such as glutaraldehyde tanning, to stabilize and render non-immunogenic. The mechanism of cross-linking is not completely understood, however the literature indicates that amino acids such as methionine, tryptophan, histidine and tyrosine may be oxidised by irradiation with visible light in the presence of a photosensitiser resulting in the formation of cross-links that stabilise the collagenous material to enzymatic degradation (Moore et al., 1994) and (Schmidt and Baier, 2000).

Cross-linking was assessed in terms of resistance to enzymatic degradation with RP-HPLC by comparing treated with untreated (control) tissue. Collagen polypeptides are

distinctive in their repetitive sequences in which every third residue is glycine (Gly), (-Gly-X-Y-)<sub>n</sub>) with a prevalence of proline (Pro) in the Y position (Creighton, 1993). Many of the proline residues in the Y position are hydroxylated after incorporation into the peptide chain to form hydroxyproline (Hyp). This distinctive amino acid composition has been used as a diagnostic tool to determine Hyp content and thus estimating the collagen content of tissues (Vincent, 1982). When collagen is cross-linked, it becomes more resistant to degradation by proteolysis due to the formation of non-digestible cross-links. Thus by comparing the concentration of free Hyp in solution after digestion in an enzyme solution for samples of cross-linked and untreated tissue samples the extent of degradation can be determined. The assay used in this thesis has been based on a protocol developed by (Bank et al., 1996).

Initial assessment of collagen degradation by the enzyme pepsin utilised lower concentrations of the enzyme (1-100 activity units/ml over a variety of time courses). At these lower concentrations and time courses, the extent of collagen degradation even with untreated tissue was minimal with no free Hyp detected. Pepsin concentration was increased to 1000 and finally to 5000 activity units/ml, with measurable quantities of Hyp not being resolved against background noise until 5000 activity units/ml was used as the digestion concentration (16.5 hours at 37°C). This alone gave a strong indication that the process has an effect in terms of stability or resistance to pepsin degradation. RP-HPLC showed the cross-linked tissue to yield only 21% of Hyp compared to control or untreated samples. Similarly the total peak area of the cross-linked tissue was less than a third (32%) of untreated control tissue.

Evaluation of the total peak area (as above) was an alternate method of accessing tissue degradation. This value is related to the total amount of amino acids and other detectable degradation products from the collagen break down, not specifically Hyp. This was used to give an estimation of the overall extent of the tissue degradation where Hyp is not present or where the concentration cannot be measured. The total peak area of tissue in the cross-linked samples was approximately a third (32.5%) of the control tissue which corresponds well with the results obtained for the digestion at 1000 units/ml, of only 23.4% of the amount of free Hyp digested from the unprocessed tissues. These results also support those described by (Mechanic, 1994) where cross-linked tissue was as low as a third of the unprocessed material.

After the trypsin digestion DNA from disrupted cell nuclei remains associated with the tissue, shown as light blue strands, Figures 4.16a and 4.17a, both the luminal and abluminal surfaces, respectively. Following cross-linking and subsequent washing of the matrix to remove residual components, DNA on the surface has been removed, Figures 4.16b and 4.17b. The exact mechanism of DNA clearance is not clear but is likely to be combination of the cross-linking steps, where tissue is immersed in 4M NaCl, precipitating DNA and washing steps that facilitate removal non-bound particulates. The effect matrix cross-linking on cells seeded onto the matrix and their behaviour once seeded is discussed in Chapter 5.

#### **4.4.4 WASHING**

Amongst the selection criteria when choosing the method of photo-catalysing cross-links in collagen using methylene green was to use a method where residual compounds posed no cytotoxic effect. Although methylene green is considered non-toxic it was desirable to remove as much of the residual stain as possible after the cross-linking procedure. In the series of images (Figures 4.16a-b and 4.17a-b) removal of DNA is shown after the washing steps, this process removes (in addition to the precipitated DNA and residual cellular debris) the bulk of the methylene green dye from the tissue. A third requirement of the washing process is to remove residues of the cross-linking process itself, in particular a 4M NaCl is used to allow the cross-linking solution to be held at 0°C without freezing also acting to osmotically shock and thus rupture cells. In addition, the hostility of the salt environment helps retain sterility of the tissue. Figures 4.21 an SEM of the abluminal surface post initial washing shows the presence of unidentified debris and Figure 4.15 a SEM of a 'sliced' transverse section displaying salt crystals within the matrix. Section 4.2.2.5 details the washing protocol where tissue is exposed to multiple washes in distilled H<sub>2</sub>O over a two week period. Clearly this protocol has not removed the undesirable processing debris from the tissue. This issue is discussed in Chapter 6 'Perfusion Bioreactor Studies' where the preparation and preconditioning treatments of the matrix within the bioreactor perfusion system further enhances the removal of salt deposition and processing debris.

#### 4.4.5 COMPARATIVE METHODOLOGY ANALYSIS

In terms of the success of a product the ultimate test is with implantation studies, any improvements from one tissue treatment methodology to the next without these implantation studies can only be speculative, with the literature used to support directive studies to theoretical advancements to the current technology. This section of work was carried out to determine any comparative improvement over the tissue preparation methodology described by Mechanic *et al* (1994) cross-linking with the photo-oxidative process described in section 4.1.3. The product development from Mechanic *et al* (1994) earlier work has undoubtedly been enhanced since the publication of the initial patent, unfortunately the details of this work are unavailable for commercial reasons. The current product developed by Sulzer Medica, Austin Texas, using 'PhotoFix® Technology' (the development of Mechanic *et al* (1994) work) has been granted FDA approval and CE authorisation for human implantation. Comparisons made here are in no way meant as a direct comparison of their current methodology, only as an interpretation of one method described from the earlier publication (Mechanic, 1994) see section, 4.2.2.4. These methodological changes made from Mechanic *et al* (1994) work in this thesis may or may not improve the current technology as discussed below.

Although the cross-linking method described and utilised in this thesis is based on the said publication, the process has been theoretically enhanced with the addition of specific extraction steps for the removal of lipid and non-structural protein. Figure 4.27 displays an expanded flow chart of processing events, where the main differences between the two methodologies are the lipid and protein extraction steps, which are in addition to the Mechanic *et al* (1994) patent. As a means to gauge relative differences between the two different treatment regimes, tissue lipid content and protein content were assayed.

Not surprisingly a reduction in both assayed components (lipid and protein) can be seen between the Mechanic *et al* (1994) process and this method due to the addition of specific lipid and protein extraction steps. Figure 4.22a, a chromatogram shows a dramatic reduction in tissue lipid content, where the Mechanic *et al* (1994) process retains all detected lipid components of untreated tissue. As discussed in the introduction to this chapter the extraction of lipids from the matrix has an important



potential benefit, particularly with the use of EtOH as the extraction mechanism, where potentially immunogenic epitopes associated with lipids and lipoproteins are extracted and the associated reduction in tissue calcification. EtOH treatment as a method to reduce tissue calcification has been well documented in the literature, for example, (Courtman et al., 1994; Demer, 1997; Lee et al., 1998; Shen et al., 2001; Vyavahare et al., 1997; Vyavahare et al., 1998)

Figure 4.22b, an SDS-PAGE analysis of the tissues gross protein content, shows a progressive decline in total detected protein from untreated tissue to the Mechanic et al (1994) process to the method described in this thesis. Although the Mechanic et al (1994) process does not include a specific protein extraction step, the reduction in protein can be largely attributed to cellular proteins released into the ECM when exposed to high molarity preconditioning solutions and subsequently removed during the washing process. The further reduction of detected protein can be ascribed to two mechanisms. Firstly the process of lipid extraction will free (into the ECM) proteins associated with cell membranes (lipoproteins) and secondly proteolysis, where there is an increased efficiency of amino acid and peptide extraction/diffusion from the matrix results due to the smaller molecular weights of the digestion products. Results of the SDS-PAGE analysis clearly show a reduction in detected protein. This result is iterated with the results displayed in Figure 4.23, tissue weight loss. This establishes a significant difference in the weight of the tissue pre and post treatment between the two methods. Tissue processed according to Mechanic et al (1994) has no significant reduction in tissue weight with approximately 2%. Conversely, and predictably, the developmental matrix showed a significant weight loss of almost 18% compared to control tissue.

When considering the removal of protein from the tissue, a fine balance must be achieved between over-digestion and under-digestion. The ideal matrix would retain all the appropriate mechanical characteristics that maintain cellular phenotype and non-structural proteins critical to allow rapid adhesion, proliferation and migration of seeded cells. An important issue with the use of biological materials is the fact that they are not uniform. Along with variation in vessel wall thickness and diameter, the vessels are tapered. This variation complicates processing, where the process must either be modified to account for the variation or the variation must be reduced by tightening the

selection criteria. Without this balance, materials will have dramatically differing mechanical properties and compositions. The selection criteria used in the section of work was deemed adequate for experimental use where arteries measured 80-110 mm in length with lumen diameters from 3.5 - 6.5 mm (proximal) tapering to 2 - 3 mm (distal). Within this selection group variation was found to be acceptable, however arteries with dimensions at the extreme end of the selection range displayed inconsistent results, for example the trypsin digest was found to be ineffective at disrupting cell nuclei when the arterial wall thickness exceeded approximately 2.5 mm (qualitative observations). As preliminary studies in the development of this material, variation has proved a useful tool, for example EC prefer (qualitative observations) to adhere to the compressed section of the matrix, see Chapter 3, which has a similar morphology to the arterial basement membrane compared to the loose fibrous sections. These observation have promoted the idea that in preference to extracting all non-structural protein, retaining the basement membrane may allow a more rapid development of the endothelium, critical for a tissue engineered vascular graft.

#### **4.4.6 MECHANICAL PROPERTIES**

To reiterate the objective of tissue engineering a vascular graft, an acellular matrix is prepared onto which cells of a known lineage are seeded. The developed construct is then 'grown' within a bioreactor, mimicking the *in vivo* environment to generate a neo-organ that will behave in a similar fashion to the disease free native organ it is to replace. The research discussed in this chapter describes the development of a biomaterial suitable for use as a biomatrix for tissue engineering applications. Each phase, from matrix development to tissue engineering vascular grafts, required independent analysis. During the transition from an acellular matrix to a cellular neovessel, cells will lay down their own matrix materials, increase the density of the vessel and alter the physiology of the material by specific protein expression, for example SMC expression of  $\alpha$ -actin, a contractile protein. In line with these concepts, the fully developed neovessel is likely to have markedly differing mechanical properties to the acellular matrix and in the case of vessel mechanics would ideally be analysed at three time points: untreated controls, as an acellular matrix and finally as a neovessel. Assessment of the acellular materials mechanical properties prior to cell seeding was

deemed important to establish whether or not the decellularisation processing steps had altered the matrix to such a degree that recovery of the critical mechanical attributes, such as burst strength, was impossible, if indeed the mechanics had changed. Two analytical techniques were used to assess the mechanical attributes of the processed material: burst pressure and load extension.

## PRESSURE TESTING

Although not a specific mechanical property of a material, pressure testing is a common property of all cylindrical vessels. Measurement of the burst pressure is a fundamental pre-requisite for a tissue engineered vascular prosthesis due to the haemodynamic stresses a prosthetic device will encounter on implantation. A variety of methods have been used to determine the point at which a vessel may fail at a given pressure, including pressurising the vessel with gas, (Roeder et al., 1999), where the pressure testing was measured by injecting regulated high pressure nitrogen gas into the artery. Contradictory to previous testing by Roeder et al (1999) the approach taken with this project has aimed to increase accuracy and yield more informative results by using an incompressible fluid ( $H_2O$ ) to pressurize the system. Initialisation of fracture is a function of the force applied by the fluid, whereas propagation of fracture is a function of the energy of the load. Gas is compressible and will retain some of the energy during propagation of fracture, resulting in a higher observed burst pressure than the true value (Vincent, 1982). The use of  $H_2O$  enabled the system to behave in a more appropriate *in vivo* 'like' manner and allowed accurate identification of leakage points within the artery. Design aspects are detailed in the Section 4.2.4.

Burst pressure values reported in this investigation (1987 & 2260 mmHg mean values) are among the few reported in the literature. Roeder et al (1999) reported an average burst pressure of 2069-4654 mmHg for small intestine submucosa (SIS) vascular grafts of 5.5mm internal diameter; and Hiles et al (1995) reported a burst pressure of 5800 mmHg for remodelled 5mm internal diameter SIS grafts in the dog (Hiles et al., 1995). It is clear that these values far exceed average pressures of approximately 80-120 mmHg. In contrast to the initial presumption that the mean values at pressure failure would indicate an increase in the ability of the cross-linked tissue to withstand pressure over the untreated controls, no significant difference was found between the two

data sets with a  $p > 0.05$ , see Figure 4.2.5. The important take home message is that although the pressure testing control, untreated porcine carotid arteries is only comparative to the fully processed acellular matrices and no direct comparison to the human arterial system is made, it can be said that processing has not been detrimental to the mechanical capacity of the material. Furthermore any remodelling of the material during the growth phase of development is likely to increase this capacity.

## LOAD-EXTENSION TESTS

Load-extension tests involve cutting the artery into ringlets or strips and pulling them apart until the section structure failed. As a single 10cm artery could be used for twenty 5mm length ringlets a large amount of data is produced thus reducing the effect of variation, often associated with biological tissue. Although convenient for mechanical analysis, the samples do fail to maintain their correct *in vivo* geometry. But since the tests are for a comparative analysis (raw and cross-linked tissue), this type of mechanical testing has been deemed acceptable (Dobrin, 1978). Hiles et al (1995) cut annular in the form of 3-5mm width ringlets and strained them to rupture in the radial direction, in open air, measuring force with extension. Courtman et al (1995) cut 4mm wide ringlets from the vascular sample, then cut them across to form strips, which were then attached to brass grips and stretched, all contained in an aqueous solution, giving force-extension results. The solution allowed the tissue to equilibrate and simulated *in vivo* conditions to some extent. Although this approach resembled *in vivo* conditions more closely, a piece of equipment similar to that described by Hiles et al (1995) was not available for use. Hence ringlet stretching in open air was chosen for this investigation. The error associated with testing (open air) is constant from test to test and is considered negligible in this comparative study. Load-extension measurements show how a material will act under increasing tensile force. Increasing the tensile load on a sample of material causes it to stretch and eventually fracture. It is common to express the load in terms of stress, and the extension in terms of strain to standardised values (i.e. per unit dimension and percent increase) clarifying result comparisons.

A stress-strain relationship can be determined for the tissue. Tensile strength can be analysed, based on the stress and strain observed respectively at fracture (De Diego et al, 2000). The elastic behaviour can be quantified in terms of the elastic modulus,

which is a qualitative measure of stiffness; the larger the value or steepness of the gradient, the stiffer the material (Riley, 1999). The elastic modulus is equal to the gradient of the stress-strain graph.

#### MEAN FAILURE: STRESS AND STRAIN

The load-extension results, Figure 4.2.6, show the ultimate tensile strength (stress at which fracture occurs) to be over three times higher for the cross-linked material compared to the untreated raw tissue,  $632 \text{ g/mm}^2$  to  $188 \text{ g/mm}^2$  respectively. Figure 4.2.6, shows the raw material fails at 85%, and the cross-linked tissue to fail at 104%. It is most likely that cross-linking is responsible for the great increase in ultimate tensile strength. The cross-linking process induces the formation of interchain cross-links amongst proteins (Schmidt and Baier, 2000). Collagen is a fibrous protein possessing a helical structure with 3 protein chains wound round a central axis. Numerous interchain links stabilise the helix and are probably the source of its great mechanical stiffness. At large distensions much of the stiffness of arteries is attributable to collagen (Dobrin, 1978). Clearly increased cross-linking of these protein chains is likely responsible for the observed increase in ultimate tensile strength. Statistically there is no significant difference between these two values given the associated error.

Schmidt and Baier (2000) have shown significant increases in the apparent tensile extensibility and concluded that the effect is likely associated with shrinkage during fixation (Schmidt and Baier, 2000). Not dissimilar to the treatment process here, their treatment process involves an initial step where the tissue is 'fixed' with ethanol for preservation. Ethanol molecules essentially replace the water molecules within the tissue and stabilise the hydrogen bonds within the tissue protein. This has the effect of denaturing the protein as it shifts from a tertiary structure to a secondary structure whilst preserving it (Leong, 2001). It is speculated that the above-mentioned shrinkage may compress the matrix fibres, which may increase strain values (% extension) as initial stress values are higher due to earlier load uptake of the ECM fibres. In relation to the above references the results obtained in these tests, which show no significant change in strain values, maybe due to ethanol being removed from the tissue during the remaining processing steps.

## ELASTICITY

The biphasic shape of the graph (Figure 4.2.5) is expected for arterial walls distended circumferentially (Dobrin, 1978). The linear region is associated with elastin content in the wall, and the upward curving region is associated with collagen content in the wall. At extensions associated with physiological conditions (80-120 mmHg), stretched elastic lamellae and stretched collagen in the medial layer take the load and provide much of the stiffness. Above physiological pressures it is the collagen-rich medial and adventitial layers that provide the stiffness, acting as a protective outer jacket for the artery. At low strains much of the stiffness of the material is contributed by the elastin content in the arterial wall, and at high strains this is contributed by the collagen (Dobrin, 1978). As demonstrated in the previous section, the tissue has been tested far above physiological stresses. At physiological to moderate distensions it is a combination of elastin fibres and collagen fibres in the media that bears the load (Dobrin, 1978). At physiological pressures collagen fibres are not orientated and normally not taut (Dobrin, 1978). The elastic behaviour of the unprocessed and cross-linked material is illustrated Figure 4.25. The graphs are both a curvilinear shape, with the unprocessed material displaying a distinct linear and non-linear region, less obvious in the treated material. The increase in stress associated with the cross-linked material indicates an increase in stiffness or a decrease in the materials elasticity. The importance of elasticity in compliance matching of arterial grafts is an important issue, the reduction in elasticity shown in Figure 4.25 of the cross-linked material is not a positive result. Although a complete analysis comparing specific protein content (collagen III, IV and elastin) between untreated and processed tissue is yet to be carried out, it is hypothesised that the increase in stiffness not necessarily a function of reduced elastin content, rather shrinkage if the ECM proteins and intermolecular cross-links restricting the normal function of the matrix resulting in increased tensile strength. The cross-linking process induces the formation of interchain cross-links amongst proteins (Schmidt and Baier, 2000). Clearly increased cross-linking of these protein chains is likely responsible for the observed increase in ultimate tensile strength.

With the development of enhanced cross-linking agents and methodologies previous problems with mechanical failures and infection can be overcome. The high cost involved with biological graft production may in turn be reduced with improved

process control. The mechanical characteristics of biological materials are seen as its main advantage. If the vessel can be processed in such a manner that when implanted, the body accepts the conduit as a partially damaged vessel, in need of repair, i.e. it is treated as a wound, compared to foreign material, graft patency rates will improve. This is one of the important factors for the increased patency rates associated with the use of autologous veins or arteries. Characteristic of this processed artery is the retention of the basement membrane and internal elastic lamina. It has been suggested the presence of the internal elastic lamina acts as physical barrier to prevent the migration of vascular smooth muscle cells into the vessels lumen, which would otherwise result in intimal hyperplasia (Sims, 1985). Additionally the internal elastic lamina has been postulated to have an important role in the prevention of atherogenesis by acting as a diffusion barrier across the arterial wall (Hampton, 1983).

As discussed, this section of work is the first step in the development of a tissue engineered vascular graft. With a biomaterial that in theory has satisfactory biocompatible properties, the following chapters describe the use of this material initial under static conditions (Chapter 5) to monitor *in vitro* cell compatibility in terms of potential cytotoxicity and the ability of hVSMC to migrate into the matrix under static culture conditions, Chapter 5 and dynamic perfusion culture in Chapter 6.

## CHAPTER FIVE: STATIC CELL CULTURE ON A PORCINE DERIVED ARTERIAL MATRIX

### 5.1 INTRODUCTION

The previous chapter has detailed the development of a material for theoretical use as a substrate for tissue engineering purposes. The objective is to seed human vascular smooth muscle cells (hVSMC) and endothelial cells (HUVEC) onto the matrix and culture *in vitro* until a suitable cell density is achieved to function as a small diameter vascular graft. The effectiveness of a biomaterial to confer a high seeding/adhesion density of human primary cell lineages and their subsequent growth and proliferation is mainly dependent on the form in which a biomaterial is initially presented to the cells.

The aims of this chapter are to first assess the porcine derived arterial matrix developed in Chapter 4 in terms of biocompatibility under static *in vitro* culture conditions and second to determine if ECM remodelling enzymes are expressed by seeded cells. If expressed, are the cells able to migrate into the matrix via the degradative mechanisms associated with enzymes such as matrix metalloproteases during matrix remodelling or is migration a passive process where cells move from one location to the next via pores in the matrix? Third, to observe enzyme expression patterns of selected remodelling enzymes and note any unique spatial arrangements that may occur during static culture over extended time courses.

#### 5.1.1 MATRIX REMODELLING

As discussed in Chapters 3 and 4, cross-linking collagenous matrices serves several functions: first to reduce the immunogenicity of the material by masking 'foreign' epitopes, second to sterilize the tissue and third to provide some level of resistance to enzymatic degradation, that is, resistance to host proteolytic enzymes. Based on the current literature, in particular (Mechanic, 1994) and (Moore et al., 1994), and the results discussed in Chapter 4.3 with RP-HPLC, it is clear that the matrix material has been stabilised to proteolytic digestion. However the degree of cross-linking can be



further and possibly more accurately assessed by cellular migration within the biomatrix. The two main methods of cell migration within tissues are: motility between matrix fibres, much the same as when cells migrate from tissue explants onto the surrounding plastic culture plate (Kirschenlohr et al., 1996) and more importantly migration through matrix fibres by the secretion of a barrage of proteolytic enzymes, such as MMP to digest matrix components, for example in cancer metastasis (Foda and Zucker, 2001) and VSMC migration after endothelium injury (Owens and Clowes, 1999). An important aspect of this study is that cells are able to migrate into the matrix to repopulate and functionalise the tissue engineered vessel. The extent of cross-linking is an important issue where a fine balance is required between too little and excessive cross-linking. Synthetic polymers may degrade via two main mechanisms: immunological reactions mediated by cellular recognition of foreign bodies and the material's subsequent tagging for removal and the biomaterial simply dissolving in host fluids. In vascular networks, in particular the arterial system, the degradation rate is critical. If degradation is too rapid, graft tissue may fail prior to host cells repopulation and subsequent ECM production to stabilise the graft. The consequences, if utilised for coronary bypass, are likely to be fatal. At the other end of the spectrum, if the tissue is heavily cross-linked, host cells or those seeded onto the matrix during bioreactor development will not be able to penetrate into the matrix to remodel and populate the matrix to physiological levels. VSMC will ideally migrate into the matrix from the abluminal surface to a distance of approximately 250  $\mu\text{m}$ , a theoretical maximum distance between which cells can effectively communicate (Francis and Palsson, 1997), whereby cell-cell communication between VSMC and the endothelium can take place ensuring a more *in vivo* like phenotype. At this point cells will ideally be prevented from migrating or proliferating into the lumen of the vessel as a result of endothelium-induced inhibition of SMC proliferation (Owens and Clowes, 1999). It is envisaged that this will allow remodelling of a pseudo-muscular wall to confer contraction, and thus vascular tone.

As part of the cellular response to migration signals, which include: wound healing, matrix remodelling, chemotactic, mechano-transduced and cell density, a variety of proteolytic enzymes capable of degrading the ECM are expressed and localised to the immediate periphery of the cell surface allowing cells to migrate through tissues (Murphy and Gavrilovic, 1999; Owens and Clowes, 1999).

Proteases have been classified into four major classes: serine, aspartate cysteine, and metallo. Grouped according to the different manner each enzyme catalyses the hydrolysis of the covalent bonds, which cleave the protein substrate (Chapman et al., 1997). The following overview of these enzymes with emphasis on metallo and cysteine proteases clarifies the importance of these enzyme families in remodelling the ECM, particularly the vascular ECM.

## SERINE PROTEASES

Earlier studies of cell migration concentrated on the serine protease *urokinase-type plasminogen activator* (uPA) and the generation of plasmin involved in cell migration. uPA is involved in a proteolytic cascade where it cleaves (specifically) a single bond in an inactive protease 'plasminogen' to yield its active form plasmin. Plasminogen is abundant in the blood stream and at sites such as wound healing, tumours, inflammation and other sites of tissue remodelling where it is expressed locally (Alberts et al., 1994). Plasmin is less specific than u-PA and cleaves a variety of proteins including laminin, fibronectin, and fibrin (Murphy and Gavrilovic, 1999). This is presumably to allow cells to migrate into the damaged area or tissue to be remodelled through a variety of different ECM molecules to elicit matrix repair, or in the case of tumour cells to allow cell migration through basement membranes during metastatic activity. uPA has been shown to play a role in VSMC migration through the basement membrane following denudation of the endothelium to initiate intimal repair and that uPA activity is essential but not sufficient for tumour cell migration in matrigel (Murphy and Gavrilovic, 1999). A further example of a serine protease relevant to this study is trypsin. Trypsin is one of the many mammalian digestive enzymes secreted from the pancreas. Its activity is strictly controlled by a series of inactive proforms or zymogens to prevent premature activation of this potentially destructive enzyme (Creighton, 1993). In this case trypsinogen is selectively cleaved by enterokinase to form active trypsin. Applications of this enzyme in the development of biomaterials are discussed further in Chapter 4.

## MATRIX METALLOPROTEINASES

The group 'metalloproteinases' consist of the proteolytic enzymes where heavy metal co-factors in the enzymes active site, such as zinc confer catalytic activity. As the name suggests matrix metalloproteases (MMP) comprise a family of enzymes that hydrolyse various ECM components. A selection of mammalian MMP and their known *in vitro* substrates are shown in Table 5.01 (Shapiro, 1998). With direct reference to the two MMP analysed for this part of the project, MMP-2 and 9, have a diverse range of catalytic activity with regard to components of the ECM. Both enzymes effectively degrade elastin, a range of collagens and multiple components of the ECM basement membrane. The earlier view that MMP are utilised as "weapons of mass destruction of the ECM" has recently been described as too simplistic, (McCawley and Matrisian, 2001). Many observations describing the increasing complexity of protease function within the matrix depict several mechanisms where cleavage of matrix components may directly affect cell function McCawley and Matrisian et al (2001). For example fibroblast growth factor (FGF) and transforming growth factor- $\beta$  (TGF- $\beta$ ), which have a strong affinity for matrix components, are released into solution when ECM components such as the proteoglycan perlecan which binds FGF is cleaved by MMP-1/3, similarly when decorin is cleaved by MMP-2, 3 or 7 to release TGF- $\beta$  (McCawley and Matrisian, 2001). In addition, both MMP-2 and 9 have been reported to convert the proform of TGF- $\beta$  into an active ligand, which has effects ranging from the regulation of cell differentiation to increasing or decreasing cellular sensitivity to other growth factors (Alberts et al., 1994).

**Table 5.01:** An overview of selected MMP and their substrates. With reference to MMP-2 and 9 (highlighted), substrates of particular relevance to the arterial wall, which are studied here, are bold text. Modified from Shapiro (1998)\*.

MMP	Interstitial collagens	Basement Membranes	Elastin
<b>Collagenases</b>			
MMP-1	I, II, III, VII, X	FN, LN, EN, PG	-
MMP-8	I, II, III, (VII, X?)	FN, LN, EN, PG	-
MMP-13	I, II, III, GL (VII, X?)	FN, LN, EN, PG	-
<b>Gelatinases</b>			
MMP-2	GL, I, VII, X, XI	Col IV/V, FN, LN, EN, PG	++
MMP-9	GL	Col IV/V, FN, LN, EN, PG	++
<b>Stromelysins</b>			
MMP-3	-	FN, LN, EN, PG	+/-
MMP-10	-	FN, LN, EN, PG	+/-
<b>Stromelysins-like</b>			
MMP-7	-	FN, LN, EN, PG	+
MMP-12	-	FN, LN, EN, PG, PS col IV	++
<b>Furin-recognition sites</b>			
MMP-11	-	-	-
MMP-14	I, II, III	FN, LN, EN, PG	
MMP-15		FN, LN, EN, PG	
MMP-16	?		
MMP-17	?		

\* As noted by Shapiro (1998), this is an incomplete list, representing only selected substrates tested to date (tested *in vitro* not *in vivo*). En, entactin; FN, fibronectin; GL, gelatin; LN, laminin; PG, proteoglycan; PS col IV, pepsinized collagen IV

## CYSTEINE PROTEASES

Cathepsin L belongs to the class of cysteine proteases. Cysteine proteases are further partitioned subgrouped into two super families: those relating to interleukin 1 $\beta$  converting enzymes and papain superfamily of which Cathepsin L is a member (Chapman et al., 1997). Cysteine proteases are known to be specifically located within cellular lysosomes, although their localisation to outside the cell has been described in pathological circumstances such as cancer, rheumatoid arthritis and apoptosis (Turk et al., 2000). Lysosomes, membrane-bound vacuolar organelles, form part of the intracellular digestive system, within which an array of hydrolytic enzymes digest both unwanted cellular protein and extracellular material via phagocytosis or endocytosis. The more extensive role of cysteine proteases has only recently come to light. The significant role that cysteine proteases have outside the lysosomes, even within the ECM as part of normal physiology is only beginning to be understood in detail.

There are currently 11 human cathepsins characterised (B, H, L, S, C, K, O, F, V, X and W). Cathepsin L appears to be ubiquitous in vertebrates, its main role within the cellular lysosome system being for protein degradation. Cathepsin L has also been identified outside the cell in both pro- and mature forms. Typically expressed by macrophages, fibroblasts, osteoclasts and others, cathepsin L has been found to have a variety of specific functions for example: Degradation of basement membranes (pH 3.5-6), elastin (pH 5.5), fibronectin (pH 5.5) and collagens (pH 3.3-6). Although these are optimal pH ranges, reduced activity will occur at physiological levels (Turk et al., 2000) and (Kirschke and Barrett, 1998).

The physiological role of these enzymes in tissue modification/remodelling clearly predicts their potential significance during the development of tissue engineered prostheses. It was with this view that experiments were designed to analyse the relationship between the degree of cross-linking and the ability of cells to migrate into and through the processed matrix.

This chapter describes the analysis of the arterial derived matrix, whereby initial studies focused on biocompatibility and methods to improve the efficiency with which cells adhere to the biomaterial. After static culturing on the matrix, hVSMC were assessed for expression of  $\alpha$ -actin and their ability to migrate into the matrix. This was followed by immunohistochemical analysis of specific matrix metalloproteinases (MMP-2 and 9) and cathepsin L by to determine firstly, expression and secondly the spatial arrangement of expression. Examples from two classes of proteolytic enzymes, MMP (MMP-2 and 9) and Cathepsins (cathepsin L) have been assayed for their presence and general pattern of expression when hVSMC have been seeded onto this material. (Two conditions were studied, static culture (this chapter) and perfusion culture with hVSMC in Chapter 7). The rationale for choosing and limiting analysis to these three enzymes is discussed in Section 5.3.

## **5.2 MATERIAL AND METHODS**

### **5.2.1 MATERIALS**

Unless stated otherwise all reagents and material details are described in Chapter 2.1.4. All culture media was changed from either DMEM (hVSMC) or M199 (HUVEC) based media to those supplied by PromoCell, Heidelberg, Germany. These media have been detailed in Chapter 2.1.3. This was due to the new media having improved buffering capacity.

### **5.2.2 EXPERIMENTAL METHODS**

Cells and cell conditions remain as described in Chapter 2.1.1 and 2.2.2 respectively. Matrix preparation, from unprocessed porcine carotid arteries to the processed and cross-linked matrix was carried out as described in Chapter 4.2.2, with an overview of the process in Figure 4.27. Immunohistochemistry, fluorescent immunohistochemistry and histological analysis were conducted as described in Chapter 2.3.6.

#### **MATRIX STERILISATION PROCEDURE**

Sterilization and depyrogenation was a modification based on a method supplied by Dr. S. Badylak, Purdue University, USA, (personal communication). 0.1 % peracetic acid (v/v) and 4% EtOH (v/v) in distilled H<sub>2</sub>O was prepared in a solution ratio of 20:1 solvent (ml) to tissue weight (g) e.g. 5 g tissue required 100 ml sterilising solution, consisting of 100 µl peracetic acid, 4 ml EtOH and 96 ml H<sub>2</sub>O. Matrix sections were immersed in the sterilising solution for a total of 2 hours on a rotator/shaker then rinsed in 1 L volumes of sterile PBS on the rotator/shaker until the pH was stable at 7.4, minimum 24 hours and 3 PBS changes.

## PRECONDITIONING TREATMENTS AND HUVEC SEEDING TO THE LUMENAL SURFACE OF THE ARTERIAL DERIVED MATRIX

To enhance the cell seeding efficiency a number of media or salt solutions were tested to determine an optimal preconditioning treatment immediately prior to cell seeding. Solutions tested; PBS, low serum EC media, (PromoCell), Smooth muscle cell media, Low serum VSMC media, (PromoCell), DMEM, FCS and FCS in a 1:1 ratio with DMEM. Media is described in detail in Chapter 2.1.3.

The matrix was dissected into sections approximately 5x5 mm and immersed in the test solutions (above) at 37 °C, 5% CO<sub>2</sub> for 48 hours prior to cell seeding. Immediately prior to cell seeding the pre-treatment solution was removed and HUVEC suspensions ( $1.8 \times 10^4$  cell/ml/well) were seeded to a final density of 90 cells/mm<sup>2</sup> onto the luminal surface of the arterial matrix. Cell densities were assessed at days 3 and 9. Non-seeded matrix maintained in low serum VSMC media served as control samples.

## hVSMC SEEDING TO THE ABLUMENAL SURFACE OF THE ARTERIAL DERIVED MATRIX

Matrix sections approximately 5 x 5 mm of fully process matrix was used and preconditioned with low serum SMC media for 48 hours at 37 °C 5 % CO<sub>2</sub>. hVSMC (PIV) were seeded to a final density of  $6.7 \times 10^4$  cell/ml or 333 cells/mm<sup>2</sup> on the tissue. Data was collected on days 3 and 7 for DAPI staining and day 21 for histological analysis. Wax embedded 5 µm sections were cut and stained as appropriate for the final analytical technique utilised, see Chapter 2.3.6 for histological method.

### 5.2.3 ANALYTICAL METHODS

All analytical methods used in this chapter are described in Chapter 2, Material and Methods.

## 5.3 RESULTS

All cell lineages were phenotypically assessed prior to seeding cultures on matrix sections. As described in Appendix A1, HUVEC were assessed for their characteristic cobble stone morphology and for specific antigens CD 31 and von Willebrand factor (Factor 8). Similarly hVSMC were assessed for the spindle shape and characteristic 'hill and valley' formations and for the specific hVSMC antigen for  $\alpha$ -actin, see Appendix A2.

### 5.3.1 LUMENAL SEEDING AND STATIC CULTURE OF HUVEC ON PORCINE DERIVED ARTERIAL MATRIX

Matrix biocompatibility was tested by seeding HUVEC at PIII onto the matrix at  $1 \times 10^5$  cells/ml. A qualitative assessment was conducted by comparing cell adhesion to the matrix used straight from rinsing ( $H_2O$ ) to matrix pretreated for 48 hours in low serum EC growth media. After 3 days culture on the pretreated matrix, HUVEC were confluent, compared with cells on the non-treated matrix that remained at low densities, Figure 5.01, cell nuclei are stained light blue.

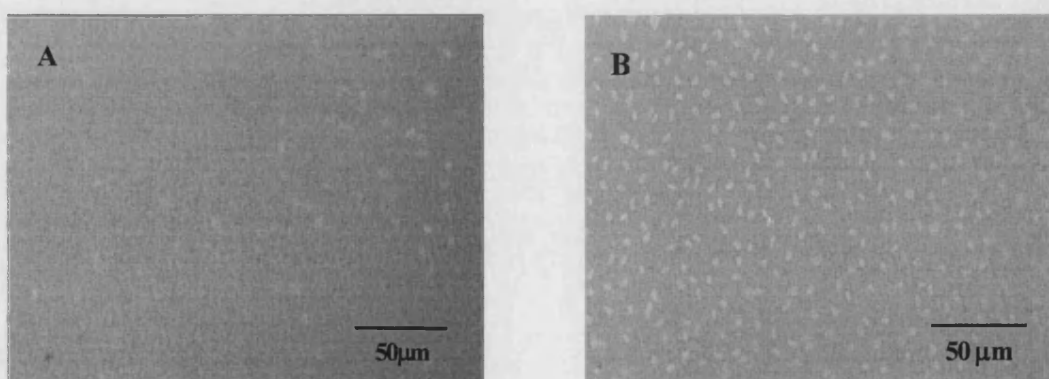


**Figure 5.01:** HUVEC seeded and cultured for 3 days on the porcine derived arterial matrix sections. HUVEC seeded onto control samples (non-treated matrix direct from washing) (A) show a lower retention than matrix pretreated with low serum EC media (B). Light stained cell nuclei were detected with the florescent nuclear stain DAPI.



## TREATMENTS TO ENHANCE HUVEC ADHESION ON LUMENAL SURFACE OF THE PORCINE DERIVED ARTERIAL MATRIX

From previous work (Smith et al., 2000) we have found that pre-treatment of porcine derived type I collagen scaffolds lead to improved fibroblast adhesion/proliferation. To determine if the same was correct for this matrix the scaffold was pretreated with a number of media or salt solutions. Solutions included HBSS, EC media, SMC media, DMEM, FCS and a 1:1 ratio FCS and DMEM, as described in Section 5.2.2. HUVEC were seeded at 90 cells/mm<sup>2</sup> onto the luminal surface of fully processed tissue sections. Results were assessed on days 3 and 9 using the fluorescent DNA stain DAPI, see Figure 5.02. As described in Chapter 2.3.1.2, 5 counts were taken on each of 2 tissue sections, with results expressed as mean values  $\pm$  1 sd, n = 2. The results show FCS and FCS:DMEM (1:1) have the highest seeding and proliferative efficiency with 1082 % and 871 % increase (respectively) in cell density from initial seeding. It was found that there was no significant differences between PBS, EC media, SMC media and DMEM in cell density at day nine  $p > 0.05$ , (n.s.).

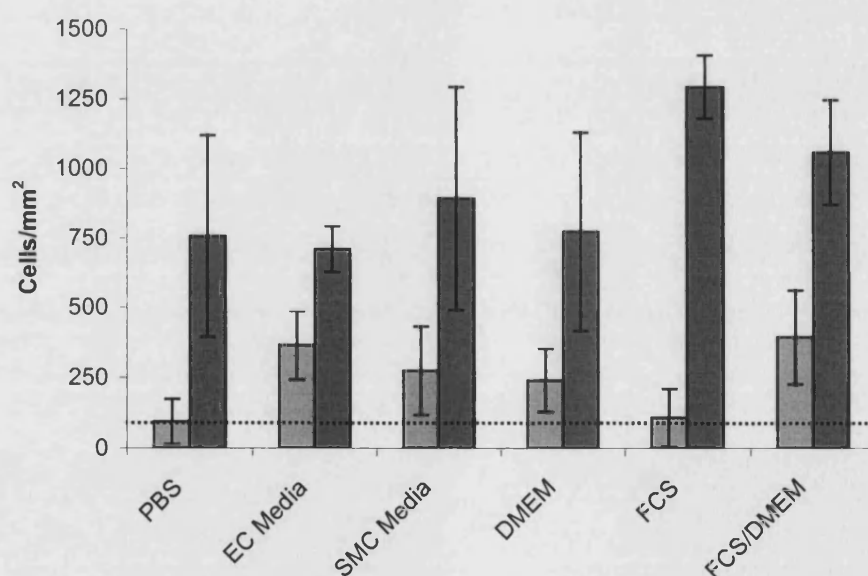


**Figure 5.02:** Effect of matrix pre-treatment on HUVEC adhesion to fully processed, cross-linked porcine carotid arteries. Day 3  Day 9 . The dotted line represents initial seeding density of 90 cells/mm<sup>2</sup>. Results are expressed as mean values  $\pm$  1 sd, n = 2.

### **5.3.2 ABLUMENAL SEEDING AND STATIC CULTURE OF hVSMC ON PORCINE DERIVED ARTERIAL MATRIX**

Based on the results in Section 5.3.2 where matrix sections were preconditioned in low serum SMC media for 48 hours as described in Section 5.2.2. hVSMC (PIII) were seeded at  $6.7 \times 10^4$  cell/ml (333 cells mm<sup>2</sup>) and results assessed on days 3 and 7 for DAPI analysis and 3 and 5 weeks for immunohistochemistry analysis. As described in Chapter 2.3.1.2, 5 counts were taken on each of 2 tissue sections. Results from seeding hVSMC onto the abluminal surface and cultured under normal conditions yielded variable cell densities that were not necessarily representative of the true cell density. Assessment of cell number/density was difficult due to the 3-dimensional fibrous structure of the matrix, limited by minimal depth-of-field at high magnification of cells embedded within the matrix during counting procedures could not be assessed, see discussion for further details.

After 3 days static culture cells are clearly seen among the abluminal fibres of the processed matrix 5.04. Cell morphology was difficult to assess due to fibrous and more 3-dimensional nature of the matrix fibres surrounding the medial layer of the processed artery. This is compared with the near 2-dimensional viewing of HUVEC on the undulating basement membrane of the luminal surface.

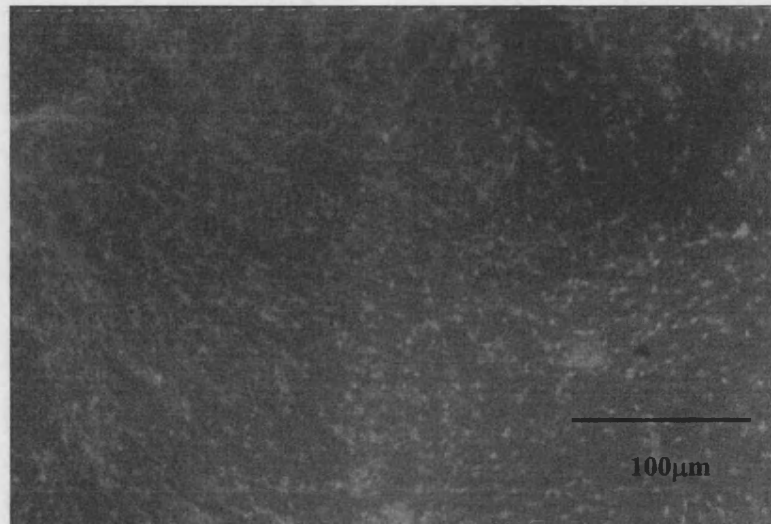


**Figure 5.04:** hVSMC seeded onto the abluminal surface of the porcine derived arterial matrix and assessed at three days. DAPI stained hVSMC can be seen, (like luminal HUVEC, Figure 5.02) as light blue 'spots' against a darker blue background.

Extended cultures of hVSMC seeded onto the abluminal surface at  $333 \text{ cell/mm}^2$  were assessed after static culture periods of 3 and 5 weeks for a phenotypic marker of SMC,  $\alpha$ -actin. Figure 5.05 displaying the migration of cells stained with haematoxylin into the matrix, with Figure 5.06 showing immunohistochemically localised  $\alpha$ -actin from the same cultures. It was speculated that cells have migrated into the matrix via the cut edge not necessarily through the EMC fibres. In all sections studied it was noted that hVSMC which often proliferated to multiple cell layers on the cut edge of the matrix and occasionally on the abluminal surface, cell were only seen as monolayers on the luminal surface.

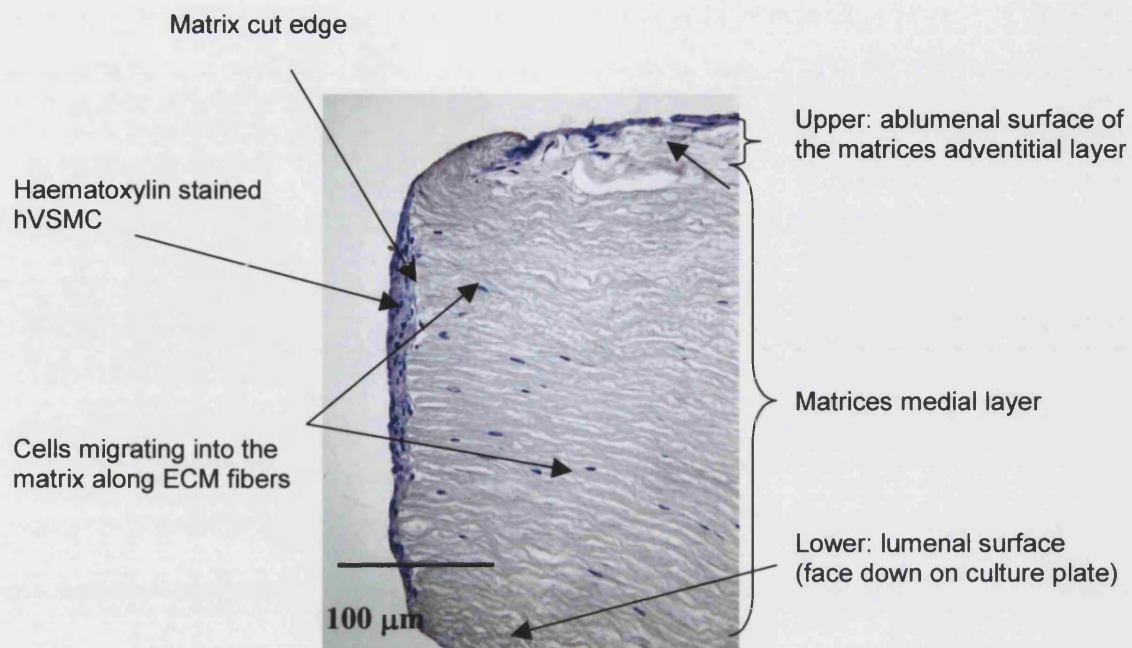


**Figure 5.05:** Extended culture of hVSMC on porcine derived arterial matrix. hVSMC seeded onto the abluminal surface and cultured for 5 weeks, sections stained with haematoxylin showing hVSMC encasing the matrix and migrated into the arterial wall via the cut section of the matrix

Either initial cell adhesion, higher proliferation rates or migratory cues appear to favour hVSMC density at the cut edge of the matrix compared with either luminal or abluminal surfaces, see Figure 5.06. hVSMC were positive for expression of  $\alpha$ -actin, particularly the outer layer of cells where cells were more than one cell layer deep. The matrix displays a non-quantified ability to maintain the phenotypic expression of  $\alpha$ -actin by the hVSMC at 5 weeks, which contrasts static cultures on plastic surfaces where expression is often lost over time.

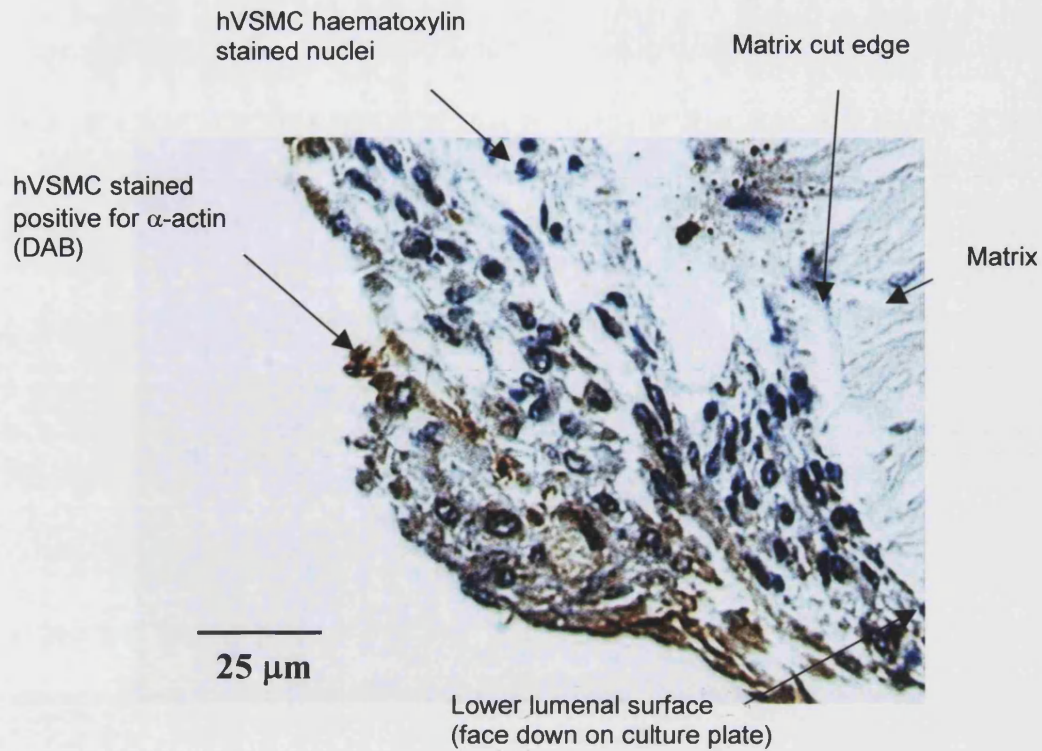


**Figure 5.06:**  $\alpha$ -actin expression by hVSMC on arterial derived matrix. A higher magnification of hVSMC on the cut edge of the medial layer of the matrix after 5 weeks having been immunohistochemically stained for  $\alpha$ -actin (shown as brown colouration by DAB) around the haematoxylin counter stained cell nuclei. Note the image orientation is the same as figure 5.05 gauged by the orientation of the collagen fibres.



### 5.3.3 ASSESSMENT OF MATRIX PENETRATION AND REMODELLING BY hVSMC

Figure 5.07 shows the matrices outer adventitial layer seeded with hVSMC after 5 weeks in culture, stained by haematoxylin. Cells were interspersed throughout the adventitial layer, showing an observable predominance for the outer surface. This contrasts Figure 5.06 where cells have adhered directly to the medial layer. Figure 5.07 shows the adventitial layer of the matrix wall, which contrasts the medial layer shown in Figure 5.06. The adventitial layer, which is less structured than the medial layer provides a very different physical environment for cell adhesion and viability.

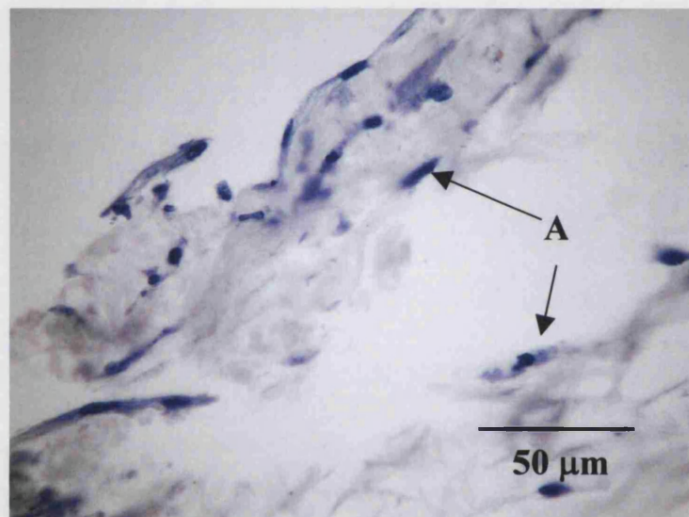


**Figure 5.07:** Culture of hVSMC on the abluminal surface of the porcine derived arterial matrix. hVSMC were seeded at  $333 \text{ cell/mm}^2$  and cultured for 3 weeks under static culture conditions. hVSMC nuclei have stained dark purple (A) by haematoxylin, note the random dispersion of cells within the loose adventitial layer compared to Figure 5.06.

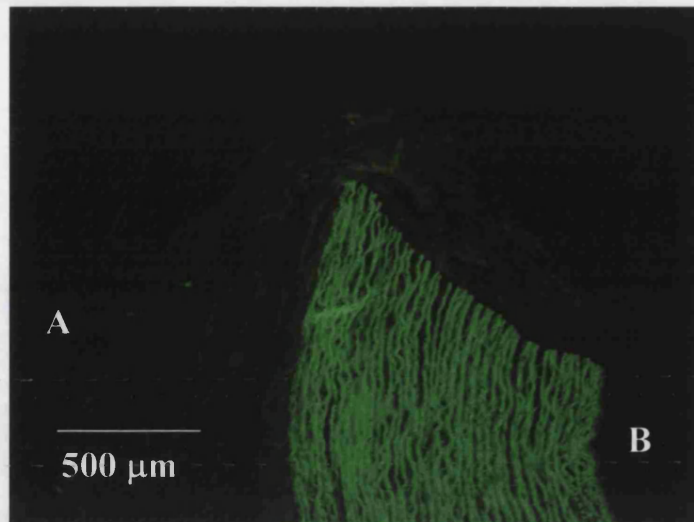
A range of proteolytic enzymes: MMP-2, 9 and cathepsin L which are known to be involved in the mechanisms of cell migration and matrix remodelling were assessed for expression at two time points; 3 and 5 weeks. This was to gain an initial understanding of the expression pattern, if any, of these enzymes in static culture on the developed matrix. In this section all hVSMC were seeded onto the abluminal surface at  $333 \text{ cell/mm}^2$  and were assessed after static culture periods of 3 and 5 weeks. Results

are shown for each immunolabelled enzyme from each time point at 3 and 5 weeks. The first image for each time/enzyme set is the negative control tissue section. Negative controls used the same tissue sections as the immunolabelled sections, i.e. with hVSMC adhered, the immunofluorescent staining process was identical except the step where the primary antibody is incubated with the sample was omitted. This was to determine the extent of background and non-specific staining by the antibody and to ensure, with evidence from H & E section that the localised staining is the actual enzyme targeted. As the controls are only for the immunolabelling procedure, which was the same for each time point, only one time point is shown.

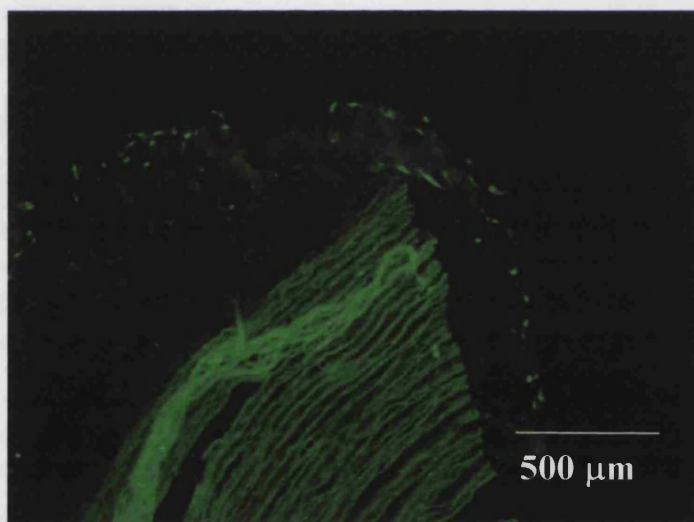
#### MMP-2 EXPRESSION BY hVSMC ON ARTERIAL DERIVED MATRIX

Figure 5.08 shows a control section (as described above) illustrating a strong background staining of the acellular medial layer. Little background or non-specific staining of the adventitial layer is noted where the hVSMC were known to reside. Sections stained for MMP-2 at 3 weeks clearly identify the presence of hVSMC adhered to and within the adventitial layer of the matrix, Figure 5.09 at three weeks. Cells expressing MMP-2 are sparsely populated with no distinct pattern other than randomly dispersed throughout the adventitial layer of the matrix. Figure 5.10 where hVSMC are present large multicellular aggregates present on the cut surface of the matrix, having been cultured for 5 weeks on the matrix show similar positive staining for MMP-2.

In this study, as previously in Section 5.32, the matrix was laid, luminal surface down on the culture plate, with the hVSMC seeded directly onto the adventitial layer. As with all images in this section, the collagen fibres, which were parallel to the culture surface, can be used to orient the image, see Figure 5.08.



**Figure 5.08:** Control section, hVSMC seeded for 3 weeks on processed matrix and stained for MMP-2. The upper, adventitial surface **B** and lower luminal surface **A**, can be used to orientate the image. Note the strong background staining of the medial layer (acellular), with little background or non-specific staining of the SMC layer on and within the adventitial layer of the matrix (A).



**Figure 5.09:** Matrix staining positive for MMP-2 after 3 weeks culture, the presence of cells corresponds with areas of immunolabelled enzyme within the adventitial layer of the matrix.



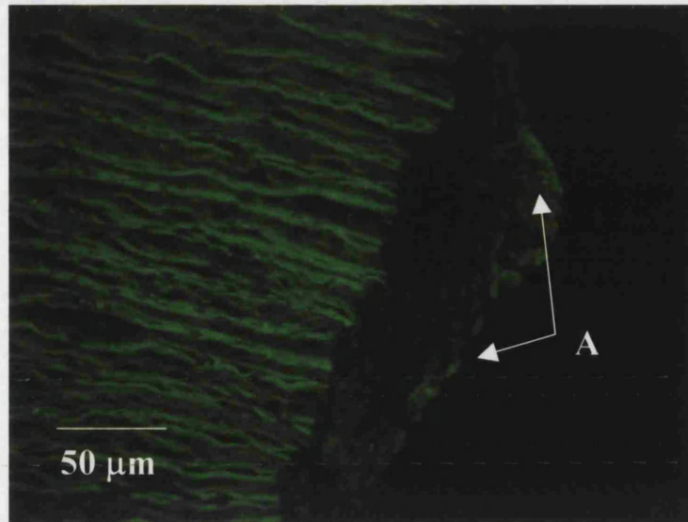
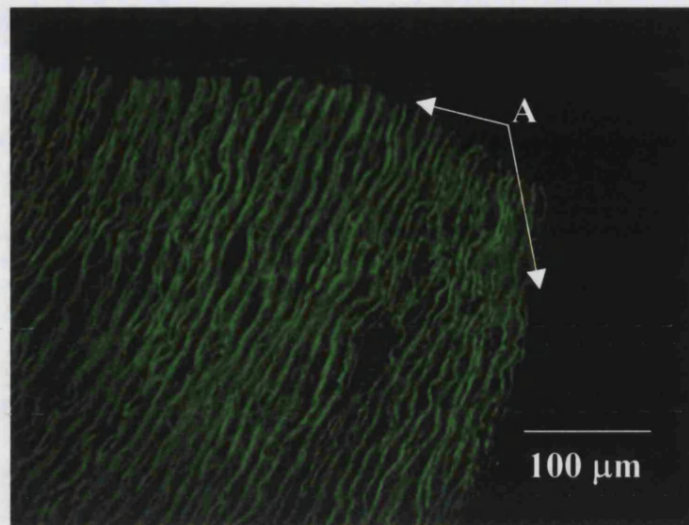


**Figure 5.10:** Positive staining for MMP-2 after 5 weeks culture, the presence of cells corresponds with areas of immunolabelled enzyme (A) within the large cellular aggregates present on the cut surface of the matrix.

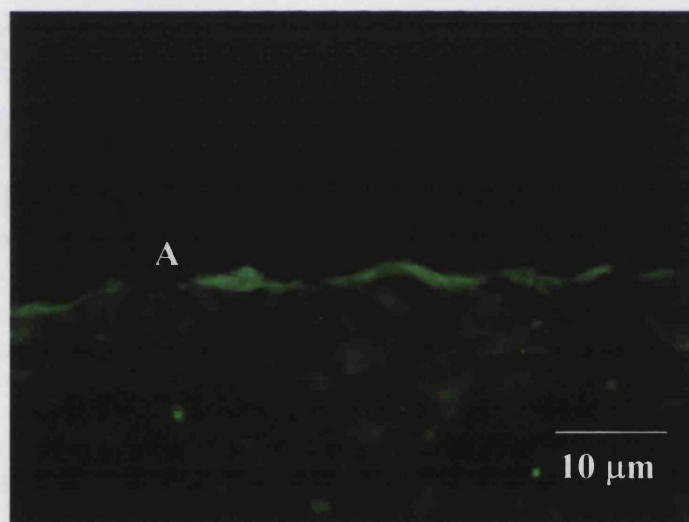
#### MMP-9 EXPRESSION BY hVSMC ON ARTERIAL DERIVED MATRIX

Figure 5.11 shows a control section (as described above) illustrating strong background staining, similar to the MMP-2 analysis, of the acellular medial layer. Little background or non-specific staining of the adventitial layer is noted where the hVSMC were known to reside, see Figure 5.05. Sections stained specifically for MMP-9 at 3 weeks clearly identify the presence of MMP-9 having been expressed by hVSMC adhered to and within the adventitial layer of the matrix. The most intense staining (qualitative) of MMP-9 was at three weeks appearing on the extreme outer surface of the matrix, see Figure 5.12.

Figure 5.13 where hVSMC are present large multicellular aggregates present on the cut surface of the matrix, having been cultured for 5 weeks under static culture conditions on the matrix showing a similar positive staining as MMP-2. The pattern of MMP-9 positive regions within the cell aggregates is the extreme abluminal surface, at the matrix-cell interface as expected.



**FIGURE 5.11:** Control section, hVSMC seeded for 5 weeks on processed matrix and stained for MMP-9. Strong background staining of the medial layer (acellular), with little background or non-specific staining of the SMC layer (A).



**FIGURE 5.12:** Positive staining for MMP-9 after 3 weeks culture, the presence of cells corresponds with areas of immunolabelled enzyme (A) in this case as a monolayer on the surface of the adventitial layer.

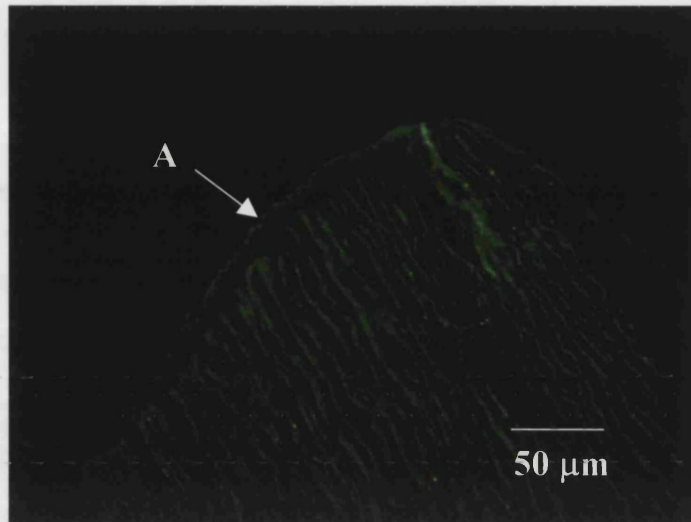


**FIGURE 5.13:** Positive staining for MMP-9 after 5 weeks in culture, the presence of cells corresponds with areas of immunolabelled enzyme (A) within the large cellular aggregates present on both the cut surface and areas of the adventitial layers of the matrix

#### CATHEPSIN L EXPRESSION BY hVSMC ON ARTERIAL DERIVED MATRIX

Control sections of hVSMC seeded and cultured under static conditions for 3 and 5 weeks on processed matrix, like previous controls where incubated without the specific primary antibody to determine background or non-specific staining. Figure 5.14 shows a control section displaying minimal background or non-specific staining within the hVSMC layer (A). Like previous controls for MMP-2 and 9 the collagen and elastin ECM (where hVSMC may reside but in low densities, see Figure 5.05) has a strong non-specific background staining. Little background or non-specific staining of the adventitial layer is noted where the hVSMC were known to reside, see Figure 5.05. Sections of matrix stained specifically for cathepsin L after 3 weeks static culture with hVSMC do not display a distinct increase in staining where hVSMC are present, indicating minimal, if any gene expression and subsequent processing of this protein, see Figure 5.15. Conversely static cultures extended out to 5 weeks clearly identify the presence of MMP-9 having been expressed by hVSMC that have adhered to and within the adventitial layer of the matrix, see Figure 5.16. Like MMP-2 and 9 immunolocalisation of the gene product appears to be restricted to the adventitial layer of the matrix. The strong background staining within the matrix made it impossible to determine whether or not cathepsin L was expressed by cells within the matrix.

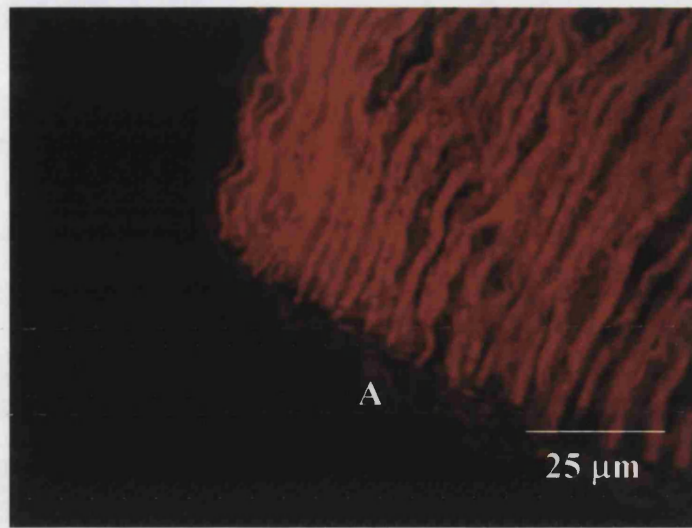


**Figure 5.14:** Control section of hVSMC seeded for 3 weeks on processed matrix and stained for Cathepsin L. Strong background staining of the medial layer (acellular), with little background or non-specific staining of the SMC layer (A).

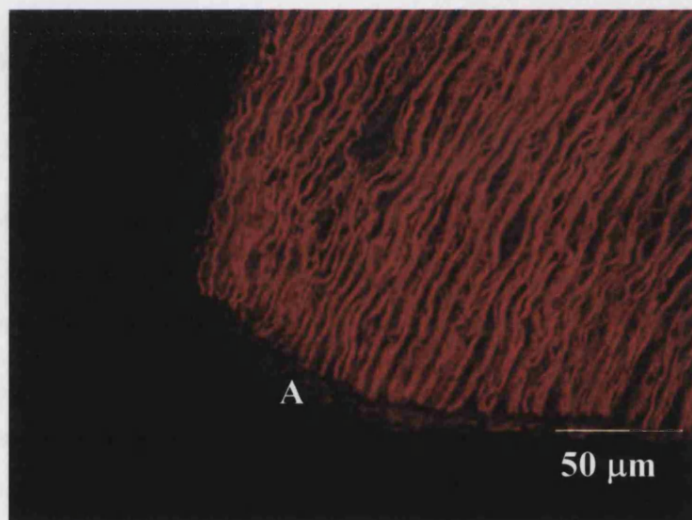


**Figure 5.15:** No definitive positive immunolocalisation for Cathepsin L after 3 weeks of hVSMC static culture.



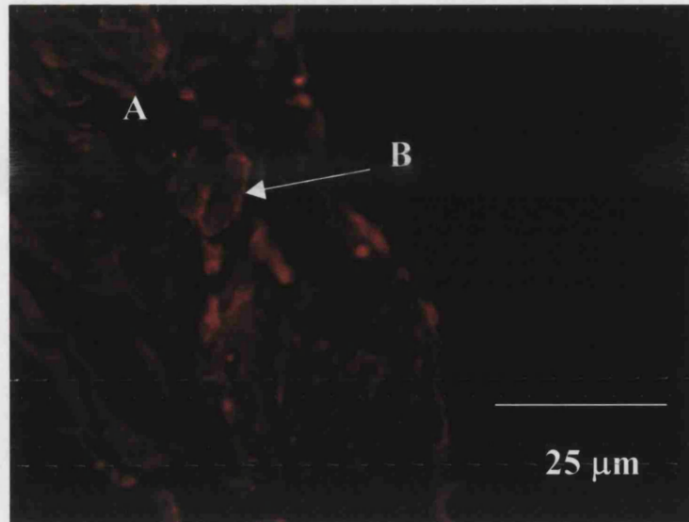


**Figure 5.16:** Unlike SMC cultured for 3 weeks and stained for Cathepsin L, 5 week cultures have stained positive (A), with some sections showing a strong presence of cathepsin L in a circular pattern speculated to be the periphery of cell structures (B).

## 5.4 DISCUSSION

The objective of this chapter was to establish *in vitro* biocompatibility of the porcine derived arterial matrix, enhance HUVEC and hVSMC adhesion to the luminal and abluminal surfaces (respectively) and establish if seeded hVSMC were actively remodelling the matrix by analysing the expression of selected proteolytic enzymes.

Cell seeding studies have demonstrated that the matrix confers cell adhesion, growth and proliferation under static conditions. Previous experience with cross-linked porcine dermal collagen (Smith et al., 2000) has shown direct seeding, without preconditioning can result in sub-optimal adhesion, initial growth and proliferation of cells seeded onto the matrix surface. Similar observations were made with this developed matrix, when HUVEC were seeded directly onto the luminal surface after rinsing with H<sub>2</sub>O, (see Figures 5.01a compared to low serum EC media preconditioned matrix, Figure 5.01b), displayed noticeably different cell adhesion/growth rates. In order to optimise the cell seeding efficiency a variety of treatments were applied to the matrix. Duplicate studies of preconditioning treatments revealed that the use of 100% FCS resulted in very low

cell counts on day 3, it was speculated that this was due to cells being washed off the surface during slide preparation. The likely cause of this result was that as the more dense fractions of the FCS settled during the 48 hour pretreatment phase a relatively thick layer of protein covered the surface of the tissue section, this in turn prevented cells at day 3 from fully adhering to the matrix and subsequently being washed off during slide preparation. Cells cultured over 9 days have more time to penetrate the protein/FCS boundary layer to adhere to the matrix resulting in higher cell densities of adhered cells. As the ultimate goal is to be able to implant the prosthesis, a defined media with minimal FCS, ideally none, is preferable. This is due to the unknown components (particularly growth factors) within serum that acceptable for use for products presented for implantation in humans by the FDA. For this reason both the SMC media (2 % FCS) and EC media (2 % FCS) with increases of 721 % and 558 % respectively, were not initially used. DMEM displayed a higher adhesion at day 3 (134 %) than HBSS (3.6 %), although the day 9 results are not significantly different with 615 % and 600 % increases respectively. Based on these results the media specific to the cells to grown was used to pre-treat the matrix prior to seeding, offering a qualitative increase in cell adhesion over H<sub>2</sub>O washed matrix preparations.

An important aspect with the use of biologically derived matrices is that the matrix material is presented to the seeded cells as a physical environment that is likely to be preferable over synthetic or reconstituted collagen matrices. It was intuitive that if the environment (both physical and chemically) more closely resembles the origins of the cells seeded onto the matrix, that cell phenotype may be maintained resulting in potentially improved graft patency. Direct evidence is not available in the literature to support this speculation, however the application of mechanical forces on cell seeded matrices, which is discussed in Chapter 7.1, undoubtedly demonstrate a link between the cells physical environment and gene expression. The ideal biologically derived graft would be immunologically inert and would retain components (e.g. basement membrane) that would confer an improved environment for cell adhesion, growth and proliferation over other materials. Comparative studies are required to determine any significant effect. In addition the application of further foreign materials could unnecessarily complicate graft development and the patients immune response to the implanted material. For these reasons methodologies to enhance cell adhesion involving, for example, immobilising biologically active molecules to inhibit thrombin

formation or platelet adhesion (Phaneuf et al., 1997), have not been employed.

Characteristic of these processed biological arteries has been the retention of the internal elastic lamina; see Figures 4.18, 4.19 and LT-SEM Figures 4.23 and 4.24 which include elements of the basement membrane, although this has not been empirically confirmed. Providing remnant immunogenic epitopes associated with the internal elastic lamina (from the digestion step) have been masked by the cross-linking step, in concert with endothelium development during the tissue culture prior to implantation, the retention of the basement membrane is perceived as positive aspects towards a successful graft material. Although it is recognized that a fine balance exists between over digesting the vessel resulting in poor mechanical performance and inadequate digestion period where potentially immunogenic protein remains within the vessel. It has been suggested the presence of the internal elastic lamina (IEL) acts as physical barrier preventing the migration of vascular smooth muscle cells into the vessels lumen resulting in intimal hyperplasia (Sims, 1985). In addition the IEL has been postulated to have an important role in the prevention of atherogenesis by acting as a diffusion barrier across the arterial wall (Hampton, 1983).

The effect of having the appropriate cell-specific surface for cell to adhere to can be compared with earlier studies with the type I dermal collagen used in Chapter 3. Initial cell seeding density for this dermal derived matrix (after extensive washing and soaking in SMC media) was approximately 600 cell/mm<sup>2</sup>, after 30 days culture cell densities remained below seeding density at 400 cell/mm<sup>2</sup>. Modification of the same matrix with NaOH, where the same seeding density allowed cells to reach 400 cell/mm<sup>2</sup> still took 20 days in tissue culture. This arterial derived matrix, under the same culture conditions when cells were seeded at 90 cell/mm<sup>2</sup> reached almost 900 cell/mm<sup>2</sup> with the same pre-treatment regime by day 9. This may in part be due to the retention of the basement membrane, where, for example perlecan, an important proteoglycan located in basement membranes and associated with cell attachment (Haralson and Hassell, 1995). As the porcine derived dermal collagen matrix has no basement membrane, this could account for the increased adhesion of HUVEC to the arterial derived matrix, where the basement membrane had been retained. Basement membranes are specialized extracellular matrices fundamental to a diverse range of biological processes, including: embryonic development, maintenance of tissue architecture during remodelling and the ultra

filtration of blood. The basement membrane has been described as an amorphous sheet-like structure positioned between a cell layer and a thick collagenous stroma, composed of several macromolecular constituents, including type IV collagen, laminin and entactin interacting to form a supramolecular structure anchored to the underlying stroma by collagen VII fibrils (Haralson and Hassell, 1995). In blood vessels the basement membrane lies between the extreme luminal surface of the endothelium and the internal elastic lamina, see Figures 4.18, 4.19 and LT-SEM Figures 4.23 and 4.24. Chapter 6, it is speculated that the specialised structure of the basement membrane offers improved anchorage to HUVEC under flow conditions. This effect was not noted in this section of work due, likely due to reduced stress on cells allowing them to adhere to non-optimal surfaces (i.e. matrix not pretreated) during static growth.

Adhesion of hVSMC to the matrix is less clear, although appears to follow a similar pattern where the surface to which these cell naturally reside offers a preferred environment for growth and proliferation. SMC appear to favour adhesion and growth on the cut surface (exposed medial layer) as apposed to the adventitial surface. The cut surface, see Figure 5.05 is the area of the matrix, the media, that VSMC normally populate, whereas the adventitial layer is predominantly populated with fibroblasts. Results show that the density of seeded hVSMC within the adventitial layer is much lower than where hVSMC have adhered (or migrated to) the medial layer. This occurs in two places, 1. where the adventitial layer has been completely removed during tissue processing and 2. the cut edge exposes the medial layer as described earlier. It is hypothesised that the variation in cell density is a result of the cell-specific signal being retained in the medial layer, compared to the adventitial layer that, under normal conditions is predominantly populated with a lower density of fibroblasts (Wheater et al., 1979). This is based on the premise that hVSMC require higher densities within the medial layer of the arterial wall in order to perform the function of contraction conferring vaso-control of the arterial wall. This contrasts the lower density of fibroblasts, which sparsely populate the outer adventitial layer which have no physical role in contraction of the arterial wall (Sunthareswaran, 1998).

This chapter has explored the ability of the arterial derived matrix to support cell adhesion, growth and proliferation. Further to adhesion, growth and proliferation of HUVEC and hVSMC seeded onto the matrix the expression of matrix remodelling



enzymes: matrix metalloproteinase 2 (MMP-2), matrix metalloproteinase 9 (MMP-9), Cathepsin L and general histology has been studied with the objective to determine if cells are migrating into the matrix, if they are expressing typical proteolytic enzymes and what type of barrier, if any, the cross-linked matrix offers to cells expressing these proteins. These and other enzymes serve as a barrage of proteolytic activity that under normal conditions readily allow cells to migrate through elastin and collagen fibres, to effectively remodel tissue as part of the natural course of growth and wound healing (Shapiro, 1998). The ability of transplanted cells to digest and migrate into the engineered tissue is of critical importance to confer high densities that may ultimately allow the construct to behave as native artery.

The rationale for choosing and limiting analysis to these three enzymes was based on several issues. MMP expression and function in the ECM plays a critical role in both physiological and pathological settings. *In vivo* remodelling of the vascular system is in a state of constant flux, where variations in blood pressure, heart rate and general health all contribute to this remodelling process. Inappropriate activity of these potentially damaging enzymes has received much attention in recent years due to their involvement in diseases such as rheumatoid arthritis and the progression of tumour cells during metastasis, have been shown to be mediated by members of the MMP family (McCawley and Matrisian, 2001). The requirement for general representatives of a wide variety of different protease groups was necessary. The activity of these enzymes is directly linked to cell migration with MMP-2 and 9 intimately linked in tumour cell metastasis and the turnover of arterial basement membranes (Foda and Zucker, 2001). Further, up regulation of MMP-2 and 9 is associated directly with abdominal aortic aneurysms (Crowther et al., 2000) and the reduction in scleroprotein content during plaque calcification (and its destabilisation) of the coronary arteries (Kieffer et al., 2001). It is therefore expected that if expression occurs, providing the material is not presented as an impenetrable barrier, cells will migrate to a greater or lesser degree within the arterial wall. Also, between the gelatinases, MMP-2 and 9 a wide range of substrates are available within the vascular ECM that may present differing expression patterns.

In this study it was found that MMP-2 and 9 were expressed at both time points (3 and 5 weeks). Confirmation of expression shows that cells are 'attempting' to modify the

matrix in some manner. Due to the limited nature of this study one can only speculate as to the intended nature of this expression, ECM remodelling, migration or both. It is with some certainty that the assumption can be made that the cross-linked matrix forms an impenetrable barrier at the medial layer to cellular migration, where close knit and non-degradable (due to extensive cross-linking) collagen fibres reside. It is noted in Figure 5.05 that migration does occur into the matrix, this is believed to be from the cut edge of the matrix only. As the collagen fibres lie in concentric layers around the matrix, cutting perpendicular to the fibres allows hVSMC direct access into the matrix without having to rely on matrix degrading enzymes to degrade collagen or elastin fibres. Cells adhered to the medial layer, via the adventitial surface do not appear to have migrated into the outer medial layer and remain as cell layers or dispersed within the adventitial matrix, Figure 5.07. The prevention of cell migration into heavily cross-linked biological tissue is supported by evidence with the matrix used in Chapter 3, where Smith et al (2001) unpublished data, noted human primary fibroblasts failed to penetrate into matrix after 5 weeks in culture. It is possible that cells are not receiving the correct cues to initiate migration, however the expression and subsequent immunolocalisation of specific matrix degrading enzyme to cells, clearly indicate cells are intending to migrate but are prevented in doing so.

The surfaces that hVSMC have adhered to (adventitial and/or directly onto the medial layer) show a variation in cell proliferation and spatial arrangements, as discussed earlier. Cells within the adventitial layer are sparsely populated, Figure 5.06 which directly contrasts cells adhered on or near to the medial layer, Figure 5.05 that are densely packed in multiple cell layers. In both of these regions cells display MMP-2 and 9 immunolocalisation. The pattern of immuno-localisation was expected to be intense staining at the base of the cell layers immediately adjacent to the collagen barrier that would indicate the cellular intention to migrate or remodel the adjacent matrix. It was interesting to observe that 5 week cultures where cells are densely packed the localisation of both MMP-2 and MMP-9 was around cells on the outer most layer, that is the layer *not* adjacent to the matrix, see Figures 5.11 and 5.15. An explanation for this is speculative in that cells adjacent to the matrix have been in close association with the impenetrable ECM for the longest period, it is possible that by the first time point these cells have completed ECM expression and remodelling, whereas cells in the outer layers are still in the process. It is also possible that it is an artefact of

specimen preparation, however controls eradicate this possibility.

The selection of the cysteine protease cathepsin L was based on several factors; firstly and primarily as an integral part of the cellular degradations system, this enzyme along with other lysosomal enzymes maybe highly expressed due to large amounts of protein fragments from the matrix processing steps, in particular trypsinisation remaining in the ECM. Secondly as a secreted protease, compared to other cathepsins, the function of cathepsin L outside the cell membrane is not fully understood. As discussed in the introduction, procathepsin L or cathepsin L it has been noted that a wide range of cells express this gene and export the gene product to the ECM. The functions of this proteolytic enzyme range from degradation of basement membranes, elastin, fibronectin and collagens to the activation of *urokinase-type plasminogen activator* (uPA) involved in the proteolytic cascade that generates plasmin which is implicated in the processes cell migration, (Kirschke and Barrett, 1998) and (Alberts et al., 1994).

Results from this series of experiments, done in concert with the MMP work, have shown, firstly that cathepsin L did not appear to be expressed in 3 week cultures whereas the enzyme was immuno-localised in 5 week cultures. In 5 week cultures cathepsin L was not localised where cells were present in monolayers, nor where cells were densely packed in cell layers, the enzyme was localised in clusters within the adventitial section of the ECM, Figure 5.19. In this image, a circular arrangement of the localised enzyme is associated with what appears to be the cell membrane, this supports the hypothesis that cells focus proteolytic activity at the cell surface to degrade ECM components presented as barriers to migration or as a mechanism of cell detachment (Murphy and Gavrilovic, 1999). This was however only one tissue section of many and was atypical, a majority of expressed enzyme was seen as smaller amorphous zones that are possibly associated with the lysosomal activity which cathepsin L is mainly associated.

Initial studies of the porcine derived arterial matrix, in terms of cell compatibility, have shown that like the porcine derived dermal collagen matrix used in Chapter 3, preconditioning is an important prerequisite to seeding primary human cells. Studies designed to determine an appropriate pretreatment have illustrated that different solutions provide (not surprisingly) a range of environments, some more compatible

than others for cell growth on this matrix under these conditions. The resulting choice, DMEM was found to be substantially better than distilled H<sub>2</sub>O. Evidence in this chapter has shown that this matrix is superior to the dermal collagen used in chapter 3 as a material for adhesion, growth and proliferation of HUVEC on the luminal surface under static conditions. Results from hVSMC culture on the abluminal surface are more difficult to interpret due to technical issues with the method used to determine cell density, though it appears to offer a stable environment that is conducive to cell maintenance with no evidence of the matrix cytotoxicity displayed with the former matrix. Immuno-localisation of MMP and cathepsin L proteases has clearly shown the expression of these enzymes. The primary aim of this study was see if these enzymes were being expressed and if so, are cells capable of migrating into the matrix given the 'machinery' is present. Evidence from immuno-localisation of MMP-2 and 9 and Cathepsin L suggests that under static culture condition hVSMC are *unable* to penetrate into the medial layer of the processed matrix.

Results have shown that the porcine vascular matrix retains a large degree of its native biomechanics (Chapter 4) and *in vitro* biocompatibility properties. The growth inhibition displayed by the dermal collagen used in Chapter 3 (cross-linked with HMDI) is not noted with this specifically designed and developed biomaterial. Under static conditions both HUVEC and hVSMC have been shown to maintain adhesion over extended culture periods and express enzymes involved in the processes of matrix remodelling. It is clear that these results support continued studies using this matrix to further develop a tissue engineered small diameter vascular graft.

The following section of work, Chapter 6, describes the progressive development of a dynamic perfusion system. The system incorporates bioreactors that maintain the porcine derived arterial matrix in sterile containment whilst allowing the application of dynamic forces that mimic *in vivo* conditions. Chapter 7 progresses this work further by seeding human primary cell lineages onto the matrix, within the bioreactors to 'grow' the graft under defined conditions.

## CHAPTER SIX: DEVELOPMENT OF A VASCULAR PERFUSION CULTURE SYSTEM

### 6.1 INTRODUCTION

Typically, static cell culture within tissue engineered matrices is limited by reduced mass transfer of key components, for example O<sub>2</sub>, metabolic by-products, growth factors, glucose etc. The limit with which these components can effectively diffuse into and out of a matrix to provide the adhered cell populations with an environment conducive to cell growth and proliferation is approximately 100  $\mu\text{m}$  (Vanjak-Novakovic, 2002). A methodology to reduce these mass transfer limitations is with the use of bioreactors. The second design parameter is that the bioreactor needs to deliver to the matrix an environment that mimics the environment that the developing matrix is to replace. With specific regard to this project, the bioreactor has been designed to deliver media (that emulates the human bodies blood) through the matrix lumen media in a pulsatile fashion (that emulates the pressure and flow of blood delivered through the vasculature by the heart).

The design and calculation of the bioreactor and its support infrastructure has taken into consideration two important criteria, first the emulation of physiological conditions in a system that allows for the continuous modification of flow parameters, much the same as the heart under normal operating conditions where pulse, flow and pressure are in a state of dynamic flux delivering blood throughout the circulatory system. Second, the system must be compact and functional in its use in both sterile and non-sterile environments. Importantly, concessions have been made that have sacrificed the principle aim, to emulate physiological conditions, in order to develop a system that that is both useable and is capable of delivering the desired results. These concessions will be discussed in this chapter along with the developmental process where a three-part system including a functional bioreactor and process flow and support infrastructure has been created. As an overview to the three primary components of the vascular perfusion system a brief description of each component and its primary function is given.

As part of the closed circuit pumping system the bioreactor, which contains the matrix, is the focal point of the system. Connected to the pumping circuit via lumenal and ablumenal flow connectors the reactor receives the pulsed flow generated by the peristaltic pump and delivers it to the matrix with minimal disruption to the prescribed flow regime. The reactor, using the principles of convective flow, aims to deliver uniform transmatrix pressure differentials that allow for uniformity of matrix processing and the delivery of nutrients/gases to the cellular populations to confer optimal cell growth and proliferation. The flow circuit and pump contained within it comprises a pumping unit where pulsatile media flow, pressure, and the pulsatile wave form are developed, the characteristics of which emulate *in vivo* physiological conditions. Media is delivered to the bioreactor by the flow circuit, a recirculatory system allowing for multiple passes of media. Coupled to the flow circuit are a number of devices, ports that allow for the efficient running and monitoring of the system, the support infrastructure. The media within the system was maintained within set parameters. A multitude of different components (discussed in this chapter) provide an environment conducive to long-term mammalian, specifically, primary human cell culture. These include: temperature control, CO<sub>2</sub> and O<sub>2</sub> gas regulation, nutrient maintenance, pH control and pulsatile pressure wave analysis, via a specifically designed computer program. The system has also been designed to allow transfer of the whole system into and out of sterile containment for process manipulation, sample analysis and media exchange etc.

The objectives of this chapter have been the development of a pulsatile perfusion system that mimics human small arterial blood flow and retains the ability to modulate pressure in both lumenal and ablumenal volumes. The reactor and support infrastructure must transfer to the matrix a physiological-like environment, which is conducive to long-term culture of human primary cell cultures.

### 6.1.1 THE EFFECT OF MECHANICAL FORCES

The important of mechanical forces applied to a tissue engineered graft cannot be understated. The physical environment in which a cell persists has a profound effect on cellular behaviour. Why are these effects so important? Cells persist in a state of constant flux, molecular attachment to the matrix, cell-cell adhesion and diffusible molecules or ligands modulate the cellular phenotype. Furthermore mechanical forces contribute directly as the matrix surrounding the cells expands, contracts or blood shear forces act on the cell surface. These shear forces act by stressing a variety of different molecules attached to the cell membrane that transmit via cell signalling cascades or directly through actin filaments or other transmembrane proteins connecting to the cells interior organelles, (Davies 2002).

Over the last 30-40 years cell culture technology has profoundly affected the cell biologist ability to culture specialised cells in the laboratory, however this has usually been at the expense of using undefined media, for example when supplementing with foetal calf serum, the addition of multiple growth factors, or both. The use of such media, from a FDA perspective, is undesirable due in large to our lack of knowledge of the specific action of undefined serum components. Even with the use of these complex medias, terminally differentiated primary human cells progressively loose their specific phenotype after prolonged maintenance in static tissue culture. The use of tissue engineering principles, such as the application of mechanical forces to maintain cellular phenotype for extended periods *in vitro* prior to implantation is an important aspect of this approach.

In this section an overview complementing the review on tissue engineering applications in chapter 1, outlining the forces acting on EC and VSMC biology that critically modulate cell function. This includes mechanical forces, gas concentrations, waste and nutrient gradient. It is therefore necessary to emulate as closely as possible the conditions the graft will be placed in, in order to precondition the living graft to its intended environment.

## RESPONSES ENDOTHELIAL CELLS TO MECHANICAL STRESSES

The heart provides the driving force for blood flow; where the systolic contraction of the ventricles ejects blood into the circulatory system; see Table 6.01 for pressure wave velocities. When contraction is complete the heart relaxes, 'diastole', and some back flow is evident in the aorta and blood vessel elasticity acts to store blood volume during systole allowing forward flow to continue as the heart cycles back to diastole. The pressure wave is generated as blood is ejected from the heart and is dependent on stroke volume, heart rate, blood volume, peripheral resistance and elasticity of the arterial wall.

**Table 6.01:** Arterial pressure wave velocities (Milnor, 1989).

Artery	Wave Velocity (cm/s)
Ascending aorta	440-520
Abdominal aorta	500-620
Iliac	700-880
Femoral	800-1800
Carotid	680-830

Pulse pressure is determined by the difference between systolic and diastolic pressures, where the mean arterial pressure is averaged over time. As a larger portion of time is spent in diastole than systole, the mean average arterial pressure is not merely taken as the midpoint between systolic and diastolic pressures. Approximate mean arterial pressure is calculated by adding one third of the pulse pressure to the diastolic pressure. (Sunthareswaran, 1998). At rest, the normal blood pressure for a healthy adult male is 120/80 mmHg. Variations in blood pressure are caused by factors including age, sleep, exercise, anger, stress, sexual excitement, pregnancy, respiration, physiological and pathological processes. The three main flow regimes in systemic and pulmonary circulation are turbulent, laminar and single-file flow. Systemic and pulmonary blood flow is predominately laminar. Turbulent flow occurs in the heart ventricles, as blood passes through the valves, and as blood immediately leaves the heart via the pulmonary artery and aorta, as well as in abnormally narrowed regions e.g. arteriosclerosis. Blood flow through capillaries is defined, as is single-file due to the single file manner in which red blood cells travel through the capillary (Sunthareswaran, 1998).



The endothelium was once thought of a simple passive nonthrombogenic barrier but is now recognised as a dynamic participant in the active physiology of the vasculature by controlling vascular tone and haemostasis (Sumpio, 1993) and (Nerem et al., 1993). Haemodynamic forces acting on the endothelium include: tensile stress, acting along the vessel wall due to circumferential deformations, hydrostatic pressure stress (cyclic strain) and shear stress acting along the length of the vessel due to blood flow (Sumpio, 1993). All of which are generated by the pulsatile action of the cardiac cycle and the resulting blood flow through the arterial system. The action of these forces on the endothelium results in a host of different responses ranging from morphological changes to secretion of bioactive compounds. At a morphological level the application of fields of force on a confluent layer of endothelial cells results in an elongation of the cells to align tangential to the flow field. In an earlier study Ives, et al (1986) had shown HUVEC, which under static growth conditions form a cobble stone pattern, when exposed to cyclic stress, the cells align in the direction of stretch (Ives et al., 1986). Thoumine et al (1995) exposed confluent bovine aortic endothelial cells (BAEC) to a range of conditions that included exposure to laminar steady shear stress of 30 dynes/cm<sup>2</sup> for 24 hours. Similar to Ives et al (1985) the BAEC elongated in the direction of flow between 12 and 24 hours after the commencement of the flow regime. Not surprisingly a direct relationship was noted between the cytoskeletal proteins (f-actin, vimentin, and vinculin) with this change in morphology. Interestingly they had shown that four other conditions also produced elongation of cells, including: altering Ca<sup>2+</sup> concentrations, culture on collagen gels, adhered c.f. floating monolayers and culturing cells on patterned surfaces (Thoumine et al., 1995). A change in morphology is therefore not necessarily a result of one condition alone, but a process in which cells adapt to each unique environment, unless with direct chemical intervention, such as altering Ca<sup>2+</sup> concentrations, to alter a variety of different cell mechanisms such as the concentration of intracellular second messengers.

The effects on endothelium physiology are reported extensively in the literature and have not been reviewed; rather it is suffice to say that forces (as mentioned above) acting on EC biology critically modulate cell function (Davies 2002). It is therefore necessary to emulate as closely as possible the conditions the graft will be placed in, in order to precondition the living graft to its intended environment. For example a decrease in cell proliferation as shear stress increases and the lack of any stress may induce apoptosis in

vascular endothelial cells, where a basal level of apoptosis occurs in normal static culture conditions of 0.5-3% (Kaiser et al., 1997). In addition there is a strong influence on secretion of active molecules, in some cases up regulated others down regulated and others show no change at all (Nerem et al., 1998). Importantly, the application of a specific shear regime determines a specific result or change in cell behaviour. For example pulsed compared to steady flow produces different patterns of gene expression, Nerem et al (1998) have shown HUVEC expression of VCAM-1, an adhesion molecule altered differentially between culture conditions from static to steady and pulsed flow (Nerem et al., 1998).

## RESPONSES OF VASCULAR SMOOTH MUSCLE CELLS TO MECHANICAL STRESSES

Vascular smooth muscle cells are a critical component of the vasculature residing in the medial layer of the vessel wall and as such are directly exposed to mechanically dynamic environment (Kim et al., 1999). If environmental cues are lost, for example when explanted vascular tissue is cultured statically in a laboratory, cells, particularly specialised primary human cells such as hVSMC, revert back to a more simplistic or less specialised phenotype. Like the endothelium, smooth muscle cells provide a specific function to a vessel wall, not least to confer the ability of vessel contraction, thus providing control over peripheral blood flow. The loss of the *in vivo* phenotype is often associated with an increase in proliferation and a loss their specialised expression. In the case of hVSMC they loose the ability to contract, which confers vasomotor action to the arterial wall and as such do not behave *in vitro* as they do *in vivo* (Jones, 1996). This loss of contractile ability can be identified immunohisto/cytologically by localising the protein  $\alpha$ -actin, as part of this contractile machinery, within the cell cytoplasm. The anti-human smooth muscle actin antibody binds to the  $\alpha$  smooth muscle isoform of actin. This technique has been used in this thesis to identify and confirm the different cellular phenotypes cultivated in this thesis, see Appendix A1.

It has been widely shown that the application of mechanical forces akin to the cells native *in vivo* environment prolong their specific phenotypic expression in *in vitro* culture, and certainly affects or modulates a gene expression. PDGF is a potent mitogenic stimulus to VSMC proliferation and is likely to mediate the response of VSMC to cyclic strain, Ma et al (1999) demonstrated the expression of platelet-

derived growth factor-B (PDGF-B) and its receptor PDGF  $\beta$  (PDGF  $\beta$ ) on the cell surface in response to exposure to cyclic strain (Ma et al., 1999). Birukov et al (1995) have clearly shown the application of cyclic stress on VSMC selectively induces expression of the phenotypic marker h-caldesmon, whereas omission of the stress reduces expression (Birukov et al., 1995). Interestingly Kim et al (1999) showed that rat cells cultured on fibronectin or vitronectin responded to mechanical stimulation (Flexercell unit) by an increase in proliferation, however the same cells cultured on laminin or collagen exposed to the same conditions did not when cultured in serum free media, when changed to serum-containing media proliferation was induced. This was explained by the adsorption of fibronectin and vitronectin from the 10% serum-containing media onto the surface the cells were cultured on. Similarly Kim et al (1999) cited an increase in elastin and collagen synthesis on fibronectin-coated bonded PGA scaffolds but not on type I collagen sponges when cells were cultured in serum-free media, again when cultured in 10 % serum media and exposed to cyclic strain cell on the collagen sponge produced increased levels of elastin. In both cases western blot analysis had shown that fibronectin had been adsorbed to the matrix, concluding the adsorbed proteins were responsible for the positive response of SMC when exposed to cyclic strain. Costa et al (1991) also reported an increase of elastin synthesis by bovine aortic SMC when subjected to repetitive cyclic strain (Costa et al., 1991).

Mechanical strain of this nature can be seen as an indirect force applied to the arterial wall as a consequence of cardiovascular output. Intimal hyperplasia and medial thickening is a critical factor, particularly in vein grafts, where VSMC migrate and proliferate into the vessel lumen effectively restricting blood flow. The significant histological changes undergone in this process have been reported to be a response to mechanical stimuli and has been shown that when blood flow or velocity has been reduced the occurrence of intimal hyperplasia increases (Sumpio, 1993).

The importance of blood flow characteristics and vessel wall structure/mechanics are not to be underestimated in the development of a tissue engineered vascular graft. The cells that populate blood vessels (endothelial, smooth muscle and fibroblasts) maintain a specific phenotype largely due to the direct effect of chemical and physical factors in the local environment e.g. matrix structure, mechanical properties and the fluid flow regime. Structural and dynamic effects on cell populations *in vivo* are an important

factor in the prevention of graft thrombosis, the main cause of small diameter graft failure. For this reason this project aims to progressively develop *in vivo* fluid and mechanical characteristics that aims to improve the patency of small diameter vascular grafts.

### **6.1.2 BIOREACTORS**

The previous section describes why the mechanical environment is critically important in maintaining cellular phenotype, this section describes the design and application of a pulsed perfusion flow circuit using a unique bioreactor to apply or direct the appropriate mechanical stimuli to the cultured graft. The importance of these forces in maintaining function of a prosthesis are seen as a critical preconditioning step that allows the cellular component to interact and in theory improve performance prior to implantation. In addition the application of convective flow will generate uniform transmatrix pressures, see Figure 6.01, that will allow cells to migrate into the matrix without subjecting them to the same nutrient and gas diffusion limitations of cells in static culture. Due to the relative infancy of the subject area, literature describing the development of vascular bioreactors is limited with little in the way of standardised design (L'Heureux et al., 1998; Nerem and Seliktar, 2001; Niklason et al., 1999; Niklason et al., 2001; Seifalian et al., 1999; Smith et al., 2000; Surowiec et al., 2000; Teebken et al., 2000; Werkmeister et al., 1995; Zilla et al., 1994). With few exceptions the descriptions of vascular bioreactors have tended to either overly simplistic or appear to have avoided accurate description of the reactor due presumably to intellectual property issues. For this reason a unique system has been developed that draws on design features from a variety of different perfusion culture systems, see Figure 6.01.

## DESIGN OBJECTIVES:

Control chemical environment; e.g. CO<sub>2</sub>, PO<sub>2</sub>, nutrients, pH

Control physical environment; e.g. pulsed flow rate and frequency, and pressure

Maintenance of sterility

Accessibility; e.g. removal and addition of culture/growth components

Material compatibility; e.g. cell-media exposure to all components within the system

Maintenance of long-term cell culture

Reproducibility of 'standardised' reactor design

Reproducibility of 'standardised' culture conditions

Ability to monitor system: e.g. construct progression

Simplicity in design and implementation

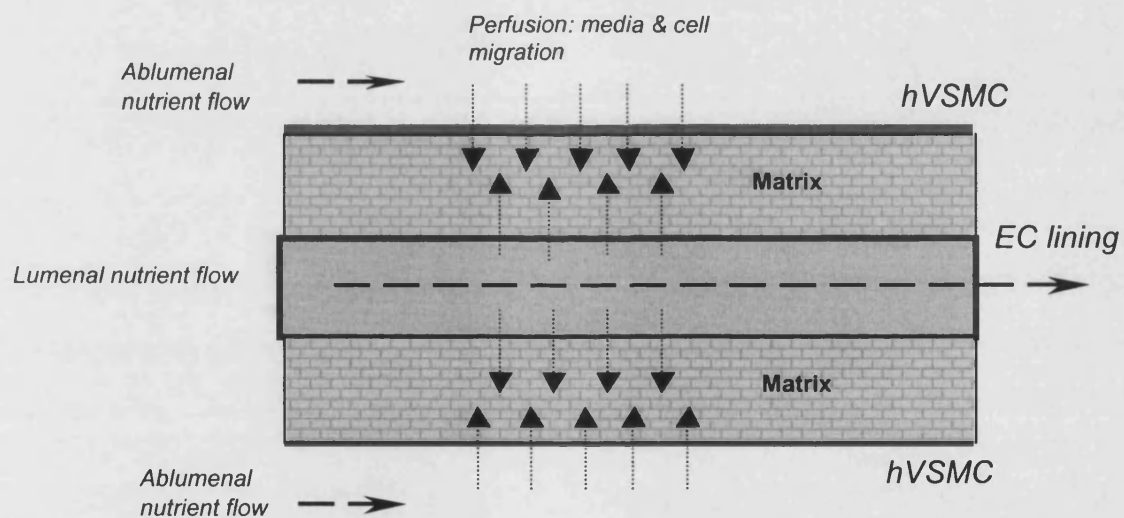


**Figure 6.01:** An illustration of perfusion conditions and construction theory: .....► Indicates cell migration into vessel, media perfusion and transmembrane differential pressure, → indicates nutrient flow indicated.

A major challenge in reactor design is the analysis of the tissue engineered construct within the reactor. Current technology requires off-line analysis, where the construct is harvested for each sample. Several analytic methodologies can be employed to determine the progress the construct during the culture phase of development, however many of these are indirect approaches that are dependent on the metabolic activity of the cells being cultured. Current methods employed to analyse cellular metabolic activity from media samples include: glucose consumption, lactate production and concentration of O<sub>2</sub> and CO<sub>2</sub>. These methods are likely to perform well with cell lines such as 3T3 fibroblasts where cell growth and proliferation are relatively uniform within a defined environment. Where the challenge lies is with the use of autologous or patient specific primary human cells. The process of isolating specific cell lineages from a patient further complicates this issue, however the important point is that each patients cells behave differently. Parameters such as age, cell source, patients general health and the potential diseased nature of some cell isolations results in a huge variation in metabolic activity which makes in-line construct monitoring vital. The clinical use of tissue engineered vascular constructs by its very nature requires rapid expansion of a very limited number of isolated cells and growth of the product *in vitro*. Due to this limitation there may only be one construct generated, off-line analysis is therefore not an ideal option.

As discussed above, initial aims and concepts for reactor development are very similar for different tissue engineering applications; the main functional differences are due specific organs requirements. The imposed requirements are to reproduce the *in vivo* mechanical environment *in vitro*, in addition to reducing problematic mass transfer issues by developing uniform trans matrix pressures. For example, it would be illogical to expose a skin equivalent to the same fluid shear forces as the endothelium of a tissue engineered vascular graft and expect a positive outcome. The following sections describe the progressive development of a three-component bioreactor system that delivers to the tissue engineering matrix and seeded cells, an *in vivo* like environment.

## 6.2 MATERIALS AND METHODS

### 6.2.1 MATERIALS

As in previous chapters all reagents and material details including vendor are shown in Chapter 2 unless stated otherwise. Materials noted in this section are primarily from the final design other materials are described in the text, see Table 6.02. Materials from earlier developmental bioreactors are omitted as they are too numerous to mention and irrelevant to the final system used.

**Table 6.02: Materials**

Materials	Cat. No.	Supplier
Silicon tubing 4.8 mm ID, 7.0 mm OD	326/0512/18	BDH, Poole, UK
PharMed tubing 4.8 mm ID, 7.0 mm OD	275/1145/24	BDH, Poole, UK
Clamps	221/0140/01	BDH, Poole, UK
Watson Marlow Peristaltic pumps	503U	Jencons, London, UK
Watson Marlow Peristaltic pump	504U	Jencons, London, UK
Glass (all sizes) borosilicate glass	275/0080	BDH, Poole, UK
Media containment vessels (1)	215/0150/12	BDH, Poole, UK
Media containment vessel (2)	215/0150/11	BDH, Poole, UK
Plastic tubing connectors (straight)	275/0284/01	BDH, Poole, UK
Plastic tubing connectors (Y shaped)	275/0287/01	BDH, Poole, UK
Stainless steel tubing 4.8 mm ID, 6.0 mm OD	SS/0048.006	BDH, Bath, UK
Duran bottles (100 ml -2 L)	215/0150/15	BDH, Poole, UK

### 6.2.2 METHODS

Figure 6.02 shows the Watson Marlow pump calibration carried out to ensure accurate delivery (in terms of flow rate and pressure wave modelling) of media to the bioreactor

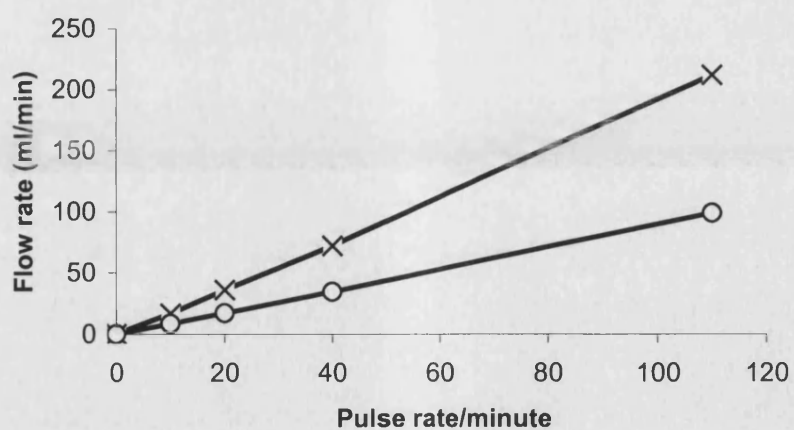


**Figure 6.02:** Watson Marlow 505U pump calibration for 3.2 -o- and 4.8 mm -X- ID peristaltic tubing.

Further methodologies used to design and build the reactor system were based on a pragmatic approach to component design and assembly, as such are not described here.

All analytical methods are described in Chapter 2.



## 6.3 RESULTS

### 6.3.1 REACTOR DEVELOPMENT

The design of the perfusion culture system has been a progressive development with incremental modifications to achieve a satisfactory result. Initial design concepts reflected the list of design aims in section 6.1. In this section the developmental process has been condensed to major design or concept changes rather than individual modifications. Preliminary reactor designs, which included reactors capable of containing multiple matrices, have not been included for reasons of space in this report. An overview of the main reactor design changes are tabulated in Table 6.03 and described in further detail in the following text.

**Table 6.03:** Overview of main bioreactor design and modifications. With reference to 'complexity' as a design issue/problem, was found during handling and general use of the reactor to maintain sterility.

Reactor	Design concept	Problem	Design solution
Mark 1A	Initial design PTFE/glass	Leakage	Alter seals
Mark 1B	"	Leakage	Change to a taper seal
Mark 1C	"	Leakage	Compress taper
Mark 1D	"	Leakage/complex	Alter fundamental design
Mark 2	All glass with multiple tapered Quickfit style connections	Too complex	Reduce complexity
Mark 3	Similar to Mark 2 but with reduced connections	Still too complex	Remove tapered fittings, use only glass treaded attachments
Mark 4	Final and current design		

#### **Mark 1A**

The first fully functional reactor (Mark 1a) was constructed from PTFE (extruded) rod 65 mm in diameter, RS Components, Corby, UK, and glass tube. PTFE was used due to its ability to withstand long-term exposure to saline solutions and super heated steam, with a maximum service temperature of 260°C the PTFE could withstand autoclaving without deforming or degrading and was capable of being machined to the precision dimensions, Figure 6.03.

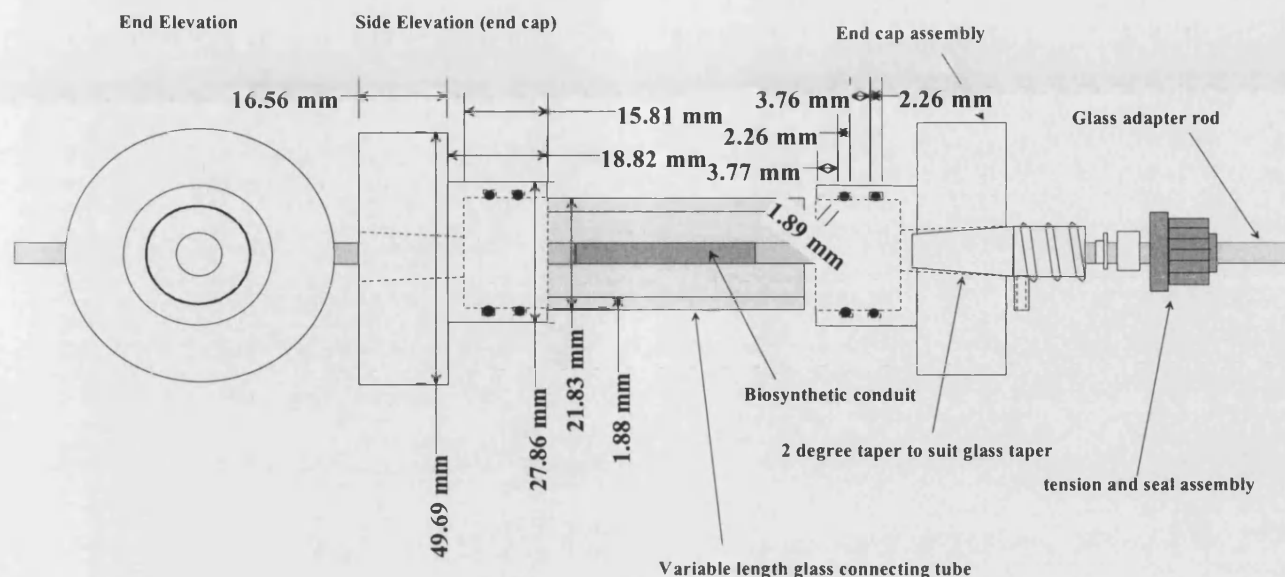


**Figure 6.03:** Technical specification of Mark 1A reactor.

Interchangeable lengths of glass tube (the reactor's main body) connected the machined PTFE copolymer end caps. The end caps were machined to allow fitment of Viton 'O' rings (2 per end cap), Barnwell, Warley, UK, to seal the glass main body once assembled, see Figure 6.03. The design allowed for the central glass body to be interchangeable to accommodate arteries with large variations in length, while the luminal adapters may be adjusted to fine tune for length and to tension (laterally) the inserted matrix. Processed porcine derived matrix was fitted between glass adapter rods (6 mm OD, 3 mm ID) drawn out to a hollow point and blunted to create a ridge to which the artery/matrix could be secured with the use of plastic zip ties, Sigma, Poole, Figure 6.04. Under trial conditions (37°C 5 % CO<sub>2</sub> with pulsed flow rates of 80 bpm/140 ml/min, used throughout testing) the reactor leaked between the PTFE end caps and the abluminal glass body, resulting in unacceptable media loss and possible system infection. It was initially thought the non-uniform circumference of the glass tubing resulted media leakage.

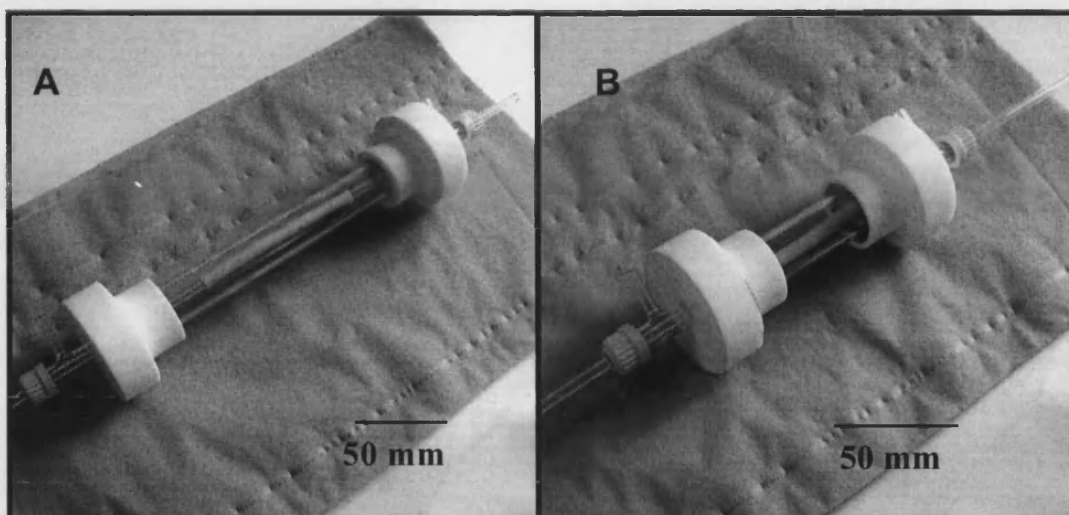


**Figure 6.04:** A. Mark 1A reactors of differing lengths (B), showing both luminal and abluminal inlets and outlets with glass connectors for connection to the simulated tan coloured matrix.

#### **Mark 1b**

The Mark 1B reactor had the PTFE end caps redesigned with 1 'O' ring and a 'lip-seal' BDH, Bath, UK, to improve the seal to the glass main body as the 'lip-seal' has a higher tolerance to variation in the glass main body, see Figure 6.05. Like the Mark 1A reactor these seals were inadequate and the reactor leaked under operating conditions (as above).

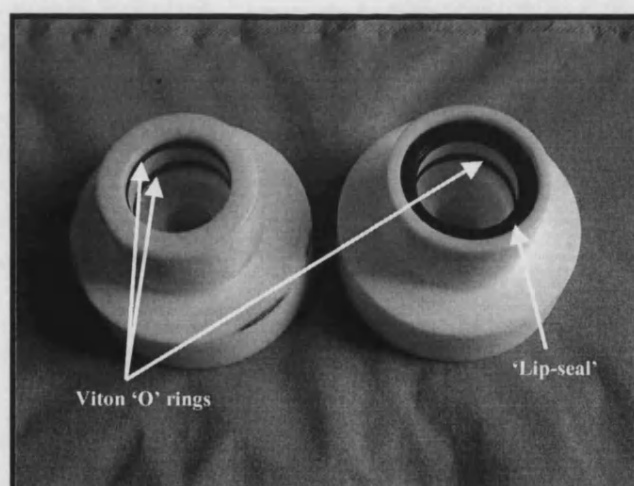


**Figure 6.05:** Mark 1 reactor PTFE end caps showing the two different sealing methods between Mark 1A (2 Viton 'O' rings) and Mark 1B reactors (1 Viton 'O' ring and 1 lip-seal).

**Mark 1c:**

A further modification to prevent leakage between the PTFE end caps and the glass main body, a 2° female taper was machined into the PTFE end caps and the parallel glass main body was replaced with tapered ground glass male fittings at each end of the glass body, (Quickfit style) to suit the female taper within the PTFE end caps, see Figure 6.06A. Like reactors Mark 1a and 1b this modification failed to prevent leakage. It was found that the PTFE end caps became loose after the transition from ambient to operating temperatures.

**Mark 1d:**

In a bid to hold the PTFE end caps secure to the glass body a series of adjustable springs were added to pull these components together. It was at this point that it was observed that the two different materials (glass and PTFE) have differing thermal expansion properties where the glass would expand approximately 0.25 mm less than the PTFE end caps during the transition from ambient temperature to 37°C in the incubator, see Figure 6.06B. However the springs pulled the PTFE end caps together which prevented leakage.

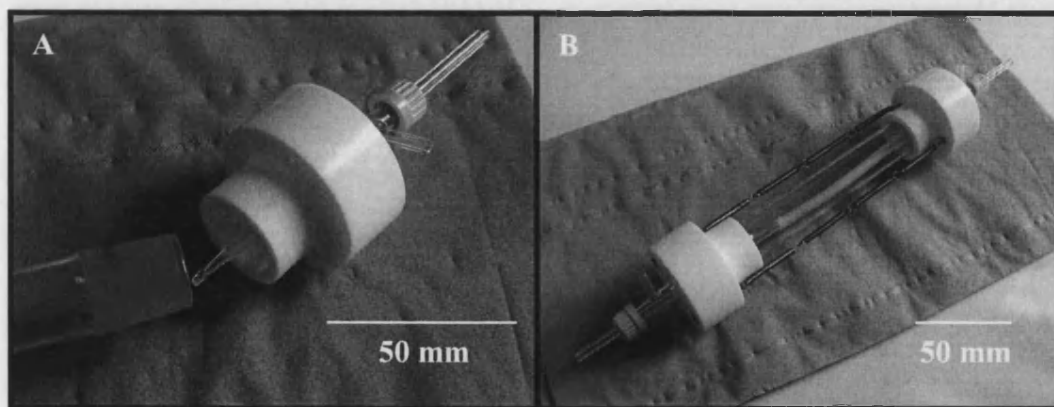


**Figure 6.06.** Mark 1c (A) reactor showing the tapered male ground glass, which fits the equivalent female taper machined into the PTFE end cap. Mark 1d (B), the first leak-proof reactor, showing the attached springs that 'pulled' the two PTFE end caps together preventing leakage due to differing thermal expansion properties.

**Mark 2:**

To eliminate differing thermal expansion properties of two materials the first ‘all glass’ reactor was designed. The luminal glass diameter measured (OD) 25 mm (ID) 20 mm. This design (*not shown*) used a variety of Quickfit adapters to allow attachment of abluminal glass housing (male ends) to fit the reduced size of the female tapered luer holders, however the operation of this design proved to complicated for continued use.

**Mark 3:**

Due to the complexity (and expense) of the Mark 2 reactor the Mark 3 was developed. This reactor consisted of a central glass body with *female* tapered ground glass couplings to which the luminal adapters fitted. This reactor had a reduced diameter main body from (OD) 25 mm (ID) 20 mm to (OD) 18 mm (ID) 14 mm, with a length of 170 mm, reducing the abluminal volume from 53.41 cm<sup>3</sup> to 26.12 cm<sup>3</sup>, see Figure 6.07. This decrease in surface area ratio of the glass abluminal void from 10.68 cm<sup>2</sup> to 7.48 cm<sup>2</sup> to the matrix, increasing the potential for cells seeded into the abluminal void to adhere to the matrix at higher densities. In addition to the potential of increasing seeding efficiency, the reduced abluminal volume reduces the total media content of the system, thus reducing costs.

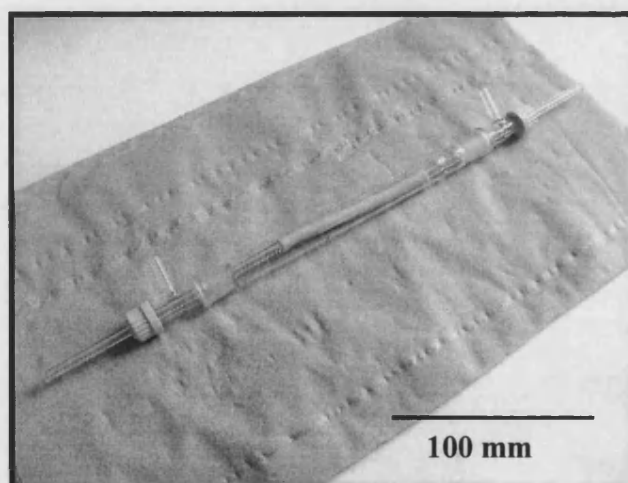


**Figure 6.07:** Mark 3 reactor showing the central glass body with *female* tapered ground glass couplings to which the luminal *male* adapters connected directly, thus eliminating the need for either PTFE or numerous glass adapters (Mark 5) to fit the inlet/outlet manifolds.

#### **Mark 4: Final Design and Specification**

The mark 4 reactor was again constructed with glass, with the main body reduced in diameter to (OD) 10 mm (ID) 8 mm x 180 mm long. This further reduced the abluminal volume from the mark 3 reactor of 26.2 cm<sup>3</sup> to 9.1 cm<sup>3</sup>. This design was later altered to an overall length of 200 mm to suit longer arteries increasing the abluminal volume to 10.1 cm<sup>3</sup>. To further reduce complexity and cost and simplify use the male tapered manifolds at either end of the reactor were eliminated and replaced by a quick-fit 10/4 threaded tube with complementary screw cap couplings (BDH, UK) to attach to the reactors main body and the luer-type adaptors that connected to the artery/matrix.

The transition to this model saw the replacement of the glass to stainless steel luer-type adaptors to connect the matrix (within the bioreactor) to the tubing of the flow circuit. The rationale for changing from the glass to the stainless steel luer-type adaptors (London Surgical, UK) was for several design considerations. Firstly retention of the artery to the glass under flow conditions proved problematic due to the smooth surface (even when buffed) vessels tended to disconnect under pressure. The addition of flattened or bulbous end solved the disconnection problem, however flow dynamics were compromised. Using the equation for velocity:

$$V = Q/A \quad (6.1)$$

where V = velocity, Q = flow rate and A = cross-sectional area flow rates within the normal range (~140 ml/min) with arterial diameters of 3 mm ID were calculated with a velocity of 0.33 m/s. The reduction from 3 mm ID to 1.2 ± 0.3 mm as the glass was moulded increased media velocity to 2.09 m/s under the test conditions (rt 16 ± 2°C with pulsed flow rates of 80 bpm/140 ml/min). At this magnitude (over 6x) of velocity increase was found to strip cells off the matrix surface even at flow rates as low as 50 ml/min (results not shown). With the aim of reduced abluminal media volume the glass was replaced with the stainless steel adaptors as a thin wall thickness was desirable to allow fitment into the vessel and reactor housing (8 mm ID).

To ensure flow into the reactor was within the laminar flow range the Reynolds number ( $N_{Re}$ ) was calculated using the test conditions above, which are at the high end of the flow regime for initial system testing (Best and Taylor, 1991).

$$N_{Re} = \frac{\rho u d}{\mu} \quad (6.2)$$

where  $d$  = vessel diameter,  $u$  = velocity,  $\rho$  = density and  $\mu$  = viscosity. It is generally accepted that as the calculated Reynolds number increases over 2300, there is a transition from laminar to turbulent flow. Fluid viscosity ( $\mu$ ) is assumed to be the same as water at 20 °C. The Reynolds numbers for the three conditions set out above were: 1. artery mean diameter 3 mm, 2. modified glass and 3. stainless steel, where  $N_{Re} = 987$ , 6270 and 801 respectively. A further advantage of using stainless steel was to reduce the wall thickness of the luer-type adapter, where the glass adapter had an end thickness ranging from 1-2 mm whereas the stainless steel was 0.3 mm. This reduction reduces the potential for flow disruption where the adapter is connected to the vessel, as such further justifies the modification to the stainless steel tube with 3.3 mm ID, 4.1 mm OD.

To enhance the fluid dynamics of the reactor a modified luminal inlet was designed that provided improved flow into the bioreactor that ensured fully developed flow entered the reactor, thus improving flow by minimising disruption within the flow field. To confer fully developed laminar flow into the bioreactor the equation for ‘entry port flow conditioning’ was used, (Perry and Green, 1998).

$$L_{ent}/D = 0.370 \exp(-0.148Re) + 0.0550 Re + 0.260 \quad (6.3)$$

Where  $D$  = diameter,  $Re$  = Reynolds number (801) and  $L_{ent}$  is the flow conditioning entry port length required to ensure 99% of fully developed flow into the reactor.



With the use of stainless steel luer adapters with a 3.3 mm ID, under the test flow conditions described above, the right side of equation 6.3 equals 44.32, combined with the left side of the equation equals an entry length of 146.3 mm. The final design length of the lumen entry length was 250 mm to allow for variation in flow conditions. By contrast if the original glass inlet adapters had been retained where flow was turbulent with a Re of 6270, equation (6.4) is used:

$$L_{ent}/D = 40 \quad (6.4)$$

The inlet length calculated (under the same conditions) would be 41.2 mm to achieve similar developed flow (99 %) (Perry and Green, 1998). The outlet port is only long enough to allow a degree of adjustability or tensioning of the artery once connected, no consideration was given to down stream fluid dynamics, an illustration of reactor 4 is shown in Figure 6.08.

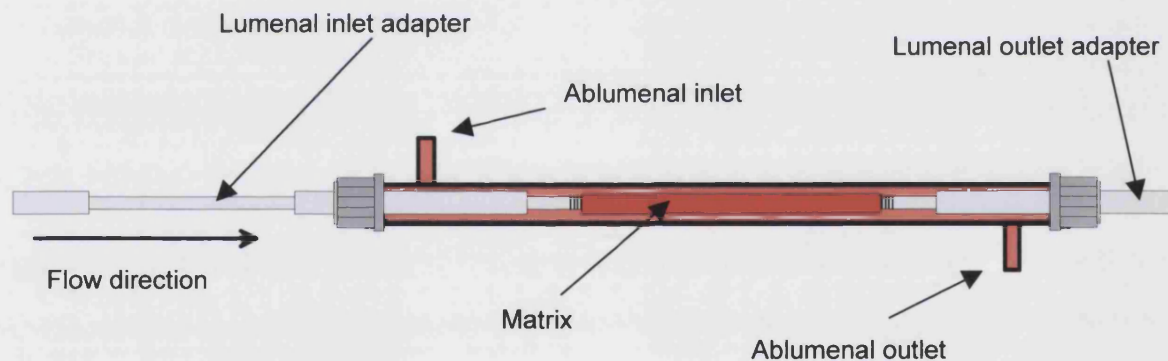


**Figure 6.08:** An illustration of the Mark 4 bioreactor displaying inlet and outlet ports of the reactors main body.



### 6.3.2 PROCESS FLOW DEVELOPMENT

The final process flow system was designed to operate in concert with the bioreactor to deliver media to the cellular population/s within the matrix under pulsatile flow conditions, see Figure 6.09. Although earlier systems were considerably more complex in design, where a variety of parameters such as pH and temperature were monitored real time (data not shown), due to the cost of media, the relatively high flow rates that necessitates media recycling and ease with which complete media changes could be made, media was completely (100 %) replaced every 3 days which negated the requirement for real time analysis. The consequence was that much of the system support apparatus was not required, for example continuous pH monitoring, where the media was buffered and shown to maintain physiological pH over extended periods, see Figure 6.14. Factors influencing media pH in this system include: media type, media volume, flow rate, gas environment and the process flow design that exposes media to the surrounding gas environment. Parameters and media analysis under flow conditions are given in section 6.3.3.

Initial designs used 1-litre fermentation vessels for bulk media containment. This vessel was later reduced in size to 500 ml, with the media return passing through an inverted sparge, situated at the top of the media vessel for gas exchange purposes. Originally this was to increase gas exchange within the returning media in a sterile atmosphere. Due to pH issues this was later replaced with a 100 ml Duran bottle with a modified lid to have 4 ports: 1. Media pick up port 2 and 3 were connected to 0.2  $\mu\text{m}$  filters, which were open for atmospheric gas exchange (5 %  $\text{CO}_2$  + air) the final port on the media storage vessel was the return for recycled media. Media was drawn and pulsed by a Watson Marlow 503U peristaltic pump, from the media storage vessel through a one way check valve to prevent back flow, into a compliance chamber, designed to reduced system noise or vibration caused by the roller action of the peristaltic pump head. The flow was then directed to the luminal inlet port on the bioreactor, see Figure 6.09. At this point the flow was split into the abluminal and luminal inlets. Immediately prior to the abluminal inlet a progressive clamp controlled the flow rate into the abluminal of the reactor at a flow rate of approximately 0.5 ml/minute. The only changes to this basic design was the inclusion of a second reactor. Initial testing attempted to run reactors in a parallel configuration to reduce complexity and handling issues with

‘plumbing’. Variation in matrix dimensions resulted in inconsistent pressure drops between luminal inlet and outlets, resulting in differential flow rates between each reactor system. As the media was recirculating all later models utilising multiple reactors were run in series.

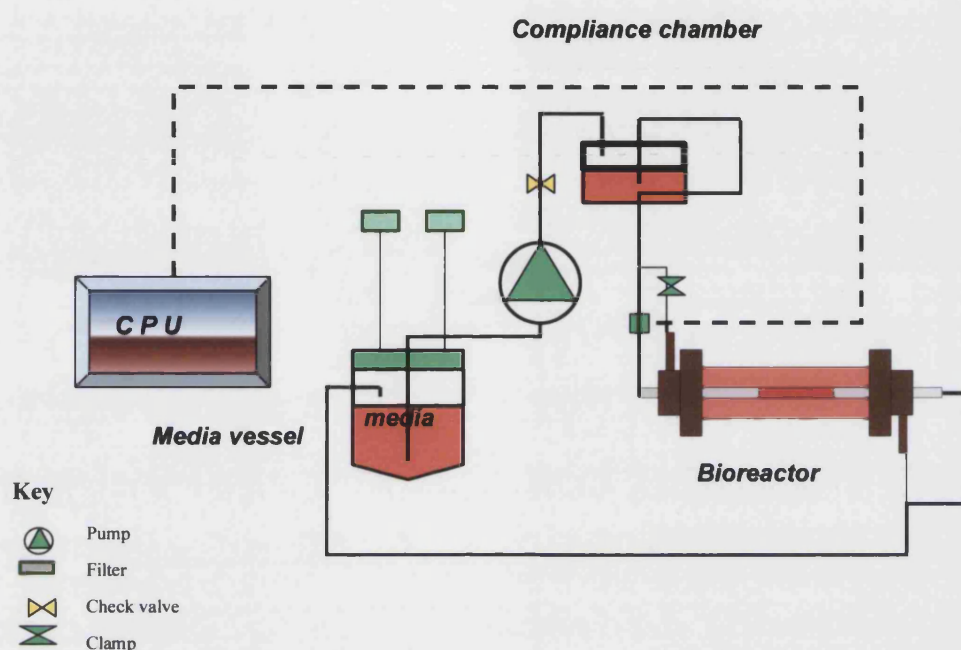


**Figure 6.09:** Schematic of the final process flow circuit, illustrating a single reactor. This design was retained when using dual reactors that were run in series. The compliance chamber serves to reduce system ‘noise’, thus improving the flow regime.

System tubing as above in Figure 6.09, consisted of silicone tubing 4.8 mm ID, 8 mm OD, with the exception of PharMed medical grade peristaltic tubing around the pump head due to its increased resistance to compression failure. This section of PharMed was progressively moved around the pump head to prevent failure after prolonged exposure (up to 5 weeks) to the compressive nature of the pump head rollers.

Total system volume was calculated by adding all discrete sections together. From table 6.04 the total media volume for a dual reactor system (in series) are listed with the addition of a second reactor ( $10 \text{ cm}^3$ ), giving a total volume of  $200 \text{ cm}^3$  (200 ml media). The total volume for a single reactor system is  $183 \text{ cm}^3$ . This compares with the earlier the Mark 1 reactor system volume of  $237 \text{ cm}^3$  with a single reactor.

**Table 6.04:** Component media volumes for perfusion system

Component	Media volumes (cm <sup>3</sup> )
System	63.4 cm <sup>3</sup>
Each Bioreactor	10 cm <sup>3</sup>
Additional tubing for second reactor	7.2 cm <sup>3</sup>
Compliance chamber	10 cm <sup>3</sup>
Media reservoir	100 cm <sup>3</sup>

## PULSE PRESSURE WAVE ASSESSMENT, DEVELOPMENT

The current method to develop a pressure wave analogous to in vivo blood flow has been based on the reproduction of images from the literature, Figure 6.10 (Berne and Levy, 1992). The progressive development of an accurate representation of in vivo blood flow is seen as critical to this project success.

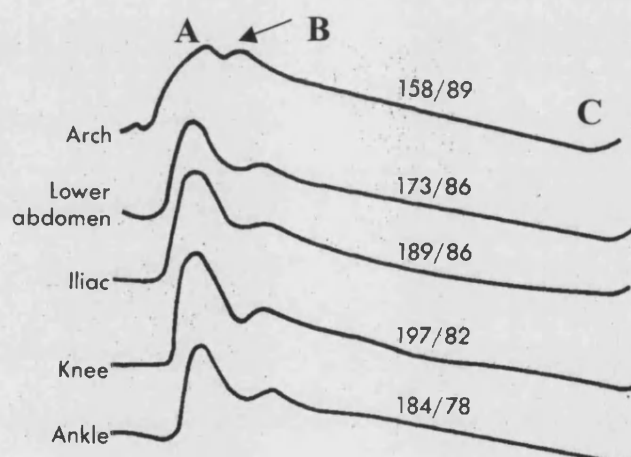


**Figure 6.10:** Arterial pressure curves recorded from several sites in an anaesthetised dog, modified from (Berne and Levy, 1992). **A**, peak systolic pressure, **B**, dicrotic notch (caused by the closure of the aortic valve) and **C**, minimum diastolic pressure.

Figure 6.11 shows progress made towards replication of the peripheral arterial pressure wave form. Initial testing of the pulsatile flow system was conducted using 4.8 mm ID silicon tubing at pulse rates of 80 beats (40 rpm) per minute, which resulted in a flow rate of 150 ml per minute, see Figure 6.12 for pump calibration.

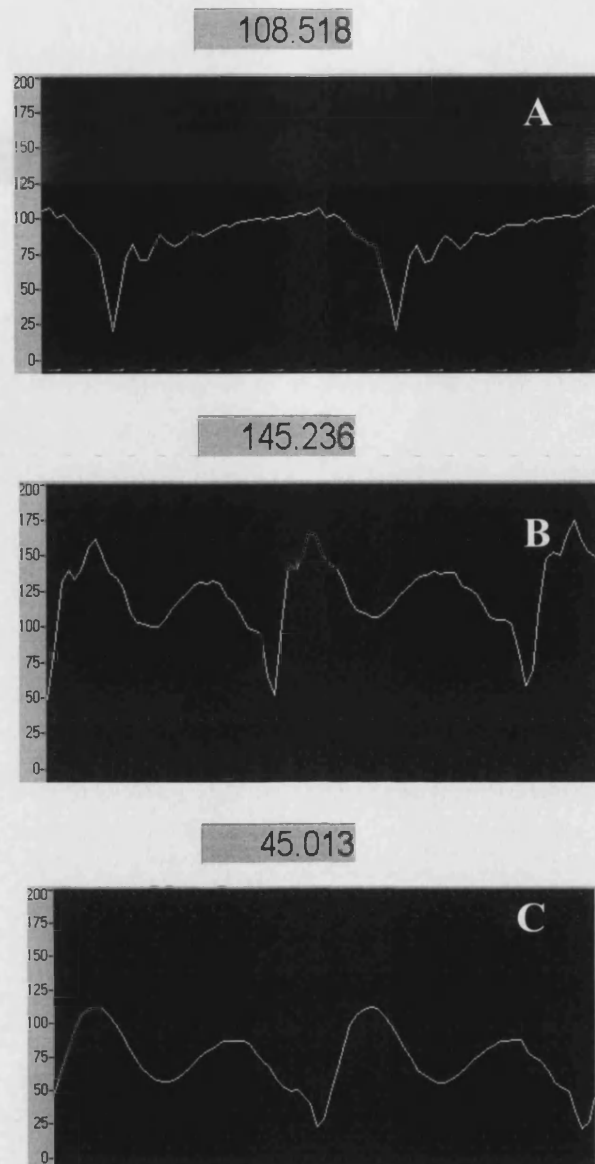


**Figure 6.11:** **A**, Illustrates the basic pulsatile pressure wave characteristics of the Watson-Marlow 503U peristaltic pump when integrated into the flow system. **B**, The addition of a compliance chamber alters both the waveform and removes much of the system noise. **C**, To prevent back flow a one way check valve (cracking pressure of 0.33 p.s.i.) was integrated into the flow system immediately after the peristaltic pump. Pressure readings (Y axis) in mmHg with real time capture shown above each image.

*In vivo*, reverse blood flow occurs only in the aorta due to the elastic recoil of the arterial wall, this event closes the heart valves prior to the next pulsed ejection of blood; the peripheral vasculature has no such back flow. Prior to the final process flow circuit shown in Figure 6.09, reverse flow occurred through out the flow circuit, resulting from the roller mechanism of the peristaltic pump. To prevent back flow a one-way check valve was inserted into the system after the pumps outlet. In addition to preventing back flow, the one-way check valve almost completely removed system noise; compare Figure 6.11 A, B and C.

#### FINAL PROCESS FLOW WITH INTEGRATED REACTOR/S

Perfusion culture described in this thesis was carried out using an apparatus similar to the process flow represented in Figure 6.12. Unlike the in model in Figure 6.12, multiple reactors were always set up in series and lumenal and ablumenal flow was not a separate pumped circuit. The model shown in Figure 6.12 shows 2 Mark 4 reactors set-up in parallel with the lumenal flow pumped separately from the ablumenal circuit. As discussed in Future Work, when the system is used to coculture EC and hVSMC, separate media will be required. For this reason modifications were taken to prepare for this eventually.

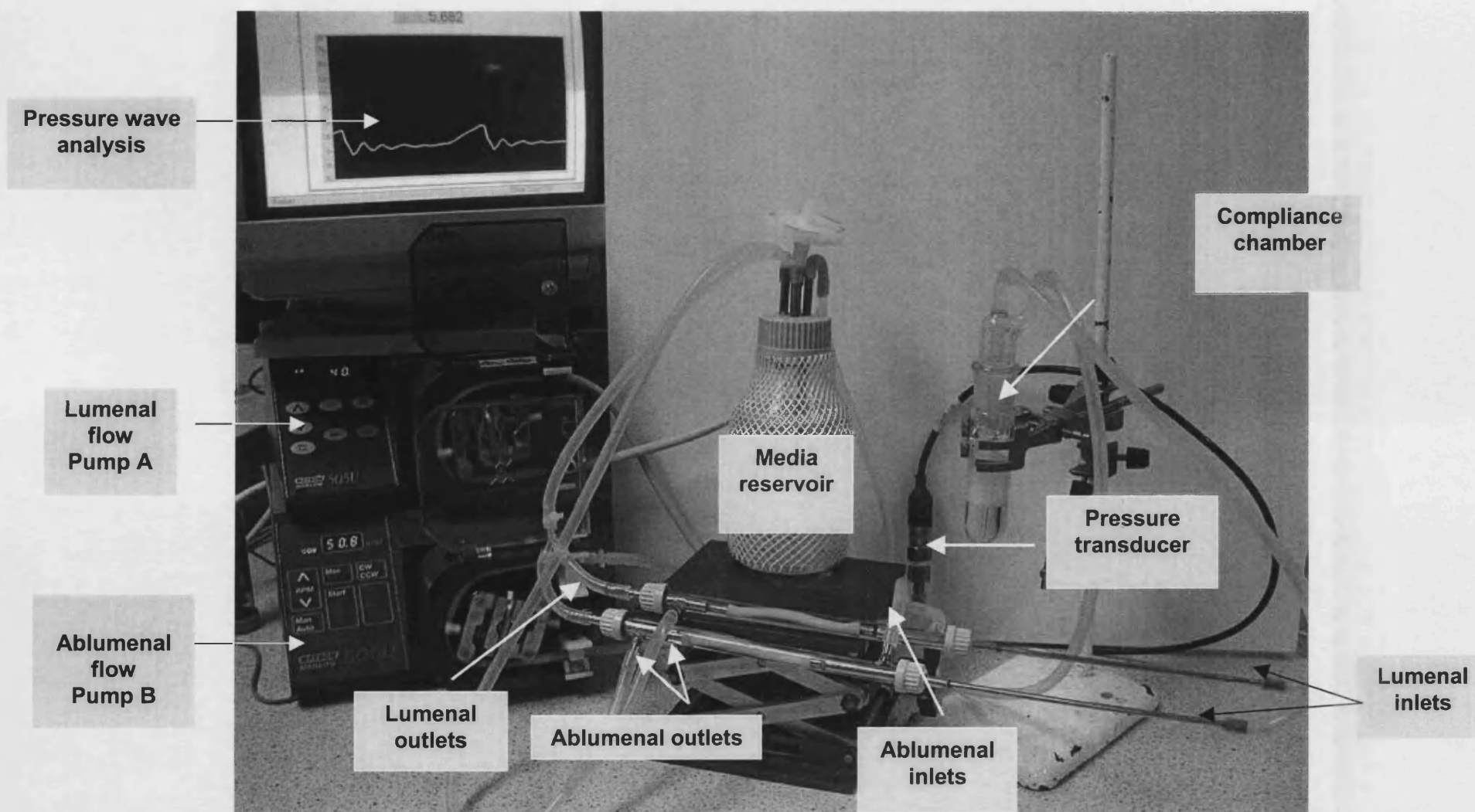


**Figure 6.12:** Representation of the systems final operating design.

### 6.3.3 MEDIA ANALYSIS AND STABILISATION

Static cultures on the developed biomaterial had shown that incubating the matrix in media prior to seeding cells provided a significant improvement in cell adhesion and subsequent growth compared to matrix samples with no pre-treatment, Chapter 5.3.1. Initial trials used DMEM due to the high cost of specific low serum media's and minimal gain shown in cell density by the other pretreatment methods. Preconditioning the matrix within the bioreactor with DMEM resulted in a rapid increase in media pH, according to the media manufactures this was due to oxidation of media components, see Figure 6.13. This result was not characterised. DMEM as the basic component of some medias has a pH 7.4 approximating physiological arterial conditions (Coster et al., 2000).

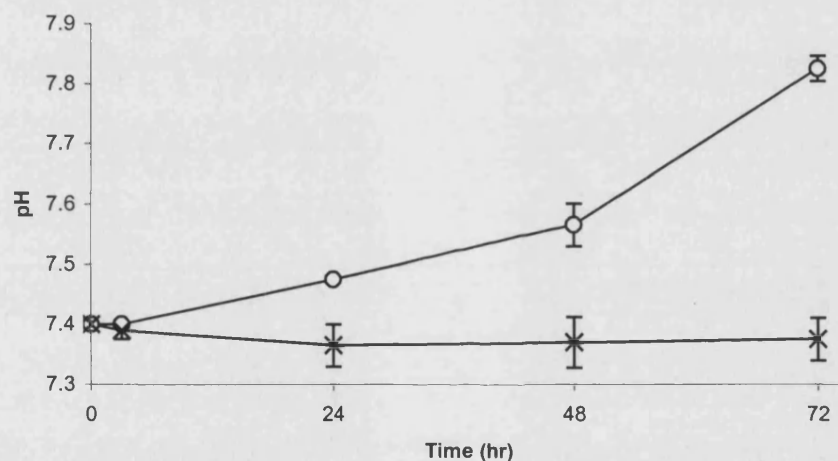


**Figure 6.13:** Variation in media pH: perfusion compared to static cultures. (○) DMEM oxidation under pulsed flow (standard conditions for testing), resulting in a dramatic increase in pH comparative to (x) the same media in static culture conditions.

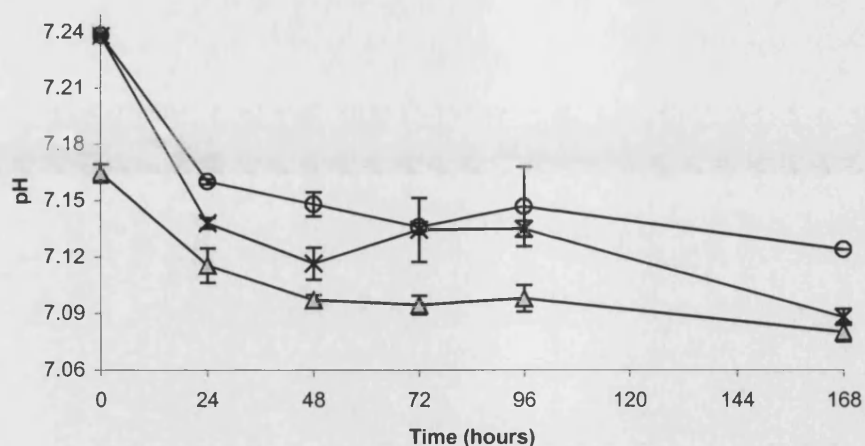


In order to control the pH and reduce the extent of oxidation several modifications were made to the apparatus to reduce gas exchange, these included: removal of the inverted sparge to allow media to enter the return vessel smoothly reducing mixing effects and reduction in the volume size of the bulk media vessel. Due to these results a variety of HEPES buffered media was analysed but failed to maintain media pH at acceptable levels (data not shown). Of these media PromoCell Media (specific for each cell type) was used as a preconditioning treatment due to its improved buffering capacity. Analysis was conducted over a test period of 7 days at 37°C and 5% CO<sub>2</sub> (standard test conditions). For each analytical test the same three conditions were evaluated: 1 pulsed perfusion system with no cells and 200 ml HUVEC media recirculating at 80 bpm, 150 ml/minute, 2 T-75 culture flask with 10 ml HUVEC media (no cells) and 3, T-75 culture flask with 10 ml HUVEC media (confluent with HUVEC). Analytical parameters tested were gas composition (PCO<sub>2</sub> and PO<sub>2</sub>), HCO<sub>3</sub><sup>-</sup>, and pH variations and compared to arterial measurements (Hornick, 2002) and glucose (Coster et al., 2000).

Theoretical cell density within the bioreactor was estimated to be considerably less than the 3 x10<sup>6</sup> cells typically found in a confluent T75 static culture flask, in concert with experimental evidence illustrating pH (Figure 6.14) and glucose (Figure 6.15) and at these cell densities has little effect on media quality. Given that the ratio of media to cells in perfusion system is 20X that in static culture (and replaced at the same rate), it was assumed the influence of cells within the system has little effect on media life span, given their low density to media ratio.

Figure 6.14 displays results of media pH analysis conducted over a 7 day time course. The PromoCell media (EC) clearly shows improved pH buffering over DMEM shown in Figure 6.13. Although the pH in all these tests are below the physiological range, (pH 7.4 ± 0.2), the pH remains within the range indicated in the literature supplied by the media supplier (PromoCell, Heidelberg, Germany).

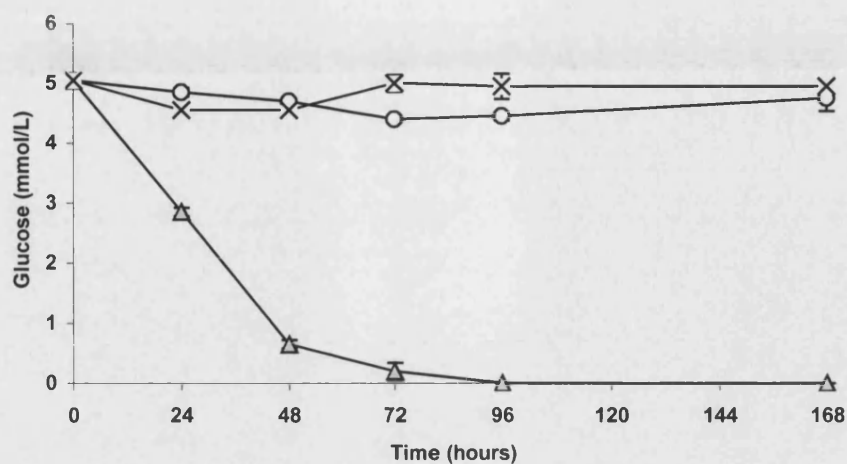




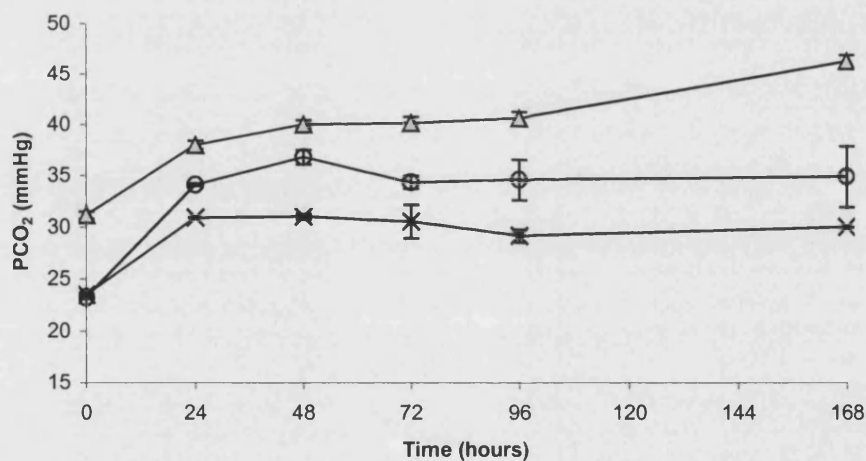
**Figure 6.14:** Comparative change in pH between static and perfusion systems. pH analysis -○- reactor (no cells), -x- T-75 flask (no cells) and -Δ- T-75 flask (confluent HUVEC cells). In both systems pH falls, with the perfusion system maintaining pH closer to the physiological conditions (pH  $7.4 \pm 0.2$ ) over the extended time course.

Glucose consumption was monitored over time using the same three conditions evaluated previously, see Figure 6.15. *In vivo* blood glucose levels vary considerably depending on the dietary status of the individual, a range between 3.8 and 6.7 mmol/L is considered within the acceptable physiological range (Coster et al., 2000). HUVEC media contains 5 mmol/L or 0.005 mmol/ml glucose, it was calculated that 10 ml media contains 0.05mmol and the 200 ml in the perfusion system 1 mmol. Data estimates that  $3 \times 10^6$  cells in this population of HUVEC utilises approximately 0.0022 mmol/ml glucose in 24 hours. Therefore the total glucose in the perfusion system (200 ml = 1 mmol glucose) would theoretically maintain  $3 \times 10^6$  cells in excess of 40 days, glucose is not therefore a limiting factor in this system.

PCO<sub>2</sub> analysis shows that only the T75 flask with HUVEC maintains a PCO<sub>2</sub> close to the *in vivo* environment over the first 4 days, after which PCO<sub>2</sub> levels increase above physiological conditions, see Figure 6.16. Although the level of Levels of PCO<sub>2</sub> are higher (~5 mmHg from 48 hours) in the perfusion system than the T-75 flask, a closer resemblance of the *in vivo* environment where arterial PCO<sub>2</sub> is approximately 40 mmHg.

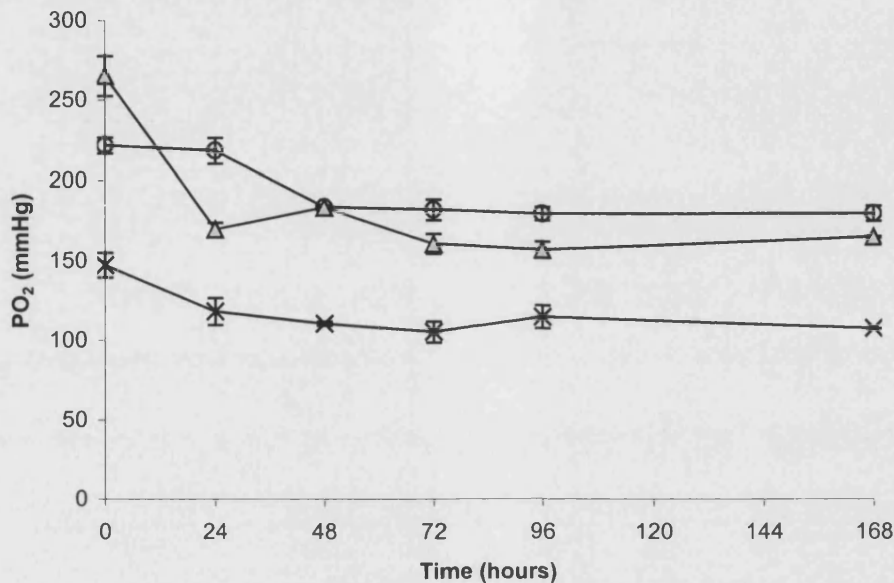


**Figure 6.15:** Comparative change in glucose concentration between static and perfusion systems. Glucose concentration: -o- reactor (no cells), -x- T-75 flask (no cells) and -Δ- T-75 flask with confluent HUVEC.



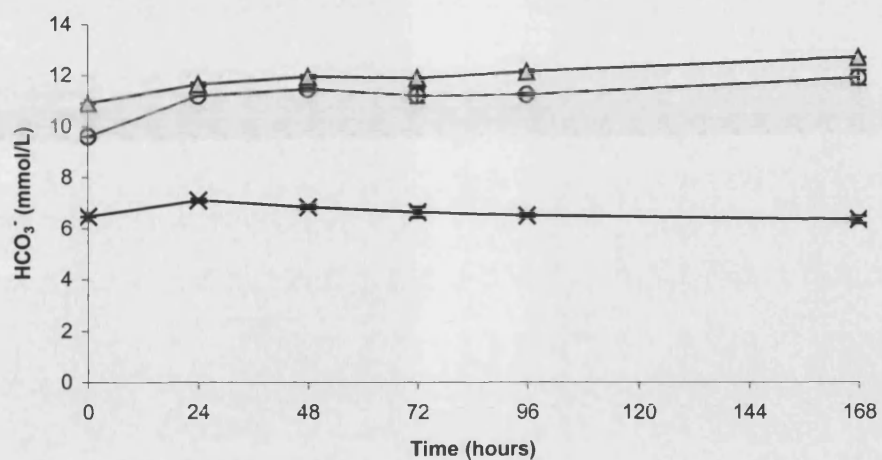
**Figure 6.16:** Comparative change in PCO<sub>2</sub> between static and perfusion systems. **PCO<sub>2</sub> analysis:** -o- reactor (no cells), -x- T-75 flask (no cells) and -Δ- T-75 flask (confluent HUVEC cells). The PCO<sub>2</sub> is highest in the T75 culture flask with confluent HUVEC, consistently 4-6 mmHg higher than PCO<sub>2</sub> in the perfusion system and 7-10 mmHg in the T75 without cells. *In vivo* arterial PCO<sub>2</sub> is approximately 40 mmHg.

Figure 6.17 shows  $PO_2$  under the same conditions as described above. Surprisingly the results show increased  $PO_2$  in the T75 with confluent HUVEC over a T75 flask allowed to equilibrate within the incubator.  $PO_2$  within the perfusion circuit is similar to the  $PO_2$  in the T75 with confluent HUVEC, both of which are higher than arterial  $PO_2$ , which approximates 98 mmHg.



**Figure 6.17:** Comparative change in  $PO_2$  between static and perfusion systems.  $PO_2$ : -o- reactor (no cells), -x- T-75 flask (no cells) and -Δ- T-75 flask (confluent HUVEC cells). Levels of  $PO_2$  are considerably higher than arterial  $PO_2$ , which approximates 98 mmHg. The perfusion system is consistently higher (~65 mmHg) than the T-75 flask (120 mmHg at 24 hours). Reduction in  $PO_2$  within the perfusion system to closer resemble the *in vivo* environment remains an objective.

Bicarbonate concentrations in both perfusion ( $11.1 \pm 0.78$  mEq/L) and static cultures ( $6.44 \pm 0.28$  mEq/L media alone and  $11.88 \pm 0.59$  mEq/L with HUVEC) are lower than the *in vivo* serum bicarbonate concentration of approximately 24 mEq/L, see Figure 6.18.



**Figure 6.18:** Comparative change in HCO<sub>3</sub><sup>-</sup> between static and perfusion systems. HCO<sub>3</sub><sup>-</sup> (bicarbonate) concentration: -○- reactor (no cells), -x- T-75 flask (no cells) and -Δ- T-75 flask (confluent HUVEC cells). Both perfusion and static cultures (with and without cells) are lower than *in vivo* serum bicarbonate concentrations of approximately 24 mEq/L.

## 6.4 DISCUSSION

### REACTOR DEVELOPMENT

In order for the system to function as proposed, the parameters of a normal healthy individual have been used as a base line, such that blood pressure and flow rates are akin to normal physiology. These conditions were determined as flow rates up to 150 ml/min, pulse rates up to 80 bpm and pressure approximating 120/80 mmHg. The validity of this base line if a prosthetic is to be implanted into a section with non-normal flow begs the question; should the flow regime for individual graft be determined by the haemodynamics of the patient receiving the graft? As a baseline for the development of this system, the parameters serve as intended to test the perfusion system for everything from leaks to media oxidation. It is intended that perfusion cultures (Chapter 7), particularly EC cultures will be exposed to a progressive flow regime to allow the seeded cells time to develop *in vivo*-like adhesion sufficient to withstand shear stresses associated with arterial blood flow.

The design and application of this perfusion system has been an incremental development where concept and ideas were modified to realise a functional reactor system. A variety of different systems have been described in the literature varying substantially on this design. Of the systems described, the fundamental difference with this system is the ability to control and monitor both abluminal and luminal pressure, making possible uniform transmembrane pressure differentials, either luminal to abluminal or visa versa. Minimising the abluminal volume improves efficiency both in media and adhesion dynamics by allowing the system to operate as a completely sealed unit. Niklason *et al* (1999) have detailed a bioreactor used in perfusion culture of small diameter arteries seeding bovine SMC and EC onto a biodegradable PGA scaffold. The significant difference between the reactor described by Niklason *et al* (1999) reactor, where pulsed flow is controlled through the reactors lumen by a bellows-style pump, is a considerably larger reactor abluminal compared to the reactor developed in this thesis. Designed like a box with a hinged lid, the reactors luminal inlets/outlets are midway up the walls of the box, the lid designed to allow gas exchange is secured to the top. The potential advantages of this system would include: improved access to the matrix

abluminal surface for either analysis or cell seeding and reduced shear stresses. Prior to EC seeding in the system used by Niklason *et al* (1999), the shell-side surface of the matrix (seeded with SMC) is immersed in a tank media that is changed at regular intervals. Media does not perfuse through the tube-side circuit until EC have been seeded to the luminal surface. PBS is used as the luminal perfusate until EC seeding (Niklason *et al.*, 1999). The advantages of the Niklason *et al* (1999) system are reduced media usage, reduced oxygenation of media resulting in a more stable pH over long-term cultures and easier access to the abluminal surface of the reactor. Improved access for cell seeding is an important issue, with this system SMC can be seeded directly onto the PGA scaffold in high concentrations dramatically improving adhesion efficiency. Although not currently seen as an important issue, seeding a uniform cell layer using this method onto the matrix may prove problematic. With human autologous cells in limited supply other methods may require visitation.

Another system design recently published by Hoerstrup *et al* (2001), typifies presentation of the system and reactor design. Other than an illustration of the systems process flow, and naming the pumping circuit as a 'pulse duplicator', no other information is published. The experimental design seeds ovine cells onto a PGA scaffold, and applies pulsed flow (progressively) up to 750 ml/min (Hoerstrup *et al.*, 2001). It is difficult to comment accurately with the information published, but several potential design flaws are apparent. Firstly the system uses as many as 4 vessels in a parallel array. No mention is made of pressure drop between and across the 4 reactors. Unless resistance is applied to the downstream side of the reactors and monitored, flow rates may vary widely from the published description. In a worst case, the bulk flow will take the path of least resistance, increased pressure drop, which may shear all EC off the luminal surface of the one graft, whereas the remaining three are exposed to considerably less shear stress and display an intact endothelium. Similarly the illustration shows no evidence of an extended luminal inlet to allow flow to develop. Given the maximum flow rates result in a  $Re$  in the turbulent flow range of 3190, the inlet adapter, using equation 6.3, would need to be 200 mm to allow flow to fully develop. Given that the illustration is not likely scaled, using the graft dimension of 40 mm, the inlet is not more than 50 mm. Either the system illustration is wholly inaccurate, equation 6.3 from (Perry and Green, 1998) is not applicable under these conditions or the adhesion of ovine EC is remarkable to yield a confluent endothelium.

The important benefit of controlling abluminal and luminal pressure is to provide an environment *within* the matrix wall that is conducive to cell growth and proliferation. As illustrated in previous chapters the matrix is acellular, prior to removing the porcine cell population the arterial wall is densely paced with VSMC, that depending on the thickness of the arterial wall maybe in close association with smaller arteries or vasa vasorum that are intercalated through the medial, though predominantly adventitial layers. Once the porous acellular matrix has been placed within the bioreactor and pulsed flow applied, fresh media needs to permeate through the matrix wall to allow seeded cells that may migrate into the matrix wall to thrive. Potential limitations in mass transfer of key components such as O<sub>2</sub>, metabolic by-products, growth factors, glucose etc can be reduced by convective flow applied by increasing or decreasing the pressure gradient across the matrix wall. Without these pressure gradients cell in growth is limited to approximately 100 µm (Vanjak-Novakovic, 2002). Additionally these pressure gradients may increase the effective distance with which cell-cell communication is possible, which has been theorised at approximately 250 µm, at least in the direction of the pressure gradient (Francis and Palsson, 1997).

An enclosed abluminal can be advantageous in several respects. Firstly, as discussed above pressure can be applied and modulated to attain desired gradients across the matrix wall, secondly SMC can be seeded directly into the shell-side void and under specific circumstances this can have an improved seeding distribution over the entire surface of the graft. Briefly this method involves the coating the bioreactors inner shell-side surface with poly-HEMA (Sigma, Poole, UK) to prevent cells adhering to the glass surface and rotating the bioreactor around its axis allowing the cells in suspension to 'fall' onto the matrix material thus increasing the percentage cell adhesion to the matrix compared with the glass wall of the reactor, in addition to producing a more uniform cell layer. Secondly environmental factors such as, trans-matrix pressure and the associated delivery of nutrients and gases can be more precisely controlled and monitored.

Like the bioreactor, the perfusion support system was a series of progressive modifications designed to deliver to the matrix, within the bioreactor, a suitable *in vivo-like* environment. Once the initial bioreactor and process flow system were operational it was possible to adjust components of the system to achieve the desired

result. The system component that required considerable adjustment was the media reservoir, many of the assumptions first made were proven inaccurate, for example gas tensions. The first media reservoir had a 1L capacity where returning media was forced through a sparger at the top of the vessel. As a result of increased exposure to oxygen the media oxidised rapidly becoming alkaline, see Figure 6.13. Subsequent vessels where reduced in size (1L, 500 ml, 250 ml and finally 100 ml capacities) and returning media was directed to reduce oxygenation. Like other environmental factors, the control over O<sub>2</sub> levels is particularly important, Lee *et al* (2001) have shown that elevated levels of O<sub>2</sub> reduces VSMC proliferation. Previous work of this group had shown that at the artery-prosthesis anastomosis resulted in significant arterial wall hypoxia, which returns to control conditions after 42 days. In this study it was shown that the first 7 days post implantation of a prosthetic graft were the most hypoxic which correlated with significant VSMC proliferation. However the mechanism for reduced proliferation is unclear with the authors acknowledging that both low and high O<sub>2</sub> tension results in oxidative stress, shown to cause VSMC apoptosis, interestingly they indicate a possible antioxidant effect from supranormal O<sub>2</sub> levels, although no clear argument is presented (Lee et al., 2001).

Under static culturing conditions and in accordance with PromoCell's culturing protocols, media for both hVSMC and HUVEC was replaced every 2-3 days. As a base unit to ensure media volumes would be adequate for cell viability under pulsed flow conditions, the static culture of HUVEC in T-75 culture plates was used. Confluent cultures of HUVEC in T-75 culture flasks have densities approximating  $3 \times 10^6$  cells or 4000 cells/mm<sup>2</sup>, maintained in 10 ml of media replaced every 2-3 days. The surface area of the matrix, assuming it is smooth is 10.37 cm<sup>2</sup> and 16.65 cm<sup>2</sup> ID and OD respectively, with a T-75 culture flask having 75 cm<sup>2</sup>. Contact inhibition of these cells will prevent, particularly during initial adhesion, higher than confluent densities adhering. Under ideal conditions and 100% adhesion of the available surface area, the total number of cells able to adhere to both the luminal ( $4.15 \times 10^5$  cells) the abluminal ( $6.66 \times 10^5$  cells) surfaces would total  $1.08 \times 10^6$  of the total  $3 \times 10^6$  cells seeded. This approximates to 36 % of the initial cell number. As  $3 \times 10^6$  cells (cells in a confluent T-75 flask) are maintained in 10 ml media (every 2-3 days), the reactor initially supports only ~36 % of this number in concert with substantially increased media (183.38 ml) it was assumed media components would be in excess for similar culture durations. Initial



tests were run for 5-7 days before changing media (data not shown), however due to degradation of growth factors in the media this time frame was reduced to 2-3 days. It was concluded that media would not be a limiting factor under these conditions. Other factors such as growth factor degradation at 37°C, media oxidation, volume and flow rate play a more significant role in stabilising the media over the duration of the 3 day exchange cycle. The extended duration of this set of experiments (7 days) past the three day media changing schedule was to gather data in the event the bulk media would be retained and supplements such as growth factor added rather than replacing total media. The advantage of this method would be the ability to analyse metabolites within the media over a longer time frame.

The extended duration of the media testing (7 days) past the three day media changing schedule, was to gather data in the event the bulk media would be retained and supplements such as growth factors would be added rather than replacing total media. The advantage of this method would be the ability to analyse metabolites within the media over a longer time frame thus assessing cell growth or metabolism. The results after these modifications and using the PromoCell HUVEC media, the pH in both the perfusion system and the control T-75 flask falls with the perfusion system maintaining pH closer to the physiological conditions ( $\text{pH } 7.4 \pm 0.2$ ) over the extended time course.  $\text{O}_2$  tension (225 falling to 185 mmHg over 48 hours) was still above normal arterial conditions of  $\sim 98$  mmHg. Reduction of the  $\text{PO}_2$  within the perfusion system to closer resemble the *in vivo* environment remains an objective. Levels of  $\text{PCO}_2$  are higher ( $33 \pm 4.89$  mmHg) in the perfusion system than the T-75 flask, ( $29.89 \pm 2.89$  mmHg) a closer resemblance of the *in vivo* environment where arterial  $\text{PCO}_2$  is approximately 40 mmHg. The current system design allows for simple adjustment of several parameters, for example avenues to reduce  $\text{PO}_2$ , 1. Removing one, or both, of the  $0.2 \mu\text{m}$  filters situated at the top of the media vessel, 2. Replacing silicone tubing for non-permeable tubing or 3. Redesigning the media return outlet to be below the surface of the bulk media. Any adjustment will require complete revaluation of the media conditions as change in  $\text{PO}_2$  will affect  $\text{PCO}_3^-$  and media pH.

The overall aim of this section of work was the development of a pulsed perfusion system to allow adhesion, growth and proliferation of vascular cell lineages under *in vitro* conditions that emulate the *in vivo* physiological environment. As described

on the first page of this chapter, objectives were divided into three categories: 1. The perfusion system to generate appropriate mechanical forces and transmit them to the bioreactor while simultaneously allowing sampling and media changes. 2. The design and development of a bioreactor that allows for the seeding of specific cell lineages to both the luminal and abluminal surfaces. Once seeded the mechanical forces generated by the perfusion system must be transferred to the matrix and 3. Design a support infrastructure to allow long-term culture of human primary cell cultures. Although these objectives are complex and multifactorial the system presented in this thesis has accomplished all the major tasks presented to the level of a working prototype. The perfusion system generates pulsed flow with waveforms and pressures similar to *in vivo* haemodynamics where pressure, frequency and flow can be modulated to suit the researchers specific requirements. Like the perfusion system, the bioreactor has been modified progressively as new challenges have occurred during development. The underling theme was to keep moving parts and complexity to a minimum, where a single researcher must be able to assemble the reactor, insert the matrix, inoculate primary human cell cultures and transfer the entire apparatus to the appropriate gas environment, whilst maintaining strict sterile conditions.

Although several properties of this system require further adjustment, e.g. gas tensions, to more accurately emulate the *in vivo* haemodynamic environment, the prerequisites have been met with this working reactor system. The next chapter in this thesis, Chapter 7, utilises the perfusion bioreactor system described in this chapter to apply conditions mimicking physiological parameters to the porcine derived vascular matrix upon which hVSMC and HUVEC have been seeded and cultured.

# CHAPTER SEVEN: PERFUSION BIOREACTOR STUDIES OF HUMAN VASCULAR CELLS CULTURED ON PORCINE DERIVED VASCULAR MATRICES

## 7.1 INTRODUCTION

The arterial derived porcine matrix was first tested in Chapter 6, where sections were assessed for biocompatibility under traditional static culture conditions using two primary human cell lines. The conclusions drawn indicated that although the material is biocompatible with primary human cells (HUVEC and VSMC) the matrix required media pre-treatment to achieve efficient seeding densities. After treatment, seeded HUVEC attained confluence rapidly. hVSMC were more difficult to assess numerically due to the 3 dimensional structure of the abluminal surface. Sections of the matrix had shown hVSMC had adhered and expressed distinctive matrix remodelling enzymes, MMP-2, MMP-9 and Cathepsin L. Cells appeared unable to migrate fully into the tissue after 5 weeks in static culture when assessed by the same matrix remodelling enzymes. Following results in Chapter 5 and the prototype reactor designed and developed in Chapter 6, a number of objectives were ascertained to progress toward a tissue engineered vascular conduit with the use of the reactor based perfusion culture system. The initial objective was to develop static cell seeding protocols for both luminal and abluminal surfaces of the matrix, ideally within the reactor system, then to optimise HUVEC seeding conditions and cell retention under preliminary flow conditions and allow cells to reach equilibrium within the perfusion bioreactor over extended time courses. Once the culture conditions had been evaluated, expand on the static studies to determine differences between 'like' cell populations cultured under the two different regimes (static verses perfusion cultures). Similarly, optimise seeding methodologies for hVSMC onto the abluminal surface via the abluminal port inoculation, and finally culture under pulsed perfusion conditions that mimic the *in vivo* environment to assess matrix remodelling enzyme activity and contrast with static cultures. As outlined above the aims of this part of the project were to assess the biomatrix and seeded cell populations under a variety of mechanical conditions such as fluid and mechanical shear stresses. The spatial arrangement of the same matrix remodelling enzymes as in chapter 5 (static cultures) was assessed

immunocytochemically and histochemically paying particular attention to differences in the cell migration profile within the matrix under both static and pulsed flow cultures.

HUVEC and hVSMC have previously been cultured under static conditions on the porcine derived vascular matrix, results from static cultures, Chapter 5, have shown HUVEC adhere to and were maintained on the matrix. hVSMC adhesion and growth on the abluminal surface under static culture conditions, Chapter 5, has shown the inability of primary hVSMC to migrate into the medial layer of the matrix. It was shown that in the presence of specific matrix degrading enzymes (MMP-2 and 9 and cathepsin L), hVSMC were unable to migrate directly into the medial section of the matrix wall from the abluminal surface. This chapter describes and discusses the use of the novel bioreactor described in Chapter 6 to apply physical and chemical conditions that mimic the *in vivo* environment to seeded HUVEC on the luminal and hVSMC on the abluminal surfaces. The first section of this chapter describes HUVEC seeding conditions that are specific to the perfusion culture system and determined the ability of cells to maintain adhesion to the luminal surface when exposed to arterial-like haemodynamic flow. The second section of work describes hVSMC seeding to the abluminal surface within the perfusion culture system. Followed by assessment of cell adhesion and migration using the same matrix degrading enzymes (MMP-2 and 9 and cathepsin L). These results were then compared and contrasted to the results from static cultures conducted in chapter 5 to assess differences in hVSMC migration behaviour when cells are cultured with the perfusion bioreactor. It must be noted that a direct comparison between static and perfusion results is limited as the two experiments were not conducted in parallel and different batches of cells (from different individuals) were used.

## **7.2 MATERIALS AND METHODS**

### **7.2.1 MATERIALS**

Unless stated otherwise all reagents and material details including vendor and purity are shown in chapter 2.1.

### **7.2.2 EXPERIMENTAL METHODS**

All hVSMC and HUVEC were cultured using materials described in Chapter 2.1.3 and cultured using methodologies described in Chapter 2.2.2. Matrix preparation, from unprocessed porcine carotid arteries to the fully processed, cross-linked and washed matrix was carried out in accordance to the protocol described in Chapter 4.3.5.

#### **7.2.2.1 REACTOR SETUP**

Mark 4 reactors were used in all cultures and set up in a similar fashion to Figure 6.12. All tubing throughout the process flow other than around the peristaltic pump head was 4.80 mm I.D. 8.00 mm O.D silicone, as described in Chapter 6.2.1. Tubing around the pump head was 4.8 mm I. D. 8 mm O. D. PharMed, peristaltic pump tubing, MERCK, Poole, UK. Two reactors were set up in series, as described in 6.3.2 with two fully processed arteries, see Section 7.2.2.3. Matrix within both reactors (number one closest to the pump head) measured, 100 mm long with the inlet or proximal I.D. being ~6.5 mm O.D. ~5 mm and the ~3 mm I.D. and ~4.5 mm O.D. at the distal end. Inserting the matrix into the bioreactor is detailed in Section 7.2.2.3.

#### **7.2.2.2 REACTOR AND MATRIX ASSEMBLY**

Due to the variety of different reactor versions only the final (Mark 4) design is described. All materials with the exception of the matrix material were first rinsed in

distilled H<sub>2</sub>O and autoclaved (standard conditions: 121°C 15 minutes) prior to assembly. The reactor is laid out within a sterile class II safety cabinet with all reactor or components in contact with internal surfaces resting on sterile surfaces. The matrix material was selected and briefly inspected to ensure no gross fractures or leaks were apparent and any loose ends trimmed. A 300 mm long x 3mm OD sharpened spike was inserted into distal end of the luminal outlet until the tapered end was just proud of the proximal end. This was used to draw the narrow end of the tapered matrix over the outlet adapter. Using the ligation device, two rubber rings clamped the matrix to the adapter. The spike was then removed ensuring the matrix was not overly stressed. The wider end of the tapered matrix was then selected and the luminal inlet inserted. The same process was applied to the proximal end of the matrix to connect it to the inlet adapter. Once the matrix was firmly attached to the inlet and outlet adapters the outlet adapter was lowered into the body of the glass reactor body. A silicon seal was placed over the adapter with the locking cap securing and sealing the adapter to the reactor. The same procedure was followed to secure the opposite end. The assembled reactor was then connected to the process flow circuit with silicon tubing. Section 7.2.2.3-7, describes the method used to precondition and seed cells into the bioreactor.

#### 7.2.2.3 MATRIX PREPARATION

Once the processed arteries had been inserted into the bioreactor and all ports connected to the perfusion system, the matrix was sterilized and depyrogenated based on a method supplied by Dr. S. Badylak, Purdue University, USA, (personal communication). A 0.1 % peracetic acid (v/v) and 4% EtOH (v/v) in distilled H<sub>2</sub>O was prepared in a solution ratio of 20:1 solvent (ml) to tissue weight (g) e.g. 5 g tissue required 100 ml sterilising solution, consisting of 100 µl peracetic acid, 4 ml EtOH and 96 ml H<sub>2</sub>O. The solution was perfused through the system for 3 hours at 50 bpm, 37°C, 5% CO<sub>2</sub> to ensure sterility within the system. PSB was then flushed through the system at 50 bpm, 37°C, 5% CO<sub>2</sub> in batch lots of 150 ml until pH was stabilized to 7.4. The matrices were then preconditioned for 48 hours with 150 ml SMC specific media, (PromoCell, Heidelberg, Germany), perfused through the system at 20 bpm, at 37°C, 5% CO<sub>2</sub>.

#### 7.2.2.4 SEEDING CELL SUSPENSIONS ONTO THE LUMENAL SURFACE OF THE MATRIX

Prior to cell seeding, all preconditioning media was pumped back to the media reservoir and discarded. Seeding HUVEC was carried out by inoculating the lumenal void (including the inlet and outlet leuc adapters) by attaching a 10 ml plastic pipette containing known volume and density of cells to the inlet leuc and pumping cell into the lumenal void. For all HUVEC experiments the ablumenal void was clamped off to prevent disrupting flow within the lumen. Media in both the lumenal and ablumenal flow circuits was replaced every 48 hours with fresh media.

#### 7.2.2.5 SEEDING HUVEC

**Method 1:** Using the same seeding methodology as described in section 7.2.2.4, cell suspensions were injected into the matrix lumen via the inlet leuc adapter and allowed to adhere for three hours before rotating the reactor body 180 degrees and leaving for a further 24 hours. A progressive flow regime was then applied, where the flow rate was increased from 0 bpm to 5 bpm (0-8.25 ml/min) for the first day post seeding, days 2 through to 3 the rate was increased from 5 bpm to 10 bpm (8.25-16.5 ml/min), then increased progressively by 20 bpm (33 ml/min), except day 7 at 10 bpm, each 48 hour period until 80 bpm (165.5 ml/min) was reached. Media was 100% changed every 48 hours.

**Method 2:** The same inoculation and application of flow was followed as method 1, differing only immediately post inoculation where the reactor body was rotated 120 degrees, each for 3 hours, where at the final rotation the progressive flow regime was followed (as above in Method 1). Media was 100% changed every 48 hours.

**Method 3:** The same inoculation and rotation procedure was followed as method 2. Prior to the application of the graduated flow regime the reactor (and seeded cells) were cultured under minimal flow conditions, 1 bpm (1.65 ml/min) for two weeks prior to applying the same flow regime (as above in Method 1). Media was 100% changed every 48 hours.

#### 7.2.2.6 SEEDING hVSMC

**Method A:** Seeding hVSMC was carried out in a similar fashion to HUVEC except cell suspensions were injected directly into the abluminal void. Using a 25 ml pipette, cell suspensions were injected into the inlet port of number one reactor. As the two reactors were in series the cell suspension was pumped in until both reactor abluminal voids were full of the cell suspension. All abluminal inlets and outlets were then clamped to prevent the cell suspension flooding into the return media flow. Post inoculation the reactor body was rotated 120 degrees, each for 3 hours to allow cells to adhere, where 3 hours after the final rotation a flow rate of 80 bpm (165.5 ml/min) was applied through the lumen. In all hVSMC monoculture experiments the abluminal void was clamped off to prevent disrupting flow within the lumen. Media in the abluminal void was refreshed every 24 hours by diverting flow from the luminal flow at approximately 1.65 ml/min or 1 bpm. Every 48 hours media discarded and 100% replaced with fresh media.

**Method B:** Each fully processed matrix was pretreated in 45 ml SMC media on a rock/rolling table at 37°C for 48 hours. In preparation for cell seeding the preconditioning media was evacuated and 2 matrices were placed in the well of a 6-well culture plate forming concentric rings to completely cover the surface of the culture plate. Cells were divided into 2 equal densities and seeded at 3 hour intervals onto the matrices surface (rotating the matrix 180° between seeding). Cell suspensions were in minimal media to enhance adhesion to the matrix surface. After two weeks in static culture (maintained using standard feeding methodologies) seeded matrices were transferred to the reactor system under sterile conditions. A flow rate of 80 bpm. (165.5 ml/min) was applied through the lumen and maintained as above in ‘method 1’.

**Method C:** Essentially the same as method 2 with the exception of placing whole cell ‘sheets’ onto the matrix abluminal surface. hVSMC cultures were bulked up in the normal fashion until cells were confluent for three weeks within T-75 culture flasks. A cell scraper was used to remove large sections of cells from the plastic in sheet form. These sheets of cells were transferred onto the matrix material and cultured in minimal media for one week prior to insertion into the bioreactor system. A flow rate of 80 bpm.



(165.5 ml/min) was applied through the lumen and maintained as above in ‘method 1’.

#### **7.2.2.7 HUVEC AND HVSMC CULTURE WITHIN THE BIOREACTOR**

All monocultures used the appropriate media, as described in chapter 2.1.3.1-2. Complete media changes were made every 48 hours by removing the reactor system from the incubator, draining the old media from the system using a separate peristaltic pump (5 rpm). Fresh, prewarmed media at 37°C (200 cm<sup>3</sup> for dual reactors and 185 cm<sup>3</sup> for single reactor systems) was progressively added to the media reservoir and pumped around the system ensuring all bubbles had been removed before sealing and replacing the unit in the 800 L capacity incubator (Cat. 394-049 Millennium XL, Jencons, Bedfordshire, UK) at 37°C 5% CO<sub>2</sub>.

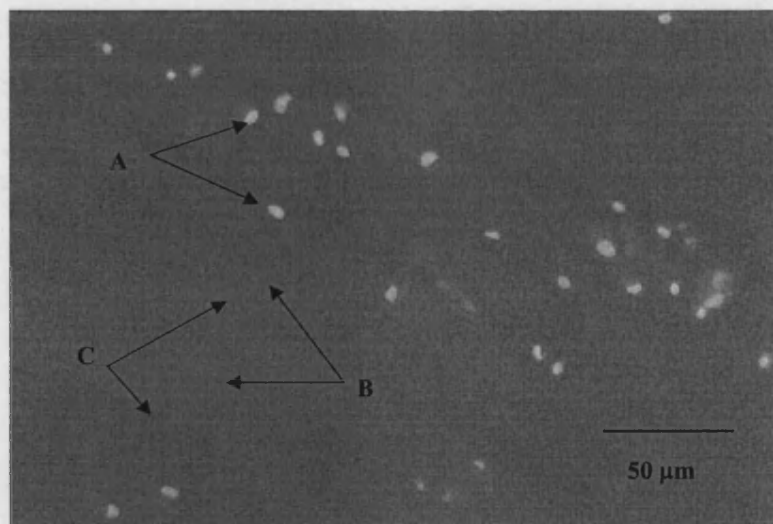
#### **7.2.3 ANALYTICAL METHODS**

All analytical methods used in this chapter including fixing cells for DAPI staining and subsequent counting are described in Chapter 2.3, Analytical Methods.

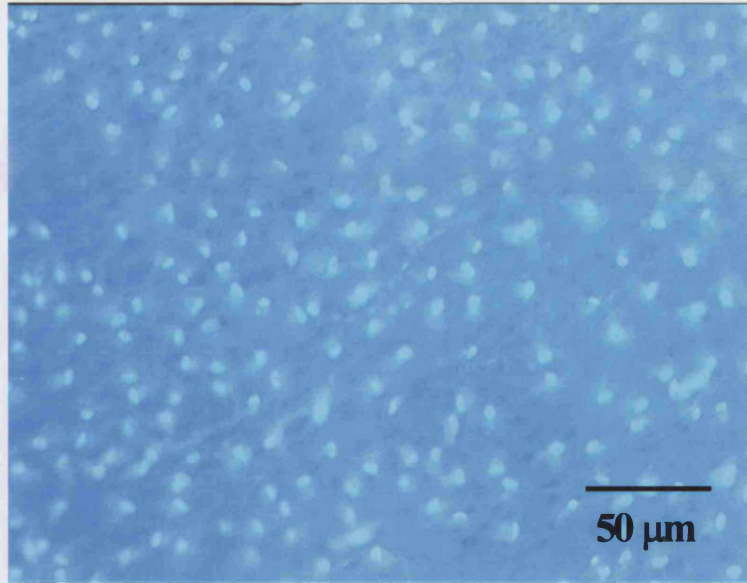
## 7.3 RESULTS

### 7.3.1 LUMEN CULTURES OF HUVEC ON THE ARTERIAL DERIVED MATRIX

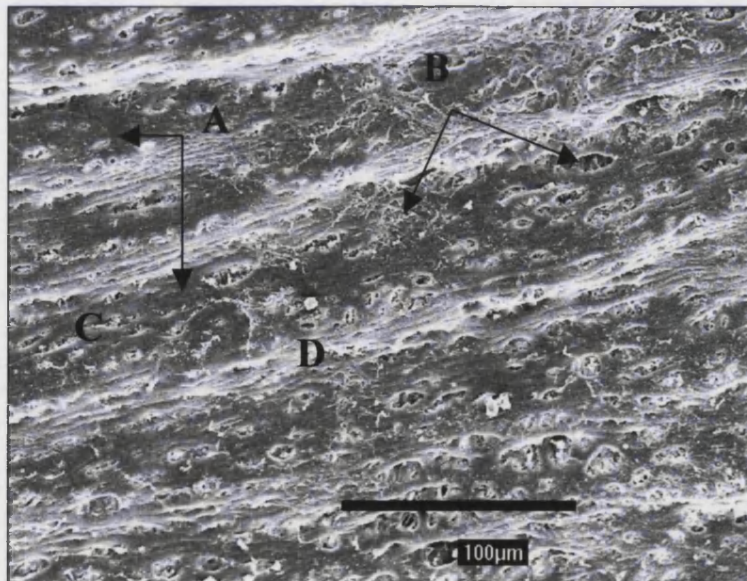
Results from the earlier tests, which did not use the compliance chamber, show minimal retention of HUVEC by the end of the flow regime (detailed in section 7.2.2.4), see Figure 7.01. The addition of a compliance chamber to smooth out the vibration in the pulsed flow further increased cell retention over the experimental time course. In both of these initial methods cells were seeded directly into the lumen, later methods that were shown to improved cell adhesion/retention, seeding methods 1-3 are detailed in Section 7.2.2. Figure 7.01 shows the remaining cells after application of the progressive flow regime where the pulse flow was applied without the compliance chamber to reduce high frequencies vibrations. Like Figure 7.01, Figure 7.02 (DAPI stained cell nuclei) and Figure 7.03 (SEM image) illustrate increased cell density on the matrix surface using application of method 3 for seeding HUVEC. Although the viability of these cells was not directly assessed, SEM images show cells of normal morphology compared to apoptotic of lysing cells



**Figure 7.01:** HUVEC adhered to the luminal surface of matrix after trial flow conditions. HUVEC were seeded at  $4 \times 10^5$  cells/ml (6 ml) directly into the matrix lumen with no rotation during initial adhesion and no compliance chamber to reduce high frequencies vibrations. Cells remaining on the luminal surface after flow (**A**) are shown stained with the nuclear stain DAPI. The undulating surface is noted with protruding sections (**B**) and recessed sections (**C**).

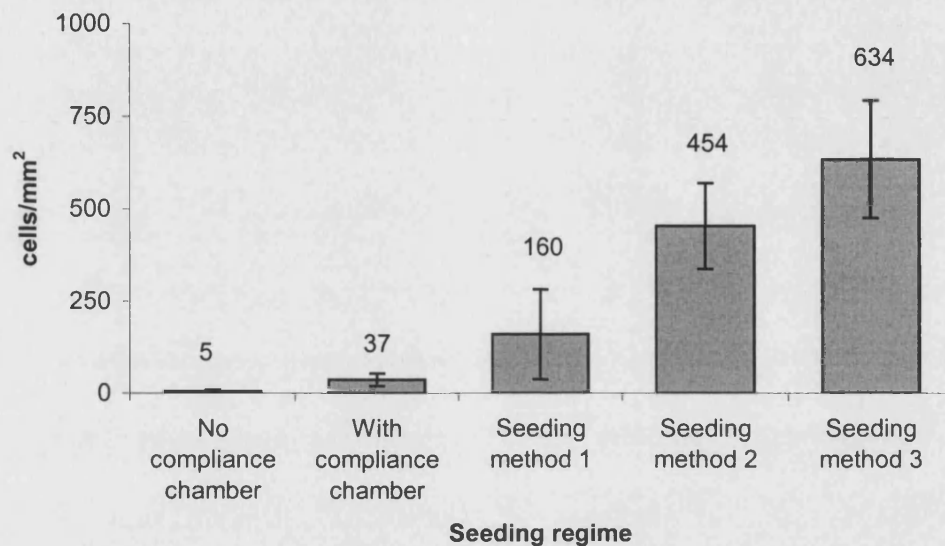


**Figure 7.02:** Improved HUVEC adhesion after modifying seeding conditions. D.A.P.I. stained HUVEC nuclei seeded at  $4 \times 10^5$  cells/ml directly into the matrix lumen using HUVEC seeding method 3. A clear visual increase in cell density is noted over Figure 7.01.



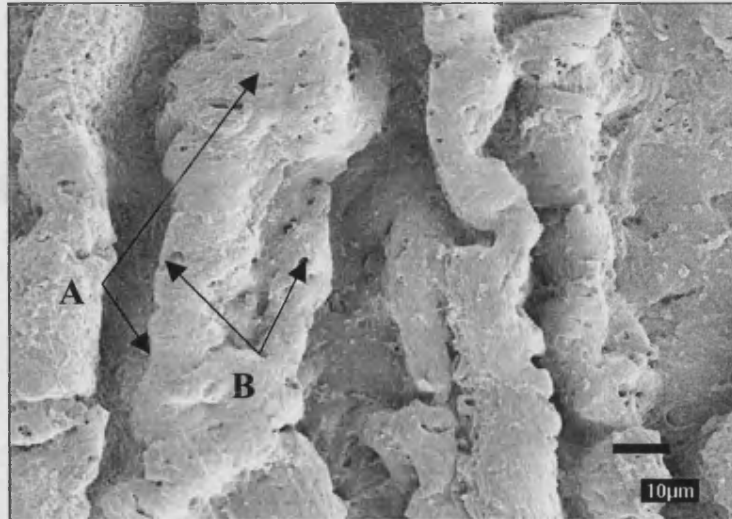
**Figure 7.03:** Improved HUVEC adhesion after modifying seeding conditions, surface analysis with LT-SEM showing matrix and HUVEC morphology seeded at  $4 \times 10^5$  cells/ml directly into the matrix lumen using seeding method 3. Cells remaining on the luminal surface (A) are shown, with sections of the matrix void of cells (B). The undulating surface of the matrix can be seen with protruding sections (into the lumen) (C) and recessed sections (D).

Figure 7.04 illustrates progression towards a confluent endothelium, where cell densities would approach 600 cells/mm<sup>2</sup> (based on cell dimensions of 20 x 30 µm) after a total culture time (each) of 10 days.



**Figure 7.04:** Quantitative analysis of improved HUVEC adhesion with variation in system and seeding methodologies. Displays increased cell densities after a total of 10 days culture (each) using different seeding methodologies and reactor/system design.

Earlier results with DAPI stained HUVEC nuclei (Figure 7.01) clearly show the presence of cells on the matrix material after cells had been exposed to pulse flow conditions for a total culture time of 10 days. Non-seeded control matrix was negative for DAPI staining. SEM images of the same matrix material were more difficult to interpret. Figures 7.05 displays a much higher degree of intimal convolutions compared to Figure 7.06, which in turn shows higher convolutions than Figure 7.07, where HUVEC had been seeded using method 3 and exposure to pulsed flow conditions as described in section 7.2.2 for a total of 10 days.



**Figure 7.05:** A SEM showing matrix and HUVEC morphology seeded at  $4 \times 10^5$  cell/ml and cultured for a total of 10 days using seeding method 3. This image displays a deeply convoluted luminal surface with HUVEC adhered (A). Gaps between cells are shown (B).

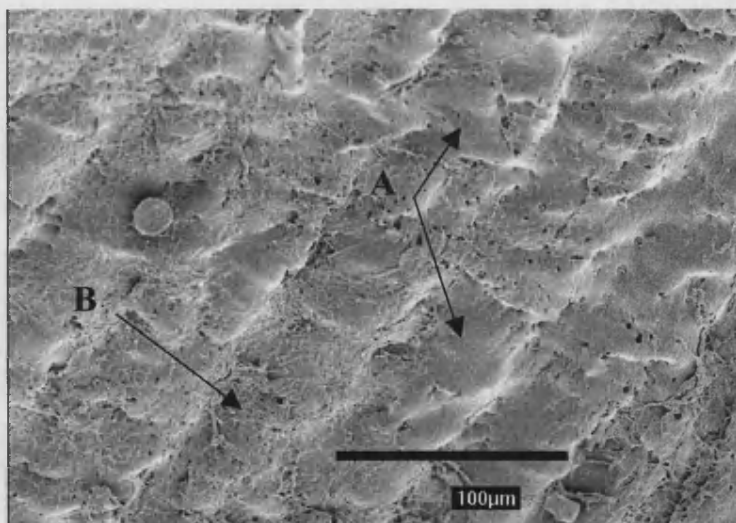


**Figure 7.06:** A SEM showing matrix and HUVEC morphology seeded at  $3.5 \times 10^5$  cells/ml and cultured for a total of 10 days after seeding using method 3. This image shows a reduction of surface convolutions compared to Figure 7.05. Smooth surface of HUVEC cells are shown (A), with areas void of cells (B).



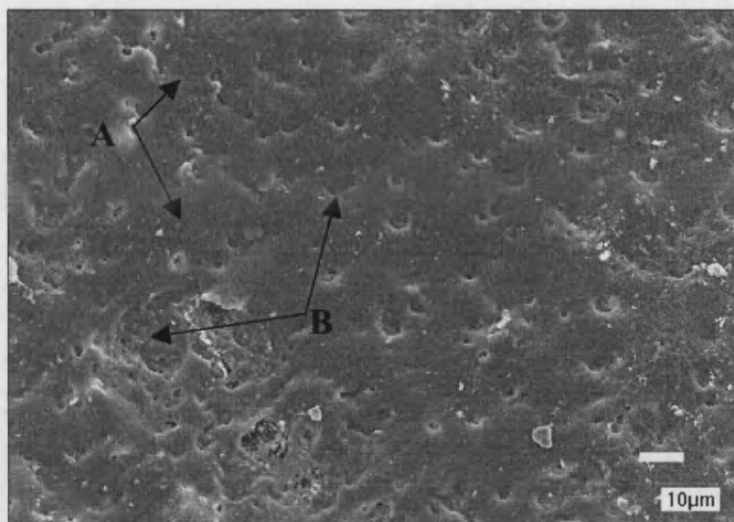


**Figure 7.07:** A SEM showing matrix and HUVEC morphology seeded at  $4.5 \times 10^5$  cells/ml and cultured for a total of 10 days using seeding method 3. This image shows a near flat surface compared to Figures 7.05 and 7.06. Smooth surface of HUVEC cells are shown (A), with gaps between cells or areas void of cells (B).

### 7.3.2 ABLUMENAL hVSMC CULTURES ON THE ARTERIAL DERIVED MATRIX

In this section of work, results from hVSMC seeding methodologies and adhesion were qualitatively assessed. hVSMC phenotype was confirmed by immunolocalisation of  $\alpha$ -actin (see Appendix A2) and analysis of cell migration and expression patterns of MMP-2 and 9 and cathepsin L was conducted. Attempts to seed hVSMC onto the matrix using method A., see section 7.2.2.6, via the abluminal port, into the abluminal void proved unsuccessful. Histological analysis displayed very few cells adhered to the matrix. It was postulated that the loose fibrous nature of the matrices abluminal surface was unfavourable as an environment for cell adhesion, particularly when submerged in media. The second seeding method, method B, was designed to allow hVSMC to be seeded onto the matrix prior to inserting the matrix into the reactor assembly. With this method a total culture time of 5 weeks consisting of 2 weeks static and three weeks under pulsed flow conditions as described in section 7.2.2.6. Figure 7.08 shows a section of matrix viewed by SEM after the total of 5 weeks culture, few cells appear viable. Although cell adhesion improved (qualitative histology), cell density remained comparatively low. The final method used was to seed or attach cell sheets onto the matrix (method C, see Section 7.2.2.6), this was used as an attempt to bind-up the

loose outer layer (adventitial) of fibrous collagens to improve cell adhesion. Figure 7.09 displays an SEM image of hVSMC taken from confluent cultures in T-75 plastic culture dishes, removed by cell scraping and laid upon the matrices abluminal surface. Cells were cultured for two weeks in static culture to allow cells to adhere then three weeks under pulsed flow conditions.

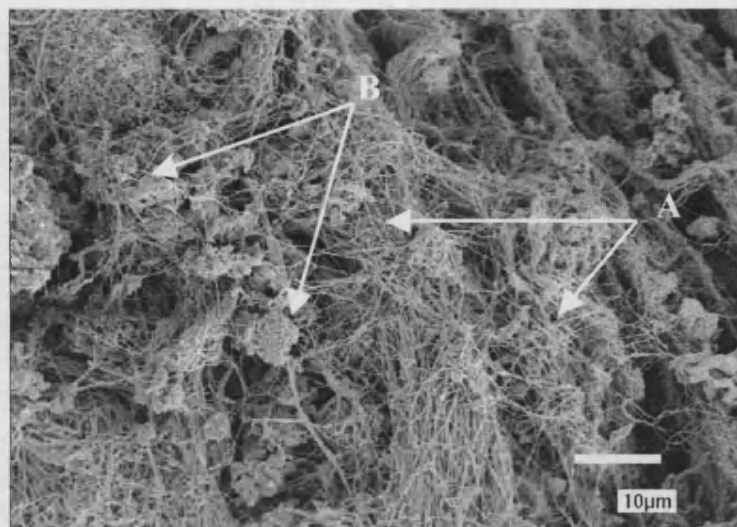


**Figure 7.08:** SEM of the abluminal surface displaying loose ECM fibres (A) of the adventitial layer with remnants of cells (B) interlaced between the fibres after 5 weeks culture.

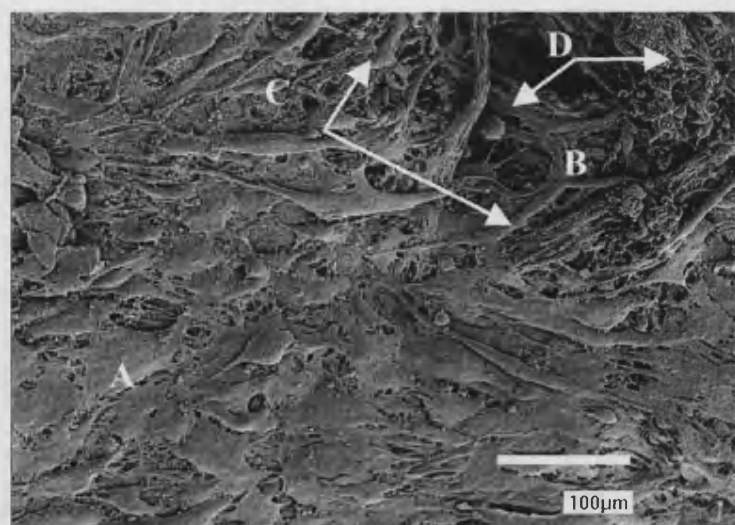


**Figure 7.09:** SEM image of hVSMC upon the abluminal surface of the matrix after 5 weeks pulsed flow culturing. Note two distinct areas, (A) confluent hVSMC (B) cell free matrix. Cells appear to be migrating from the cell sheet (C) to the acellular region. Evidence of cell debris is also noted among the loose fibres of the matrix (D).

## PHENOTYPIC EXPRESSION OF $\alpha$ -ACTIN BY hVSMC SEEDED ONTO THE ARTERIAL DERIVED MATIX

Extended cultures of hVSMC seeded onto the abluminal surface as described in Section 7.2.2. A total of approximately  $5 \times 10^5$  cells were seeded under static conditions (see Section 7.2.2.6) and cultured for two weeks prior to insertion into the reactor assembly and a further 3 weeks culture under pulsed flow. Figure 7.10 shows hVSMC migration within the adventitial layer of the matrix by counterstaining with haematoxylin. No evidence was found of cells migrating past the adventitial/medial boundary. Figure 7.10 also shows immunohistochemically labelled hVSMC for  $\alpha$ -actin from the same cultures. Cell adhesion appears to favour the outer most surface of the adventitial layer with a reduced number of cells present within the adventitial layer and none observable within the medial layer.

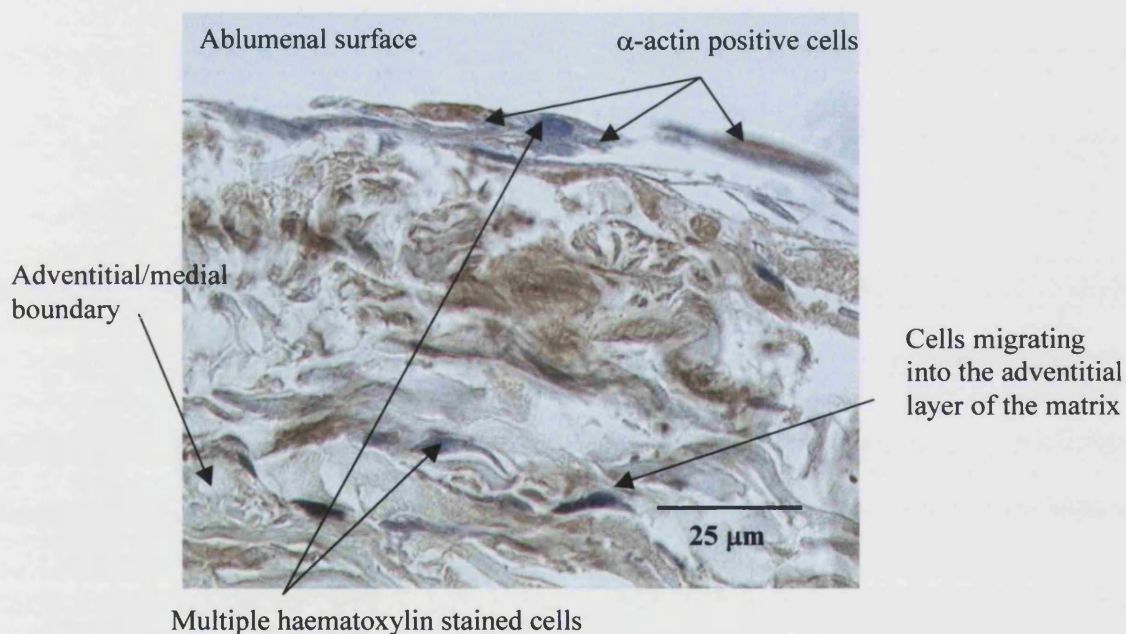


**Figure 7.10:** hVSMC were seeded at a total of  $5 \times 10^5$  cells under static conditions for two weeks onto the abluminal surface and a further 3 weeks within the bioreactor being exposed to mechanical stresses.  $\alpha$ -actin expression was confirmed by the presence of brown stained (DAB) hVSMC above. Sections were counter stained with haematoxylin to identify the location of all cells within the matrix.



### 7.3.3. ASSESSMENT OF MATRIX PENETRATION BY hVSMC

As discussed previously, a range of proteolytic enzymes: MMP-2, 9 and Cathepsin L known to be involved in the mechanisms of cell migration and matrix remodelling were assessed for expression at 5 weeks to attain an initial understanding of the expression pattern, if any, of these enzymes when exposed to mechanical stresses imposed by pulsed flow conditions transmitted through the arterial wall. Figure 7.11 is shown to provide reference to other images in this chapter to further appreciate that the adventitial layer is less structured than the medial layer and provides a different environment for cell viability.

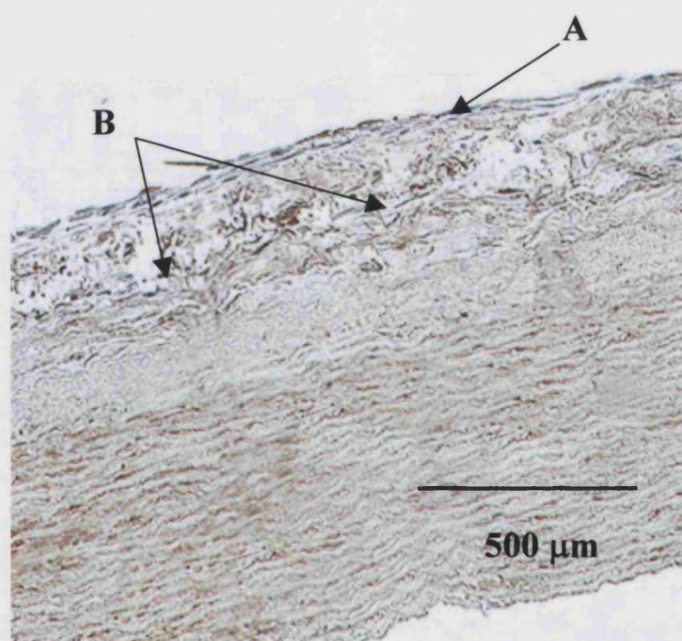


**Figure 7.11:** Cross-section of hVSMC adhesion to the adventitial surface of the matrix. Seeded at  $5 \times 10^5$  cell mm under static conditions for two weeks onto the abluminal surface and a further 3 weeks within the bioreactor being exposed to mechanical stresses. hVSMC are stained dark purple (A,B) by haematoxylin, note the layers of cells on the matrix surface (A) and the random dispersion of cells within the loose adventitial layer (B).

Similar to Chapter 5, a range of proteolytic enzymes: MMP-2, 9 and cathepsin L which are known to be involved in the mechanisms of cell migration and matrix remodelling were assessed for expression at 5 weeks. The earlier time point at 3 weeks used in Chapter 5 was omitted to give cells cultures an extended time frame to extend the opportunity for cellular migration. In this section all hVSMC were seeded or wrapped onto the abluminal surface at as cell sheets and cultured using the method described in Section 7.2.2.6, seeding method C. The exact cell density is unknown as the normal counting method was not applicable. It was estimated to be approximately 600 cells/mm<sup>2</sup>. Like the static cultures the negative controls used the same tissue sections as the immunolabelled sections, for example sections with hVSMC adhered were processed using the immunofluorescent staining protocol described in Chapter 2.3.3.6/7. The method was identical except the step where the primary antibody is incubated with the sample was omitted. This was to determine the extent of background and non-specific staining by the antibody and to ensure, with evidence from H & E sections that the localised staining is the actual enzyme targeted. As with all results in this section, the first image for each time point/enzyme is the negative control with the following image displaying the section incubated with the primary antibody.

#### **MMP-2 EXPRESSION BY hVSMC CULTURED UNDER PERFUSION CONDITIONS ON THE PORCINE DERIVED ARTERIAL MATRIX**

Figure 7.12 shows control sections of hVSMC seeded and cultured for 5 weeks on processed matrix show little background staining in the areas where hVSMC were know to reside, see Figure 7.11. Similar to static cultures the medial layer of the matrix stains non-specifically for the MMP-2 antibody in the same control sections. Figure 7.13 shows no distinct immunolocalisation of MMP-2, after 5 weeks perfusion culture was evident.

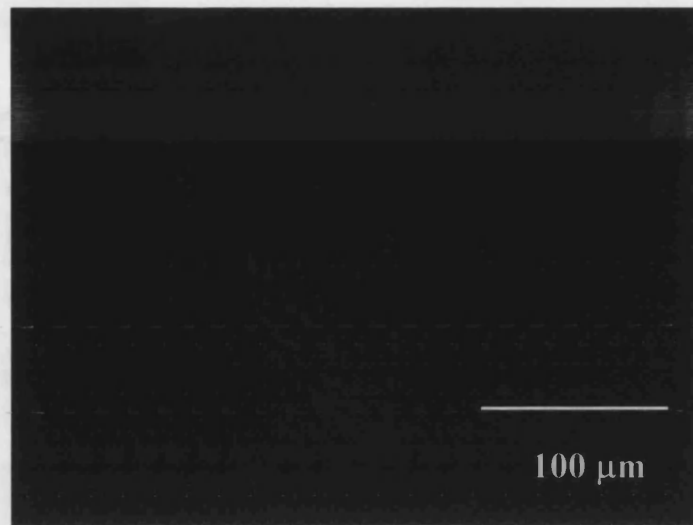


**Figure 7.12:** Control section of hVSMC seeded and cultured for 5 weeks on processed matrix and stained for MMP-2. Note minimal background staining of the medial layer (acellular), with little background or non-specific staining of the adventitial layer where the hVSMC reside.

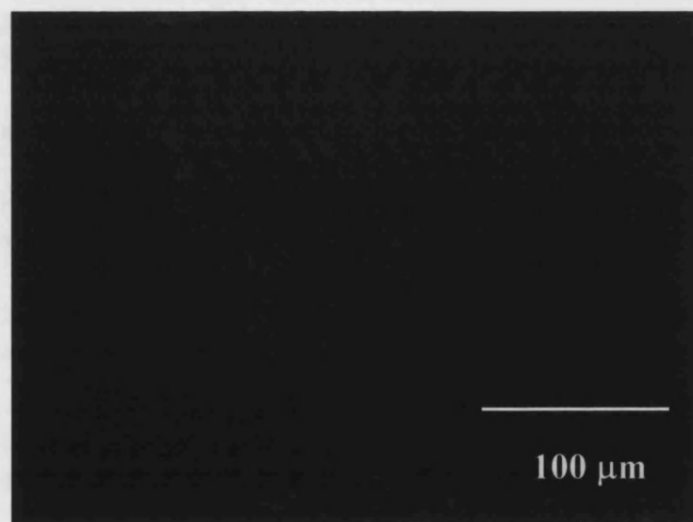


**Figure 7.13:** Matrix and cell populations staining negative for MMP-2 after 5 weeks culture.

#### MMP-9 EXPRESSION BY hVSMC CULTURED UNDER PERFUSION CONDITIONS ON THE PORCINE DERIVED ARTERIAL MATRIX

Figure 7.14 shows control sections of hVSMC seeded and cultured for 5 weeks on processed matrix show little background staining in the areas where hVSMC were known to reside, see Figure 7.11. Unlike previous controls these sections had minimal non-specific staining of the medial layer. Figure 7.15 clearly displays the positive immunolocalisation of MMP-9 in the outer adventitial layer of the matrix.

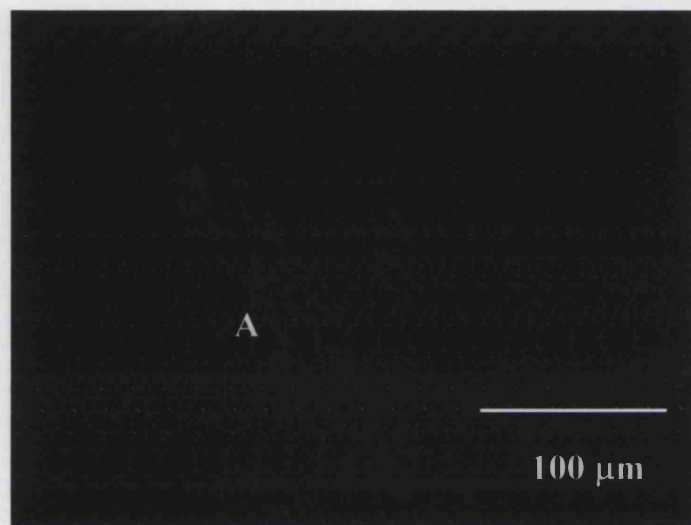


**FIGURE 7.14:** Control, no background or non-specific staining of MMP-9 in the SMC layer (A).

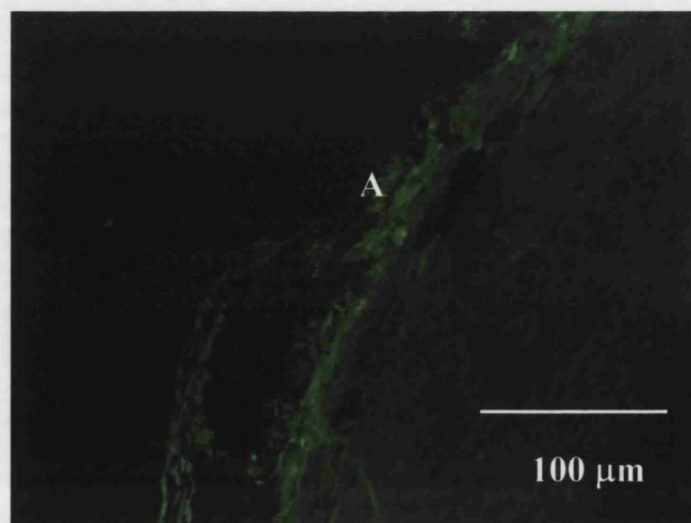


**FIGURE 7.15:** Positive immunolocalisation for MMP-9 after 5 weeks in perfusion culture (A).

#### ASSESSMENT OF CATHEPSIN L EXPRESSION BY hVSMC CULTURED UNDER PERFUSION CONDITIONS ON THE PORCINE DERIVED ARTERIAL MATRIX

Control sections of hVSMC seeded and cultured under perfusion conditions for 5 weeks on processed matrix, like previous controls where incubated without the specific primary antibody to determine background or non-specific staining. Figure 7.16 shows a control section displaying minimal background or non-specific staining within the hVSMC layer (A). Like previous controls for MMP-2 and 9, the collagen and elastin ECM (where hVSMC may reside but in low densities, see Figure 7.11) has a strong non-specific background staining. Little background or non-specific staining of the adventitial layer is noted where the hVSMC were known to reside, see Figure 7.11.

Perfusion cultures at the 5 week time point clearly show the presence of MMP-9 having been expressed by hVSMC within the adventitial layer of the matrix, see Figure 7.17. Like MMP-2 and 9 immunolocalisation of the gene product appears to be restricted to the adventitial layer of the matrix, where hVSMC reside, in this section with reduced background staining of the medial layer no distinct staining is evident in the medial or intimal layers. This data supports H & E stained sections, see Figure 7.11.

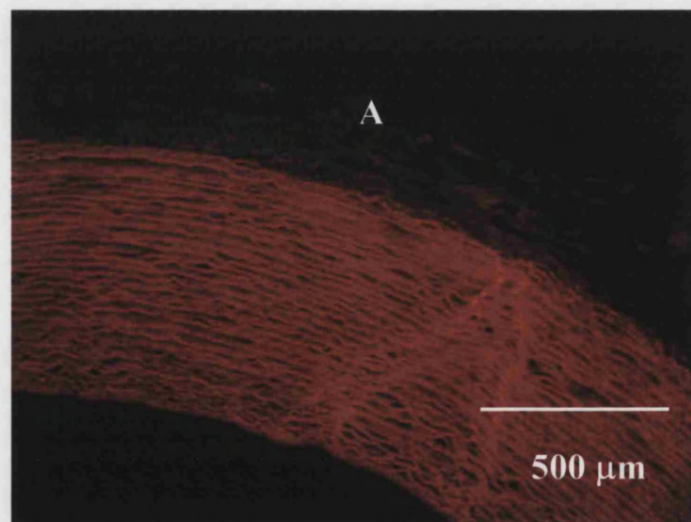


**FIGURE 7.16:** Control section of hVSMC seeded and cultured for 5 weeks on processed matrix and stained for Cathepsin L. Strong background staining of the medial layer (acellular), with little background or non-specific staining of the SMC layer (A).



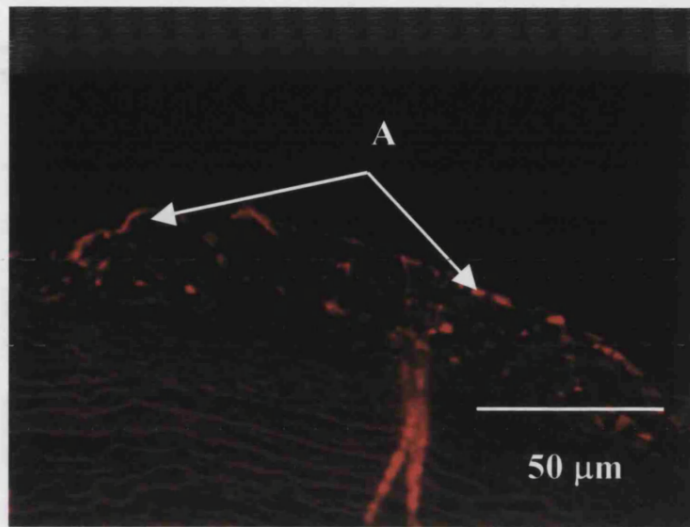


**Figure 7.17:** Sections stained for Cathepsin L after 5 weeks perfusion culture have stained strongly positive (A).

## 7.4 DISCUSSION

A vascular replacement graft that could be removed from its sterile packaging, immediately used while providing optimal biocompatibility would be the simplest and most cost effective option for vascular replacements. While manufactures of synthetic replacements work towards this goal, methodologies to enhance existing and prototype prostheses are actively researched. The advantage of autologous endothelial cell seeding is to enhance graft patency by exposing the only known 100% nonthrombogenic surface. To provide a graft with viable autologous cells to a patient in the operating theatre adds new levels of complexity to production, where cells must firstly be isolated from patient tissue (until immunologically inert cells are available for use) then grown rapidly *in vitro* prior to seeding onto the matrix and culturing under *in vivo* 'like' conditions. Once the graft has been seeded and surgically implanted, problems remain during reperfusion where the endothelial cell lining maybe stripped from the matrix wall. This is seen as one of the advantages of the tissue engineering approach where the application of a progressive flow regime (*in vitro*) to seeded and cultured EC allows acclimatization and adaptation time and facilitates endurance against the rigors of pulsed flow.

In order to seed cells onto a matrix, they must be first sourced. In this thesis human primary cells were chosen over immortalized human cell lines as they offer a phenotype/genotype closer to the patient cells. The main advantage with immortalized cell lines is consistency. These include consistently high proliferation rates and consistent phenotypic expression compared to primary cell cultures extracted from multiple human donors. This consistency allows experimental conditions to be optimised, but does not take genotypic or phenotypic variation between patients into account. Isolation of adult vascular endothelial cells in densities high enough for graft seeding are not only technically more difficult but may have a negative impact on the patient, such as removal of 'nonessential' vessels e.g. saphenous vein. Although this method is successful in isolation of EC, the question must be asked if the vessel may be better served as the prosthesis. In addition, these vessels may have been used previously in other reconstructive surgery. Other sources of EC include: microvascular endothelial cells harvested from microvessels (arterioles, capillaries and venules) found in adipose tissue (Williams et al., 1994) and extraction of EC progenitor cells from

circulating blood. The choice of SMC to seed onto the abluminal surface was simplified by the ready availability of adult saphenous vein from which hVSMC were isolated. Although slow to culture, appropriate densities were achievable for seeding purposes within 4-6 weeks of explanting tissue. In addition, variability between cell cultures adds validity to results as they are seen to more closely replicate the perceived surgical application with multiple patients and autologous cells.

Ideally, only autologous cells should be used in the final phases of graft development to ensure methodologies are repeatable with the more sensitive, adult cells. This is in reference to neonatal EC as the hVSMC are adult derived. A balance between the use of rapidly growing immortalized cell lines and the difficult to source and cultivate autologous cells from potentially diseased patients is required for research purposes. Much of the current research in Tissue Engineering have used non-autologous cells, such as HUVEC, such as bovine derived (Niklason et al., 1999; Niklason et al., 2001; Patel et al., 1988) murine derived (Kim et al., 1999) and human cell lines (Fernandez et al., 2001). These cell lineages are comparatively easier to grow and maintain in culture, unlike the fore mentioned adult human primary cells. The validity of experiments conducted with cells of this origin has been questioned. Justification for the use of these cells is that they offer a considerable advantage over human cell lines (immortal) in that they represent a more appropriate phenotype, but still have the advantage of the rapid replication associated with neonatal cells or non-human cell lineages.

Numerous techniques have been used to seed EC into the luminal surface of prosthetic devices. As described by Schmidt et al (1999) these methodologies can be divided into three main categories: 1. Gravitational 2. Hydrostatic, application of either external vacuum or internal pressure and 3. Electrostatic. Methods 1 and 2 have had reduced success due to the time required for cells to flatten and fully adhere to the surface prior to implantation. Delays of this nature during an operative procedure prior to closure are far from ideal. Application of electrostatic charges to improve EC adhesion was first applied by Bowlin and Rittgers (1997) and later described and applied by Schmidt and Bowlin (1999), electrostatic seeding, utilises the properties of ePTFE whereby the surface polarity is temporarily changed to a positive charge which attracts and speeds up a more mature HUVEC adhesion (Bowlin and Rittgers, 1997) and (Schmidt and Bowlin, 1999). The approach taken with tissue engineering, with the application of



flow would increase the time taken for graft maturation, the benefits in specific cases where time is less critical are clearly obvious. It is accepted that this is a serious limitation of the Tissue Engineering methodology.

#### **7.4.1 LUMEN CULTURES**

The vascular graft bioreactor and support systems described in this thesis was designed to allow direct seeding or inoculating cells through the shell or luminal inlet ports, using the gravitational method of seeding. An advantage of this method was a reduction in handling compared with seeding cells onto the matrix prior to assembling the reactor, which reduces the likelihood of bacterial or fungal infection. Furthermore, multiple reactors could be seeded in a single step, again minimising potential contamination. Seeding the lumen with HUVEC displayed a progressive improvement in cell retention after application of pulsed flow conditions. Initial trials where HUVEC were injected into the reactor without rotation of the reactor (to allow cells to adhere over the surface), in concert with the lack of a compliance chamber to smooth out high frequency vibrations in the flow, resulted in poor cell retention. All normal mammalian cells in tissue culture are contact inhibited, where upon contact with other cells (higher densities) remain in G1 prior to the restriction or 'start' point of the mitotic cell cycle, (Alberts et al., 1994). Amongst other reasons, contact inhibition is part of the body's self-defence mechanism against excessive or uncontrolled proliferation. EC, which grow as a monolayer, do not as a rule form 3-dimensional structures. As soon as an EC contacts other EC, proliferation ceases thus preventing layers of cells forming. Although SMC are contact inhibited they are not as strongly inhibited by cell-cell contact EC. SMC, to a degree begin to form 3-dimensional structures. This can be seen in the Appendix A2 with the formation of 'hills and valleys' characteristic of the VSMC phenotype. Earlier seeding methods where large numbers of cells were seeded directly into the lumen failed in part due to contact inhibition. As the cell suspension settles or gravitates to the bottom of the matrix, only those cells in immediate contact with the substrata (matrix) will begin the adhesion process. The remaining cells are loosely stacked and unable to adhere. With the application of flow through the lumen these cells are likely to be washed out of the system. The result illustrated in Figure 7.01 show that the only cells remaining on the matrix are those on the lower surface where

cells had initially adhered as the reactor was not rotated during seeding. The addition of a compliance chamber and reactor rotation during the seeding process (methods 1 and 2, see section 7.2.2.) significantly improved cell retention. As seen in figures 7.02, 7.03 and 7.05-07 the density of cells adhering to the matrix approach densities of a complete endothelium. Qualitative analysis showed that on average these cultures have densities a little over 1.6 times less than that of flat surface and potentially much less than a native convoluted endothelium. Estimation of the size of a HUVEC in culture is approximately  $25 \times 40 \mu\text{m}$  ( $1000 \mu\text{m}^2$ ) giving a density of approximately 1000 cells/ $\text{mm}^2$ , compared to  $634 \pm 158$  cells/ $\text{mm}^2$  of these cultures. Cross-linking collagenous matrices alters the structure of the natural matrix. This may be the basis for the differences between the theoretical and the observed cell densities per unit area.

The method described in chapter 4 was aimed at minimising structural change whilst removing immunogenic epitopes. As reviewed by Schoen and Levy (1999) some of the potential changes a matrix may incur are: cross-linking proteins, locking structures in one phase of the cardiac cycle, loss of collagen 'waviness', loosening of collagen bundles, loss of the amorphous acellular matrix and loss of compliance (Schoen and Levy, 1999). As discussed in chapter 4 this matrix has undergone most of these structural changes to a greater or lesser degree. In this section of work a far greater degree of SEM surface analysis was conducted above initial studies that obtained representative images of the matrix luminal surface. Although the initial assessment that the basement membrane remained essentially intact after processing is correct, what became apparent was variation in the luminal surfaces structural morphology after cells were seeded onto the matrix and flow conditions applied. The luminal surface of the matrix is predominantly convoluted (qualitatively) see Figure 7.07, however as shown in images 7.06 and 7.05 this varies from convoluted to wavy and a flat morphology in some areas. Areas where there is a loss of the convoluted structure of the ECM fibres are likely to strongly affect the mechanical and fluid handling properties of the matrix, as physical forces are transmitted during the pulse flow regime. Further research is required to quantify this effect if indeed it has a negative impact on graft patency.

#### 7.4.2 ABLUMENAL CULTURES

Like luminal seeding, it was envisaged that the abluminal inoculation protocol would prove successful, however, the use of this particular matrix seeding and subsequent adhesion proved problematic. As the matrix material was suspended within the abluminal cavity, the percentage cell adhesion to the matrix material was considerably lower than if cells were seeded directly onto the matrix. When cells were seeded into the abluminal void those not directly above the matrix would gravitate to the bottom of the reactor, resulting in only a small section of the matrix being seeded. To improve the seeding efficiency a number of methods were assessed, including: variation in seeding densities and periodic rotation of the reactor/s about their longitudinal axes. Histological and SEM analysis of the 'seeded' matrices after 7 day culturing had shown that these methods failed to improve cell adhesion onto the matrix, and few cells had adhered to the matrix, (see Figure 7.09). This initial experiment was designed to evaluate seeding efficiency of cells seeded directly into the abluminal void with a preconditioned artery present, without any material, such as Poly-HEME present on the reactor wall to prevent cell adhesion. Poly-HEME or poly (2-hydroxethylmethacrylate) has been used widely as a coating to prevent cell adhesion. Folkman and Moscona (1978) used poly-HEME to observe the relationship between cell shape, DNA synthesis and growth in cells by coating plastic culture plates with varying thickness of poly-HEME (Folkman and Moscona, 1978). Although coating the inside of the glass reactor with poly-HEME and rotating the reactor to improve adhesion was considered, it was found that the main issue with seeding cells onto the abluminal surface was not limitations with initial adhesion. As mentioned above, densities as high as  $4 \times 10^6$  cells were injected into the abluminal to literally flood the matrix with cells. After histological and SEM analysis little differences were noted other than an increase in cell debris among the adventitial fibres on the abluminal surface. Assessment of these results indicated a need for a fundamental change in seeding methodology. It was predicted that the problem was not one of biocompatibility with the matrix surface as static cultures had shown positive cell adhesion, growth and proliferation, but the way in which the surface was presented to the cells in free suspension. When supported in the reactor, collagen fibres on the matrices abluminal surface literally 'float' in the media within the abluminal void. Thus, the surface is not stable or static enough for

cells to adhere. In order to improve this each matrix was seeded outside the reactor in tissue culture plates, as described in section 7.2.2. Although an improvement was noted, the fibres were still essentially in free solution and each time the media was changed (every 48 hours) these fibres were disrupted. The use of method three for abluminal seeding was designed to bind up the loose fibres by seeding down not cell suspensions, but sheets of cells wrapped around the matrix. The method, described in section 7.2.2 was not fully optimised but results show that the cell sheets adhered well to the matrix and layers of viable layers are present. Figure 7.10 shows an SEM image of the cell layer bordering an acellular region of the matrix. The positive result is clear compared to cell seeded as a suspension either into or in static culture, as illustrated in Figure 7.09. Histological analysis of 5  $\mu$ m haematoxylin stained sections show, like static cultures presented in Chapter 5, that some areas of the matrix displayed a capacity to maintain the phenotypic expression of  $\alpha$ -actin, contrasting static cultures where expression is lost over time, see Figures 7.11-2. Figures 7.11 and 7.12 typify the migration pattern of hVSMC cultured under these conditions. Cells remain as a sheet of multiple cell layers on the extremity of the abluminal surface, displaying some migration into and up to the adventitial-medial boundary.

The ultimate purpose of seeding hVSMC onto the abluminal side of the matrix is to fully populate the medial layer of the matrix with functional SMC. Static cultures have shown the inability of hVSMC to migrate through the matrix, while samples grown under pulsed flow conditions follow a similar pattern. Analysis of a representative group of matrix remodelling enzymes was conducted to determine if cells were expressing the matrix-degrading enzymes whether they were migrating.

An inherent lack of chemical or physical signals 'instructing' cell/s to migrate would result in cells remaining in a similar region (other than proliferative expansion) to where they were seeded. One would expect that if the cellular machinery is activated to express these enzymes then a stimulation to migrate would be provided to the cells. It can therefore be speculated, that if the cells are unable to penetrate the adventitial-medial boundary it is because they are unable to break down the bonds holding the ECM components, together which prevents migration. Static cultures have shown that hVSMC seeded or adhered to the *cut surface* of the matrix migrate along (not through) the matrix fibres into the vessels medial layer. hVSMC seeded onto the surface of the

matrix were unable to migrate, via degradative mechanisms associated with the presence of the above mentioned matrix remodelling enzymes. By the very nature of cross-linking and the methods used to determine cross-linking efficiency to stabilize proteins against enzymatic degradation, it is not surprising that cellular migration across ECM is not observed. Methods to test the effectiveness of cross-linking have used collagenase or pepsin to degrade the ECM and either colorimetric or RP-HPLC to quantify soluble by-products such as hydroxyproline. Studies in Chapter 4 have shown this matrix has a three-fold increase in resistance to pepsin digestion over non-cross-linked samples.

Similar to the static cultures of chapter 5, several enzymes involved in matrix remodelling were immunologically detected to determine their expression and potential effectiveness at degrading the cross-linked matrix. Chapter 5 concluded that under static culturing conditions MMP-2 and 9 were expressed at both 3 and 5 week time frames, with Cathepsin L only being expressed at 5 weeks. Under pulsed flow conditions, expression of MMP-2 was not evident at 5 weeks while both MMP-9 and Cathepsin L were strongly expressed. The main role of Cathepsin L is within the cellular lysosome system for protein degradation. As discussed in chapter 5 the understanding of cathepsin L with regard to its role outside cellular lysosomes is not fully understood. Kirschke et al (1998) and Turk et al (2000) support the evidence found here that cathepsin L is expressed both intercellular and extracellularly (Turk et al., 2000) and (Kirschke and Barrett, 1998). The difference here is that firstly hVSMC are expressing the enzyme and secondly expression is in a “foreign” environment. Cathepsin L has a variety of functions outside the cell including: degradation of basement membranes, elastin, fibronectin and collagens all of which are present in these cultures. Optimal pH ranges between pH 3 and 6, indicative of the acidic lysosomal environment cathepsins are normally associated. This may mean reduced extracellular activity unless; acidic microenvironments exist, the enzyme is post-translationally modified to increase its activity outside the cell. Conversely the reduced extracellular activity/active life span is part of the control mechanism for these potentially dangerous enzymes when outside the protective walls of the lysosome. It is difficult to determine if expression is increased between static and flow cultures due to differences in density, however these preliminary results indicate some factor has induced a higher expression, with physical forces acting on the cells being a likely cause. It is clear that there is

differences in expression patterns between the static and pulsed flow cultures. It is difficult however to draw firm conclusions from the data due to differences in seeding methodology and the density.

It was hypothesized that the application of pulsed flow would provide the mechanical signals required for hVSMC to express a barrage of proteolytic activity, and to allow cells to effectively migrate through the matrix. Either the stimulation to migrate was ineffective or the matrix is extensively cross-linked whereby seeded hVSMC are unable to migrate into the medial section. Analysis of MMP-2, 9 and cathepsin L has shown the enzymes are expressed indicating an attempt to remodel the matrix, but neither activity nor concentrations are quantifiable. Based on hVSMC normal proliferative rate in static culture it was expected cell densities would be considerably higher than a layer of cells 2-3 deep over the adventitial surface after 5 weeks culture. Glucose, pH and gas analysis show that the culture parameters are not limiting and range from static conditions to physiological *in vivo* conditions. The most likely conclusion that can be drawn from the inability of cells to migrate into the medial layer is that the tissue is over cross-linked. It is important to note that both static and pulsed flow cultures of hVSMC were conducted as mono-cultures, that is hVSMC were the only cell type present. In normal vascular physiology the two main cell types present are hVSMC and EC and communication between is a requirement to normal function. It is possible that co-culturing hVSMC with HUVEC in the reactor system may provide the EC with a stronger chemical signal that would induce the expression of other proteolytic enzymes, such as MMP-1,8 and 13 (specific collagenases) not analysed in this study. Further studies are required to determine which of these hypotheses are correct.

The aim of this section of work was to develop an understanding of the comparative differences between the results gathered in Chapter 5, which assessed the developed matrix in terms of biocompatibility under simple static *in vitro* conditions and results in this chapter, application of mechanical forces such as fluid and mechanical shear stresses to the matrix and cell populations.

Seeding HUVEC into the lumen of the matrix and exposing them to a prescribed flow regime has shown a progressive increase in cell adhesion as the system was modified. Final densities remain below that of a confluent endothelium. Continued system

development is likely to improve this issue. hVSMC adhesion to the abluminal surface follows a similar prescription to HUVEC seeding, where progressive system and protocol development has shown that a continuous layer of cells on the abluminal surface is possible. Unfortunately, it was not possible to seed cells directly into the abluminal void and achieve high adhesion efficiencies due to the fibrous nature of the matrices abluminal surface.

Given the range of ECM components capable of being degraded by the two matrix metalloproteinases and cathepsin L chosen for this study, see Figure 5.01, it is not surprising that these enzymes are indeed being expressed. The lack of MMP-2 maybe explained as a temporal expression whereby signals for its transcription are blocked by feed back signals. It can be concluded that the altered structure, by means of exposure to the numerous processing steps, particularly cross-linking of the matrix prevents cell migration into the medial layer. This is a critical aspect of this project and further study is required to determine if reduced exposure to the cross-linking step may allow cell to migrate freely through the matrix. A high level of matrix cross-linking confers resistance to enzymatic degradation and increased biocompatibility prevents cells from migrating freely into the matrix. Conversely reduced cross-linking results in a matrix that is susceptible to degradation *in vivo* and is more likely to be recognised as 'foreign' when implanted. It is essential that a balance between stability, biocompatibility and allowance for cell migration be met if the aim remains to fully populate the medial layer with VSMC.

The likely consequences of reduced migration into the medial layer and thus out of effective communicative range of the endothelium is reduced control of both VSMC and EC growth and proliferation. Co-cultures within the bioreactor system will be an important aspect of future studies to determine the effectiveness of this processed matrix in allowing cellular migration and matrix remodelling, resulting in a physiologically competent graft suitable for vascular reconstructive surgery.

## CHAPTER EIGHT: CONCLUSIONS AND FUTURE WORK

### 8.1 CONCLUSIONS

Progress towards a tissue engineered small diameter vascular graft began with the use of porcine derived dermal collagen as a matrix material; supplied in sheet form, see Chapter 3. Results have shown that this matrix (after extensive washing to remove residual cross-linking chemicals) supports primary human cell adhesion growth and proliferation. Preparation of the matrix by means of incubation in cell culture media has been shown to improve cell-matrix biocompatibility, as does treatment by modification of the ECM proteins with chemical treatments, such as NaOH, see Chapter 3.3.3. However the material was not found to be an ideal matrix material for the development of a tissue engineered vascular graft. By comparison to a native artery, the sheets of collagen would require fashioning into a tube, creating a longitudinal ridge (0.75 mm) within the matrix lumen that is likely to detrimentally affect flow dynamics and thus EC adhesion. In addition, further handling of the material increases the potential for graft infection. Both experimental and cited literature have shown that cross-linked matrices are resistant to host degradation, an attribute desired in bioartificial heart valves where degradation may result in failure. The object of the tissue engineering approach is to allow the graft to remodel using the matrix as a platform to guide cellular growth and development into a functional shape/organ. For remodelling to occur cells must be able to digest matrix components, freeing the way for cells to migrate into the matrix, thus populating the full thickness of the graft. This is one of the design objectives to ultimately confer vascular tone by attaining a high density of VSMC throughout the medial layer of the matrix. Extended cultures on the dermal collagen matrix have shown the inability of human primary fibroblasts to migrate into the tissue suggesting, like other chemically cross-linked matrices, that excessive stabilisation was the reason for this effect.

In seeking an alternative matrix material for use as a small diameter vascular graft, several options were considered, including the alternative of full synthetic materials. As biological materials can offer superior mechanical properties compared to synthetic



matrices the potential for maintaining the *in vivo* cell phenotype is increases. This is due to a closer replication of a more natural *in vivo*-like environment. Further, previous experimental knowledge working with biological biomaterials contributed to the selection of porcine carotid arteries as a starting material for matrix preparation.

After treatments the porcine derived arterial matrix described in Chapter 4 has a reduced lipid and protein content compared to unprocessed tissue, with the bulk of the cellular components removed. The effect of cross-linking the matrix has increased its mechanical strength in terms of burst pressure and ultimate failure (stress/strain), whilst retaining a similar structure and ECM morphology to the native artery. The processing methodology preserves the bulk of the basement membrane and internal elastic lamina, central to maintaining the matrices mechanical and cell adhesion properties. The internal elastic lamina has also been suggested to act as physical barrier to prevent the migration of hVSMC into the vessels lumen, which would otherwise result in intimal hyperplasia. The effect cross-linking and ethanol treatment has on the matrix with regard to immunogenicity and resistance to calcification are theoretical and based on literature cited within the chapter, further studies are required to ascertain the effectiveness of these and other combined treatments.

An assessment of the processed porcine matrix described in Chapter 4, in terms of compatibility with primary human cell lineages (HUVEC and hVSMC), was conducted under static culture conditions in Chapter 5. Unlike the dermal collagen matrix used in Chapter 3, HUVEC remained adhered to the matrix after 9 days static culture when used directly from the final processing step. Initial compatibility tests concluded that pre-treatment of the matrix after processing and washing in H<sub>2</sub>O was essential to attain efficient adhesion of HUVEC under static conditions. Under static conditions DMEM basal media was chosen due to its low cost and that it provided no significant advantage over the substantially more expensive cell specific medias. Due to the restrictive depth-of-field of the analytical technique used and the 3-dimensional structure of the matrix, no conclusions could be drawn from abluminal seeding of hVSMC, other than cells had adhered and were maintained up to 5 weeks in culture, as assessed by H&E, DAPI staining. Extended culture of hVSMC on the arterial derived matrix appears to offer a stable environment conducive to cell maintenance with no evidence of the matrix cytotoxicity displayed with the former porcine derived dermal matrix.

Immuno-localisation of MMP-2 and 9 and cathepsin L proteases within the matrix clearly identifies expression of these matrix remodelling enzymes by hVSMC under static culture conditions. Based on the inability of hVSMC to migrate into the matrix medial layer other than by the cut edge of the matrix, it was concluded that the adventitial/medial boundary acts as a physical barrier to cell migration. The mechanism preventing cell penetration was not clear; as no chemical or mechanical stimuli was applied, it is possible there was no driving force for migration, however cell migration via the matrix cut edge does imply that the necessary stimuli was provided. As shown in Chapter 4.3.3 the matrix is stabilised against pepsin digestion as a result of the cross-linking process. This would indicate, in concert with extended cultures of hVSMC, that once cells have migrated through the adventitial layer up to the medial boundary they were unable to migrate further into the matrix as the dense fibrillar medial ECM poses as a barrier to migration as direct result of cross-linking the matrix. When a matrix is not cross-linked cells from surrounding tissue are able to migrate fully into a similar matrix (Clarke et al., 2000).

In Chapter 6 a perfusion bioreactor was designed and implemented in concert with a pulsed flow system that aimed to deliver to the matrix, sealed within the bioreactor, conditions that simulated the *in vivo* peripheral arterial environment. The first aim was to generate appropriate mechanical forces and transmit them to the bioreactor while simultaneously allowing sampling and media changes. Secondly the bioreactor was required to allow direct cell seeding into both the luminal and abluminal cavities, with the support infrastructure allowing long-term, sterile culture of human primary cell cultures.

These objectives were complex and compromises were required to achieve certain goals. For example system design, with regard to on-line monitoring, was limited to ensure the unit was useable and transportable to a sterile facility for routine cell culture maintenance. As a conclusion to this section, all of the major tasks to develop a workable reactor and support infrastructure have succeeded. The perfusion system generates a user defined pulsed flow with waveforms and pressures similar to *in vivo* haemodynamics. Similarly the Mark 4 bioreactor allows for the delivery of nutrients and extraction of by-products, including gasses. Although not quantified, the reactor by

design is likely to deliver uniform transmembrane/matrix pressures that have allowed hVSMC to remain viable within the matrix wall, inside the 100  $\mu\text{m}$  cell in-growth limit, whilst shown to maintain strict sterile conditions.

The aim of Chapter 7 was to develop an understanding of the comparative differences between the results gathered in Chapter 5, which assessed the porcine derived arterial matrix in terms of biocompatibility under static *in vitro* conditions, and results from perfusion bioreactor studies in this chapter, where mechanical forces such as fluid and mechanical shear stresses were applied to the matrix and cell populations. Seeding of HUVEC into the lumen of the matrix and exposing them to prescribed flow regimes has shown a progressive increase in cell adhesion as the system was modified. Final densities remain below that of a confluent endothelium. Continued system development is likely to improve this issue. hVSMC adhesion to the abluminal surface follows a similar pattern to HUVEC seeding, where progressive system and protocol developments have shown that a continuous layer of cells on the abluminal surface is possible. Unfortunately, it was not possible to seed cells directly into the abluminal void and achieve high adhesion efficiencies due to the fibrous nature of the matrices abluminal surface. The final method of hVSMC seeding (method C) to the abluminal surface applied cell sheets and a period of static culture to allow cells to adhere. This methodology was successful in stabilising the free fibrous nature of the matrices outer abluminal surface by allowing hVSMC to adhere to the matrix. Either extended cultures or reduced cross-linking may allow cells to migrate further into the matrix.

Studies in Chapter 5 and 7 have shown a range of matrix degrading enzymes are expressed by hVSMC under both static and perfusions culture conditions. Both MMP-9 and cathepsin L displayed the same expression pattern under both static and perfusion culture, where there is a qualitative increase in expression in the perfusion cultures after 5 weeks culture. MMP-2 was strongly expressed in 3 and 5 week static cultures but was not localised in 5 week perfusion cultures. In terms of cell expression patterns, little can be concluded from the observed data, other than there appears to be a temporal change in expression (MMP-2 / 9). Given further resources, a more restrictive study over defined time points would help elucidate this variation. In addition to these and other results, it was concluded that the altered structure of the matrix prevents cell migration into the medial layer. This is a critical point with the project and further study is

required to determine the steps required to allow cells to migrate freely through the matrix. Again, it must be noted that the ability for cells to freely migrate means that the matrix is susceptible to degradation *in vivo*. It is essential that a balance between stability, biocompatibility and allowance for cell migration be met if the aim remains to fully populate the medial layer with VSMC.

## **8.2 FUTURE WORK**

Future work has been subdivided into 3 sections each outlining a research objective by identifying issues that may lead to a more complete understanding of why small diameter grafts fail, followed by experimental methodologies to further develop the process of tissue engineering to overcome these problematic issues.

### **8.2.1 BIOMATRIX UNIFORMITY**

Any developed tissue engineered product must meet strict parameters in order to be issued licence for human implantation. One of those requirements is that the product must be uniform with limited variation between each individual product. Inherent in biological systems is the fact that they are non-uniform. This issue became obvious during the extraction process at the abattoir, although all animals were of the same age and breed, variation in carotid arteries usable length (range ~50-130 mm) vessel wall thickness (range ~ 0.8-2.5 mm) and taper over the usable length (range 9.5- 4 mm OD) added to compound the issue. As discussed in Chapter 4, the first step in the process was to narrow the potential range of variation by the initial selection process at the abattoir. Although the arteries selected for processing were within a given dimension range the observed variation at the macroscopic level is indicative of the variation that is likely to occur at the microscopic and molecular level.

The problem of uniformity or lack of it is yet to be resolved; if a methodology is to be pursued further these issues must be addressed and logical steps taken to ensure product homogeneity.

A list is shown below that pinpoints process steps requiring modification in order to produce a more uniform product.

Tighten initial vessel selection criteria

Adventitial ECM to be removed using a dissection microscope: to reduce damage to the medial layer and produce a more uniform excision of surrounding connective tissue layer, identification of arterial flaws such as disease and to aid the vessel selection to reducing variation

Cross-linking carried out within the reactor system using a motorized revolving system to confer 360° rotation and uniform cross-linking of vessel surface

Optimise cross-linking duration to ensure the balance between reduced immunogenicity and cell migration and establish light penetration into tissue, i.e. is the tissue more heavily cross-linked on the vessels surface than the lumen?

Seeding both EC and hVSMC to be carried out within the revolving reactor, where cells are prevented adhering to the glass reactors abluminal and adhere uniformly on the appropriate surface, e.g. EC lumen and hVSMC the abluminal surface.

Optimise flow conditioning for EC retention

Although far from a complete list of modifications to the system/process design, if these things are carried out a more uniform product is likely to result. It is unlikely that a 'one-fit-system process' will solve the problem due to tissue variation irrespective of the initial selection process, unless the processing method is changed from the system described herein.

### **8.2.2 DEVELOPMENT OF A VARIABLE PULSE FLOW MODEL**

Changes in cellular phenotype and chemical responses as a result of physiological stresses, such as pressure, pulse and shear conditions have received considerable attention in the last two decades. Most if not all studies have focused on phenotypic changes to cells under a predefined flow protocol (often linear) that encompasses an initial flow regime to prepare cells for a primary flow rate that approximates a single physiological flow condition. It has become clear that in order to replicate a true *in vivo* cellular phenotype in an *in vitro* model, the application of a variety of growth factors alone is not enough. The mechanical or physical conditions cells are exposed to is

critical in the maintenance of the *in vivo* phenotype.

In this series of studies, it is proposed to develop a physiological flow regime that fluctuates as a normal (or diseased) heart, altering pulse rate and associated pressure changes in concert with modulation of peripheral vascular tone. A number of questions require answering. Is any change in cell phenotype or gene expression noted when comparing the proposed dynamic perfusion system to non-pulsed or a single pulsed flow regimes? Is any variation noted in cell densities, particularly SMC? For example VSMC density is an important aspect of tissue engineered vascular prostheses to confer vascular tone and allow the matrix to remodel ECM components giving the ability to withstand arterial pressures. Particularly important is the expression of matrix components, such as collagen and elastin, essential if the matrix is degraded over time. Studies required to answer these questions would include modelling heart and vascular haemodynamics, where pulse, flow and pressure data (over time) from a number of appropriate adults is collected and used to define a programme that models real time vascular haemodynamics. Development of a pulsed flow system to mimic 'real time' vascular haemodynamics, where the pump and reactor systems will allow fully developed flow conditions and be computer monitored and controlled throughout all stages, from cell seeding to flow modulation. The choice of matrix material will be fundamental as results and performance vary considerably from one material to another. Finally all these studies would need to be integrated to produce a generic methodology for perfusion cultures that incorporates the dynamic flow system with the perfusion bioreactors conferring reproducibility, with design strategies for scaling up the process.

Key steps include the development of a pump, pump-head that can produce physiological pulse pressures waves at prescribed frequencies that models normal and diseased vascular systems. A computer programme designed to incorporate data from the modelling of physiological conditions that can control pump output and frequency. Added to this, bioreactor design, development and integration to realise the desired pressure and pulse wave conditions prescribed from physiological modelling. This brief overview is obviously not one project but a series of studies that can be used in concert to develop a model system for continued research. These projects are not limited to vascular studies but can be integrated into all areas of tissue engineering.

### 8.2.3 DEVELOPMENT OF A SECOND GENERATION MATRIX

This thesis has described the use of established tissue engineering and biochemical principles to progress our knowledge towards a biocompatible nonthrombogenic small diameter vascular graft. It is now possible to critically assess the initial findings and fully optimise the graft preparing it for *in vivo* modelling. To achieve this, an assessment of cell adhesion, growth, proliferation and the maintenance of cell specific phenotype would be required. In combination with aspects from Sections 8.21 and 8.22, the product may be optimised to allow the matrix to be fully remodelled conferring full functionality, where the graft is capable of regulating vascular tone and maintaining the integrity of the endothelial layer. With respect to the prototype porcine vascular graft a 'second generation' graft would be developed to generate a unique product that would preferentially use autologous cells.

The experimental programme would consist of 4 major section of work. The first stage would entail optimisation of the solvent and enzyme extraction steps leading to not only complete removal of undesirable non-structural ECM components but to an efficient process in preparation for a potential scaling up for industrial application. The second section of work, once process optimisation is complete would be characterised with reference to:

Histological appearance and structural analysis

Maintenance of cellular phenotypes

Strength and elasticity in relationship to cell density

Cell proliferation rates, both EC (time to achieve confluence) and hVSMC with relevance to intimal hyperplasia.

Once the graft has been fully characterised in terms of content (protein, lipid, carbohydrates etc), the abluminal and luminal surfaces would need to be assessed under perfusion conditions to allow efficient adhesion, growth and proliferation of cocultured primary EC and VSMC. A reduction in graft lead time (reduction in the time required for the culture phases of the tissue engineered graft) is crucial if this technology can be employed in situations where patients require urgent treatment.

The perfusion culture system would ideally be fine-tuned to match more closely arterial pulse, pressure and optimisation of PO<sub>2</sub>, PCO<sub>2</sub>, pH and other *in vivo* biochemical parameters, with the degree of cross-linking optimised to allow cell migration whilst maintaining biocompatibility. Once characterisation is complete, the final step is to test with an *in vivo* animal model, followed by scale up for clinical trials (~3 years from start date).



## REFERENCES

- Alberts, B., Bray, D., Lewis, J., Raff, M., Roberts, K., and Watson, J. D. (1994). "Molecular biology of the cell." Garland Publishing, Inc., New York.
- Antiplatelet Trialist's Collaboration (1994). Collaborative overview of randomised trials of antiplatelet therapy-II: Maintenance of vascular graft or arterial patency by antiplatelet therapy. *British Medical Journal* **308**, 159-168.
- Bader, A., Schilling, T., Teebken, O. E., Brandes, G., Herden, T., Steinhoff, G., and Haverich, A. (1998). Tissue engineering of heart valves - human endothelial cell seeding of detergent acellularized porcine valves. *European Journal of Cardio-thoracic Surgery* **14**, 279-284.
- Badylak, S. F., Liang, A., Record, R., Tullius, R., and Hodde, J. (1999). Endothelial cell adherence to small intestinal submucosa: an acellular bioscaffold. *Biomaterials* **20**, 2257-2263.
- Badylak, S. F., Record, R., Lindberg, K., Hodde, J., and Park, K. (1998). Small intestinal submucosa: a substrate for in vitro cell growth. *Journal of Biomaterial Science. Polymer edition* **9**, 863-878.
- Bank, R. A., Jansen, E. J., Beekman, B., and te Koppele, J. M. (1996). Amino acid analysis by reverse phase high-performance liquid chromatography: Improved derivatisation and detection conditions with 9-fluorenylmethyl chloroformate. *Analytical Biochemistry* **240**, 167-176.
- Belden, T. A., Schmidt, S. P., Kalkow, L. J., and Sharp, W. V. (1982). Endothelial cell seeding of small-diameter vascular grafts. *Trans. American Society Artificial Organs* **28**, 173-177.
- Bellincampi, L. D., and Dunn, M. G. (1997). Effect of cross-linking method on collagen fiber-fibroblast interactions. *Journal of Applied Polymer Science* **63**, 1493-1498.
- Berglund, J.D. and Nerem, R.M. (2002). Towards the development of a biological tissue engineered vascular graft: incorporating intact elastin scaffolds into collagen based constructs (abstract). *Cardiovascular Pathology*. **11**, 35.
- Berne, R. M., and Levy, M. N. (1992). "Cardiovascular Physiology." Mosby Year Book, St. Louis.
- Best, C. H., and Taylor, N. B. (1991). "Best and Taylors physiological basis of medical practice." Williams and Wilkins, Baltimore, MD 21202, USA.
- Birukov, K. G., Shirinsky, V. P., Stepanova, O. V., Tkachuk, V. A., Hahn, A. W. A., Resink, T. J., and Smirnov, V. N. (1995). Stretch effects phenotype and proliferation of vascular smooth muscle cells. *Molecular and cellular biochemistry* **144**, 131-139.
- Blakemore, A., and Voorhees, A. B. (1954). The use of tube made of Vinyon 'N' cloth in bridging arterial defects: experimental and clinical. *Annals of Surgery* **140**, 324-334.
- Bodnar, E., Olsen, E. G. J., Florio, R., and Dobrin, J. (1986). Damage of porcine aortic valve tissue caused by the surfactant sodium dodecylsulphate. *Thoracic cardiovascular Surgeon* **34**, 82-85.
- Bos, G. W., Poot, A. A., Beugeling, T., van Aken, W. G., and Feijen, J. (1998). Small-diameter vascular graft prostheses: current status. *Archives of Physiology and Biochemistry* **106**, 100-115.
- Bos, G. W., Scharenborg, N. M., Poot, A. A., Engbers, G. H. M., Beugeling, T., van Aken, W. G., and Feijen, J. (1999). Proliferation of endothelial cells on surface-immobilized albumin-heparin conjugate loaded with basic fibroblast growth factor. *Journal of Biomedical Materials Research* **44**, 330-340.
- Bos, G. W., Scharenborg, N. M., Poot, A.A., Engbers, G. H. M., Terlingen, J. G. A., Beugeling, T., VanAken, W. G., and Feijen, J. (1998). Adherence and proliferation of endothelial cells on surface immobilized albumin-heparin conjugate. *Tissue Engineering* **4**, 267-279.
- Bowlin, G. L., and Rittgers, S. E. (1997). Electrostatic endothelial cell seeding technique for small diameter (6mm) vascular prostheses: feasibility testing. *Cell Transplantation* **6**, 623-629.
- Boyd, K. L., Schmidt, S., Rippert, T. R., Hite, S. A., and Sharp, W. V. (1988). The effect of pore size and endothelial cell seeding upon the performance of small-diameter ePTFE vascular grafts under controlled flow conditions. *Journal of Biomedical Material Research* **22**, 163-177.
- Bull, D. A., Hunter, G. C., Holubec, H., Aguirre, M. L., Rappaport, W. D., and Putnam, C. W. (1995). Cellular origin and rate of endothelial cell coverage of PTFE grafts. *Journal of Surgical Research* **58**, 58-68.
- Callow, A. D. (1982). Current status of vascular grafts. *Surg. Clin. North America* **62**, 501-.
- Cameron, A., Davis, K. B., Green, G., and Schaff, H. V. (1996). Coronary bypass surgery with internal-thoracic-artery grafts: effects on survival over a 15 year period. *New England Journal of Medicine* **334**, 216-219.
- Campbell, J. H., Efendy, J. L., and Campbell, G. R. (1999). Novel vascular graft grown within recipient's own peritoneal cavity. *Circulation Research* **85**, 1173-1178.

- Cartmell, J. S., and Dunn, M. G. (2000). Effect of chemical treatments on tendon cellularity and mechanical properties. *Journal of Biomedical Materials Research* **49**, 134-140.
- Chanda, J., Kuribayashi, R., and Abe, T. (1999). Heparin coupling in inhibition of calcification of vascular prostheses. *Biomaterials* **20**, 1753-1757.
- Chapman, H. A., Riese, R. J., and Shi, G. P. (1997). Emerging roles for cysteine proteases in human biology. *Annual Review of Physiology* **59**, 63-88.
- Charlesworth, P. M., Brewster, D. C., Darling, R. C., Robison, J. G., and Hallet, J. W. (1985). The fate of polytetrafluoroethylene grafts in lower limb bypass surgery: a six year follow up. *British Journal of Surgery* **72**, 896-899.
- Cheshire, N. J. W., Wolfe, J. H. N., Noone, M. A., Davies, L., and Drummond, M. (1992). The economics of femoral reconstruction for critical leg ischemia with and without autologous vein. *Journal of Vascular Surgery* **15**, 167-175.
- Chvapil, M. (1992). Method of using tendon/ligament substitutes composed of long, parallel, non-antigenic tendon/ligament fibres. In "United States Patent 5,078,744". Bio-products, Inc., Tucson, Arizona, USA.
- Clarke, D. R., Lust, R. M., Sun, Y. S., Black, K. S., and Ollerershaw, J. D. (2000). Transformation of nonvascular acellular matrices into durable vascular conduits. *Annals of Thoracic Surgery* **71**, S433-436.
- Costa, K. A., Sumpio, B. E., and Cerreta, J. M. (1991). Increased elastin synthesis by bovine aortic smooth muscle cells subjected to repetitive mechanical stretching. *FASEB J.* **5**.
- Coster, S., Gulliford, M. C., Seed, P. T., Powrie, J. K., and Swaminathan, R. (2000). Monitoring blood glucose control in diabetes mellitus: a systematic review, pp. 1-105. Health Technology Assessment NHS R&D HTA Programme, London.
- Courtman, D. W., Pereira, C.A., Kashef, V., McComb, D., Lee, J.M. and Wilson, G.J. (1995). Biomechanical and ultrastructural comparison of crypreservation and a novel cellular extraction of porcine aortic leaflet valves. *Journal of Biomedical Materials Research* **29**, 1507-1516.
- Courtman, D. W., Errett, B., and Wilson, G. J. (2000). The role of cross-linking in modification of the immune response elicited against xenogenic vascular acellular matrices. *Journal of Biomedical Materials Research* **55**, 576-586.
- Courtman, D. W., Pereira, C. A., Kashef, V., McComb, D., Lee, J. M., and Wilson, G. J. (1994). Development of a pericardial acellular matrix biomaterial: biochemical and mechanical effects of cell extraction. *Journal of Biomedical Materials Research* **28**, 655-666.
- Creighton, T. E. (1993). "Protein structure and molecular properties." W. H. Freeman and company, New York.
- Crowther, M., Goodall, J., Bell, P., and Thompson, M. (2000). Localization of matrix metalloproteinase 2 within the aneurysmal and normal aortic wall. *British Journal of Surgery* **87**, 1391-1400.
- Dardik, H., Baier, R. E., and Meenaghan, M. (1982). Morphologic and biophysical assessment of long term human umbilical vein implants used as vascular conduits. *Surgical Gynecology and Obstetrics* **154**, 17.
- Dardik, H., Miller, N., Dardik, A., Ibrahim, I. M., Sussman, B., Berry, S. M., Wolodiger, F., Khan, M., and Dardik, I. (1988). A decade of experience with the glutaraldehyde-tanned human umbilical cord vein graft for revascularisation of the lower limb. *Journal of Vascular Surgery* **7**, 336-346.
- Davids, L., Dower, T., and Zilla, P. (1999). Lack of healing in conventional vascular grafts. In "Tissue Engineering of Vascular Prosthetic Grafts" (P. Zilla and H. P. Greisler, Eds.), pp. 3-44. R.G. Landes Company, Austin.
- Davies, P. F. (2002). Spatial structural and genomic responses of endothelial cells to haemodynamic shear stress (abstract). *Cardiovascular Pathology* **11**, 25.
- DeBlois, C., Cote, M. F., and Doillon, J. (1994). Heparin-fibroblast growth factor-fibronectin complex: in vitro and in vivo applications to collagen based materials. *Biomaterials* **15**, 665-672.
- Demer, L. L. (1997). Lipid Hypothesis of Cardiovascular Calcification. *Circulation* **95**, 479-488.
- Dobrin, P.B. (1978). Mechanical Properties of Arteries. *Physiological Reviews*, **58** (2), pp. 397-449.
- Doi, K., and Matsuda, T. (1997). Enhanced vascularisation in a microporus polyurethane graft impregnated with basic fibroblast growth factor and heparin. *Journal of Biomedical Material Research* **34**, 361-370.
- Eickhoff, H., Broomé, A., Ericsson, B. F., Jørgen, H., Hansen, B., Kordt, K.F, Mouritzen, C., Knut Kvernebo, K., Norgren, L., Rostad, H., and Trippstad, A. (1987). Four years' results of a prospective, randomised clinical trial comparing polytetrafluoroethylene and modified human umbilical vein for below-knee femoropopliteal bypass. *Journal of Vascular Surgery* **6**, 505-511.

- Esquivel, C. O., and Blaisdell, F. W. (1986). Why small calibre vascular grafts fail: A review of clinical and experimental experience and the significance of the interaction of blood at the interface. *Journal of Surgical Research* **41**, 1-15.
- Fasol, R., Zilla, P., Deutsch, M., Fischlein, T., Minar, E., Hammerle, A., and Wolner, E. (1987). "Endothelial cell seeding: experience and first clinical results in Vienna." Karger, Basel.
- Fasol, R., Zilla, P., Deutsch, M., Grimm, M., Fischlein, T., and Laufer, G. (1989). Human endothelial cell seeding: evaluation of its effectiveness by platelet parameters after one year. *Journal of Vascular Surgery* **9**, 432-436.
- Fernandez, P., Bareille, R., Conrad, V., Midy, D., and Bordenave, L. (2001). Evaluation of an in vitro endothelialised vascular graft under pulsatile shear stress with a novel radio labelling procedure. *Biomaterials* **22**, 649-658.
- Foda, H., and Zucker, S. (2001). Matrix metalloproteinases in cancer invasion, metastasis and angiogenesis. *Drug Discovery Today* **6**, 478-482.
- Folkman, J., and Moscona, A. (1978). Role of cell shape in growth control. *Nature* **273**, 345-349.
- Francis, K., and Palsson, B. O. (1997). Effective intercellular communication distances are determined by the relative time constants for cyto/chemokine secretion and diffusion. *Proc. Natl. Acad. Sci.* **94**, 12258-12262.
- Friess, W. (1998). Collagen-biomaterial for drug delivery. *European Journal of Pharmaceutics and Biopharmaceutics* **45**, 113-136.
- Gahtan, V., Esses, G. E., Bandyk, D. K., Nelson, R. T., Dupont, E., and Mills, J. L. (1995). Anti staphylococcal activity of rifampin-bonded gelatin-impregnated dacron grafts. *Journal of Surgical Research* **58**, 105-110.
- Galdbart, J. O., Branger, C., Andreassian, B., Lambert-Zeckovsky, N., and Kitzis, M. (1996). Elution of six antibiotics bonded to polyethylene vascular grafts sealed with three proteins. *Journal of Surgical Research* **66**, 174-178.
- Gemmell, C. H., Gorbet, M. B., and Sefton, M. B. (1998). Novel strategies for enhancing surface thromboresistance. Proceedings of the VI Biennial Meeting of the International Society of Applied Cardiovascular Biology, Munich, Germany, III-04.
- Gerdes, R., Wohrle, D., Spliier, W., Schneider, G., Schnurpfeil, G. and Schulz-Ekloff, G. (1997). Photo-oxidation of phenol and monochlorophenols in oxygen-saturated aqueous solutions by different photosensitizers. *Journal of Photochemistry and photobiology A: Chemistry* **111**, 65-74.
- Goissis, G., Suzigan, S., Parreira, D. R., Maniglia, J. V., D.M., B., and Raymundo, S. (2000). Preparation and characterization of collagen-elastin matrices from blood vessels intended as small diameter vascular grafts. *Artificial Organs* **24**, 217-223.
- Graham, L. M., Vinter, D. W., Ford, J. W., Kahn, R. H., Burkel, W. E., and Stanley, J. C. (1980). Endothelial cell seeding of prosthetic vascular graft. Early experimental studies with cultured autologous canine endothelium. *Arch. Surgery* **115**, 929-933.
- Gray, J. L., Kang, S. S., Zenni, G. C., Kim, D. U., Burgess, W. H., Winkles, J. A., Haudenschild, C. C., and Greisler, H. P. (1994). FGF-1 affixation stimulates ePTFE endothelialisation without intimal hyperplasia. *Journal of Surgical Research* **57**, 596-612.
- Gregory, K.W., Hinds, M., Judd, J., Roberts, T., Kenned, K., Burke, R. and Beck, T. (2000). Porcine derived populated with porcine aortic endothelial cells during pulsatile perfusion with controlled shear stress (abstract). In "Cardiovascular Pathology", Vol. 9, pp. 165.
- Greisler, H. P., Gosselin, C., Ren, D., Kang, S. S., and Kim, D. U. (1996). Biointeractive polymers and tissue engineering blood vessels. *Biomaterials* **17**, 329-336.
- Greisler, H. P., Petsikas, D., Lam, T. M., Patel, N. E., Cabusao, E. (1993). Kinetic of cell proliferation as a function of vascular graft material. *Journal of Biomedical Materials Research* **27**, 955-961.
- Guidoin, R., Marceau, D., Couture, J., Jian Raio, T., Merhi, Y., Roy, P. E., and De la Faye, D. (1989). Collagen coatings as biological sealants for textile arterial prostheses. *Biomaterials* **10**, 156-165.
- Guidoin, R., Marceau, D., Jian Raio, T., King, M., Roy, P. E., Martin, L., and Duval, M. (1987). In vitro and in vivo characterisation of an impervious polyester arterial prosthesis: the Gelseal Triaxial graft. *Biomaterials* **8**, 433-441.
- Hampton, J.R.E. (1983). "Cardiovascular Disease." William Heinemann Medical Books Ltd., London.
- Haralson, M. A., and Hassell, J. R. (1995). "The Practical Approach Series." Oxford University Press, Oxford.
- Harmand, M. F., and Briquet, F. (1999). In vitro comparative evaluation under static conditions of the haemocompatibility of four types of tubing for cardiopulmonary bypass. *Biomaterials* **20**, 1561-1571.
- Hasson, J. E., Newton, D. W., Waltman, A. C., Fallon, J. T., Brewster, D. C., Darling, R. C., and Abbott, W. M. (1986). Mural degeneration in the glutaraldehyde tanned umbilical vein graft: Incidence and implications. *Journal of Vascular Surgery* **4**, 243-250.

- Herring, M. B., Compton, R. S., Gardner, A. L., and Le Grand, D. R. (1987). "Clinical experiences with endothelial cell seeding in Indianapolis." Karger, Basel.
- Herring, M., Gardner, A., and Glover, J. (1979). Seeding endothelium on to canine arterial prostheses. *Arch. Surgery* **114**, 679-682.
- Hiles, M. C., Badylak, S. F., Lantz, G. C., Kokini, K., Geddes, L. A., and Morff, R. J. (1995). Mechanical properties of xenogenic small-intestinal submucosa when used as an aortic graft in the dog. *Journal of Biomedical Materials Research* **29**, 883-891.
- Hirai, J., and Matsuda, T. (1996). Venous reconstruction using hybrid vascular tissue composed of vascular cells and collagen: Tissue regeneration process. *Cell Transplantation* **5**, 93-105.
- Hoerstrup, S. P., G. Z., Sodian, R., Schnell, A. M., Grunenfelder, J., and Turina, M. I. (2001). Tissue engineering of small diameter vascular grafts. *European Journal of Cardio-thoracic Surgery* **20**, 164-169.
- Hornick, D. B. (2002). An approach to the analysis of arterial blood gases and acid-base disorders, Vol. 2002. The University of Iowa.
- Hubble, J. A., Massia, S. P., Desai, N. P., and Drumheller, P. D. (1991). Endothelial cell-selective materials for tissue engineering in the vascular graft via a new receptor. *Biotechnology* **9**, 568-572.
- Hunt, C. J., Song, Y. C., Bateson, E. J. A., and Pegg, D. E. (1994). Fractures in cryopreserved arteries. *Cryobiology* **31**, 506-515.
- Hynes, R. O. (1992). Integrins: versatility, modulation and signalling in cell adhesion. *Cell* **68**, 11-25.
- Ito, R. K., and Lo Gerfo, F. W. (1990). Hirudin-immobilized biocompatible substances for manufacture of antithrombogenic prostheses. In "Patent EU 357242 A1 900307", pp. 19.
- Ives, C. L., Eskin, S. G., and McIntire, L. V. (1986). Mechanical effects on endothelial cell biology. *In vitro Cell Developmental Biology* **22**, 500-507.
- Jackson, C. J., Garbett, P. K., Nissen, B., and Schrieber, L. (1990). Binding of human endothelium to Ulex europaeus: I-coated Dynabeads: application to the isolation of microvascular endothelium. *Journal of Cell Science* **96**, 257-262.
- Jaffe, E. A., R. L. Nachman, et al. (1973). "Culture of human endothelial cells derived from umbilical vein: identification by morphologic and immunologic criteria." *Journal of Clinical Investigations* **52**: 2745-2756.
- Jeschke, M. G., Hermanutz, V., Wolf, S. E., and Koveker, G. B. (1999). Polyurethane vascular prostheses decreases neointimal formation compared with expanded polytetrafluoroethylene. *Journal of Vascular Surgery* **29**, 168-176.
- Johnson, W. C., and Lee, K. K. (2000). A comparative evaluation of polytetrafluoroethylene, umbilical vein, and saphenous vein bypass grafts for femoral-popliteal above-knee revascularisation: A prospective randomised Department of Veterans Affairs cooperative study. *Journal of Vascular Surgery* **32**, 268-277.
- Jones, G. E. (1996). "Methods in Molecular Medicine." Humana Press, Towowa.
- Kaiser, D., Freyberg, M. A., and Friedl, P. (1997). Lack of haemodynamic forces trigger apoptosis in vascular endothelial cells. *Biochemical and Biophysical Research Communications* **231**, 596-590.
- Karim, N., Mertsching, A., Haverich, A., and Bader, A. (1999). Remodelling of acellularized porcine aorta by matrix-producing human myofibroblasts ( XII ISAO conference Edinburgh, abstract only). *International Journal of Artificial Organs* **22**, 417.
- Karkow, W. S., Cranley, J. J., Cranley, R. D., Hafner, C. D., and Ruoff, B. A. (1986). Extended study of aneurysm formation in umbilical vein grafts. *Journal of Vascular Surgery* **4**, 486-492.
- Khor, E. (1997). Methods for the treatment of collagenous tissues for bioprostheses. *Biomaterials* **18**, 95-105.
- Kiaei, D., Hoffman, A. S., and Horbett, T. A. (1992). Tight binding of albumin to glow discharge treated polymers. *Journal of Biomaterial Science Polymers* **4**, 35-44.
- Kieffer, P., Giummelly, P., Schjoth, B., Carteaux, J., Villemot, J., Hornebeck, W., and Atkinson, J. (2001). Activation of metalloproteinase-2, loss of matrix scleroprotein content and coronary artery calcification. *Atherosclerosis* **157**, 251-254.
- Kim, B. S., Nikoloviski, J., Bonadio, J., and Mooney, D. J. (1999). Cyclic mechanical strain regulates the development of engineered smooth muscle tissue. *Nature Biotechnology* **17**, 979-983.
- Kim, B., and Mooney, D. (1998). Development of biocompatible synthetic extracellular matrices for tissue engineering. *Trends in Biotechnology* **16**, 224-230.
- Kirkpatrick, C. J., Mueller-Schulte, D., Roye, M., Hollweg, G., Gossen, C., Richter, H., and Mittermayer, C. (1991). Surface modification of polymers to permit endothelial cell growth. *Cells and Materials* **1**, 93-108.

- Kirschenlohr, H. L., Metcalfe, J. C., and Grainger, D. J. (1996). Cultures of proliferating vascular smooth muscle cells from adult human aorta. In "Methods in Molecular Medicine" (G. E. Jones, Ed.), pp. 319-334. Humana Press, Towowa.
- Kirschke, H., and Barrett, A. J. (1998). "Lysosomal Cysteine Proteinases." Oxford University Press, New York.
- Kobashi, T., and Matsuda, T. (1999). Fabrication of a branched hybrid vascular prosthesis. *Tissue Engineering* **5**, 515-524.
- Kodama, M. (1990). Small diameter cardiovascular graft. Proceedings from the 33rd Japanese Congressional Materials Research, 153-155.
- Koskas, F., Goëau-Brissonnière, O., Nicolas, M., Bacourt, F., and Kieffer, E. (1996). Arteries from human beings are less infectible by *Staphylococcus aureus* than polytetrafluoroethylene in an aortic dog model. *Journal of Vascular Surgery* **23**, 472-476.
- Kottke-Marchant, K., Anderson, J. M., Umemura, Y., and Marchant, R. E. (1989). Effect of albumin coating on the in vitro blood compatibility of Dacron arterial prostheses. *Biomaterials* **10**, 147-155.
- Kuntz, E. (1964). Preparation of collagenous materials. In "United States Patent Office". Ethicon, Inc., United States of America.
- Laemmel, E., Penhoat, J., Warocquier-Clerout, R., and Sigot-Luizard, M. F. (1998). Heparin immobilized on proteins usable for arterial prostheses coating: growth inhibition of smooth muscle cells. *Journal of Biomedical Materials Research* **39**, 446-452.
- Laemmli, U. K. (1970). "Cleavage of structural proteins during the assembly of the head of bacteriophage T4." *Nature* **15**(227 (259)): 680-685.
- Lee, C., Vyavahare, N., Zand, R., Kruth, H., Schoen, F. J., Bianco, R., and Levy, R. J. (1998). Inhibition of aortic wall calcification in bioprosthetic heart valves by ethanol pretreatment: Biochemical and biophysical mechanisms. *Journal of Biomedical Materials Research* **42**, 30-37.
- Lee, E. S., Caldwell, M. P., Tretinyak, A. S., and Santilli, S. M. (2001). Supplemental oxygen controls cellular proliferation and anastomotic intimal hyperplasia at a vascular graft-to-artery anastomosis in the rabbit. *Journal of Vascular Surgery* **33**, 608-613.
- Leong, A.S.Y. (2001). [WWW] <http://home.primus.com.au/royellis/fix.htm> (March 22, 2001)
- L'Heureux, N., Germain, L., Labbe, R., and Auger, F. A. (1993). In vitro construction of a human blood vessel from cultured vascular cells: a morphologic study. *Journal of Vascular Surgery* **17**, 499-509.
- L'Heureux, N., Paquet, S., Labbe, R., Germain, L., and Auger, F. A. (1998). A completely biological tissue-engineered human blood vessel. *FASEB Journal* **12**, 47-56.
- Loop, F. D., Lytle, B. W., Cosgrove, D. M., and et al. (1986). Influence of the internal mammary artery graft on 10-year survival and other cardiac events. *New England Journal of Medicine* **314**, 1-6.
- Ma, Y.-H., Ling, S., and Ives, H. E. (1999). Mechanical strain increases PDGF-B and PDGF-beta receptor expression in vascular smooth muscle cells. *Biochemical and Biophysical Research Communications* **265**, 606-610.
- Malone, J., Brendel, K., Duhamel, R. C., and Reinert, R. L. (1984). Detergent-extracted small-diameter vascular prostheses. *Journal of Vascular Surgery* **1**, 181-191.
- Marois, Y., Chakfe, N., Deng, X., Marois, M., How, T., King, M. W., and Guidoin, R. (1995). Carbodiimide cross-linked gelatin: a new coating for porous polyester arterial prostheses. *Biomaterials* **16**, 1131-1139.
- Marois, Y., Chakfe, N., Guidoin, R., Raymond, C., Duhamel, Roy, R., Marois, M., King, M. W., and Douville, Y. (1996). An albumin coated polyester arterial graft: in vivo assessment of biocompatibility and healing characteristics. *Biomaterials* **17**, 3-14.
- Mary, C., Marois, Y., King, M. W., Laroche, G., Douville, Y., Martin, L., and Guidoin, R. (1997). The in vitro and in vivo studies of polyester arterial prosthesis with a warp knitted sharkskin structure. *Journal of Biomedical Materials* **35**, 459-472.
- McCawley, L. J., and Matrisian, L. M. (2001). Matrix metalloproteinases: they're not just for matrix anymore! *Current Opinion in Cell Biology* **13**, 534-540.
- Mechanic, G. L. (1992). Cross-linking collagenous product. Assignee University of North Carolina, Patent number 5 332 475, USA.
- Meinhart, J., Deutsch, M., and Zilla, P. (1997). Eight-years of clinical endothelial cells transplantation - Closing the gap between prosthetic grafts and vein grafts. *American Society of Artificial Internal Organs* **43**, M515-M521.
- Milnor, W. R. (1989). "Hemodynamics." Williams and Wilkins, Baltimore.
- Moore, M. A., Bohachevsky, I. K., Cheung, D. T., Boyan, B. D., Chen, W.-M., Bickers, R. R., and McIlroy, B. K. (1994). Stabilization of pericardial tissue by dye-mediated photooxidation. *Journal of Biomedical Materials Research* **28**, 611-618.

- Morgan, D. M. (1996). Isolation and culture of human umbilical vein endothelial cells. *Methods in Molecular Medicine*. G. E. Jones. Towowa, Humana Press. 101-110.
- Murphy, G., and Gavrilovic, J. (1999). Proteolysis and cell migration: creating a path? *Current Opinion in Cell Biology* **11**, 614-621.
- Nackman, G. B., Schloss, R., Graham, A. M., and Moghe, P. V. (2000). Endothelial response to flow is improved by heterotrophic smooth muscle cell interactions (abstract). *Cardiovascular Pathology* **9**, 190.
- Naughton, G. (1999). The advanced tissue sciences story. *Scientific American* **280**, 60-61.
- Nerem, R. M., Alexander, W. R., Chappell, D. C., Medford, R. M., Varner, S. E., and Taylor, R. W. (1998). The study of the influence of flow on vascular endothelial biology. *American Journal of Medical Science* **316**, 169-175.
- Nerem, R. M., and Seliktar, D. (2001). Vascular Tissue Engineering. *Annual Review of Biomedical Engineering* **3**, 225-243.
- Nerem, R. M., Harrison, D. G., Taylor, R. W., and Alexander, W. R. (1993). Haemodynamics and vascular endothelial biology. *Journal of Cardiovascular Pharmacology* **21** (supplement 1), S6-S10.
- Nevelsteen, A., Smet, G., Wilms, G., Marchal, G., and Suy, R. (1988). Intravenous digital subtraction angiography and Duplex scanning in the detection of late human umbilical vein degeneration. *British Journal of Surgery* **75**, 668-670.
- Niklason, L. E., Gao, J., Abbott, W. M., Hirschi, K. K., Houser, S., Marini, R., and Langer, R. (1999). Functional arteries grown in vitro. *Science* **284**, 489-493.
- Niklason, L. E., Gao, J., Abbott, W. M., Klagges, B., Hirschi, K. K., Ulubayram, K., Conroy, N., Jones, R., Vasanawala, A., Sanzgiri, S., and Langer, R. (2001). Morphologic and mechanical characteristics of engineered bovine arteries. *Journal of Vascular Surgery* **33**, 628-638.
- Oliver, R. F., and Grant, R. A. (1985). Implant Tissue. In "World Intellectual Property Organisation", pp. 1-22. Oliver, R.F., UK.
- Olivier, L. A., Yen, J., Reichert, W. M., and Truskey, G. A. (1999). Short term cell/substrate contact dynamics of subconfluent endothelial cells following exposure to laminar flow. *Biotechnology Progress* **15**, 33-42.
- Osol, G. (1995). Mechanotransduction by vascular smooth muscle. *Journal of Vascular Research* **32**, 275-292.
- Oster, G., Bellin, J.S., Kimball, R.W and Schrader, M.E. (1959). Photochemical oxidation. *Journal of the American Chemical Society*. **81**, 5095.
- Ott, M. J., and Ballermann, B. J. (1995). Shear stress-conditioned endothelial cell-seeded vascular grafts: improved cell adherence in response to in vitro shear stress. *Surgery* **117**, 334-339.
- Owens, E. L., and Clowes, A. W. (1999). Pathobiology of hyperplastic intimal responses. In "Tissue Engineering of Vascular Prosthetic Grafts" (P. Zilla and H. P. Greisler, Eds.), pp. 231-240. R.G. Lanes Company, Austin.
- Patel, N. E., Padera, R., Sanders, G. H., Cannizzaro, S. M., Davies, M. C., Langer, R., Roberts, C. J., Tendler, S. J., Williams, P. M., and Shakesheff, K. M. (1988). Spatially controlled cell engineering on biodegradable polymer surfaces. *FASEB J.* **12**, 1447-1454.
- Perry, R. H., and Green, D. W. (1998). "Perry's Chemical Engineers Handbook." McGraw-Hill International Editions, Chemical Engineering Series,
- Phaneuf, M. D., Berceli, S. A., Bide, M. J., Quist, W. C., and LoGerfo, F. W. (1997). Covalent linkage of recombinant hirudin to poly (ethylene terephthalate) (Dacron): creation of a novel antithrombin surface. *Biomaterials* **18**, 755-765.
- Phaneuf, M. D., Quist, W. C., Bide, M. J., and LoGerfo, F. W. (1995). Modification of polyethylene terephthalate (Dacron): via denier reduction: effects on material tensile strength weight and protein binding capabilities. *Journal of Applied Biomaterials* **6**, 289-299.
- Pieper, J. S., Oosterhof, A., Dijkstra, P. J., J.H., V., and van Kuppevelt, T. H. (1999). Preparation and characterization of porous crosslinked collagenous matrices containing bioavailable chondroitin sulphate. *Biomaterials* **20**, 847-858.
- Probst, M., Dahiya, R., Carrier, S., and Tanagho, E. A. (1997). Reproduction of function smooth muscle tissue and partial bladder replacement. *British Journal of Urology* **79**, 505-515.
- Probst, M., Piechota, H. J., Dahiya, S., and Tanagho, E. A. (2000). Homologous bladder augmentation in dog with the bladder acellular matrix graft. *British Journal of Urology* **85**, 362-371.
- Ramshaw, J. A. M., Stephens, L.J. and Tulloch, P.A. (1994). Methylene blue sensitised photo-oxidation of collagen fibrils. *Biochim Biophys Acta* **1206** (2) 225-230.
- Ramshaw, J. A. M., Werkmeister, J. A., and Glattauer, V. (1995). *Collagen-based biomaterials. Biotechnology and Genetic Engineering Reviews* **13**, 335-382.
- Ratcliffe, A. (2000). Tissue engineering of vascular grafts. *Matrix Biology* **19**, 353-357.

- Reid, L. C., and Rojkind, M. (1987). Method for the isolation of connective tissue biomatrix. Albert Einstein College of Medicine of Yeshiva University, Bronx, N.Y., USA.
- Robotin-Johnson, M. C., Swanson, P. E., Johnson, D. C., Schuessler, R. B., and Cox, J. L. (1998). An experimental model of small intestinal submucosa as a growing vascular graft. *Journal of Thoracic Cardiovascular Surgery* **116**, 805-811.
- Roeder, R., Wolfe, J., Lianakis, N., Hinson, T., Geddes, L. A., and Obermiller, J. (1999). Compliance, elastic modulus, and burst pressure of small-intestine submucosa (SIS), small-diameter vascular grafts. *Journal of Biomedical Materials Research* **47**, 65-70.
- Rosenburg, N., Thompson, J. E., Keshishian, J. M., and VanderWerf, B. A. (1976). The modified bovine arterial graft. *Arch. Surg* **111**, 222.
- Schmidt, C. E., and Baier, J. M. (2000). Acellular vascular tissues: natural biomaterials for tissue repair and tissue engineering. *Biomaterials* **21**, 2214-2231.
- Schmidt, S. P., and Bowlin, G. L. (1999). Endothelial cell seeding: A review. In "Tissue Engineering of Vascular Prosthetic Grafts" (P. Zilla and H. P. Greisler, Eds.), pp. 61-67. R.G. Lanes Company, Austin.
- Schmidt, S. P., Evancho-Chapman, M., Sims, R. L., and Anderson, J. M. (1998). A controlled evaluation of the hemashield woven single velour polyester vascular graft and Gor-tex ePTFE vascular graft for patency and healing characteristics in a canine aorto-iliac model. Proceeding of the VI Biennial Meeting of the International Society of Applied Cardiovascular Biology, Munich, Germany, III-20.
- Schmidt, S. P., Sharp, W. V., Evancho, M. M., and Meerbaum, S. O. (1991). Endothelial cell seeding of prosthetic vascular grafts - current status. In "High Performance Biomaterials" (S. M, Ed.), pp. 287-292. Technomic Lancaster.
- Schoen, F. J., and Levy, R. J. (1999). Tissue heart valves: Current challenged and future research perspectives. *Journal of Biomedical Materials Research* **47**, 439-465.
- Seifalian, A. M., Giudiceandrea, A., Schmitz-Rixen, T., and Hamilton, G. (1999). Noncompliance: The silent acceptance of a villain. In "Tissue Engineering of Vascular Prosthetic Grafts" (P. Zilla and H. P. Greisler, Eds.), pp. 45-58. R.G. Lanes Company, Austin.
- Shapiro, S. D. (1998). Matrix metalloproteinase degradation of extracellular matrix: biological consequences. In *Current Opinion in Cell Biology* **10**, pp. 602-608.
- Shayani, V., Newman, K. D., and Dichec, D. A. (1994). Optimisation of recombinant t-PA secretion from seeded vascular grafts. *Journal of Surgical Research* **57**, 495-504.
- Shen, H.R., Spikes, J.D., Smith, C.J. and Kopecek, J. (2000) Photodynamic cross-linking of proteins IV. Nature of His-His bond(s) formed in the rose Bengal-photosensitised cross-linking of N-benzoyl-L-histidine. *Journal of Photochemistry and photobiology A: Chemistry* **130**, 1-6.
- Shen, M., Mostefa, A., Chen, L., Daudon, M., Thevenin, M., Lacour, B., and Carpentier, A. (2001). Effect of ethanol and ether in the prevention of calcification of bioprostheses. *Annals of Thoracic Surgery* **71**, 413-416.
- Sherma, J. (1986). "Thin-layer and paper chromatography." *Analytical of Chemistry* **58**: 69R-81R.
- Shinoka, T. S.-T., D., Ma, P. X., Tanel, R. E., Isogai, N., Langer, R., Vacanti, J., and Mayer, J. E. (1998). Creation of viable pulmonary artery autografts through tissue engineering. *Journal of Thoracic and Cardiovascular Surgery* **115**, 536-146.
- Shinoka, T., Ma, P. X., Shum-Tim, D., Breur, C. R., Cusick, R. A., Zund, G., Langer, R., Vacanti, J. P., and Mayer, J. E. (1997). Tissue-engineered heart valves: autologous valve leaflet replacement, study in a lamb model. *Circulation (Supplement II)* **96**, 164-168.
- Shinoka, T., Imia, Y., Kashiwagi, J., Watanabe, M., Matsumura, G., Kosaka, Y., Konuma, T., Hibino, N., Naito, T., Miyake, T. and Murata, A. (2002). Successful clinical application of tissue engineered blood vessel (abstract). *Cardiovascular Pathology*. **11**, 59.
- Sims, F. H. (1985). Discontinuities in the internal elastic lamina: a comparison of coronary and internal mammary arteries. *Artery* **13**, 127-143.
- Sipehia, R., Martucci, G., Barbarosie, M., and Wu, C. (1993). Enhanced attachment and growth of human endothelial cells derived from umbilical veins of ammonia plasma modified surfaces of PTFE and ePTFE synthetic vascular graft biomaterials. *Biomaterials, Artificial Cell Immobilisation Biotechnology* **21**, 455-468.
- Slimane, S. B., Guidoin, R., Mehri, Y., King, M., Domurado, D., and Sigot-Luizard, M. F. (1988). In vivo evaluation of polyester arterial grafts coated with albumin: the role and importance of cross-linking agents. *European Surgical Research* **20**, 66-74.
- Smith, M., McFetridge, P. S., Bodamyali, T., Chaudhuri, J. B., Howell, J. A., Stevens, C. R., and Horrocks, M. (2000). Porcine-Derived Collagen as a Scaffold for Tissue Engineering. *Transactions Institution of Chemical Engineers* **78**, 19-24.

- Stanley, J. C., Burkel, W. E., Ford, J. W., Vinter, D. W., Kahn, R. H., and Graham, L. M. (1982). Enhance patency of small-diameter externally supported Dacron iliofemoral grafts seeded with endothelial cells. *Surgery* **92**, 994-1005.
- Stevens, C. R., V. G. Oberholzer, et al. (1988). "Lactosylceramide in inflammation bowel disease: a biochemical study." *Gut* **29**: 580-587.
- Sumpio, B. E. (1993). "Haemodynamic forces and vascular cell biology." R.G. Landes Company, Georgetown.
- Sunthareswaran, R. (1998). "Mosby's crash course." Mosby, London, UK.
- Surowiec, S. M., Conklin, B. S., Li, J. S., Lin, P. H., Weiss, V. J., Lumsden, A. B., and Chen, C. (2000). A new perfusion culture system used to study human vein. *Journal of Surgical Research* **88**, 34-41.
- Szilagyi, D. E., Elliot, J. P., Smith, R. F., Reddy, D. J., and McPharlin, M. (1991). A thirty-year survey of the reconstructive surgical treatment of aortoiliac occlusive disease. *Journal of Vascular Surgery* **3**, 421-436.
- Tamura, N., Terai, H., Iwakura, A., Yamamoto, Y., Matsumoto, K., Ueda, H., Inoue, M., Nakamura, T., Shimizu, Y., and Komeda, M. (1999). An "acellular" vascular prosthesis may provide a scaffold for the host tissue regeneration. *International Journal of Artificial Organs* **22**, 419 (abstract).
- Teebken, O. E., Bader, A., Steinhoff, G., and Haverich, A. (2000). Tissue engineering of vascular grafts: Human cell seeding of decellularised porcine matrix. *European Journal of Vascular and Endovascular Surgery* **19**, 381-386.
- Tennant, C. (2000). Product Properties, Vol. 2000. Charles Tennant & Company.
- Thomas, J. B., Smith, L. A., and Hamilton, I. N. (1999). Vascular reconstruction utilizing artery from an amputated extremity: a case report. *Journal of Vascular Surgery* **29**, 1159-1161.
- Thoumine, O., Ziegler, T., Girard, P. R., and Nerem, R. M. (1995). Elongation of confluent endothelial cells in culture: The importance of fields of force in the associated alterations of their cytoskeletal structure. *Experimental Cell Research* **219**, 427-441.
- Tomita, M., Irie, M. and Ukita, T. (1969). Sensitized photooxidation of Histidine and its derivatives. Products and mechanisms of the reaction. *Biochemistry* **8**, 12, 5149-5160.
- Tran, C. N. B., and Walt, D. R. (1989). Plasma modification and collagen binding to PTFE grafts. *Journal of colloidal Interface* **132**, 373-381.
- Turk, B., Turk, D., and Turk, V. (2000). Lysosomal cysteine proteases: more than scavengers. *Biochimica et Biophysica Acta*, 98-111.
- Undeland, I., Härröd, M., and Lingnert, H. (1998). Comparison between methods using low-toxicity solvents for the extraction of lipids from herring. *Food Science* **61**, 355-365.
- Van der Rest, M., and Garrone, R. (1991). Collagen family of proteins. *The FASEB Journal* **5**, 2814-2823.
- van Luyn, M. J., Van Wachem, P. B., Nieuwenhuis, P., Olde Damink, L., Ten Hoopen, H., and Feijen, J. (1991). Methylcellulose cell culture as a new cytotoxicity test system for biomaterials. *Journal of Materials Science: Materials in Medicine* **2**, 142-148.
- van Luyn, M. J., van Wachem, P. B., Olde Damink, L., Dijkstra, M. J. A., Feijen, J., and Nieuwenhuis, P. (1992a). Relations between in vitro cytotoxicity and cross-linked dermal sheep collagens. *Journal of Biomedical Research* **16**, 1091-1110.
- van Luyn, M. J., van Wachem, P. B., Olde Damink, L., Dijkstra, M. J. A., Feijen, J., and Nieuwenhuis, P. (1992b). Secondary cytotoxicity of cross-linked dermal sheep collagens during repeated exposure to human fibroblasts. *Biomaterials* **13**, 1017-1024.
- Vanjak-Novakovic. (2002). Tissue engineering approach to functional myocardium. *Cardiovascular Pathology* **11**, 23.
- Vann, R. D., Ritter, E. F., Plunkett, M. D., Wyble, C. W., Benson, C. V., Gerth, W. A., Barwick, W. J., and Klitzman, B. (1993). Patency and blood flow in gas denucleated arterial prostheses. *Journal of Biomedical Research* **27**, 493-498.
- Vincent, J. F. V. (1982). "Structural Biomaterials." Macmillan Press Ltd, London.
- Voorhees, A. B., Jaretski, A., and Blakemore, A. H. (1952). The use of tubes constructed from Vinyon 'N' cloth in bridging arterial defect. *Annals of Surgery* **135**, 332-336.
- Vyavahare, N., Hirsch, D., Lerner, E., Baskin, J. Z., Schoen, F. J., Bianco, R., Kruth, H. S., Zand, R., and Levy, R. J. (1997). Prevention of Bioprosthetic Heart Valve Calcification by Ethanol Preincubation: Efficacy and Mechanisms. *Circulation* **95**, 479-488.
- Vyavahare, N., Hirsch, D., Lerner, E., Baskin, J. Z., Zand, R., Schoen, F. J., and Levy, R. J. (1998). Prevention of calcification of glutaraldehyde-crosslinked porcine aortic cusps by ethanol preincubation: Mechanistic studies of protein structure and water-biomaterial relationships. *Journal of Biomedical Materials Research* **40**, 577-585.



- Walker, M. G., Thompson, G. J. L., and Shaw, J. W. (1987). "Endothelial cell seeded versus non-seeded ePTFE grafts in patients with severe peripheral vascular disease. Preliminary results." Karger, Basel.
- Watkins, M. T., Sharefkin, J. B., Zajchuk, R., Maciag, T. M., D'Amore, P. A., Ryan, U. S., Van Wart, H., and Rich, N. M. (1984). Adult human saphenous vein endothelial cells: assessment of their reproductive capacity for use in endothelial cell seeding of vascular prostheses. *Journal of Surgical Research* 36, 588-596.
- Weadock, K. S., and Goggins, J. A. (1993). Vascular graft sealants. *Journal of Medical Implants* 3, 207-222.
- Weil, L., Seibles, T.S. and Herskovits, T.T. (1965). Photooxidation of bovine insulin sensitised by methylene blue. *Archives of Biochemistry and Biophysics* 111, 308-329.
- Weinberg, C. B., and Bell, E. (1986). A blood vessel model constructed from collagen and cultured vascular cells. *Science* 231, 397-400.
- Werkmeister, J. A., White, J. F., Edwards, G. A., and Ramshaw, J. A. M. (1995). Evaluation of the Omniflow collagen-polymer vascular prosthesis: immuno-histological analysis using monoclonal antibodies. *Advances in Science Technology* 12, 767-776.
- Wheater, P. R., Burkitt, H. G., and Baniels, V. G. (1979). "Functional Histology: a text and colour atlas." Churchill Livingstone, Edinburgh, London and New York.
- Williams, S. K., Jarrell, B. E., Rose, D. G., Pontell, J., Kapelan, B. A., Park, P. K., and Carter, T. L. (1989). Human microvessel endothelial cell isolation and vascular graft sodding in the operating room. *Annals of Vascular Surgery* 3, 145-152.
- Williams, S. K., Wang, T. F., Castrillo, R., and Jarrell, B. E. (1994). Liposuction-derived human fat used for vascular graft sodding contains endothelial cells and not mesothelial cells as the major cell type. *Journal of Vascular Surgery* 19, 916-923.
- Williams. (1998). Collagen: Ubiquitous in nature, multifunctional in devices. *Medical Device Technology* 9, 10-13.
- Wilson, G. J., MacGregor, D. C., Klement, P., Weber, B. A., Binnington, A. G., and Pinchuk, L. (1993). A compliant corethane/Dacron composite vascular prosthesis. *ASAIO J.* 39, M526-M531.
- Zeff, R. H., Kongtahworn, C., Iannone, L. A., and et al. (1988). Internal mammary artery versus saphenous vein graft to the left anterior descending coronary artery: prospective randomised study with 10-year follow-up. *Annals of Thorac Surgery* 45, 533-536.
- Ziegler, T., and Nerem, R. (1994). Tissue engineering a blood vessel: regulation of vascular biology by mechanical stresses. *Journal of Cellular Biochemistry* 56, 204-209.
- Zilla, P., Deutsch, M., Meinhart, J., Puschmann, R., Eburn, T., Minar, E., Dudczak, R., Lugmaier, H., Schmidt, P., Noszian, I., and Fischlein, T. (1994). Clinical in vitro endothelialisation of femoropopliteal bypass grafts; An actuarial follow-up over three years. *Journal of Vascular Surgery* 19, 540-548.

# APPENDIX

## A1: DETERMINATION OF ENDOTHELIAL CELL PHENOTYPE

In this section the primary human cell lineages used in this thesis are characterised and confirmed as HUVEC and VSMC by immunocytochemistry and visual analysis of cell morphology. HUVEC were confirmed by their characteristic 'cobble stone' morphology when confluent and staining antigens for both von Willebrand factor (vWF) and CD31 surface markers. Human VSMC were characterised morphologically by 'hill and valley' formations, characteristic of this cell type confirmed by staining for  $\alpha$ -actin. Chapter 2.3.3.5 describes the protocols for immunocytochemical staining procedures.

Eukaryotic cell behaviour is critically dependent on a cells terminal or differentiated state, therefore determination of cell phenotype, or terminally differentiated state, was an essential requisite to ensure the intended cell type was indeed the specific phenotype used experimentally. The aim of this section was to firstly determine specific cell lineages by immunocytochemical staining methods, then to characterise

EC lining the luminal surface of arteries as described in chapter one, provide a number of distinct and important roles that allow a blood vessel to function normally. HUVEC as the name implies were isolated from neonatal umbilical cords, using the now standard technique described by (Jaffe, 1973) to enzymatically remove the endothelium, which is subsequently cultured as described in 2.2.2. Figure A.01 displays EC in normal culture conditions using phase-contrast microscopy. Cell morphology when cultured on plastic shows the characteristic cobble stone morphology (Bicknell, 1996).

Immunocytochemical phenotype characterisation was carried out with two separate monoclonal mouse antibodies, anti-human Von Willebrand Factor (vWF) and anti-human endothelial cell, CD31. The antibody to vWF binds to a family of vWF multimeric plasma glycoproteins with molecular weight ranging from 40,000 to 20 million and is expressed in both EC *and* megakaryocytes to facilitate platelet adhesion to the underlying vascular wall. The vWF glycoprotein links the platelet membrane

receptors to the subendothelium and serves as the plasma carrier for Factor VIII, in addition the vWF glycoprotein stabilizes the molecule Factor VIII. (DAKO, 2000). EC stained positive for vWF show spherical Weibel-Palade bodies (A) adjacent to the cell plasma membrane figure A.02.

The second EC identifier was the **platelet/endothelial adhesion molecule (PECAM-1)** or CD31 belongs to the immunoglobulin superfamily with adhesive properties. It is a single chain type 1 transmembrane glycoprotein with a molecular mass of 130 kD. CD31 is strongly expressed by all endothelial cells and more weakly on several types of leucocytes. Functionally CD31 is an adhesion molecule with both homophilic and heterophilic binding. The homotypic binding involves interaction as an important step in leucocyte transendothelial migration (diapedesis) and passage through the extracellular matrix. The heterotypic ligands have been reported to include integrin  $\alpha v \beta 3$  and glycosaminoglycans. Figure A.03 shows clearly the EC stained positive for CD31 cell surface antigen.

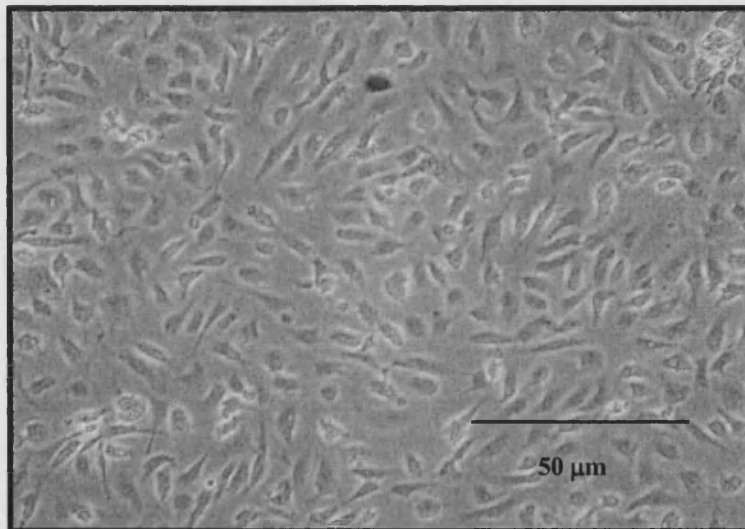


**Figure A.01:** HUVEC displaying 'cobblestone' morphology

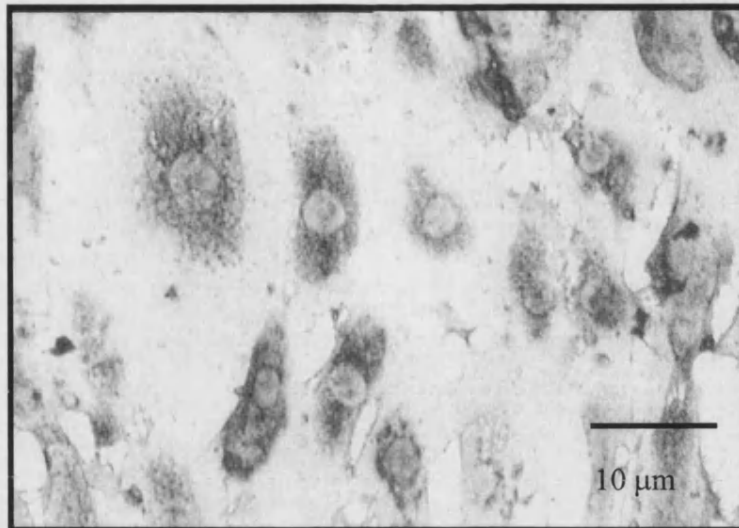


**Figure A.02:** HUVEC positively staining for vWF

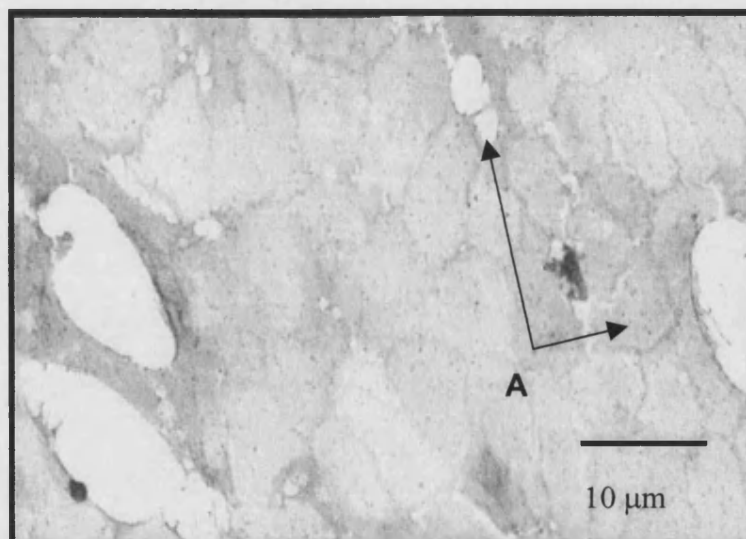


**Figure A.03:** Showing the CD31 surface marker (A) outlining the cell periphery

## **A2: DETERMINATION OF SMOOTH MUSCLE CELL PHENOTYPES**

Human vascular smooth muscles (hVSMC) were derived from several sources, including: adult human saphenous vein, umbilical cord artery and vein. Cell isolation methods are described up in Chapter 2.2.1.1. Most cell lineages have been cultured using explanted tissue. The exception being hVSMC isolated from umbilical cords by exposure to a second collagenase treatment after EC have been extracted, refer to

Chapter 2.2.1.1 for protocols. Umbilical artery SMC initially isolated by enzyme extraction were shown to proliferate readily in contrast to other studies using human aortic SMC, found high levels of TGF- $\beta$  a potent inhibitor of SMC proliferation (Kirschenlohr et al., 1996). Possible differences in cell phenotype and resulting gene expression due to cell source may explain these differences. Later experiments used hVSMC isolated using the explant method, this was primarily due to using a standard protocol for a range of tissue types that were in some cases unsuitable to use the enzyme extraction method. In addition, although umbilical arterial SMC proliferated readily when isolated enzymatically, higher cell densities were achieved by the explant method.

Like the endothelium, smooth muscle cells provide a specific function to a vessel wall, not least to confer the ability of vessel contraction, thus providing control over peripheral blood flow. Isolation of immunocytochemically proven hVSMC is therefore important to confirm the cell lineage and resulting patterns of adhesion, growth and proliferation. Figure A.04 shows umbilical vein hVSMC in normal culture conditions, displaying characteristic 'hill and valley' formations indicative of this cell type.

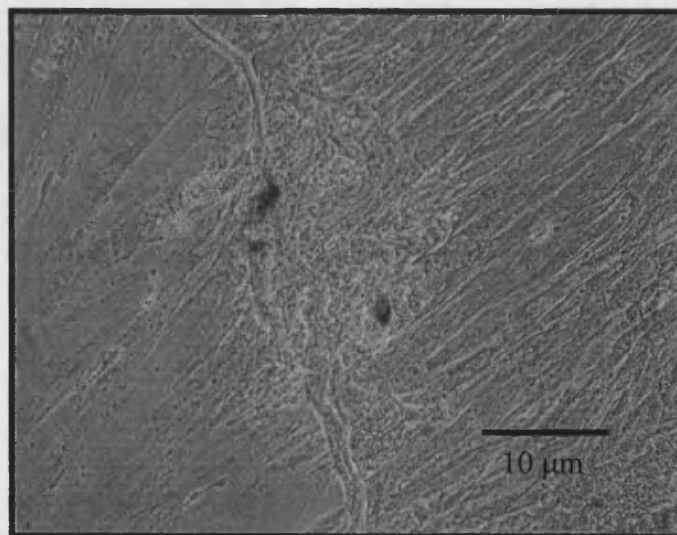


**Figure A.04:** hVSMC displaying the characteristic 'hill and valley' formation

Figures A.05 and A.06 having been immunohistochemically stained for  $\alpha$ -actin with Vector-RTU kits using the DAB substrate kit for peroxidase yielding a brown stain. Monoclonal mouse – anti-human smooth muscle actin: clone 1A4 code No. M0851 lot 028 from DAKO, UK. was used to bind the  $\alpha$ -actin epitopes. The anti-human smooth muscle actin antibody binds to the  $\alpha$  smooth muscle isoform of actin and does not cross react with;  $\beta$ - and  $\gamma$ - cytoplasm actin, striated muscle or myocardial fibroblasts. The antibody reacts with smooth muscle cells, my epithelial cells and parricides of vessels and different parenchyma's without exception (DAKO, 2000).

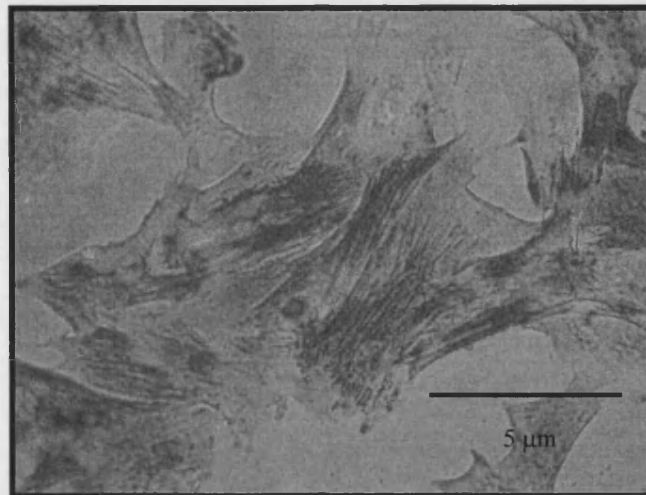


**Figure A.05:** Neonatal umbilical cord arterial derived hVSMC stained positive for  $\alpha$ -actin.

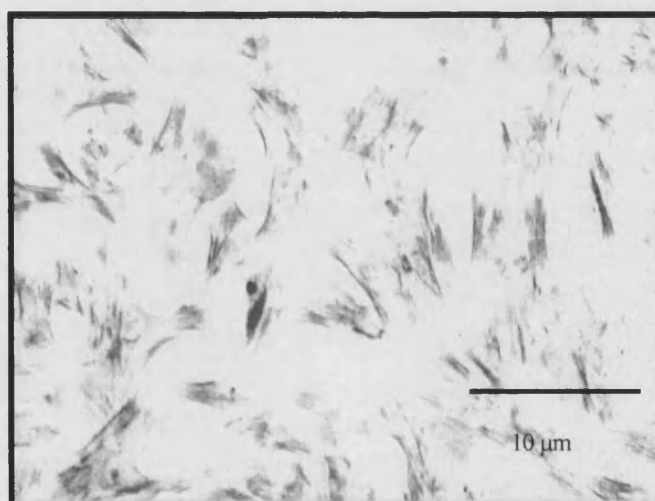


**Figure A.06:** Adult saphenous vein hVSMC stained positive for  $\alpha$ -actin

### A3: SDS-PAGE METHOD

Glass plates (two with raised spacers, two without) were set out and the plastic seals were inserted. The plain glass plates were then laid on top and clamped together. The combs were then added and tested for leaks by filling with distilled water. The resolving and stacking gels were then made up (see below) minus the final 7.5  $\mu$ l (each gel) of TEMED as this reagent sets the gel. The TEMED was added to the final solutions immediately prior to pupating the gel solution between the glass plates, this was to prevent the gel setting prematurely.

**Table A.01:** Resolving gel

Materials 8 % resolving gel (2 gels)	Concentration	Volume
Distilled Water		10.66 ml
Acrylamide (40%)		4 ml
Tris/base	18 g in 100 ml H <sub>2</sub> O pH 8.8	5.02 ml
SDS; Sodium dodecylsulfate (Lauryl Sulphate)	20 % w/v	100 $\mu$ l
AMPS (Ammonium persulphate)	10 % w/v	200 $\mu$ l
TEMED (N,N,N',N'-Tetramethylethylenediamine)		15 $\mu$ l

The resolving gel was then pipetted between the plates to a level just below the combs, ensuring that no air bubbles were trapped within the gel itself. The gel was then covered with a thin layer of ddH<sub>2</sub>O saturated with butanol to produce a straight edge across the gel. The gel was then left for 15-20 minutes to set.

**Table A.02:** Stacking gel

Materials 4 % Stacking gel (2 gels)	Concentration	Volume
Distilled Water		4.98 ml
Acrylamide (40%)		0.66 ml
Tris/base	12 g in 100 ml dd H <sub>2</sub> O pH 6.8	0.84 ml
SDS; Sodium Dodecylsulfate (Lauryl Sulphate)	20 % w/v	33.4 $\mu$ l
AMPS (Ammonium persulphate)	10 % w/v	66 $\mu$ l
TEMED (N,N,N',N'-Tetramethylethylenediamine)		8 $\mu$ l

When the resolving gel had set, the unpolymerised surface gel in saturated butanol was poured off and washed with ddH<sub>2</sub>O. The combs were then replaced and the stacking gel was pipetted on top of the resolving gel. As with the resolving gel the TEMED was added last to the stacking gel solution to prevent premature setting. The gel was then left to set for 15-20 minutes.

**Table A.03:** Running buffer

Materials running buffer (1000 ml)	Concentration	Volume
Tris/base	25 mM	3.06 g
Glycine	190 mM	14.4 g
SDS	0.001 %	1 g
Made up to a total volume of 1000 ml		total 1 L

The gel tank was set up with enough running buffer to cover the base of the tank, which was then tipped to one side to expel any bubbles that may have become trapped during the filling process. When the gels had set the clamps, combs and spacers were removed and the plates were then placed in the tank with the shaped plates facing inwards. Importantly, the tank must contain two gels to run correctly (even if only one is required). The plates were held in place by inserting supports with the ledged section upper most. The running buffer was then poured into the reservoir between the two sets of plates until full. The lid was fitted and the tank connected to the power supply. The tank was run (100V, 2-3 minutes) without the samples loaded to allow the gels to settle.

**Table A.04:** Loading buffer

Materials loading buffer (stock soln.)	Concentration	Volume
2-Mercaptoethanol	100 mM	77.125 mg
SDS; Sodium Dodecylsulfate (Lauryl Sulphate)	2%	100 mg
Glycerol (ACS Reagent)	20%	1 ml
Trizma Hydrochloride	50 mM	5 ml
Bromophenol blue	0.10%	50 ul



## A4: ANALYTICAL TECHNIQUES

### MECHANICAL TESTING CALCULATION

This section details the approach used to convert the raw load-extension data into stress-strain data. The equations developed, as well as the margins of error, were used in computations for stress and strain. The chart recorder produced graphical raw data as typified in Figure A.07. The distance along the x-axis is representative of time. Since the rate of extension is constant this is effectively the distance the ringlet is pulled apart:

$$X_{\text{dist apart}} = [ r_{\text{ext}} / v_{\text{chart}} ] \cdot X_{\text{dist chart}} \quad (4.1)$$

Where  $X_{\text{dist apart}}$  is the distance the ringlet is pulled apart (mm);  $r_{\text{ext}}$  is the rate of extension (5 mm/min);  $v_{\text{chart}}$  is the chart drive speed (50 mm/min); and  $X_{\text{dist chart}}$  is the distance measured on the chart graph x-axis (Hiles, Badylak et al. 1995). Therefore 10 mm on the chart recorder represented an extension of 1mm.

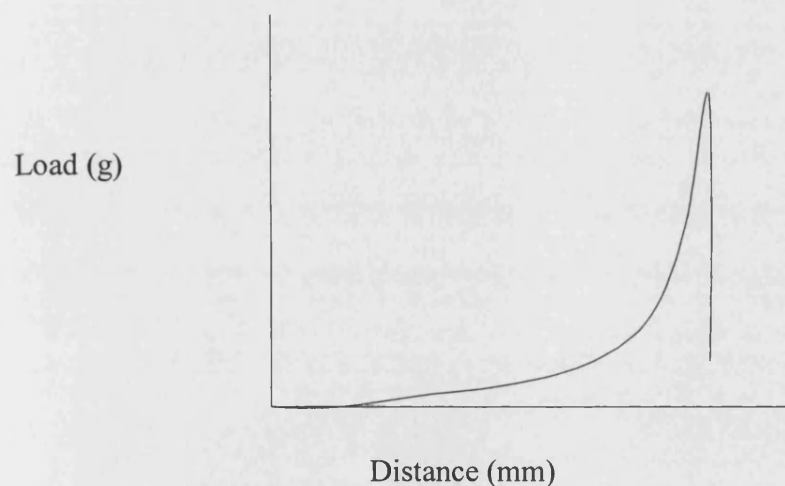


**Figure A.07:** A stylised stress-strain curve produced by the chart recorder in the load-extension tests.

Zero extension was taken to be the point where the load just began to rise above zero grams (Hiles et al, 1995). Prior to this the load did not increase with extension due to slack of the ringlet around the fittings. Due to the gradual increase in load the point of initial strain was difficult to determine, an approximation would be within  $2 \pm 0.2$  mm of initial strain. It is assumed that the rate of extension and chart drive speed, of the Instron rig, have negligible error.

#### INITIAL LENGTH CALCULATION

The ringlet can be thought of as a single strip as represented in Figure A.08. The length of this strip is thus the circumference of the ringlet, however the arterial ringlet is not a thin walled vessel. To be thin walled the ratio of the wall thickness to inner radius would have to be less than 0.1, whereas 100 % of the samples had a ratio of greater than 0.19 (mean of 0.51). The best approximation for the circumference was based on an average of the internal and external diameters (Riley et al, 1999). Hence:

$$Y_{\text{initial}} = \pi [0.5 (d_i + d_o)] \quad (4.2)$$

Where  $Y_{\text{initial}}$  is the initial strip length (mm);  $d_i$  is the internal diameter (mm); and  $d_o$  is the external diameter (mm). Measurements of the internal diameter and wall thickness were accurate to  $\pm 0.2$ mm. In equation 4.2 this gives the error in  $Y_{\text{initial}}$  of:

$$Y_{\text{initial, error}} = \pi [0.5 (0.2 + 0.2)] = \pm 0.6\text{mm} \quad (4.3)$$

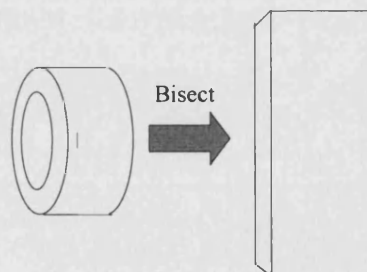


**Figure A.08:** Pictorial representation of a tissue ringlet in the form of a strip after bisection. Note that the thin side of the strip is a trapezium shape, representative of the difference in internal and external diameters of the ringlet.

## EXTENSION CALCULATION

By geometrical analysis it can be seen that the actual extension is twice the distance the ringlet has been pulled apart, assuming that the curved region at either end remains the same shape (and same length), see Figure A.09. This assumption is reasonable as the tissue stretched into constant shape around the curved metal hooks. Hence:

$$X_{\text{extension}} = 2 \cdot X_{\text{dist apart}} \quad (4.4)$$

Where  $X_{\text{extension}}$  is the actual extension (mm); and  $X_{\text{dist apart}}$  is the distance the ringlet is pulled apart (mm), from equation 4.1.

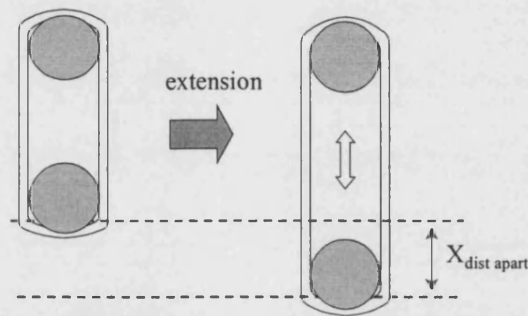


**Figure A.09:** Side-on view of the ringlet during extension by two hooks on the Instron™ 1122 rig. Note that the distance the ringlet has been pulled apart is  $X_{\text{dist apart}}$ .

It is assumed tissue thickness does not change during extension, only when the ultimate tensile strength is reached, that a ductile specimen will begin to thin or neck down (Riley, 1999). As expected it was observed that thickness was only seen to change significantly once fracture had initiated at which point the test was ended. The error involved for the actual extension is hence twice that of the distance the ringlet has been pulled apart:

$$X_{\text{extension, error}} = 2 \times 0.2 = \pm 0.4\text{mm} \quad (4.5)$$

## STRAIN CALCULATION

Strain ( $\epsilon$ ) has been defined as the extension over the initial length as a percentage (Dobrin, 1978). Using equations 4.2 and 4.4:

$$\epsilon = [ X_{\text{extension}} / Y_{\text{initial}} ] \cdot 100\% \quad (4.6)$$

The % error in the strain was calculated as the sum of the % errors of the initial length and the extension, from equations 4.3 and 4.5. hence:

$$\epsilon_{\text{error}} = ( [ X_{\text{extension, error}} / X_{\text{extension}} ] + [ Y_{\text{initial, error}} / Y_{\text{initial}} ] ) \cdot 100\% \quad (4.7)$$

It must be noted that as  $X_{\text{extension}}$  increases over the test period, the margin of error decreases as expected.

## STRESS CALCULATION

Stress ( $\sigma$ ) has been defined as

$$\sigma = F / A \quad (4.8)$$

Where F is the force exerted by the extended tissue and A is the area over which that force is exerted (Dobrin, 1978). Stress has units of pressure and the force component can be expressed as grams, as opposed to the traditional unit of force, the Newton. Throughout the tests it is assumed that the degree of error in the load is negligible, as the rig used is of a professional standard, and compared to the degree of error in the area component of the stress calculations, was insignificant.

The force is circumferential throughout these tests, and the area over which the force is exerted is the cross-sectional, annular region of the wall, depicted in Figure A.08. This area is:

$$A = w \cdot t \quad (4.9)$$

Where A is the area over which the force is exerted; w is the width of the ringlet (5mm); and t is the wall thickness (mm). As before, the change in this cross-sectional area is considered negligible throughout the test. The accuracy of measurements for both the width and wall thickness of each matrix ringlet, were  $\pm 0.2\text{mm}$ . For the wall thickness this also accounts for the variation in thickness both in the circumferential direction and the longitudinal direction, where an average value was approximated for individual samples.